THEORETICAL AND APPLIED STUDY OF THE POTENTIAL OF ION MOBILITY SPECTROMETRY

UNIVERSIDAD D CÓRDOBA

ESTUDIO TEÓRICO Y APLICADO DEL POTENCIAL DE LA ESPECTROMETRÍA DE MOVILIDAD IÓNICA

NATIVIDAD JURADO CAMPOS

TESIS DOCTORAL CÓRDOBA, 2020
Facultad de Ciencias
Departamento de Química Analítica

TITULO: *Theoretical and applied study of the potential of ion mobility spectrometry*

AUTOR: *Natividad Jurado Campos*

Campus de Rabanales
Ctra. Nacional IV, Km. 396 A
14071 Córdoba

https://www.uco.es/ucopress/index.php/es/
ucopress@uco.es

UNIVERSIDAD DE CÓRDOBA

Programa de doctorado: Química Fina

Título de la tesis (español e inglés): Estudio teórico y aplicado del potencial de la espectrometría de movilidad iónica/ Theoretical and applied study of the potential of ion mobility spectrometry

Director/Directores (Nombre y apellidos del / de los mismos)

Lourdes Arce Jiménez

Natalia Arroyo Manzanares

Autor de la tesis (Nombre y apellidos del mismo)

Natividad Jurado Campos

Fecha de depósito tesis en el Idep: 17 de Julio de 2020

UNIVERSIDAD DE CÓRDOBA

FACULTAD DE CIENCIAS
DEPARTAMENTO DE QUÍMICA ANALÍTICA

Estudio teórico y aplicado del potencial de la espectrometría de movilidad iónica

Theoretical and applied study of the potential of ion mobility spectrometry

Natividad Jurado Campos
Córdoba, España 2020

Estudio teórico y aplicado del potencial de la espectrometría de movilidad iónica

Las Directoras,

ARROYO MANZANARES NATALIA - 75116405S
Digitally signed by ARROYO MANZANARES NATALIA - 75116405S
Date: 2020.07.17 11:06:20 +02'00'

Fdo. Natalia Arroyo Manzanares
Profesora Contratada Doctora del
Departamento de Química Analítica de la
Universidad de Murcia

ARCE JIMENEZ MARIA LOURDES - 30798892Y
Firmado digitalmente por ARCE JIMENEZ MARIA LOURDES - 30798892Y
Nombre de reconocimiento (DN): c=ES, serialNumber=IDCES-30798892Y, givenName=MARIA LOURDES, sn=ARCE JIMENEZ, cn=ARCE JIMENEZ MARIA LOURDES - 30798892Y
Fecha: 2020.07.17 10:26:45 +02'00'

Fdo. Lourdes Arce Jiménez
Catedrática del Departamento
de Química Analítica de la
Universidad de Córdoba

Trabajo presentado para optar al grado de
Doctora en Ciencias, Sección Químicas

JURADO CAMPOS NATIVIDAD - 50615863Q
Firmado digitalmente por JURADO CAMPOS NATIVIDAD - 50615863Q
Fecha: 2020.07.17 10:19:24 +02'00'

Fdo. Natividad Jurado Campos

Natalia Arroyo Manzanares, Profesora Contratada Doctora del Departamento de Química Analítica de la Facultad de Química de la Universidad de Murcia, y **Lourdes Arce Jiménez**, Catedrática del Departamento de Química Analítica de la Facultad de Ciencias de la Universidad de Córdoba, en calidad de Directoras de la Tesis Doctoral presentada por Natividad Jurado Campos, con el título "Estudio teórico y aplicado del potencial de la espectrometría de movilidad iónica",

CERTIFICAN:

Que la citada Tesis Doctoral se ha realizado mayoritariamente en los laboratorios del Departamento de Química Analítica, Facultad de Ciencias, Universidad de Córdoba (España). La doctoranda también ha realizado estancias de investigación en el Departamento de Química Analítica de la Universidad de Murcia (España) y en el Departamento de Química y Bioquímica de la Universidad del Estado de Nuevo México (New Mexico State University, USA). Y que, a su juicio, reúne los requisitos necesarios exigidos en este tipo de trabajo.

Y para que conste y surta los efectos pertinentes, expiden el presente certificado en Córdoba, a 17 de Julio de 2020.

ARROYO MANZANARES NATALIA - 75116405S

Digitally signed by ARROYO MANZANARES NATALIA - 75116405S
Date: 2020.07.17 11:08:00 +02'00'

Fdo. Natalia Arroyo Manzanares

ARCE JIMENEZ MARIA LOURDES - 30798892Y

Firmado digitalmente por ARCE JIMENEZ MARIA LOURDES - 30798892Y
Nombre de reconocimiento (DN): c=ES, serialNumber=IDCES-30798892Y, givenName=MARIA LOURDES, sn=ARCE JIMENEZ, cn=ARCE JIMENEZ MARIA LOURDES - 30798892Y
Fecha: 2020.07.17 10:28:29 +02'00'

Fdo. Lourdes Arce Jiménez

Mediante la defensa de esta Memoria se pretende optar a la mención de **Doctorado Internacional**, habida cuenta de que la doctoranda reúne los requisitos exigidos para tal mención, a saber:

1. Informes favorables de dos doctores pertenecientes a Instituciones de Enseñanza Superior de otros países:
   - Stefanie Sielemann, University of Hamm-Lippstadt, Germany.
   - Štefan Matejčík, University of Comenius, Bratislava, Slovakia.
2. Uno de los miembros del tribunal que ha de evaluar la Tesis pertenece a un centro de Enseñanza Superior de otro país:
   - Bernhard Lendl, Vienna University of Technology, Austria.
3. La exposición y la defensa de parte de esta Tesis se realizarán en una lengua diferente a la materna: inglés.
4. Estancia de tres meses en un centro de investigación de otro país:

College of arts and sciences, Department of Chemistry and Biochemistry at New Mexico State University (Las Cruces, New Mexico, USA), bajo la supervisión del Profesor Gary A. Eiceman.

TÍTULO DE LA TESIS: Estudio teórico y aplicado del potencial de la espectrometría de movilidad iónica

DOCTORANDA: Natividad Jurado Campos

INFORME RAZONADO DE LOS DIRECTORES DE LA TESIS

(se hará mención a la evolución y desarrollo de la tesis, así como a trabajos y publicaciones derivados de la misma).

La licenciada Natividad Jurado Campos cursó (2009-2014) brillantemente la Licenciatura de Ciencias Químicas obteniendo el premio extraordinario. Durante su época de estudiante disfrutó de una beca de iniciación a la investigación que le permitió iniciar su carrera investigadora en el Departamento de Química Analítica de la Universidad de Córdoba (UCO). Los estudios del Máster interuniversitario en Química Fina y Nanoquímica realizado en la UCO, los compatibilizó con una beca de colaboración concedida por el Ministerio de Educación, Cultura y Deporte. Posteriormente, consiguió un contrato asociado a proyecto en la UCO, gracias al cual pudo seguir su carrera investigadora. En el año 2016 accedió a una beca de formación del profesorado universitario para la realización de la Tesis Doctoral, cuya memoria se presentará para su defensa el próximo mes de septiembre bajo la modalidad de doctorado internacional y como compendio de publicaciones. La temática de la misma ha abordado tanto estudios teóricos como aplicados para demostrar el potencial de la espectrometría de movilidad iónica (IMS).

El trabajo experimental realizado (tanto en la UCO como en otros centros de investigación nacionales (Universidad de Murcia) e internacionales (New Mexico State University)) se ha materializado en seis artículos científicos publicados en Q1 y tres trabajos enviados para su publicación a revistas especializadas del área de química analítica que se incluyen en su tesis doctoral. Además, la doctoranda ha publicado otros tres artículos científicos y dos capítulos de libro que no se incluyen en su tesis doctoral. La doctoranda ha participado en 15 congresos nacionales e internacionales presentando un total de 18 comunicaciones en formato oral, *flash* o cartel. A lo largo de estos años, ha adquirido formación en el manejo de equipos de IMS con fuentes ultravioleta y radioactivas (tritio ó niquel). También se ha formado en otras técnicas separativas como la cromatografía de gases, cromatografía de líquidos o la electroforesis capilar y en métodos de tratamiento de muestra para la determinación de analitos de interés en muestras de diferente naturaleza. Además de las competencias técnicas inherentes al trabajo en el laboratorio, ha demostrado iniciativa, capacidad para la resolución de problemas, planificación y dirección del trabajo a investigadores noveles.

Por todo ello, se autoriza la presentación de la tesis doctoral.

Córdoba,17 de julio de 2020

ARROYO MANZANARES NATALIA - 75116405S

Digitally signed by ARROYO MANZANARES NATALIA - 75116405S
Date: 2020.07.17 11:36:21 +02'00'

Firma de las directoras

ARCE JIMENEZ MARIA LOURDES - 30798892Y

Firmado digitalmente por ARCE JIMENEZ MARIA LOURDES - 30798892Y
Nombre de reconocimiento (DN): c=ES, serialNumber=IDCES-30798892Y, givenName=MARIA LOURDES, sn=ARCE JIMENEZ, cn=ARCE JIMENEZ MARIA LOURDES - 30798892Y
Fecha: 2020.07.17 10:29:08 +02'00'

Fdo.: Natalia Arroyo Manzanares

Fdo.: Lourdes Arce Jiménez

INFORME SOBRE EL FACTOR DE IMPACTO DE LAS PUBLICACIONES DE LA TESIS

TÍTULO DE LA TESIS: Estudio teórico y aplicado del potencial de la espectrometría de movilidad iónica

DOCTORANDA: NATIVIDAD JURADO CAMPOS

PUBLICACIÓN	FI*	DECIL/CUARTIL
Stability of proton-bound clusters of alkyl alcohols, aldehydes and ketones in ion mobility spectrometry. **Talanta** 185 (2018) 299-308	4.916	Q1 11/84 Analytical Chemistry
Innovative coupling of supercritical fluid extraction with ion mobility spectrometry. **Talanta** 188 (2018) 637-643	4.916	Q1 11/84 Analytical Chemistry
Thermal desorption-ion mobility spectrometry: a rapid sensor for the detection of cannabinoids and discrimination of cannabis sativa L. chemotypes. **Sensor. Actuat. B-Chem.** 273 (2018) 1413-1424	6.393	D1 6/84 Analytical Chemistry
A robustness study of calibration models for olive oil classification: targeted and non-targeted fingerprint approaches based on GC–IMS. **Food Chem.** 288 (2019) 315-324	6.306	D1 6/139 Food Science and Technology
Field induced fragmentation (FIF) spectra of oxygen containing volatile organic compounds with reactive stage tandem ion mobility spectrometry and functional group	6.785*	D1 7/86 Analytical Chemistry

classification by neural network analysis, Analytical Chemistry. **Anal. Chem.** 92 (2020) 5862-5870		
Quality authentication of Virgin Olive Oils using Orthogonal Techniques and Chemometrics based on individual and high-level data fusion information. **Talanta**, 219 (2020) 121260	5.339*	Q1 11/86 Analytical Chemistry

*Factor de impacto obtenido de Journal Citation Report (JCR). Para los datos de 2020 se usaron los correspondientes al año 2019.

ABSTRACT

1. Introduction

Ion mobility spectrometry (IMS) is an analytical technique based on the separation of gaseous ions under the influence of an electric field through an inert gas atmosphere.

Some of the main limitations of IMS, depending on the context, may be the limited quantification capacity of compounds in real samples since narrow linear quantification ranges are normally obtained; the low selectivity due to the low resolution power of this type of equipment; and the difficulty of unequivocally identifying compounds in real samples since the existing databases are not as up-to-date as for other technologies such as mass spectrometry (MS).

Therefore, it is evident that there is a demand for more selective methodologies and that provide greater analyte detection and quantification capacity.

With these premises, it can be said that the greatest current challenge of the IMS is to maximize the detection capacity of the technique in order to achieve the unambiguous identification of a high number of analytes. This challenge is currently utopian when working with complex samples.

For this reason, the main motivation of this Doctoral Thesis was to seek solutions for the different challenges that the IMS currently faces in a theoretical and applied context.

2. Research content

The *basic objective* of the research was to explore the potential of IMS by using theoretical and applied strategies to improve the detection and identification coverage of the analysis carried out with this technology. These new strategies were applied throughout the main steps of the analytical process and

allowed improving basic analytical features such as the selectivity and sensitivity of optimized analysis methods and their detection capacity. The achievement of this basic objective leaded to analysis methods of standards and real samples, such as explosives, drugs, soil, rosemary plant, olives and mainly different types of olive oils. This *basic objective* was divided into three *general objectives* according to the different research topics to address in this Doctoral Thesis: a) To take benefits derived from the study of theoretical aspects of IMS for improving the interpretation of IMS spectra and from the use of additional features such as structural information to enhance qualitative analysis; b) To develop approaches to improve the detection and identification capacity in IMS analysis; and c) To exploit the opportunities of gas chromatography (GC)-IMS and IMS devices for food analysis as an expanding application area in IMS based on untargeted analysis methods. In this context, the Thesis has included the following studies:

(i) To study about the fundamentals of the formation of product ions through the modeling of ions stability using ab initio computations to math these results with the spectral patterns and structure of ions [1].

(ii) To explore the fragmentation of ions using an external electric field and the potential of the extra information of these fragments to enhance the rates of categorization by chemical class using neural networks [2].

(iii) To explore a thermal desorption (TD)-IMS device to obtain spectral fingerprints of Cannabis herbal samples, with and without pretreatment for rapid assignment to their different chemotypes by using principal component analysis (PCA) and linear discriminant analysis (LDA) [3].

(iv) To achieve the selectivity in response to trinitrotoluene (TNT) through reactive removal of interfering ions following mobility isolation using a tandem IMS with reactive stage as detection system [4].

(v) To develop a pioneer online coupling of supercritical fluid extraction (SFE) as sample introduction system (SIS) prior IMS using a column filled with Tenax TA material as sorbent trap to coupled both devices to improve analytical properties such as sensitivity and selectivity of future IMS methods [5].

(vi) To carry out a bibliographical study which gather and critically discuss recent publications related to analytical techniques to distinguish olive oils according to their quality as extra virgin (EVOO), virgin (VOO) or lampante (LOO) [6].

(vii) To investigate and compare different chemometric approaches for olive oil classification as EVOO, VOO or LOO using GC-IMS to get the most robust model over time [7].

(viii) To evaluate the combination of the results of orthogonal instrumental techniques to differentiate EVOO, VOO or LOO to imitate the expert panels [8].

(ix) To analyze olive and olive oil samples according with their production system to classify them as organic or conventional using ultraviolet (UV)-IMS, GC-IMS, GC-MS and/or capillary electrophoresis (CE)-UV [9].

3. Conclusions

The most salient conclusions drawn from this Doctoral Thesis according to the initially proposed objectives are summarized below:

1. Benefits derived from the study of theoretical aspects of IMS for improving the interpretation of IMS spectra and from the use of additional features such as structural information to enhance qualitative analysis.

(i) Only n-alcohols from 1-pentanol to 1-octanol produced proton-bound trimers which are sufficiently stable to be observed at 35 ºC since only these alcohols formed a V-shaped arrangement for proton-bound trimers strengthening ion stability and lifetime according to computational modeling. Collision cross sections derived from reduced mobility coefficients in nitrogen gas atmosphere support the predicted ion structures and approximate degrees of hydration [1].

(ii) Field induced fragmentation (FIF) spectra obtained using a tandem IMS spectrometer with a reactive stage presented a high efficiency of fragmentation for single bond cleavage of alcohols and in six-member ring rearrangements of acetates. Fragmentation was not observed, or seen weakly, with aldehydes, ethers, and ketones due to their strained four-member ring transition states.

Neural networks were trained to categorize spectra by chemical class. Rates of categorization were class dependent with best performance for alcohols and acetates, moderate performance for ketones, and worst performance for ethers and aldehydes [2].

2. Improvement of the analytical process through new methodological developments to enhance the detection and identification capacity in IMS analysis.

(iii) The rapid detection of cannabinoids of Cannabis sativa L. plants using a portable TD-IMS was used to chemotyping these plants by analysing their solid-liquid extracts and the residues of plants on hands after their manipulation. PCA and LDA were applied over the pre-treated data and suitable results for on-site chemotaxonomic discrimination of Cannabis varieties and detection of illegal marijuana were obtained in less than 2 min [3].

(iv) The use of a tandem IMS with reactive stage allowed the selective detection of TNT in presence of Interferent B. The peaks of their product ions, $(M-1)^-$ and M_2Cl^-, were more than 90% convolved even with mobility isolation of peaks in a tandem IMS drift tube. When using the reactive stage through applying an electric field of 123 Td more than 95 % of peak area for M_2Cl^- was decomposed to $M\cdot(M-1)^-$ which is almost completely separated from TNT. Only a 5% convolution was observed which was easily removed through peak deconvolution. However, suppression of ionization in the source from excessive amounts of Interferent B was observed which caused 30% loss in response to TNT with amounts of Interferent B of 200 ng or more on a sample swipe [4].

(v) A pioneer on-line and environmentally-friendly hyphenation between a SFE and an IMS detector through a Tenax TA sorbent trap as retention interface was carried out for first time. This new coupling allows to extract and preconcentrate analytes and in a second step to determine them eliminating sample transfer from one device to another which increase the accuracy and speed of the analytical processes. The coupling was successfully evaluated determining benzene and toluene present in soil and eucalyptol in rosemary aromatic plants.

It was concluded that the proposed new hyphenation can have a strong impact on extracting and detecting different volatile analytes from complex matrices with a higher sensibility and/or selectivity, expanding the scope of the present technique to other research areas or even in different industrial applications [5].

3. Exploitation of the opportunities of GC-IMS and IMS devices for food analysis as an expanding application area in IMS based on untargeted analysis methods.

(vi) An update bibliographical study of the publications on quality classification of olive oils into EVOO, VOO or LOO categories using non-separation and separation analytical techniques to complement the official methods was carried out, showing that the GC-IMS, GC-MS and CE-UV are the most successful alternative today [6].

(vii) Two chemometric approaches for olive oil classification as EVOO, VOO or LOO were compared to get the most robust model over time by analysing 701 samples from two harvests: i) an non-targeted fingerprinting analysis and ii) a targeted approach based on peak-region features (markers). Both strategies demostrated to be suitable when they were used to build classification models of samples from the first harvest (average success > 74%). However, when these models were applied for classifying samples from the second harvest, better values were obtained using markers. The combination of data from the two harvests to build the chemometric models improved the percentages of prediction success for samples of the second harvest (> 90%). These results confirm the suitability of the recalibration of the models with samples from at least two different harvests [7].

(viii) CE-UV was selected in comparison with high performance liquid chromatography (HPLC)-UV and HPLC-fluorescence detector (FLD) as orthogonal technique of the GC-IMS to be part of an analytical platform to classify olive oils as EVOO, VOO or LOO depending on compounds perceived in the mouth (by CE-UV) and the components contributing to the olive oils aroma (by GC-IMS), respectively. Liquid-liquid extraction (LLE) proved to be a good extraction technique of olive oil prior CE-UV analysis. The potential of using this

platform was demonstrated using high-level data fusion since an improvement on the detection of samples with a uncertain category due to they are sitting on the border of two groups (e.g. EVOO-VOO or VOO-LOO) was achieved which could avoid the wrong categorization of that samples when using a single analytical technique [8].

(ix) The suitability of the optimised method using UV-IMS for the rapid and low-cost classification of organic or conventional olives of two varieties and a single harvest was demonstrated using a chemometric treatment on their volatile fingerprinting (94.39 % classification success). However, this UV-IMS device did not provide good results for the classification of organic or conventional olive oil samples. To achieve this objective, two different analytical techniques were used, GC-IMS (to analyse the volatile fingerprinting) and LLE-CE-UV (to evaluate the polar compounds present in olive oil). Both devices provided good classification results, above 93.20 % for samples from a single harvest. However, when samples from two harvest were considered, CE-UV was the more robust technique (95.76 %) in comparison with GC-IMS (75.16 %). An improvement of classification percentages of GC-IMS data was observed when samples from two harvest were separated into *Picual* (98.73 %) and *Hojiblanca* (98.78 %) variety sets. Results related to volatile fraction of olives and olive oils obtained with UV-IMS and GC-IMS, respectively, were contrasted with GC-MS (considered as a more implemented technique in analytical laboratories) and good correlation of percentages of success obtained with the aforementioned techniques was achieved. GC-MS was also employed to identify a total of 12 compounds in both matrices. However, the categorization of olives was not possible with this information and only the 3-hexenyl acetate allowed differentiation between organic and conventional olive oils [9].

4. References

[1] **N. Jurado-Campos**, R. Garrido-Delgado, B. Martínez-Haya, G.A. Eiceman, L. Arce, Stability of proton-bound clusters of alkyl alcohols, aldehydes and ketones in ion mobility spectrometry, Talanta, 185 (2018) 299-308.

[2] H. Shokri, E.G. Nazarov, B.D. Gardner, H-C. Niu, G. Lee, J.A. Stone, **N. Jurado-Campos**, G.A. Eiceman, Field induced fragmentation (FIF) spectra of oxygen containing volatile organic compounds with reactive stage tandem ion mobility spectrometry and functional group classification by neural network analysis, Analytical Chemistry, 92 (2020) 5862-5870.

[3] M.M. Contreras[#], **N. Jurado-Campos[#]**, C. Sánchez-Carnerero Callado, N. Arroyo-Manzanares, L. Fernández, S. Casano, S. Marco, L. Arce, C. Ferreiro-Vera. (**[#]Both authors contribute equally**), Thermal desorption-ion mobility spectrometry: a rapid sensor for the detection of cannabinoids and discrimination of cannabis sativa L. chemotypes, Sensors and Actuators B: Chemical, 273 (2018) 1413-1424.

[4] **N. Jurado-Campos**, U. Chiluwal, G.A. Eiceman. Improved selectivity for the determination of trinitrotoluene through reactive stage tandem ion mobility spectrometry and a quantitative measure of source-based suppression of ionization. Submitted to publication, 2020.

[5] **N. Jurado-Campos**, A. Carpio, M. Zougagh, L. Arce, N. Arroyo-Manzanares, Innovative coupling of supercritical fluid extraction with ion mobility spectrometry, Talanta, 188 (2018) 637-643.

[6] **N. Jurado-Campos**, R. Rodríguez-Gómez, N. Arroyo-Manzanares, L. Arce. Instrumental techniques to classification Olive oils according to their quality. Submitted to publication, 2020.

[7] M.M. Contreras, **N. Jurado-Campos**, L. Arce, N. Arroyo-Manzanares, A robustness study of calibration models for olive oil classification: targeted and non-targeted fingerprint approaches based on GC–IMS, Food Chemistry, 288 (2019) 315-324.

[8] **N. Jurado-Campos**, N. Arroyo-Manzanares, P. Viñas, L. Arce, 2020. Quality authentication of Virgin Olive Oils using Orthogonal Techniques and Chemometrics based on individual and high-level data fusion information. Talanta. 219, 121260.

[9] **N. Jurado-Campos**, M. García-Nicolás, M. Pastor-Belda, T. Bußmann, N. Arroyo-Manzanares, B. Jiménez, P. Viñas and L. Arce. Exploration of the potential of different analytical techniques to authenticate organic vs. conventional olives and olive oils from two varieties using untargeted fingerprinting approaches. Submitted to publication, 2020.

RESUMEN

1. Introducción

La espectrometría de movilidad iónica (IMS en inglés) es una técnica analítica que se basa en la separación de iones gaseosos bajo la influencia de un campo eléctrico a través de una atmósfera de gas inerte.

Algunas de las principales limitaciones de la IMS, dependiendo del contexto, pueden ser la limitada capacidad de cuantificación de compuestos en muestras reales ya que se obtienen normalmente rangos lineales de cuantificación muy estrechos; la escasa selectividad debido al bajo poder de resolución de este tipo de equipos; y la dificultad de identificación de forma inequívoca de compuestos en muestras reales ya que las bases de datos existentes no están tan actualizadas como para otras tecnologías como la espectrometría de masas (MS en inglés).

Por tanto, resulta evidente que existe una demanda de metodologías más selectivas y que proporcionen mayor capacidad de detección y cuantificación de analitos.

Con estas premisas, se puede decir que el mayor reto actual de la IMS es maximizar la capacidad de detección de la técnica con el fin de conseguir la identificación inequívoca de un alto número de analitos. Este reto es actualmente utópico cuando se trabaja con muestras complejas.

Por ello, la principal motivación de esta Tesis Doctoral fue buscar soluciones para los distintos retos a los que se enfrenta actualmente la IMS en un contexto teórico y aplicado.

2. Contenido de la investigación

El *objetivo básico* de la investigación fue explorar el potencial de la IMS mediante el uso de estrategias teóricas y aplicadas para mejorar la capacidad de

detección e identificación de los análisis realizados con esta tecnología. Estas nuevas estrategias se aplicaron a lo largo de las etapas principales del proceso analítico y permitieron mejorar características analíticas básicas, como la selectividad y la sensibilidad, de los métodos de análisis optimizados y su capacidad de detección. El logro de este objetivo básico condujo a métodos de análisis de estándares y muestras reales, como explosivos, drogas, suelo, plantas de romero, aceitunas y principalmente diferentes tipos de aceites de oliva. Este *objetivo básico* se dividió en tres *objetivos generales* de acuerdo con los diferentes temas de investigación para abordar en esta Tesis Doctoral: a) aprovechar los beneficios derivados del estudio de los aspectos teóricos de la IMS para mejorar la interpretación de los espectros de IMS y del uso de características adicionales como información estructural para mejorar el análisis cualitativo; b) desarrollar herramientas para mejorar la capacidad de detección e identificación en los análisis de IMS; y c) aprovechar las oportunidades de los instrumentos de cromatografía de gases (GC en inglés)-IMS e IMS para el análisis de alimentos como un área de aplicación en expansión en IMS basado en métodos de análisis no dirigidos. En este contexto, la Tesis ha incluido los siguientes estudios:

(i) Estudiar los fundamentos de la formación de iones producto a través del modelado computacional de la estabilidad de los iones utilizando cálculos ab initio para combinarlos con los patrones espectrales y la estructura de los iones [1].

(ii) Explorar la fragmentación de iones utilizando un campo eléctrico externo y el potencial de la información adicional de estos fragmentos para mejorar las tasas de categorización por clase química utilizando redes neuronales [2].

(iii) Explorar un equipo de desorción térmica (TD en inglés)-IMS para obtener huellas espectrales de muestras de plantas de cannabis, con y sin pretratamiento, para la rápida asignación de los diferentes quimiotipos mediante análisis de componentes principales (PCA en inglés) y análisis discriminante lineal (LDA en inglés) [3].

(iv) Lograr la respuesta selectiva del trinitrotolueno (TNT en inglés) a través de la eliminación con etapa reactiva de iones interferentes usando el aislamiento de iones con un IMS en tándem con etapa reactiva como sistema de detección [4].

(v) Desarrollar un acoplamiento on-line pionero de la extracción con fluídos supercríticos (SFE en inglés) como sistema de introducción de muestra previo a la IMS utilizando una columna rellena con el material Tenax TA como trampa sorbente para acoplar ambos dispositivos para mejorar propiedades analíticas como la sensibilidad y la selectividad de futuros métodos IMS [5].

(vi) Realizar un estudio bibliográfico que reúna y discuta críticamente las publicaciones recientes relacionadas con técnicas analíticas para distinguir los aceites de oliva según su calidad como virgen extra (AOVE), virgen (AOV) o lampante (AOL) [6].

(vii) Investigar y comparar diferentes estrategias quimiométricas para la clasificación del aceite de oliva como AOVE, AOV o AOL utilizando la GC-IMS para obtener el modelo más robusto con el tiempo [7].

(viii) Evaluar la combinación de los resultados de técnicas instrumentales ortogonales para diferenciar AOVE, AOV o AOL para imitar los paneles de expertos [8].

(ix) Analizar muestras de aceitunas y aceite de oliva de acuerdo con su sistema de producción para clasificarlas como ecológicas o convencionales usando ultravioleta (UV)-IMS, GC-IMS, GC-MS y/o electroforesis capilar (CE en inglés)-UV [9].

3. Conclusiones

Las conclusiones más destacadas de la Tesis Doctoral de acuerdo con los objetivos inicialmente propuestos se resumen a continuación:

1. Beneficios derivados del estudio de los aspectos teóricos de la IMS para mejorar la interpretación de los espectros de IMS y del uso de características adicionales como información estructural para mejorar el análisis cualitativo.

(i) Solo los n-alcoholes desde el 1-pentanol al 1-octanol produjeron trímeros protonados que son suficientemente estables para ser observados a 35 ºC ya que solo estos alcoholes presentaban una disposición en forma de V para los trímeros protonados que fortalecían la estabilidad y la vida útil de los iones de acuerdo con el modelo computacional. Las secciones transversales de colisión obtenidas a partir de los coeficientes de movilidad reducida en atmósfera de nitrógeno gaseoso apoyan las estructuras iónicas predichas y los grados aproximados de hidratación [1].

(ii) Los espectros de fragmentación inducida por campo (FIF en inglés) obtenidos usando un espectrómetro de IMS en tándem con una etapa reactiva presentaron una alta eficiencia de fragmentación mediante la escisión de un solo enlace en alcoholes y el reordenamiento de anillos de seis miembros en acetatos. La fragmentación no se observó, o se vio débilmente, con aldehídos, éteres y cetonas debido a sus estados de transición tensos de anillos de cuatro miembros. Las redes neuronales se entrenaron para clasificar los espectros por clase química. Las tasas de categorización fueron dependientes de la clase obteniéndose las mejores para alcoholes y acetatos, moderadas para cetonas y las peores para éteres y aldehídos [2].

2. Mejora del proceso analítico a través de nuevos desarrollos metodológicos para mejorar la capacidad de detección e identificación en el análisis IMS.

(iii) La detección rápida de los cannabinoides de las plantas de Cannabis sativa L. usando un TD-IMS portátil se usó para agrupar en función de su quimiotipo estas plantas mediante el análisis de sus extractos sólido-líquido y los residuos de las plantas en las manos después de su manipulación. Se aplicaron PCA y LDA sobre los datos pretratados y se obtuvieron resultados adecuados para la discriminación quimiotaxonómica in situ de las variedades de cannabis y la detección de marihuana ilegal en menos de 2 minutos [3].

(iv) El uso de un IMS en tándem con etapa reactiva permitió la detección selectiva de TNT en presencia de Interferente B. Los picos de sus iones producto, $(M\text{-}1)^-$ and M_2Cl^-, estaban solapados en más del 90% incluso con el aislamiento

de iones en un tubo de deriva en tándem. Al usar la etapa reactiva mediante la aplicación de un campo eléctrico de 123 Td, más del 95% del área de pico para M_2Cl^- se descompuso en $M\cdot(M-1)^-$, que está casi completamente separado del TNT. Solo se observó un solapamiento del 5% que se eliminó fácilmente a través de la deconvolución de picos. Sin embargo, se observó la supresión de la ionización en la fuente debido a cantidades excesivas de Interferente B que causó una pérdida del 30% en la respuesta del TNT con cantidades de Interferente B de 200 ng o más [4].

(v) Un acoplamiento pionero on-line y respetuoso con el medio ambiente entre un SFE y un detector IMS a través de una trampa sorbente de Tenax TA como interfaz de retención se llevó a cabo por primera vez. Este nuevo acoplamiento permite extraer y preconcentrar analitos y, en un segundo paso, determinarlos eliminando la transferencia de muestras de un dispositivo a otro, lo que aumenta la precisión y la velocidad de los procesos analíticos. El acoplamiento se evaluó con éxito determinando el benceno y el tolueno presentes en suelo y el eucaliptol en plantas de romero. Se demostró que el nuevo acoplamiento propuesto puede tener un fuerte impacto en la extracción y detección de diferentes analitos volátiles de matrices complejas con una mayor sensibilidad y/o selectividad, ampliando el alcance de la presente técnica a otras áreas de investigación o incluso en diferentes aplicaciones industriales [5].

3. Aprovechar las oportunidades de la GC-IMS y dispositivos IMS para el análisis de alimentos como un área de aplicación en expansión en IMS basada en métodos no dirigidos.

(vi) Se realizó un estudio bibliográfico actualizado de las publicaciones que tratan sobre la clasificación de los aceites de oliva según su calidad en las categorías AOVE, AOV o AOL utilizando técnicas analíticas no-separativas y separativas para complementar los métodos oficiales, demostrándose que las GC-IMS, GC-MS y CE-UV son hoy día la alternativa más exitosas [6].

(vii) Se compararon dos enfoques quimiométricos para la clasificación del aceite de oliva como AOVE, AOV o AOL para obtener el modelo más robusto a lo largo

del tiempo analizando 701 muestras de dos campañas: i) un análisis de huellas espectrales no dirigido y ii) un enfoque dirigido basado en áreas de pico de marcadores. Ambas estrategias demostraron ser útiles cuando se utilizaron para construir modelos de clasificación de las muestras de la primera campaña (valor medio de éxito > 74%). Sin embargo, cuando estos modelos se aplicaron para clasificar muestras de la segunda campaña, se obtuvieron mejores valores utilizando marcadores. La combinación de datos de las dos campañas para construir los modelos quimiométricos mejoró los porcentajes de éxito de predicción para muestras de la segunda campaña (> 90%). Estos resultados confirman la idoneidad de la recalibración de los modelos con muestras de al menos dos campañas diferentes [7].

(viii) La CE-UV se seleccionó en comparación con la cromatografía de líquidos (HPLC en inglés)-UV y HPLC-detector de fluorescencia (FLD en inglés) como técnica ortogonal de la GC-IMS para formar parte de una plataforma analítica para clasificar los aceites de oliva como AOVE, VOO o LOO dependiendo de los compuestos percibidos en la boca (por CE-UV) y los componentes que contribuyen al aroma de los aceites de oliva (por GC-IMS), respectivamente. La extracción líquido-líquido (LLE en inglés) demostró ser una buena técnica de extracción antes del análisis del aceite de oliva por CE-UV. El potencial de usar esta plataforma se demostró usando la fusión de datos de alto nivel, ya que una mejora en la detección de muestras con una categoría incierta debido a que se encuentran en el borde de dos grupos (por ejemplo, AOVE-AOV o AOV-AOL) se logró, lo que podría evitar la categorización incorrecta de esas muestras cuando se utiliza una sola técnica analítica [8].

(ix) La utilidad del método optimizado mediante UV-IMS para la clasificación rápida y a bajo coste de aceitunas ecológicas o convencionales de dos variedades y de una sola campaña se demostró utilizando un tratamiento quimiométrico sobre su huella espectral (94.39% de éxito de clasificación). Sin embargo, este dispositivo UV-IMS no proporcionó buenos resultados para la clasificación de muestras de aceites de oliva ecológicas o convencionales. Para lograr este objetivo, se emplearon dos técnicas analíticas diferentes y más potentes, la GC-

IMS (para analizar las huellas espectrales de los compuestos volátiles) y la LLE-CE-UV (para evaluar los compuestos polares presentes en el aceite de oliva). Ambos dispositivos proporcionaron buenos resultados de clasificación, por encima del 93.20% para muestras de una sola campaña. Sin embargo, cuando se consideraron muestras de dos campañas, CE-UV fue la técnica más robusta (95.76%) en comparación con la GC-IMS (75.16%). Se observó una mejora en los porcentajes de clasificación de los datos de GC-IMS cuando las muestras de dos campañas se separaron en conjuntos de variedades *Picual* (98.73%) y *Hojiblanca* (98.78%). Los resultados relativos a la fracción volátil de aceitunas y aceites de oliva obtenidos con UV-IMS y GC-IMS, respectivamente, se compararon con GC-MS (considerada como una técnica más implementada en los laboratorios analíticos) y se logró una buena correlación de los porcentajes de éxito obtenidos con las técnicas mencionadas. La GC-MS también se empleó para identificar un total de 12 compuestos en ambas matrices. Sin embargo, la categorización de las aceitunas no fue posible con esta información y solo el acetato de 3-hexenilo permitió la diferenciación entre los aceites de oliva ecológicos y convencionales [9].

4. Bibliografía

[1] **N. Jurado-Campos**, R. Garrido-Delgado, B. Martínez-Haya, G.A. Eiceman, L. Arce, Stability of proton-bound clusters of alkyl alcohols, aldehydes and ketones in ion mobility spectrometry, Talanta, 185 (2018) 299-308.

[2] H. Shokri, E.G. Nazarov, B.D. Gardner, H-C. Niu, G. Lee, J.A. Stone, **N. Jurado-Campos**, G.A. Eiceman, Field induced fragmentation (FIF) spectra of oxygen containing volatile organic compounds with reactive stage tandem ion mobility spectrometry and functional group classification by neural network analysis, Analytical Chemistry, 92 (2020) 5862-5870.

[3] M.M. Contreras[#], **N. Jurado-Campos**[#], C. Sánchez-Carnerero Callado, N. Arroyo-Manzanares, L. Fernández, S. Casano, S. Marco, L. Arce, C. Ferreiro-Vera. (**[#]Both authors contribute equally**), Thermal desorption-ion mobility

spectrometry: a rapid sensor for the detection of cannabinoids and discrimination of cannabis sativa L. chemotypes, Sensors and Actuators B: Chemical, 273 (2018) 1413-1424.

[4] **N. Jurado-Campos**, U. Chiluwal, G.A. Eiceman. Improved selectivity for the determination of trinitrotoluene through reactive stage tandem ion mobility spectrometry and a quantitative measure of source-based suppression of ionization. Submitted to publication, 2020.

[5] **N. Jurado-Campos**, A. Carpio, M. Zougagh, L. Arce, N. Arroyo-Manzanares, Innovative coupling of supercritical fluid extraction with ion mobility spectrometry, Talanta, 188 (2018) 637-643.

[6] **N. Jurado-Campos**, R. Rodríguez-Gómez, N. Arroyo-Manzanares, L. Arce. Instrumental techniques to classification Olive oils according to their quality. Submitted to publication, 2020.

[7] M.M. Contreras, **N. Jurado-Campos**, L. Arce, N. Arroyo-Manzanares, A robustness study of calibration models for olive oil classification: targeted and non-targeted fingerprint approaches based on GC–IMS, Food Chemistry, 288 (2019) 315-324.

[8] **N. Jurado-Campos**, N. Arroyo-Manzanares, P. Viñas, L. Arce, 2020. Quality authentication of Virgin Olive Oils using Orthogonal Techniques and Chemometrics based on individual and high-level data fusion information. Talanta. 219, 121260.

[9] **N. Jurado-Campos**, M. García-Nicolás, M. Pastor-Belda, T. Bußmann, N. Arroyo-Manzanares, B. Jiménez, P. Viñas and L. Arce. Exploration of the potential of different analytical techniques to authenticate organic vs. conventional olives and olive oils from two varieties using untargeted fingerprinting approaches. Submitted to publication, 2020.

INDEX

OBJECTIVES

OBJETIVOS

The ***basic objective*** of the research in this Thesis Book was to explore the potential of IMS by using theoretical and applied strategies to improve the detection and identification coverage in analysis carried out with this technology. These new strategies were applied at different steps of the analytical process and allowed improving basic analytical features such as selectivity and sensitivity of analysis methods which employ IMS and their detection capacity. The achievement of this basic objective led to the development of analytical methods to determine standards and analyze samples such as explosives, drugs, soil, rosemary plant, olives and mainly olive oils.

To address this objective, it was divided into three ***general objectives***:

- Use of theoretical aspects of IMS for improving the interpretation of its IMS spectra and use of additional features such as structural information of the ions formed to increase the potential of the technique from the point of view of qualitative analysis.
- Development of approaches to improve the detection and identification capacity in IMS analysis.
- Study of the potential of GC-IMS and IMS devices for food analysis as an expanding application area using this technology based on untargeted analysis methods.

From each general objective, we defined several ***specific objectives***:

(i) To study about the fundamentals of the formation of product ions through the modeling of ions stability using ab initio computations to math these results with the spectral patterns and structure of ions.

(ii) To explore the fragmentation of ions using an external electric field and the potential of the extra information of these fragments to enhance the rates of categorization by chemical class using neural networks.

(iii) To explore a TD-IMS device to obtain spectral fingerprints of Cannabis herbal samples, with and without pretreatment for their rapid chemotyping by using PCA and LDA.

(iv) To achieve the selectivity in response to TNT through reactive removal of interfering ions following mobility isolation using a tandem IMS with reactive stage as detection system.

(v) To develop a pioneer online coupling of SFE as SIS prior IMS using a column filled with Tenax TA material as sorbent trap to coupled both devices to improve analytical properties such as sensitivity and selectivity of future IMS methods.

(vi) To carry out a bibliographical study which gather and critically discuss recent publications related to analytical techniques to distinguish olive oils according to their quality as EVOO, VOO or LOO.

(vii) To investigate and compare different chemometric approaches for olive oil classification as EVOO, VOO or LOO using GC-IMS to get the most robust model over time.

(viii) To evaluate the combination of the results of orthogonal instrumental techniques to differentiate EVOO, VOO or LOO to imitate the expert panels.

(ix) To authenticate olive and olive oil samples according with their production system to categorize them as organic or conventional using UV-IMS, GC-IMS, GC-MS and/or CE-UV.

The formation of the future PhD, which is the ***final objective*** of a Doctoral Thesis, has also included the master on "Chemistry". Also, the necessary steps to fulfill the requirements to achieve the International Doctorate mention were developed. In parallel to the above-mentioned tasks and to the research included in the main part of this Book, a wider formation of the PhD student has been sought by development of other activities summarized below as annexes:

- Annex I: Collaborations with other members of the group and with other group, which has provided 3 published articles.
- Annex II: Book chapters non-included in the Thesis.
- Annex III: Oral and poster communications in national or international meetings.
- Annex IV: Co-direction of two Final Degree Projects (TFGs) of Degree in Chemistry students (University of Córdoba, Spain).
- Annex V: Co-direction of three Practical semester project of German Erasmus students from Hamm-Lippstadt University of Applied Sciences, Germany.
- Annex VI: Simultaneous research in education, which has provided one published article and participation in a teaching innovation project.

El ***objetivo básico*** de la investigación recogida en esta Memoria de Tesis fue explorar el potencial de la IMS mediante el uso de estrategias teóricas y aplicadas para mejorar la capacidad de detección e identificación en los análisis realizados con esta tecnología. Estas nuevas estrategias se aplicaron en distintas etapas del proceso analítico y permitieron mejorar características analíticas básicas, como la selectividad y la sensibilidad, de los métodos de análisis que usan la IMS y su capacidad de detección. El logro de este objetivo básico condujo al desarrollo de métodos analíticos para determinar estándares y analizar muestras tales como explosivos, drogas, suelo, plantas de romero, aceitunas y principalmente aceites de oliva.

Para abordar este objetivo, éste se dividió en tres ***objetivos generales***:

- Uso de los aspectos teóricos de la IMS para mejorar la interpretación de sus espectros y uso de características adicionales como información estructural de los iones formados para aumentar el potencial de la técnica desde el punto de vista del análisis cualitativo.
- Desarrollo de herramientas para mejorar la capacidad de detección e identificación en los análisis de IMS.
- Estudio del potencial de los instrumentos de GC-IMS e IMS para el análisis de alimentos como un área de aplicación en expansión usando esta tecnología basado en métodos de análisis no dirigidos.

Cada objetivo general ha dado lugar a varios ***objetivos específicos***:

(i) Estudiar los fundamentos de la formación de iones producto a través del modelado computacional de la estabilidad de los iones utilizando cálculos ab initio para combinarlos con los patrones espectrales y la estructura de los iones.

(ii) Explorar la fragmentación de iones utilizando un campo eléctrico externo y el potencial de la información adicional de estos fragmentos para mejorar las tasas de categorización por clase química utilizando redes neuronales.

(iii) Explorar un TD-IMS para obtener huellas espectrales de muestras de plantas de cannabis, con y sin pretratamiento, para la rápida asignación de quimiotipos mediante PCA y LDA.

(iv) Lograr la respuesta selectiva del TNT a través de la eliminación con etapa reactiva de iones interferentes usando el aislamiento de iones con un IMS en tándem con etapa reactiva como sistema de detección.

(v) Desarrollar un acoplamiento on-line pionero de un SFE como sistema de introducción de muestra previo a la IMS utilizando una columna rellena con el material Tenax TA como trampa sorbente para acoplar ambos dispositivos para mejorar propiedades analíticas como la sensibilidad y la selectividad de futuros métodos IMS.

(vi) Realizar un estudio bibliográfico que reúna y discuta críticamente las publicaciones recientes relacionadas con técnicas analíticas para distinguir los aceites de oliva según su calidad como AOVE, AOV o AOL.

(vii) Investigar y comparar diferentes estrategias quimiométricas para la clasificación del aceite de oliva como AOVE, AOV o AOL utilizando la GC-IMS para obtener el modelo más robusto con el tiempo.

(viii) Evaluar la combinación de los resultados de técnicas instrumentales ortogonales para diferenciar AOVE, AOV o AOL para imitar los paneles de expertos.

(ix) Autenticar muestras de aceitunas y aceite de oliva de acuerdo con su sistema de producción para clasificarlas como ecológicas o convencionales usando UV-IMS, GC-IMS, GC-MS y/o CE-UV.

La formación de la futura doctora, que es el ***objetivo final*** de una Tesis Doctoral, también ha incluido el máster en "Química". Además, se completaron los pasos necesarios para cumplir con los requisitos para lograr la mención del Doctorado Internacional. Paralelamente a las tareas indicadas anteriormente y a la investigación incluida en la parte principal de la Memoria, se ha buscado una formación más amplia de la estudiante de doctorado mediante el desarrollo de otras actividades resumidas a continuación como anexos:

- Anexo I: Colaboración con otros miembros del grupo y con otro grupo de investigación, que ha proporcionado 3 artículos publicados.

- Anexo II: Capítulos de libro no incluidos en la Tesis.

- Anexo III: Comunicaciones orales y pósters en congresos nacionales o internacionales.

- Anexo IV: Codirección de dos Trabajos Fin de Grado (TFG) de estudiantes de Grado de Química (Universidad de Córdoba, España).

- Anexo V: Codirección de tres proyectos prácticos de semestre de estudiantes Erasmus alemanes de la Universidad de Ciencias Aplicadas Hamm-Lippstadt, Alemania.

- Anexo VI: Investigación simultánea en el área de educación, que ha proporcionado un artículo publicado y la participación en un proyecto de innovación docente.

INTRODUCTION

This introduction section is intending to offer an overview of the ion mobility spectrometry (IMS) analysis from both a theoretical and applied point of view considered in the research carried out in this PhD.

1. The role of IMS in the analytical process

Since the end of 19th century, there is evidence about the formation of ions in air [1] and, at the beginning of twentieth century, the first studies about the mobility of ions under an electric field were published [2,3]. However, the first IMS devices were not developed until the 1970's by Karasek et al. [4] who employed the term "plasma chromatography" to refer to what is currently known as ion mobility spectrometers. From that moment, the development of IMS devices has risen exponentially in order to overcome problems encountered in monitoring vapors at ambient pressure. Improvements in analytical properties such as high sensitivity (low detection limits), acceptable selectivity, low price, quickness, robustness and simplicity have been achieved [5].

Nowadays, IMS is used as an analytical technique which could be part of the analytical process for sample measurement to obtain quality results that society needs. In overall terms, the analytical process can be segmented into three steps: previous operations, which integrate sample collection (sampling) and sample preparation, data acquisition and data treatment. Figure 1 illustrates a general workflow of the analytical process. IMS is considered as a vanguard analytical technique which could be used to acquire data in an analytical process providing fast and low cost results. Also, little or any sample preparation is required when using IMS devices [6]. Other remarkable advantages of IMS devices are working at atmospheric pressure, gas-phase ion separation and that IMS methods are environmental-friendly since solventless measurements are carried out.

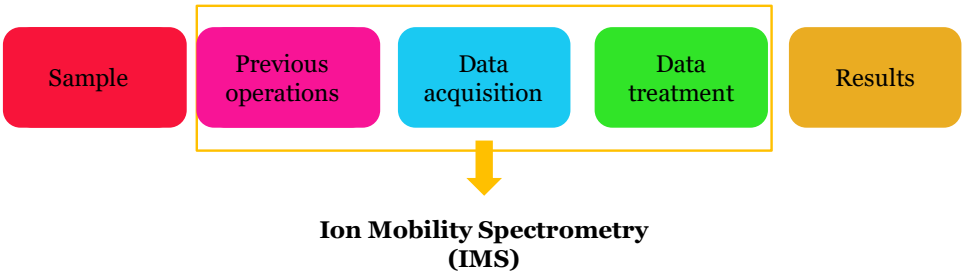

Figure 1. Scheme of a general analytical process.

2. IMS operation

IMS principle is based on the movement of swarms, defined as ensembles of gaseous ions, in an electric field and through a supporting gas atmosphere [5]. Gaseous ions in an electric field at atmospheric pressure are chaotically accelerated and it provoques collisions between them which culminates in a constant velocity of ions over macroscopic distances [7]. The velocity of ions is directly proportional to the electric field through a magnitude named ion mobility, as can be seen in *equation (1)*:

$$v = K \cdot E \tag{1}$$

where v is velocity of ions, K is the ion mobility coefficient and E is electric field.

The separation of ions on the basis of mobility differences is the principle of IMS technology. This separation is motivated by mass, charge, size and shape differences of ions. Mobility values are characteristic of each ion so K is a qualitative parameter to identify ions in IMS analysis. Also, the velocities of ions in a IMS are determined from the time that they need to traverse the distance between the ion shutter and detector or, in other words, the drift tube length as expressed in *equation (2)*:

$$v = \frac{L}{D_t} \tag{2}$$

where L is the drift tube length and D_t is the mentioned time which is called as drift time. The drift time is also characteristic for the analyte ion. *Equation (1)* and *(2)* can be joined to produce a new one, *equation (3)*, which allows to calculate the K value of an analyte ion apart from experimental parameters:

$$K = \frac{L}{D_t \cdot E} \tag{3}$$

K values are usually normalized to pressure and temperature for the value for standard conditions (T_o = *273.15 K* and P_o = *760 Torr*) in the form of reduced mobility constant (K_o), as it is shown in *equation (4)*. This enables comparisons between IMS devices data since both parameters influence on the density of molecules, and then, on their mobility:

$$K_0 = K \cdot \frac{P}{P_0} \cdot \frac{T_0}{T} \tag{4}$$

However, the calculated K_o values could vary between data reported in the literature by different researches. These differences have been attributed to instrumental variables such as inhomogeneities in temperature and electric field or contamination of buffer gas with moisture or other volatile compounds [8]. Then, the analysis of standards compounds or simultaneous mass measurements could be used to help identification purpose when using IMS [9]. Karpas suggested the use of chemical standards to correct K_o values. The compound 2,4-lutidine was selected due to its high proton affinity and because it produces a single peak at the studied conditions. The K_o value reported for 2,4-lutidine was 1.95 $cm^2 \cdot V^{-1} \cdot s^{-1}$ [10]. Also, 2,6-di-tbutylpyridine (2,6-DtBP) was used as calibrant by Eiceman and coworkers [11] based on its stability and reduced tendency for hydration, which leads to a roughly temperature-independent K_o value (1.42 $cm^2 \cdot V^{-1} \cdot s^{-1}$). Later, this value was updated to 1.46 $cm^2 \cdot V^{-1} \cdot s^{-1}$, with slight changes depending on the drift field applied [12]. Using an accepted standard, K_o values

can be calculated from measured mobility values by *equation (5)* as follows:

$$\frac{K_{0\ (unknown\ )}}{K_{0\ (standard\ )}} = \frac{D_{t\ (standard\ )}}{D_{t\ (unknown\ )}} \tag{5}$$

The mobility of an ion is also related to its collision cross section (Ω), called as CCS, and to number density (N, the number of molecules per unit volume) through experimental parameters according to Mason-Schamp equation [13] as shown in *equation (6)*:

$$K = \frac{3 \cdot q}{16 \cdot N} \cdot \left(\frac{2\pi}{\mu \cdot k_B \cdot T}\right)^{1/2} \cdot \frac{1}{\Omega} \tag{6}$$

where q is the ion charge, $\mu=mM/(m+M)$ is the reduced mass of the pair of diffusing ions (m) and carrier gas molecule (M), k_B is the Boltzmann constant (1.38065×10^{-23} J·K^{-1}) and T is the gas temperature.

Both, mobility and CCS, are suitable to ion identification and correlation although the fundamental meaning of the IMS as a structural measurement technique is more reflected when using the CCS [14]. The empirical CCS is influenced by the real CCS of the analyte, the drift gas (mometum transfer and gas polarization effects) and the ion mobility experiment (temperature and magnitude of the electric field) [15, 16]. Also, CCS is proper for comparison across different instrument platforms so, in the last years, several CCS databases have been built in an attempt to use it as a qualitative parameter in IMS [14, 17].

Separately, the number of detected ions through IMS is a measure of the concentration of analytes. Normally, this information is amplified and transduced as a voltage quantitative signal in IMS. Therefore, IMS data is commonly represented as a mobilty spectrum which includes ion peaks of the separated ions. Each peak is defined for its drift time as qualitative experimental parameter and a voltage value as quantitative analytical signal as it is shown in Figure 2**,** which represents a synthetic ion mobility spectrum.

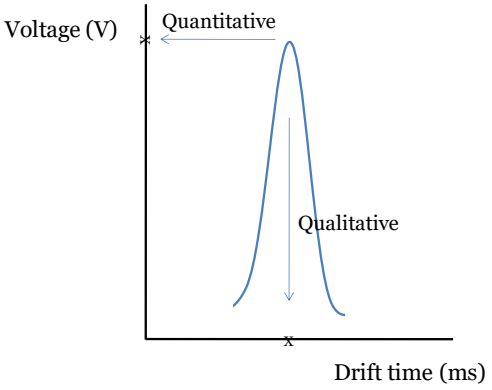

Figure 2. Synthetic ion mobility spectrum.

3. Parts of an IMS device

An ion mobility instrument is mainly composed of four parts namely sample introduction system (SIS), ionization source, drift tube and detector as it is shown in Figure 3.

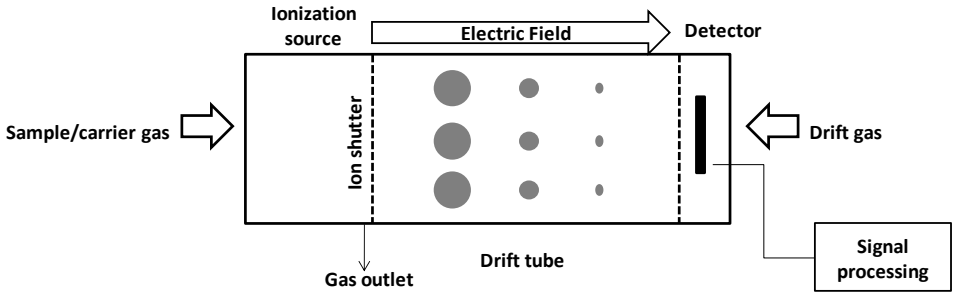

Figure 3. Basic scheme of the main components of a generic IMS device.

3.1. Sampling in IMS

One of the most crucial step of an analytical method relies on an appropriate choice of the SIS since the quality of the rest of parts of the

measurement process will depend on it. For instance, the SIS influences on the sensitivity and selectivity of the method. Suitable SIS for IMS instruments should involve the transformation of all analytes from the sample matrix to gas phase before their ionizacion, separation and detection. Thus, the selected SIS method largely depends on the physical characteristics of the analyte and type of sample analysed. According to the characteristics of the sample such as vapor, semivolatile, aqueous and solid sample, different SIS have been employed for IMS devices.

When vapor samples are analysed, direct injection [18], membranes (if the large amount of water or other contaminant in sample can be a problem with its ionization) [19] or active inlets and sniffing (by drawing gas samples past a membrane with a small air-sampling pump) [20] have been used.

Additionally, semivolatile samples are considered as those that contain compounds with vapor pressures too low to be directly detected by IMS. In that case, the most commonly employed SIS are: preconcentration, thermal desorption (TD), solid phase microextraction (SPME), stir-bar sorptive extractors (SBSE), gas chromatography (GC) and supercritical fluid chromatography (SFC) or extraction (SFE). Firstly, preconcentration is usually based on packing adsorbing material such as Tenax TA or Carbosieve® into a glass tube or stainless steel column [21]. For its part, TD is based of transforming samples from the solid or liquid state to produce neutral vapors with heat [22]. Concretely, TD from a SPME fiber is based on the adsorption of semivolatile compounds onto a nonvolatile polymeric coating or solid sorbent phase that has been coated onto a small fiber and later they are thermally desorbed into the clean carrier gas of the IMS [23]. If the sorptive materials are coated onto a stir bar, the SIS is a SBSE and then the selected organics or other analytes are adsorbed onto the surface of the bar which is stirred in solution. As previouly, these stir bars are heated to desorbed analytes into the IMS [24]. Also, the use of chromatographic injection methods prior IMS measurements is suitable and they can be interfaced directly. This coupling as SIS reduces the charge competition in IMS enabling quantitative

analysis [25]. Moreover, SFC [26] or SFE [27] can be used to carry samples into an IMS after chromatography or directly after extraction. Some advantages of using supercritical fluids are that they provide solubility for samples by solvating high molecular weight compounds with a too low vapor pressures. The CO_2 is the most common supercritical fluid used so that SFC and SFE are considered as a green technology. Moreover, CO_2 can be used as unique buffer gas for IMS.

Separately, the application of IMS as an analytical tool for analysing biological, environmental, food or other kind of samples dissolved in water is due to the possibility of introducing aqueous samples on these devices. Electrospray ionization (ESI) is the main system which allows the direct introduction of aqueous samples into an IMS [28] for stand-alone separation or for rapid preseparation before mass spectrometry (MS). ESI is based on using a heated reverse drift flow to both evaporate and prevent solvent vapors from entering the drift region of the IMS. Also, paperspray is a development related to ESI whose advantage is that the analyte can be ionized directly from filter paper which includes the sample without using a pump or capillary [29]. Futhermore, liquid chromatography (LC) can be used to introduce aqueous samples into IMS. ESI is usually employed as interface to directly introduce the eluent from LC into the IMS [30].

Finally, solid samples, which include molecules that are not volatile or have a extremely low vapor pressure, are introduced into IMS through different ionization sources. In this case, ionizacion sources also seves as SIS and samples are introduced in ionic form. The most common procedures are: direct analysis in real time (DART) [31], desorption electrospray ionization (DESI) [32] and matrix-assisted laser desorption ionization (MALDI) [33]. They are different in the ionization mechanism: The DART source uses energetic neutrals, DESI uses ions and MALDI uses light to generate ions for analysis from solid samples on surfaces. Furthermore, laser ablation can be employed as SIS of solid samples using a laser pulse over the sample and a plume of ions is produced and swepted into the ionization source of the IMS [34].

Other SIS to transform liquid or solid sample to gas such as permeation tubes [35], purge vessels and dilution gas flask [36], headspace (HS) samplers [37], pyrolyzers [38] have been used prior IMS. All the considered SIS along this section are summarized in Table 1.

Table 1. Summary of SIS employed with IMS.

Type of sample	SIS	References
Vapor samples	Direct injection	[18]
	Membranes	[19]
	Inlets and sniffing	[20]
Semivolatile samples	Preconcentration	[21]
	TD	[22]
	SPME	[23]
	SBSE	[24]
	GC	[25]
	SFC or SFE	[26, 27]
Aqueous samples	ESI	[28]
	Paperspray	[29]
	LC	[30]
Solid samples	DART	[31]
	DESI	[32]
	MALDI	[33]
	Laser ablation	[34]
Liquid or solid samples	Permeation tubes	[35]
	Purge vessels and dilution gas flask	[36]
	HS samplers	[37]
	Pyrolyzers	[38]

Five of the aforementioned SIS have been employed in different chapters of this Doctoral Thesis. TD was employed in **chapters III and IV**; SFE with a Tenax TA column were coupled with IMS as SIS in **chapter V**; and GC was directly selected as SIS in **chapter II** and it was used after an HS sampler (HS-

GC) in **chapters I, VII, VIII and IX**. Finally, HS sampler was also used without GC in **chapter IX**.

3.2. Ionization sources

Ionization of samples is needed when using IMS since measurements are based on the separation of ions in an electric field and through a supporting gas atmosphere. Then, these ions should be generated apart from neutral compounds of samples through IMS ion-generating reactions. Ionization can occur after the SIS or in the same step, depending on the type of ionization source used. Ionization in analytical IMS instruments commonly occurs at ambient pressure and thus, atmospheric pressure ionizations that have been used for IMS are shown in this section. The commonly deployed ion sources are radioactive sources, photoionization sources (photodischarge lamps and lasers), corona discharge (CD) sources and ESI sources.

3.2.1. Radioactive sources

Radioactive sources are preferred when using IMS due to their stability and reliability in operation. They do not need extra power source but special permits for a safety use are required which are difficult to obtain. The most widely used radioactive sources is based on nickel (^{63}Ni) although beta-emitting tritium (^{3}H) and alpha-emitting americium (^{241}Am) radioactive sources are also common. The ionization of samples comes from the electrons emitted from ^{63}Ni radioactive sources which produce ions and secondary electrons which collide with molecules of the supporting atmosphere inside the IMS such as N_2, H_2O or O_2 generating positive or negative ions. These ions are called reactant ions and produce a signal named as reactant ion peak (RIP). These ions are employed to ionize substances before being introduced into the drift tube. The identity of these ions is $H^+(H_2O)_n$, called hydrated proton, in positive polarity and $O_2^-(H_2O)_n$ in negative polarity. These reactant ions transfer their charge to sample

molecules (M) with greater proton affinity (in positive mode) or electronegativity (in negative mode) than them to generate ions. When reactant ions are exhausted, the upper limit of ionization is reached [39]. The ions generated apart from collision of reactant ions and M are named product ions which are stabilized through the displacement of water molecules as shown in *equation (7)* in positive mode:

$$M + H^+(H_2O)_n \rightleftharpoons MH^+(H_2O)_{n-x} + x\,H_2O \quad (7)$$

Sample + Hydrated proton→ Protonated monomer + Water

Levels of moisture and temperature govern the magnitude of n and proton-bound dimers (M_2H^+) may be formed with increased [M] as shown in *equation (8)*:

$$MH^+(H_2O)_n + M \rightleftharpoons M_2H^+(H_2O)_{n-x} + x\,H_2O \quad (8)$$

Protonated monomer + Sample→ Proton-bound dimer + Water

Ion peaks for proton-bound trimers or higher clusters are seldom observed in mobility spectra. However, this kind of product ions were observed in results of **chapter I** of this Doctoral Thesis [40].

Separately, the formation of product ions in negative ionization mode is shown in *equation (9)*:

$$M + O_2^-(H_2O)_n \rightleftharpoons MO_2^-(H_2O)_{n-x} + x\,H_2O \quad (9)$$

Sample + Negative reactant ion→ Protonated monomer + Water

3.2.2. Photoionization sources

The photoionization of neutral molecules in air at ambient pressure can be carried out by using photodischarge lamps and lasers. Since the ionization mechanism of the samples depends on the type of ionization source, when the ionization is based on photodischarge lamp a charge transfer does not take place

as it happens with radioactive sources. In this case, positive ions are formed apart from photons emitted from the electrical excitation of gases filled in the lamp [41] as shown in reaction of *equation (10)*:

$$h \cdot \nu + M \rightarrow M^{+} + e^{-} \tag{10}$$

where $h \cdot \nu$ is the photon energy and M is the neutral molecule. The energy of commercial photodischage lamps are 9.5, 10.2, 10.6 (UV), and 11.7 eV. The main advantage of photodischarge sources is the selectivity provided when an appropriate ionization energy or wavelength is selected. However, these lamps require for an external power supply and they should be replaced periodically due to their finite lifetimes.

Separately, lasers could be used to produce a photoionization of samples in the range of ultraviolet to infrared wavelengths. However, only a handful of studies have implemented ionization of sample by using lasers with IMS [42].

3.2.3. Corona discharge sources

Basically, the parts which form CD sources are a sharp needle or thin wire and a metal plate or discharge electrode. They should be separated between 2 and 8 mm and with a voltage difference of 1 to 3 kV. In the gap between these two parts, an electric discharge generates the formation of ions similar to those formed for ^{63}Ni radioactive source. These ions promote the consequent IMS ion-generating reactions of samples. Different designs of CD sources have been developed for IMS [43-46]. One disadvantage of this ionization source is that, in negative mode, ions generated from nitrogen as buffer gas are interfered by substances like oxygen or ozone with a high electronegativity. To overcome this issue, an increasing on the distance between the electrodes [47] and reversing the airflow past the corona needle [43] have been carried out. This kind of source has the value of simplicity, high ion currents, no radioactivity and some application as the possibility of the direct analysis of liquid samples. However the corrosion

of the needle causes instability which together with the formation of corrosive vapors (NO_x and ozone) involves intensive maintenance of the source. Also, an external power supply is needed.

3.2.4. Electrospray sources

Electrospray is an aerosol generated apart from the droplets of liquid samples. The aerosol is formed between a needle tip and a grid or plate which are included in a ESI source, being the former under a high potential. The liquid effluent passes through the needle tip and the charged droplets are evaporated, leaving gas-phase ions. If an analyte is dissolved in the effluent, it will receive some of this charge and become a gas-phase ion [48]. Two mechanisms have been proposed for ion formation in ESI: the ion evaporation model [49] and the charged radius model [50]. Several innovative ion sources that are based on ESI were developed, including secondary electrospray ionization (SESI) [51], DESI [52] and nanoelectrospray ionization (nESI) [53]. Some of the advantages of ESI sources are that they can be used as SIS and ionization source for liquid samples in only one step. Also, molecular information is not lost during the ionization since it is a soft process. There are limitation for the analytical applicability of ESI source with IMS since memory effects implies long rinsing times between samples.

3.2.5. Other ionization sources

Other ionization sources have been also employed with IMS technology. However, they are less common than the previouly described sources. Some of these ionization sources are MALDI [54], surface ionization sources [55], flames [56], plasma-based ion sources [57] or glow discharge ion sources [58].

One of the most important source is MALDI. This is a laser-based source suitable to analyse solid samples. In this case, samples are placed on a crystal matrix which absorbs the majority of the laser energy. The analyte molecules

receive part of the energy and they are ionized and desorbed without any or little fragmentation.

As summary, different ionization sources have been described which are compatible with IMS to ionize samples at atmospheric pressure and generate ions which could be introduced into the drift tube of the IMS. Some of the sources are universal while others have limitation with respect to types of samples or compounds and prices. Therefore, the selection of the ionization source demands the understanding of the sample and the compatibility of matrix with the configuration. Different ionization sources has been employed along this Doctoral Thesis. Mostly, radioactive ionization sources such as ^{63}Ni in **chapters II, III and IV**, and ^{3}H in **chapters I, VII, VIII and IX** were used. UV lamp was employed as ionization source in **chapters V and IX**.

3.2.6. Effect of dopants on ionization

Dopants are substances which influence the ion–molecule chemistry in sample ionization region as well as change conditions for the drift of ions. When the carrier or drift gas contains a dopant, the reactant ions are modified through reaction with this dopant. This new reactant ions are named alternative reactant ions. Improved selectivity and sensitivity of detection can be obtained by the use of dopants. For instance, the alternative reactant ions could react with the analyte but not with an interference. Also, drift times of product ions generated when using dopants can vary from using a clean gas and it could avoid the overlap of peaks. Moreover, product ions created with alternative ions can be more stable. The most commonly used dopants are acetone and ammonia for positive mode and chloride for negative mode IMS [59]. The use of dopants was applied in the **chapter IV** of this Doctoral Thesis. In that case, dichloromethane was selected as dopant and the RIP was $Cl^-(H_2O)_n$ instead of $O_2^-(H_2O)_n$ in negative ionization mode.

3.3. Drift tube

Once samples are ionized, the separation of ions is carried out at ambient pressure under an electric field in the drift tube. Normally, an ion gate or ion shutter is included before this drift region. They are made of wire grids, or etched metal analogs and mediate the entrance of ions to drift region. Ions pass when a brief pulse (between 10 and 1000 μs) is applied which is named as grid pulse width. This parameter influences on peak shape and width in mobility spectra. A high grid pulse width value produces an increase in the sensibility of the measurements at the expense of resolution [60].

Meanwhile, drift tubes consist of drift rings stacked or arranged alternately with insulating rings in a tubular geometry connected by a resistor chain. The construction of drift tubes is expensive and laborious since the assembly of pieces should be accurate. An electric field is established using a voltage divider to separate ions between the ion shutter and the detector. The separation of ions is based on their size and shape while collide with the particles of the drift gas flow, which flows counter-current with the sample flow. Smaller ions move faster than larger ions through the drift tube to the detector.

The critical parameters which affect IMS separations in the drift tube are temperature, purity and composition of the supporting gas atmosphere, electric field and drift tube length. Firstly, drift temperature influences on the mobility of ions according to *equation (6)*. Also, the drift temperature affects the degree of clustering of ions. At low temperature neutral water molecules of sample and drift gas are available to attach to ions in gas phase in the drift region which influences sensitivity, resolving power and mobility of ions. In this case, the mobility of ions is lower. Conversely, increasing the drift tube temperature causes decluster ions of water which means small variations in moisture and then, the changes on ion mobility are minimized. Also, the mobility of ions is higher when increasing drift tube temperature. However, working at a high temperature is expensive in relation with power and could produce reactivity or fragmentation of ions [61]. Other important parameter is the purity and composition of carrier and

drift gases. The carrier gas in the drift tube is used to transport sample molecules from the inlet into the reaction region and provide the supporting atmosphere for ionization to occur. The drift gas is intended to maintain a clean gas environment in the drift region, free of unwanted impurities. In relation with purity, if ambient air is used as carrier or drift gas it should be passed over a molecular sieve filter to remove moisture or reduce its content as well as that of other vapour impurities that may be present to avoid undesirable reaction in IMS devices. In fact, pure air is the most commonly used gas but the same precautions should be taken with other gases such as nitrogen, helium and so on. With respect to composition of carrier and drift gases, the accuracy of ion mobility measurements should not be affected when nitrogen or synthetic pure air are used as drift gases bases on the general conclusion of two separate works by Gunzer [62] and Kirk [63]. They concluded that no significant differences are likely for most compounds between mobility values in nitrogen and air, taking into account the polarizability constants and masses of N_2 and O_2 along with their corresponding abundances in air. Separately, other gases such as CO_2 provide unique ion mobility separation patterns relative to its higher polarizability in comparison with N_2 or air [64]. Also, the field strength applied in the drift region influences on the separation of ions into the drift tube since increasing in this parameter improves resolving power [65]. Finally, resolution can be improved using an IMS analyzer with a longer drift tube. It has been confirmed that there are fewer cluster formation and fragmentation reactions when a longer drift tube is used. It was demonstrated using benzene, toluene, and m-xylene as model analytes. For this reason, the peaks obtained in the spectrum are narrower and the resolution improves. [66].

3.4. Detector

After the separation of ions in the drift region, they are usually detected at ambient pressure in a Faraday plate. The Faraday plate is a simple flat-plate design which can be easily interfaced to an IMS. In this module, ions which

impinge on the detector are converted into current by neutralization on a collector electrode where ions are collected. The amplified ion current versus time results in ion mobility spectrum of a measurement [5]. Some authors have chosen MS as a detector coupled after IMS devices since it has the possibility of affording an additional qualitative information which faraday plate does not provide [67].

4. Types of IMS instruments

There are different types of IMS instruments. A scheme of the main types of IMS devices is shown in Figure 4.

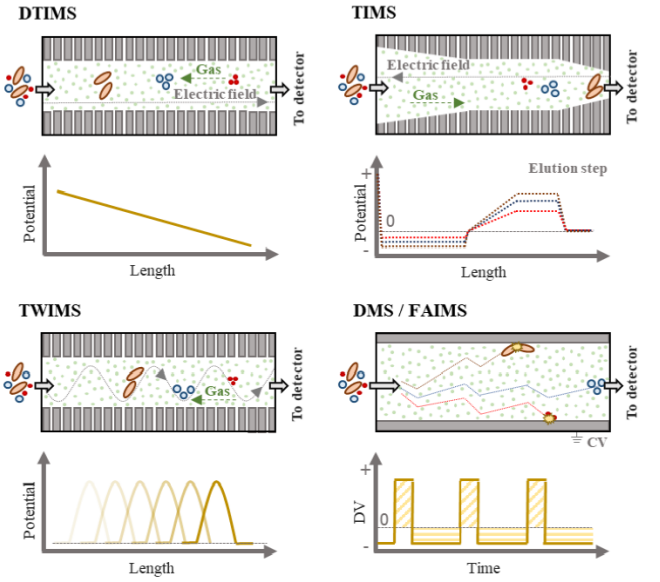

Figure 4. Scheme of the main types of IMS instruments (From M. Hernández-Mesa, D. Ropartz, A.M. García-Campaña, Hélène Rogniaux, G. Dervilly-Pinel, B. Le Bizec, 2019. Ion Mobility Spectrometry in Food Analysis: Principles, Current Applications and Future Trends. Molecules. 24, 2706.).

Apart from the classical configuration of drift time (DTIMS), the most common types of IMS instruments are travelling-wave IMS (TWIMS), which is also a time-dispersive version as DTIMS; high field asymmetric waveform IMS (FAIMS), as a space-dispersive IMS; and trapped IMS (TIMS) which is a trapping IMS model. Other types of IMS instruments are: open loop IMS (OLIMS), differential mobility analyzers (DMA), transversal modulation IMS (TMIMS) and overtone mobility spectrometers (OMS) [68]. In this section, a summary of the main IMS instruments was carried out.

4.1. Linear ion mobility spectrometer (DTIMS)

The linear ion mobility spectrometer named as DTIMS is the traditional configuration of IMS in which ions travel under a homogeneous and continuous electric field in the drift tube filled with neutral gas molecules. CCS measurements can only be carried out with IMS devices that operate at low electric fields, as is the case of DTIMS, because the K value is independent of the electric field under this condition (<1000 $V \cdot cm^{-1}$). K becomes dependent of the reduced field strength (E/N) at high electric fields (E/N > 4–10 Townsends (Td); 1 Td = 10–21 $V \cdot m^2$) and *equation (6)* cannot be applied [69]. In this Doctoral Thesis, all the stand-alone IMS devices used were DTIMS.

4.2. Travelling-Wave ion mobility spectrometer (TWIMS)

TWIMS consists on a drift tube with a stacked-ring ion guide connected in opposite phase of a radiofrequency field to produce a radially confined potential well [70]. The movement of ions is produced by applying a voltage pulse on one or two rings and then the pulse is transported to a neighbour ring and relaxed. This pattern is propagated at a 300-1300 m/s and the separation of ions is due to the control of velocity or pulse (or wave), the height of the pulse and gas pressure [5]. This device was released commercially by Waters Corporation as the Synapt™ high-definition MS (HDMS) system, including three TW-enabled

stacked-ring ion guides in combination with a quadrupole-orthogonal acceleration-time of flight (TOF) mass analyzer [71]. In fact, TWIMS devices are not stand-alone instruments since they are always hyphenated with a mass spectrometer. The TWIMS devices operate below the low-field limit as DTIMS.

4.3. High Field Asymmetric Waveform ion mobility spectrometer (FAIMS)

FAIMS instruments work under high electric fields (>7500 V cm^{-1}) taking advantages of that. This types of IMS were created because, at normal conditions, a high voltage of 200 kV would be needed if working with a DTIMS of 10 cm long drift region at a high electric field of 20000 V cm^{-1}. Then, the use of that high voltage was avoided using asymmetric waveforms and parallel plates, for the planar version of this type of IMS named as differential mobility spectrometry (DMS), or cylinders [72]. In the cylindrical version, called FAIMS, sample molecules are ionized and pass with the gas flow between two concentric tubes (the inner and outer electrodes). The asymmetric electric field is applied between these inner and outer electrodes. While DMS devices consist of two flat parallel electrodes separated by a gap through which ions are transported by a gas flow perpendicular to the electric field. As mentioned previously, FAIMS is a space-dispersive IMS since ion mobility spectrum is represented as intensity vs. the sweeping compensation voltage or compensation field instead of drift time as is the case of DTIMS and TWIMS [68]. FAIMS are shutter-free designs with continuous flow of ions from the source to the mobility region allowing continuous and real-time monitoring of samples which is the main advantage of these designs. Both stand-alone or coupled to MS or other IMS devices are available [5].

4.4. Trapped ion mobility spectrometer (TIMS)

TIMS is based on the use of a non-uniform electric field to hold ions stationary against a moving gas. A weak electric field increases along the axial section while a radiofrequency applied to the electrodes confines the ions radially. The separation of ions is based on trapping of ion packages in regions where the drift force is compensated by the electric field force depending on their size-to charge ratio. Later, the electric field is decreased, and ions packages elute from high to small size-to-charge ratios. Drift gas velocity, the ion confinement and the electric field ramp speed are the main parameters which influence the movement of ions [68]. The main characteristics of the IMS described in this section were shown in Table 2.

Table 2. Summary of characteristics of the main IMS instruments used.

Parameters	DTIMS	TWIMS	FAIMS or DMS	TIMS
Electric Field	Uniform and low	Moving, non-uniform and low	Alternating asymmetric and high/low	Radiofrequency and low
Pressure	Ambient (1 bar)	0.025-3 mbar	Ambient (1 bar)	2.6-3.4 mbar
Kind of separation	Time-dispersive	Time-dispersive	Space-dispersive	trapping
Hyphenated techniques	MCC*-IMS, GC-IMS, IMS-MS, GC-IMS-MS, LC-IMS-MS	TWIMS-MS	GC-FAIMS, FAIMS-MS, ESI-FAIMS, pyrolysis-FAIMS	TIMS-MS
Temperature	Ambient (300 K)	360 K	Ambient (300 K)	Ambient (300 K)

* MCC: Multi-capillary column

5. IMS Couplings

Despite stand-alone IMS instruments have been used in a wide range of applications, as it will be reviewed in section 8 of this introduction, sometimes the ion mobility alone is likely not sufficient for the identification of each analyte when complex mixtures are analysed due to the low resolution power of IMS devices. Therefore, hyphenated techniques are employed to overcome this problem.

5.1. Pre-separation prior IMS

Pre-separation in the liquid and gas phases can be carried out prior IMS analyzers. While LC [73, 74] has been used for the former, the most commonly employed are both GC [61, 75] and MCC [76, 77] for the latter. Firstly, using a pre-separation step can decrease the competitive ionization effects in the IMS devices since analytes enter into the ionization region sequentially. This means an improvement in the sensitivity of the methods. Also, a dual separation takes place which allows the separation of some compounds in the pre-separation step although the resolving power of the IMS was not sufficient. Therefore, more selective methods can be obtained when using a separation technique coupled to IMS. Moreover, an easier identification of compounds is possible since an additional qualitative parameter is obtained which is retention time of compounds in the chromatographic column. Nevertheless, while an IMS measurement alone is conducted in milliseconds, longer methods have to be developed if a pre-separation is included, which could take between a few minutes to several hours.

5.2. IMS-MS

MS is a well-implemented technology in analytical chemistry which is based on measuring the mass-to-charge ratio (m/z) of a molecular ion, which is

an inherited property of molecules. Meanwhile, size-to-charge ratios of ions are measured in IMS. Hybrid ion mobility-mass spectrometry (IM-MS) instruments provide new opportunities to extend the current boundaries of targeted and non-targeted analyses [78]. This coupling allows the separation of isobaric (isotopes of different elements in the same *m/z*) and isomeric molecules in the IMS and MS provides valuable information about the mass of ions to identify those compounds [79, 80]. This development has improved the selectivity and identification capacity of stand-alone IMS or MS when analysing complex matrices since and additional parameter is added when they are combined [81]. The first IM-MS analyzer was described in the 1960's [82]. Since then, IMS has been coupled with many kinds of mass analyzers such as TOF, quadrupole, ion-trap, ion-cyclotron, or magnetic-sector mass spectrometers [83]. Given that ions are separated in millisecond in IMS instruments and it is slower than microsecond scale of MS to obtain a mass spectrum, several mass spectra can be measured for each ion mobility peak. This fact enables an easy IM-MS coupling. However, a negative aspect is that MS instruments work at vacuum condition and then IM-MS instruments are more expensive and difficult to maintain than stand-alone IMS devices [84].

5.3. Multiple hyphenated methods

The combination of IMS devices with other IMS instruments is inexpensive and simple in comparison with MS spectrometers. These couplings are named tandem IMS. Tandem methods have usually a higher sensitivity due to larger signal to noise ratio are obtained. Although they imply a loss in the signal intensity, a more substantially loss in noise over baseline occurs [5]. Basically, the functioning of tandem IMS instruments is based on the entering of ions generated into the ionization source through a first shutter into a drift region where ions are separated according to their mobility. Later, some selected ions cross a second shutter located at the end of the first drift region. Ions are selected by synchronization of dual ion shutters through the control of the delay between

both shutters. Then, only a portion of drift time can pass to the second drift region, so the isolation of ions is achieved in this second region. Additionally, selective reactions, or fragmentation of ions using a strong electric field could happen in this second drift region. For all these reasons, an additional selectivity in response would arise from chemical isolation, transformation in a reactive region, and characterization in a second mobility stage of ion products from the transformation [85]. Two tandem IMS with reactive stage were employed in the **chapters II and IV** of this Doctoral Thesis. As an example, a scheme of a tandem IMS drift tube equipped with two ion shutters and a reactive stage is shown in Figure 5. Furthermore, 2D/3D tandem IMS devices have been coupled to MS (2D: IMS-IMS-MS; 3D: IMS-IMS-IMS-MS) [86, 87].

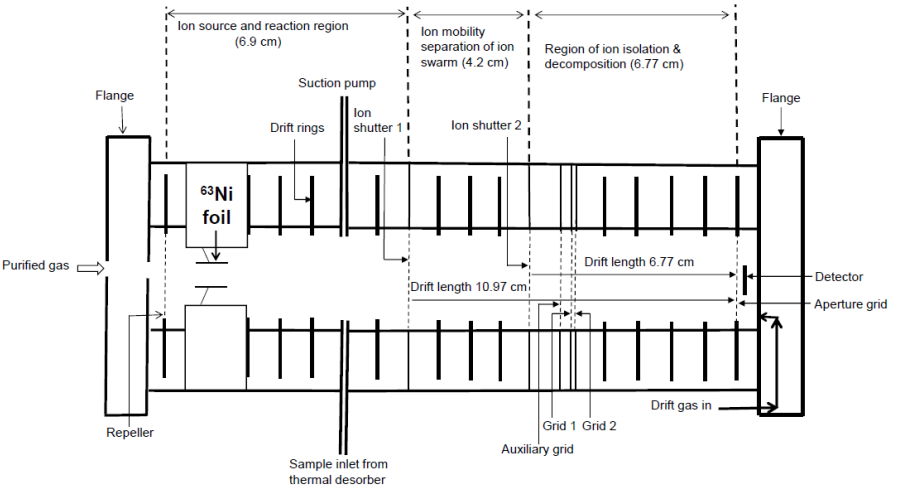

Figure 5. Scheme of a tandem IMS drift tube equipped with two ion shutters and a reactive stage (From U. Chiluwal, G. Lee, M.Y. Rajapakse, T. Willy, S. Lukow, H. Schmidt, G.A. Eiceman, Tandem ion mobility spectrometry at ambient pressure and field decomposition of mobility selected ions of explosives and interferences, Analyst 144 (2019) 2052–2061. With permission).

Additionally, combinations of pre-separation (LC, GC or MCC) with tandem IMS [88] or IMS-MS have been explored [89, 90]. A GC prior tandem IMS with reactive stage was employed in the **chapter II** of this Doctoral Thesis.

For GC/MCC/LC coupled to IMS-MS, the different separation time of each module which composes the single instrument should be firstly considered to develop these multiple hyphenated instruments. While chromatographic separation can take between minutes to hours, IMS and MS take millisecond and microsecond, respectively. Secondly, the MS module operate at significantly lower pressures than IMS. This creates a challenge of significantly different pressure zones in ion path. The commercial LC-TWIMS-TOF named as Synapt G2 instrument (from Waters) and LC-IMS-MS in general have been widely explored in proteomics [91, 92].

6. Current limitations and challenges of IMS analysis

This section summarizes some of the concepts that have been discussed throughout the introduction of this Doctoral Thesis. Moreover, new concepts in the context of improving the sensitivity, selectivity, identification and quantification of compounds using IMS are introduced.

6.1. Sensitivity and quantification

Sensitivity of IMS analyzers is not normally an analytical property which limits applications of this technology. However, sensitivity can be enhanced by selecting a suitable ionization source and/or SIS or by using a preconcentration step prior IMS when low limit of detection and quantification are required.

Also, charge and exchange reactions and competitive ionization which happen in IMS analyzers yield in narrow quantification dynamic ranges. If more of one chemical enters in the ionization chamber simultaneously, the competition

for charge available or any kind of ionization reinforces the problem of the narrow dynamic response of IMS. This problem is largely mitigated using a GC, MCC or LC column prior IMS measurement.

6.1.1. SIS and ionization source

The suitability of an ionization source depends on the type of sample and analyte studied. CD and ^{63}Ni ionization sources are more sensitive for halogenated compound detection while UV photoionization lamps are more indicated for aromatics compounds. Also, ^{3}H source is highly recommended to determine compounds with a high proton affinity in positive mode [5]. Moreover, SIS can positively influence on sensitivity of the methods as it is the case of TD which permit the detection of semivolatile analytes. This strategy was used in this Doctoral Thesis in **chapters III and IV** to determine cannabinoids and an explosive compound, respectively, with a relatively high boiling point. Also, ESI or laser-based SISs are more appropriated for the determination of analytes in aqueous or solid samples, respectively.

6.1.2. Extraction techniques

The use of an extraction technique can reduce the final volume of sample before their analysis by IMS which means an enhancement of sensitivity of the developed analytical methods. Conventional and novel smart materials in the pretreatment and preconcentration of samples previous to IMS determinations can be used for the analysis of complex samples such as biological fluids, food, or environmental samples [93].

Some conventional extraction techniques commonly employed with IMS are dispersive liquid-liquid microextraction (DLLME), solid phase extraction (SPE), SPME and SBSE. DLLME has been used to determine pesticide residues [94]or food contaminants [95] and variants of this technique such as liquid phase

microextraction (LPME) for the analysis of drugs in saliva [96], and hollow fibre liquid phase microextraction (HFLPME) for the analysis of pesticide residues in vegetables [97] or therapeutic drugs in urine and plasma [98] have been employed to improve sensitivity of IMS methods. Moreover, SPE has been used to detect traces of dichlorodiphenyl trichloroethane and its metabolites from water samples [99], and cocaine from urine samples [100] or cocaine and ecgonine methyl ester from oral fluids [101]. SPME has widely been used for the determination of dichlorvos traces in tea drinks [102], chemical warfare agents and simulants in water [103], ephedrine in urine [104], parabens in pharmaceutical formulations [105], methyl tert-butyl ether in water [106], and BTEX, naphthalene, chlorinated alkenes and chlorinated benzenes in water [107]. Other extraction formats, such as SBSE and microextraction in packed syringe (MEPS) were employed for the analysis of trace levels of organic compounds [108, 109].

Separately, smart materials are defined as those that respond to an external stimulus in a specific way. These materials incorporate unexpected advantages from the sensibility, selectivity or practical aspects of analytical determination. Smart materials such as immunosorbents, aptamers, molecularly imprinted polymers (MIPs), ionic liquids (ILs) and nanomaterial have been used with IMS [93].

6.2. Selectivity and identification

One of the main limitations of IMS instruments is their low selectivity due to their low resolving power. Also, the identification of analytes represents a challenge due to the presence of several ions generated from the same neutral compound, or additional intermediate products depending on its concentration in the sample. The selectivity of IMS methods can be improved through different ways. Firstly, choosing a suitable ionization source could suppress the ionization of interferences and/or favor the ionization of the analyte, as mentioned in section 6.1.1 of this introduction. Also, the use of a proper polarity mode of work

is an option since some interference can be avoided. In general, compounds with high electronegativities, such as explosives, are better detected as negative ions, whereas electropositive compounds such as drugs and other amines respond well as positive ions. Moreover, the selective extraction of compounds prior the IMS can be carried out following the extraction techniques mentioned in section 6.1.2 of this introduction. Furthermore, the selection of a proper electric field value and drift tube length can improve selectivity as mentioned in section 3.3 of this introduction. A higher electric field yields in a higher resolving power [65] while a longer drift tube could produce narrower peaks [66]. Additionally, the use of dopants, as explained in section 3.2.6 of this introduction, can positively influence on selectivity of IMS methods.

In addition, the employment of a pre-separation step (LC, GC or MCC) enhances both the selectivity and the identification capability of signal of real samples when using IMS as detector. The dual separation can avoid the overlapping of signals and an additional identification parameter is obtained, the retention time (see section 5.1 of this introduction). Moreover, the coupling of a MS analyzer after the IMS helps to identify compounds providing *m/z* information of ions (see section 5.2 of this introduction) or even through the fragmentation of ions by using a tandem MS/MS. A scheme of the information provided when using all the mentioned modules is shown in Figure 6.

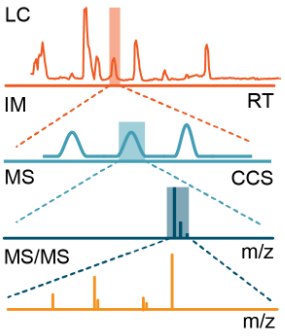

Figure 6. Scheme of information provided when using LC-IMS-MS/MS.

Tandem IMS with a reactive stage, which produces fragmentation of ions generated by IMS (see section 5.3 of this introduction), can also improve the selectivity and identification capability as it was demonstrated in **chapter II** of this Doctoral Thesis for the identification of acetates, alcohols, ketones, aldehydes and ethers; and in **chapter IV** to determine an explosive.

7. Data treatment of IMS data

Chemometrics is the discipline concerned with the application of statistical and mathematical methods to chemistry. This discipline has been fundamental for the development of application of IMS. Data treatment approaches employed in IMS are designed according to the selected strategy, being slightly different between targeted and untargeted analysis. Recent advances in multidimensional coupling of IMS to chromatography and MS has created challenges for data processing, yielding high-dimensional datasets. Data between 1 and 5 dimensions can be obtained depending on the employed analytical technique as described in Table 3.

Table 3. Data dimensionality obtained with IMS combined with different analytical techniques.

Analytical technique	Data dimensionality
IMS	1
Chromatography with IMS	2
IMS with MS	2
Chromatography with IMS and MS	3
2D Chromatography with IMS and MS	4
2D Chromatography with IMS and tandem MS	5

Normally, data analysis is divided in two steps: data pre-processing and pattern recognition or statistical analysis. The first step is usually time-consuming and crucial to be successful. A general workflow of IMS data analysis is shown in Figure 7. Noted that peak picking applies only to targeted analysis and RIP detailing when radioactive source are used.

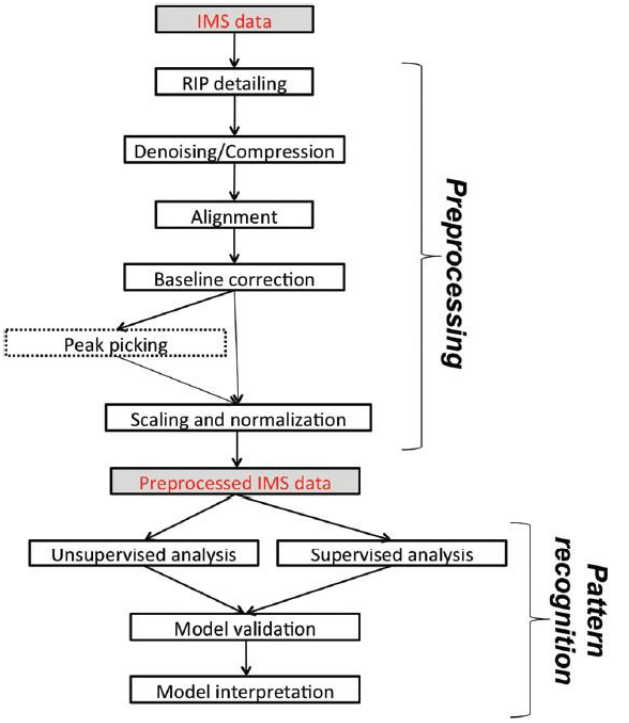

Figure 7. General workflow of IMS data analysis (From E. Szymańska, A.N. Davies, L.M.C. Buydens, Chemometrics for ion mobility spectrometry data: recent advances and future prospects, Analyst 141 (2016) 5689–5708).

The main alternatives to pre-process and analyse the most common IMS data, 1D (IMS) and 2D (chromatography with IMS) are mentioned below [110].

7.1. Data pretreatment

Data pretreatment is the first step of the workflow that attempts to prepare raw data (those provided by the analytical instrument that are exclusive of its trademark) into clean data (universal format) for processing by suited softwares for statistical analysis. IMS data pretreatment encompasses several pre-processing steps which are crucial for data quality and interpretation of the results. The workflow depends on the analysis strategy, with differences between targeted and untargeted analysis.

7.1.1. Data pretreatment in targeted IMS analysis

This process is not easy due to low selectivity of IMS instruments and the dependence of ion mobility on environmental conditions. For 1D data, it mainly consists of obtaining the peak area corresponding to the target analytes through peak deconvolution techniques or chemometric calibration models to quantify a targeted group of analytes and qualitatively identify them. Firtsly, peak deconvolution techniques include simple to use interactive self-modelling mixture analysis (SIMPLISMA) and its recursive version (RSIMPLISMA) [111, 112] as well as multivariate curve resolution (MCR) with alternating least squares (ALS) [113]. Meanwhile, chemometric calibration models include partial least squares regression (PLSR), its modifications such as non-linear PLS [114, 115], neural networks (NN) [116] and tucker 3 models [115]. They separate overlapping peaks and predict the concentrations of an analyte of interest.

And later, transformation of these areas through data compression prior to statistical analysis is part of 1D data pretreatment. Wavelet transform is the most common compression and denoising method applied to IMS data. Wavelet transform is a mathematical transformation for hierarchically decomposing signals [117].

For the 2D IMS data, analyte peaks are composed of several points grouped in circle or oval shaped spots depending on the instrument setup. The pre-processing of 2D data (chromatography with IMS) is different from 1D data.

The whole process could be divided into different steps:

- peak picking: this step can be carried out manually but automated strategies such as merged peak cluster localization (MPCL), growing interval merging, wavelet-based multiscale peak detection, watershed transformation (WST) and peak model estimation (PME) can be used [118, 119].

- RIP detailing: It is usual to find a signal on the right side of the RIP which is named RIP tailing. This signal is considered as an undesired disturbance. Then some methods are developed to remove or minimize RIP tailing. The simplest and most common strategy is data cropping to exclude a part of the data which contains the RIP tail [120]. However, it could produce a loss of information. Other option is the curve fitting to substract the tail signal [121].

- denoising and compression: This step is applied to enhance the signal to noise ration of IMS data which helps when low intensity signals are obtained. The main alternatives of denoising are Savitzky–Golay and wavelets. Additionally, discarding certain frequencies of data during wavelet transformation imply the benefit of compressing the data [122, 123].

- baseline correction: the baseline correction looks for correcting the baseline drift which can be observed in both dimensions (drift and retention time). The common solution is to subtract a "blank IMS spectrum" from the analysed IMS spectra [124]. However, for 2D data, different smoothing techniques such as assymetric least squares (AsLS) [120], locally weighted scatterplot smoothing (LOWESS) [125] and top-hat filtering [126] are used.

- alignment: The alignment is carried out to correct the drift time changes due to variations in the temperature and pressure of the drift tube over time. Different method can be applied such as correction with K_o or its inverse ($1/K_o$) [122]. Moreover, a reference peak, e.g. internal standard or RIP, can be used in further correction [127]. Warping methods widely used for chromatographic data [128] such as correlation optimized warping and icoshift are also employed in the correction of drift time changes in IMS spectra [115]. Finally, linear regression is

other alternative [129].

- data scaling and normalization: This step strongly depends on both the aim of data analysis and chemometric techniques employed in statistical analysis [130]. In most cases data are mean-centered. Scaling such as autoscaling or range scaling are commonly used [120, 131] and more rarely logarithmic transformations [132]. Separately, data can be normalized by the RIP peak intensity, the maximum intensity, or internal standards peak intensities.

7.1.2. Data pretreatment in untargeted IMS analysis.

IMS spectra could also be used directly as unique chemical fingerprints. For 1D data, pre-processing usually consists of steps described previously for data pretreatment of targeted 2D IMS data (RIP detailing, denoising, compression, alignment, baseline correction, scaling and normalization). For pretreatment of untargeted 1D data, the main differences are related to the non-use of a chromatographic dimension in these steps. Depending on data and the aim of the data treatment, the order of these steps may vary.

For 2D data, several chemometric techniques used in pre-processing i.e. alignment, denoising, compression, baseline correction, region selection and a discriminant analysis have been also applied [122].

7.2. Statistical analysis

Different strategies can be used to carry out the statistical analysis of the pre-treated IMS data. The chosen alternative is widely influenced by their popularity in the application field. When the aim of the measurements is qualitative analysis, statistical procedures are usually employed to sample classification, discrimination and marker detection. Conversely, calibrations are commonly used when the purpose is a quantitative analysis. Also, two kinds of statistical techniques can be employed, univariate and multivariate ones.

Univariate techniques focus on one variable at a time, e.g. analysis of variance (ANOVA), while multivariate techniques analyse all variables simultaneously.

Generally, the pattern recognition procedure starts with an exploratory analysis carried out with unsupervised chemometric techniques. Later, supervised techniques, which employ information of samples such as their classes are applied. At the end, results are statistically validated to provide a correct interpretation [110]. Chemometric techniques used in the statistical analysis of IMS data are shortly described below.

7.2.1. Exploratory analysis by unsupervised analysis

Unsupervised learning refers to those methods for analysis of data without measured/defined outcome (response) or when the outcome measure is not of primary concern [133]. Unsupervised learning uses procedures that attempt to find the natural patterns to facilitate the understanding of the relationship between the samples and to highlight the variables that are responsible for these relationships. By providing means for visualization, unsupervised learning aids in the discovery of unknown but meaningful categories of samples or variables that naturally fall together [134]. The main unsupervised analyses are considered into two types: projection techniques such as principal component analysis (PCA) and self-organizing maps (SOMs); and partitional clustering techniques such as hierarchical cluster analysis (HCA) and multidimensional scaling (MDS). The formers allow to achieve a simpler representation of the original data that still preserves intrinsic information; and the latters are employed to group samples based on the IMS data [110]. The most widely used explorative analysis technique in IMS studies is PCA. PCA is an orthogonal transformation of multivariate data, first formulated by Pearson (1901), and mostly used for exploratory analysis by extracting and displaying systematic variations [133]. PCA attempts to describe the maximal variance of the data, being a very useful tool for displaying purposes as it provides a low-dimension projection of the data (*i.e.,* a window into the

original K-dimensional space) by transformation into a new coordinate system [134].

7.2.2. Classification by supervised multivariate analysis

Supervised learning uses labelled data to classify samples or objects according to an observed response that generally includes several variables [134]. This classification aims at producing general hypotheses based on samples identified by known labels corresponding to the existing classes. The list of supervised multivariate analysis used with IMS data included the partial least squares discriminant analysis (PLS-DA), sparse-PLS-DA, linear discriminant analysis (LDA), recursive supporting vector machine (r-SVM), random forests (RF), genetic algorithms (GA), *k*-nearest neighbor (KNN), principal component regression (PCR), PLSR and n-way-PLSR. LDA is the most popular classification technique for the IMS data. PLS-DA is commonly employed in metabolomics studies and in food screening. Regression techniques (PCR, PLSR and n-way-PLSR) are routinely used in food quality and safety, environmental and monitoring analyses [110].

7.2.3. Validation and interpretation

The validation of the data treatment procedure can be carried out through internal and/or external approaches. IMS dataset should be splitted in training set (used to train the classification or calibration model), a validation set (employed to optimize the model parameters (internal validation)) and an independent test set employed to assess the predictive power of the model (external validation). Currently, the most common validation methods are leave-one-out cross-validation, double cross-validation, bootstrapping and permutation tests [110]. Validation results can be expressed as number of misclassifications, accuracy, sensitivity, specificity, area under ROC curve (AUROC) and root mean square error of prediction (RMSEP) [135, 136]. When

this step is finished, the assessment of model findings is carried out depending on the application. In Table 4, the data pretreatment and statistical analysis methods mentioned along this section have been summarized.

Table 4. List of data pretreatment and statistical analysis methods applied over IMS data.

Step	Methods
Data pretreatment targeted analysis (1D data)	
Peak picking through peak deconvolution	SIMPLISMA, RSIMPLISMA and MCR with ALS
Peak picking through chemometric calibration models	PLS, non-linear PLS, NN and Tucker 3 models
Transformation of areas	Wavelet transform
Data pretreatment targeted (2D data) and untargeted analysis*	
Peak picking	MPCL, growing interval merging, wavelet-based multiscale peak detection, WST and PME
RIP detailing	Data cropping, curve fitting and subtraction of baseline
Denoising and compression	Savitzky–Golay and wavelets
Baseline correction	Subtract the blank, AsLS, LOWESS and top-hat filtering
Alignment	Correction with K_o, correction with RIP mobility, warping methods and linear regression
Data scaling	Autoscaling, range scaling and logaritmic transformations
Data normalization	Using RIP peak intensity and internal standard peak intensities
Statistical analysis of IMS data	
Unsupervised analysis	PCA, SOMs, HCA and MDS
Supervised analysis	PLS-DA, sparse-PLS-DA, LDA, r-SVM, RF, GA, KNN, PCR, PLSR and n-way-PLSR.

* For untargeted 1D data, the main differences is the non-use of a chromatography.

8. Applications

In general, a deeper knowledge and the enhancement of the available or novel analytical instrumentations is necessary for the growth of their potential. It allows to improve the performance characteristics of an analytical instrument and extending the boundaries of its applications. The IMS instrumentation has historically been applied for chemical measurements of warfare agents in military preparedness [137], explosives or illicit drugs in commercial aviation security [138] and in human spaceflight [139].

In recent years, the application areas of IMS technology have been expanded through the analysis of complex samples such as pharmaceutical, food, environmental, biological and medical samples. This is largely due to the development of hyphenated techniques which improve the analysis of real samples as mentioned in section 5 of the introduction of this Doctoral Thesis through the coupling of IMS with other IMS, MS and/or chromatography modules. These couplings enhance the selective identification of analytes since stand-alone IMS instruments will likely not be sufficient for this purpose. A summary of the publications related to IMS in different application fields until 2020 was included in Figure 8. Currently, explosives and drugs represent much of the interest in the use of IMS but this technology has also acquired a major role in areas focused on the analysis of environmental, biological or food samples (see Figure 8).

Much of this Doctoral Thesis has an applied character addressing both the most classic samples as drugs or explosives in **chapters III** and **IV**, respectively; and innovative ones such as environmental (**chapter V**) and food samples (**Block III**). Specifically, an entire Block is devoted to the analysis of olive oil samples and **chapter IX** is dedicated to the measure of olive and olive oils samples for their authentication.

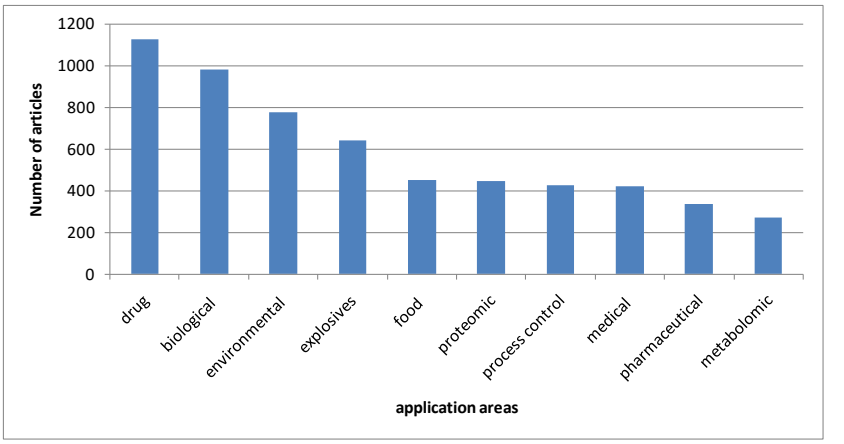

Figure 8. Summary of the number of articles concerning IMS categorized by field of application found on the database "ISI Web of Knowledge" (until May 2020).

8.1. Explosives and drugs

There is no doubt about that the application of IMS for the detection of explosives and drugs have been the objective of plenty of studies [140-143]. In the case of the detection of explosives, there are the need of rapid, efficient and reliable detectors to be used in acts of terrorism worldwide as it is the case of stand-alone IMS instruments. Moreover, the technology should be non-invasive since analysis should be carried out in control points, international borders and airports [5]. At the beginning, the emphasis of using IMS was on detecting volatile compounds such as ethylene glycol dinitrate (EGDN), nitroglycerine (NG), and trinitrotoluene (TNT), from the family of nitrated organic compounds. TNT is probably the optimum compound to be detected by IMS due to their physico-chemical properties [144] which implies that it is the most studied explosive in literature. Due to the need of safety in commercial flights, studies focused on the detection of compounds with lower vapor pressures such as RDX (cyclonite), PETN (pentaerythritol tetranitrate), HMX (octogen) and son on have been carried out. In the case of RDX, some difficulties have been found related to surface adsorption, thermal decomposition, and vapor pressures [103]. Also, it

was found that the detection of HMX requires high desorption temperatures due to its low vapor pressure [145]. Anyway, new challenges for explosives detection require improvements on sensitivity and reliability of IMS technology to expand the list of detectable explosive substances until new types of explosives different from nitrogenous compounds such as peroxide-based explosives (triacetone triperoxide or hexamethylene triperoxide diamine) or binary liquids [5]. In addition, improvements in sampling techniques have been proposed to determine explosives [141]. Also, it should be considered that the explosives based on nitro compounds have a high electronegativity and form stable negative ions at ambient pressure. For that, the ionization of explosives occurs by reactions in the negative polarity [85]. The type of ionization sources of the IMS instrument affects the sensitivity and/or identification ability of explosives. For example, ^{63}Ni source mainly produce O_2 reactant ions and corona discharge provides nitrite and nitrate ones which can react with the same explosive differently [146]. However, the low selectivity of the explosive determination when using IMS may suffer a considerable number of false positives. This is the reason of studies such as the included in **chapter IV** of this Doctoral Thesis, in which a tandem IMS with reactive stage was investigated to improve the selectivity of IMS to determine explosives.

Separately, the potential for detecting illicit drugs, especially heroin and cocaine, by IMS was recognized in the seventies [147]. Currently, the attention is also placed on the detection of recreational drugs like the amphetamines MDMA (3,4-methylenedioxy-methamphetamine) and other derivatives [5]. The use of IMS to detect illicit drugs can be carried out over material such as luggage, clothes and so on or over biological matrices, air, water, and seized materials [140]. However, the use of efficient extraction techniques and SIS is required due to the low vapor pressures of most of illicit drugs and the presence of interferences in complex samples. For example, liquid-liquid microextraction (LLME) have been used to detect MDMA [148] and MDPV [96] in oral fluids. Also, cocaine and its metabolites have been determined using SPE as sample preparation technique prior IMS in oral fluids [101] and urine [100].

Furthermore, SPME [149] and SBSE [150] are other extraction techniques explored in biological fluids to detect drugs before IMS analysis. Also, most of applications use TD at high temperature around 200 ºC as SIS. In this Doctoral Thesis, **chapter III** was dedicated to study drugs, concretely cannabinoids [151].

8.2. Enviromental applications

The unique characteristics of IMS instruments such as portability, low cost, speed and ruggedness are responsible for the selection of this technique for on-site, real-time environmental applications. However, the low selectivity of IMS devices against the complexity of environmental samples and the requirements of really low sensitivity values in this field cause the need of employing some of the strategies described in detail in sections 6.1 and 6.2 of the introduction of this Doctoral Thesis [152]. Mainly, environmental analysis using IMS are focused on the determination of contaminants in air, water and solid samples, such as soil and sediments, and aerosols [153].

Since IMS analysis needs the samples are in gaseous state, the determination of contaminants in air is the most direct situation since the volatilization of sample is not required. The on-site monitoring of volatile compounds from some process of ceramic industry was possible using a permeation setup with standard compounds [154]. Also, ammonia produced by companies that manufacture fertilizers was controlled in urban air [155]. UV-IMS devices have been widely used to detect aromatic compounds in air due to the high efficiency of this type of ionization with these analytes [156-158]. Specifically, a bipolar ionization to determine benzene, toluene, ethylbenzene and xilenes (BTEX) [156], a membrane setup to avoid humidity to determine BTX [157] and a Tenax TA column to improve selectivity for the determination of BT [158] prior UV-IMS have been explored.

Aqueous samples are the most common environmental samples analysed by IMS. Depending on their complexity, a cleaning, separation or

preconcentration steps can be required before the IMS analysis. Some examples of analytes determined in real aqueous environmental samples are the determination of methyl tert-butyl ether (MTBE) using a membrane for the extraction [159] or a HS-SPME system [160]; the determination of halogenated substances with membrane extraction [161], HS-SDME and GC [162], HS-SPME and MCC [107] and large-bore preseparation and ESI-IMS [163]; and the determination of pesticide residues such as atrazine and ametryn in water and soil samples using HS-SPME without GC separation [164]. The determination of typical pesticides of aqueous environmental samples using standards was carried out using TD-IMS for malathion, ethion and dichlorovos [165]; sevin, amitraz and metalaxyl [166]; and ethyl parathion and toluene 2,4-diisocyanate [167].

In solid environmental samples, the analysis of contaminants such as halogenated compounds in vadose soil zone was carried out with a special configuration of IMS device [168, 169]. Moreover, the determination of residues of a pesticide, malathion, in aerosol dust [170] and the study of the formation of aerosols from the interaction of volatile compounds with atmospheric oxidants using the oxidation of α-pinene as model [171] were carried out. In this context, in the **chapter V** of this Doctoral Thesis, an innovative coupling between SFE and UV-IMS using a Tenax TA column as interface, was employed to detect benzene and toluene in soil [27].

8.3. Food analysis

The number of applications focused on food analysis has increased exponentially in the last few years due to the commercialization of hyphenated IMS with MS and/or chromatography, especially for food safety and food authentication purposes. Most of the publication are focused on the determination of several known compounds through targeted or semi-targeted analysis. However, the increase of using non-targeted approaches is expected, such as in food fingerprinting [69]. A great variety of molecules, macronutrients and micronutrients, such as peptides, lipids, terpenes, polyphenols, etc [172-175]

and samples (flours, olive oil, mushrooms, ham, etc) [176-179] have been analysed using instruments based on IMS technology. Methods using stand-alone IMS instruments, which are usually portable and fast equipments, are employed for in situ analysis and real-monitoring such as the determination of histamine in tuna fish [180], trimethylamine in seafood [181] or off-flavor and contaminants generated during the processing or storage of food such as 2,4,6-trichloroanisole [182], and furfural and hydroxymethylfurfural toxicants [183]. Due to the low selectivity of IMS devices, these instruments coupled to chromatography and/or MS are widely employed in food science. Firstly, GC-IMS methods using HS as SIS are very common to study the volatile compounds of food for product discrimination according to their quality, origin, etc [75, 177, 184]. These devices have been employed for the authentication of matrices such oils [77, 185], meat products [179, 186], wines [187] and honey [188]. Also, GC-IMS is applied in the food safety field which covers the determination of a wide range of residues and contaminants. The analysis of pesticides in a great variety of vegetables (i.e., apples, tomatoes, cucumbers, etc), oils, animal feed, juices and water samples has been the most investigated topic [189]. However, GC-IM-MS is a more powerful configuration since it overcomes the current boundaries of GC–IMS approaches for food characterization and authentication [69]. Also, IMS included in LC-MS workflows is being successfully used to separate isobars and isomers [190]. Moreover, a higher number of compounds are detected by LC-IMS-MS in comparison to LC-MS. For example, drift time has been used to identify 100 pesticides in different vegetables and fruits by LC-TWIMS-TOF-MS [191]. Now, only one study has been reported about LC-IM-MS to study the metabolomic fingerprinting for food authentication [192]. In this Doctoral Thesis, a complete Block which includes **chapters VI, VII, VIII** and **IX** was dedicated to the analysis of olive oil samples and, only **chapter IX** was focused on measuring olive and olive oil samples for their authentication using GC-IMS and/or UV-IMS devices.

9. Conclusions and future trends

IMS is a vanguard analytical technique which provides the separation of ions in gaseous phase based on the differences of ion mobilities under an electric field. This permits a rapid, simple, low cost, robust and sensitive detection of volatile compounds at ambient conditions. The developments in IMS technology through a wide variety of configuration and studies to deepen the knowledge of it is reflected today, including commercial and research areas. This has led to the exponential growth of applications of IMS beyond its uses for monitoring explosive, illicit drug and chemical warfare. In recent years, the applied potential of IMS has extended its scope to the pharmaceutical, food, environmental, biological and medical fields. However, in some cases, some limitations related to sensitivity and selectivity of IMS for detection of target analytes in complex samples can be obtained. Some solutions to reduce these problems are to use a suitable ionization source/SIS and preconcentration methods prior IMS. Also, extraction techniques, polarity mode, the use of dopants and pre-separation of the constituents of the samples with a GC, MCC or LC coupled to IMS can enhance the IMS performance. Coupling IMS to MS is also advantageous because MS provides information about the mass of ions for a better identification while IMS has the capacity to differentiate isobaric and isomeric compounds using the CCS value. In addition, hyphenation of IMS instrument improved resolution. It has been seen that the utility of IMS in the agri-food field is starting to be exploited and that the key of success is the correct use of chemometrics to deal a complex and representative group of samples of the problem under study. The future of IMS technology continues to look encouraging and new developments in IMS instrumentation and applications are expected. Some of them should be based on the results obtained in the experimental work of this Doctoral Thesis.

References

[1] W.C. Rontgen, On a New Kind of Rays, Science 3 (1896) 227–231.

[2] M.P. Langevin, L'ionization des gaz, Ann. Chim. Phys. 7 (1903) 289–384.

[3] M.P. Langevin, Une formule fondamentale de théorie cinétique, Ann. Chim. Phys.

8 (1905) 245–288.

[4] F.W. Karasek, Plasma chromatography, Anal. Chem. 46 (1974) 710–720.

[5] G.A. Eiceman, Z. Karpas, H.H. Hill Jr, Ion Mobility Spectrometry, Third edition, CRC Press, United States, 2013.

[6] M. Valcárcel, S. Cárdenas, Vanguard-rearguard analytical strategies, TrAC Trend Anal. Chem. 24 (2005) 67–74.

[7] H.H. Hill, W.F. Siems, R.H. Louis, D.G. Mc Minn, Ion mobility spectrometry, Anal. Chem. 62 (1990) 1201–1209.

[8] R. Fernandez-Maestre, C.S. Harden, R.G. Ewing, C.L. Crawford, H.H. Hill Jr, Chemical standards in ion mobility spectrometry, Analyst 135 (2010) 1433–1442.

[9] M. Maurer, G.C. Donohoe, S.J. Valentine, Advances in ion mobility-mass spectrometry instrumentation and techniques for characterizing structural heterogeneity, Analyst 20 (2015) 6782–6798.

[10] Z. Karpas, Ion mobility spectrometry of aliphatic and aromatic amines, Anal. Chem. 61 (1989) 684–689.

[11] G.A. Eiceman, E.G. Nazarov, J.A. Stone, Chemical standards in ion mobility spectrometry, Anal. Chim. Acta 493 (2003) 185–194.

[12] B.C. Hauck, W.F. Siems, C.S. Harden, V.M. McHugh, H.H. Hill Jr, Determination of E/N influence on K0 values within the low field region of ion mobility spectrometry, J. Phys. Chem. A 121 (2017) 2274–2281.

[13] E.A. Mason, E.W. McDaniel, Transport properties of ions in gases, John Wiley & Sons Inc., New York, 1988.

[14] J.C. May, C.B. Morris, J.A. McLean, Ion mobility collision cross section compendium, Anal. Chem. 89 (2017) 1032–1044.

[15] W.F. Siems, L.A. Viehland, H.H. Hill, Improved Momentum-Transfer Theory for Ion Mobility. 1. Derivation of the Fundamental Equation, Anal. Chem. 84 (2012) 9782–9791.

[16] E.W. McDaniel, Collision Phenomena in Ionized Gases, Wiley, New York, 1964.

[17] J.A. Picache, B.S. Rose, A. Balinski, K.L. Leaptrot, S.D. Sherrod, J.C May, J.A. McLean, Collision cross section compendium to annotate and predict multi-omic compound identities, Chem. Sci. 10 (2019) 983–993.

[18] F.W. Karasek, The Plasma Chromatography, Res./Dev. 21 (1970), 34–37.

[19] G. Hoch, B. Kok, A mass spectrometer inlet system for sampling gases dissolved in liquid phases, Arch. Biochem. Biophys. 101 (1963) 160–170.

[20] J. Zhang, L.F. Li, D.P. Guo, Y. Zhang, Q. Wang, P. Li, X.Z. Wang, Determination of Hazardous Chemicals by Microchip-based Field Asymmetric Ion Mobility Spectrometric Technique, Chin. J. Anal. Chem. 41 (2013) 986–992.

[21] R. Garrido-Delgado, F. Mercader-Trejo, L. Arce, M. Valcárcel, Enhancing sensitivity and selectivity in the determination of aldehydes in olive oil by use of a Tenax TA trap coupled to a UV-ion mobility spectrometer, J. Chromatogr. A 1218 (2011) 7543–7549.

[22] F.W. Karasek, S.H. Kim, H.H. Hill, Mass identified mobility spectra of p-nitrophenol and reactant ions in plasma chromatography, Anal. Chem. 48 (1976) 1133–1137.

[23] J.M. Perr, K.G. Furton, J.R. Almirall, Solid phase microextraction ion mobility spectrometer interface for explosive and taggant detection, J. Sep. Sci. 28 (2005) 177–183.

[24] M.T. Jafari, M.R. Rezayat, M. Mossaddegh, Design and construction of an injection port for coupling stir-bar sorptive extraction with ion mobility spectrometry, Talanta 178 (2018) 369–376.

[25] S.P. Cram, S.N. Chesler, Coupling of high speed plasma chromatography with gas chromatography, J. Chromatogr. Sci. 11 (1973), 391–401.

[26] S. Rokushika, H. Hatano, H.H. Hill Jr, Ion mobility spectrometry after supercritical fluid chromatography, Anal. Chem. 59 (1987) 8–12.

[27] N. Jurado-Campos, A. Carpio, Z. Mohammed, L. Arce, N. Arroyo-Manzanares, Innovative coupling of supercritical fluid extraction with ion mobility spectrometry, Talanta 188 (2018) 637–643.

[28] M. Dole, C.V. Gupta, L.L. Mack, K. Nakamae, Application of the plasma chromatograph to polystyrene, American Chemical Society, Polymer Preprints, Division of Polymer Chemistry, 18 (1977) 188-193.

[29] H. Sukumar, J.A. Stone, T. Nishiyama, C. Yuan, G.A. Eiceman, Paper spray ionization with ion mobility spectrometry at ambient pressure, Int. J. Ion Mobil. Spectrom. 14 (2011) 51–59.

[30] H.H. Hill Jr, W.F. Siems, R.L. Eatherton, R.H. St. Lewis, M.A. Morrissay, C.B. Shumate, D.G. McMinn, Gas, supercritical fluid, and liquid chromatographic detection of trace organics by ion mobility spectrometry, in: R.E. Clement, K.W.M. Siu, H.H. Hill Jr (Eds), Instrumentation for Trace Organic Monitoring, Lewis, Chelsea, MI, 1991, pp. 49–64.

[31] R.B. Cody, J.A. Laramee, H.D. Durst, Versatile new ion source for the analysis of materials in open air under ambient conditions, Anal. Chem. 77 (2005) 2297–2302.

[32] Z. Takats, J.M. Wiseman, B. Gologan, R.G. Cooks, Mass spectrometry sampling under ambient conditions with desorption electrospray ionization, Science 306 (2004) 471–473.

[33] W.E. Steiner, B.H. Clowers, W.A. English, H.H. Hill Jr, Atmospheric pressure matrix-assisted laser desorption/ionization with analysis by ion mobility time-of-

flight mass spectrometry, Rapid Commun. Mass Spectrom. 18 (2004) 882–888.

[34] G.A. Harris, S. Graf, R. Knochenmuss, F.M. Fernandez, Coupling laser ablation/desorption electrospray ionization to atmospheric pressure drift tube ion mobility spectrometry for the screening of antimalarial drug quality, Analyst 137 (2012) 3039–4044.

[35] H. Borsdorf H, H. Schelhorn, J. Flachowsky, H.R. Doring, J. Stach, Corona discharge ion mobility spectrometry of aliphatic and aromatic hydrocarbons, Anal. Chim. Acta 403 (2000) 235–242.

[36] L. Arce L, M. Menéndez, R. Garrido-Delgado, M. Valcárcel, Sample-introduction systems coupled to ion-mobility spectrometry equipment for determining compounds present in gaseous, liquid and solid samples, Trac-Trend. Anal. Chem. 27 (2008) 139–150.

[37] Y. Seto, Determination of volatile substances in biological samples by headspace gas chromatography, J. Chromatogr. A 674 (1994) 25–62.

[38] S. Prasad, H. Schmidt, P. Lampen, M. Wang, R. Gueth, J.V. Rao, G.B. Smith, G.A. Eiceman, Analysis of bacterial strains with pyrolysis-gas chromatography/differential mobility spectrometry, Analyst 131 (2006) 1216–1225.

[39] C.S. Creaser, J.R. Griffiths, C.J. Bramwell, S. Noreen, C.A. Hill, C.L.P. Thomas, Ion mobility spectrometyr: a review. Part 1. Structural analysis by mobility measurement, Analyst 129 (2004) 984–994.

[40] N. Jurado-Campos, R. Garrido-Delgado, B. Martínez-Haya, G.A. Eiceman, L. Arce, Stability of proton-bound clusters of alkyl alcohols, aldehydes and ketones in Ion Mobility Spectrometry, Talanta 185 (2018) 299–308.

[41] J.N. Driscoll, Evaluation of a new photoionization detector for organic compounds, J. Chrom. A 134 (1977) 49–55.

[42] D.M. Lubman, M.N. Kronick, Plasma chromatography with laser-produced ions, Anal.Chem. 54 (1982) 1546–1551.

[43] A.J. Bell, S.K. Ross, Reverse flow continuous corona discharge ionization, Int. J. Ion Mobil. Spectrom. 5 (2002) 95–99.

[44] M. Tabrizchi, T. Khayamian, N. Taj, Design and optimization of a corona discharge ionization source for ion mobility spectrometry, Rev. Sci. Instrum. 7 (2000) 2321–2328.

[45] M. Tabrizchi, A. Abedi, A novel electron source for negative-ion mobility spectrometry, Int. J. Mass Spectrom. 218 (2002) 75–85.

[46] C.A Hill, C.L.P. Thomas, A pulsed corona discharge switchable high resolution ion mobility spectrometer-mass spectrometer, Analyst 128 (2003) 55–60.

[47] G.A. Eiceman, J.H. Kremer, A.P. Snyder, J.K. Tofferi, Quantitative assessment of a corona discharge ion source in atmospheric pressure ionization-mass spectrometry for ambient air monitoring, Int. J. Environ. Anal. Chem. 33 (1988) 161–183.

[48] C. Shumate, Electrospray Ion Mobility Spectrometry, Trac-Trend. Anal. Chem. 13 (1994) 104–109.

[49] P. Kebarle, L. Tang, From ions in solution to ions in the gas phase, Anal. Chem. 65 (1993) 972A–986A.

[50] J.V. Iribarne, B.A. Thomson, On the evaporation of small ions from charged droplets, J. Chem. Phys. 64 (1976) 2287–2294.

[51] Y.H. Chen, H.H. Hill Jr, D.P. Wittmer, Analytical merit of electrospray ion mobility spectrometry as a chromatographic detector, J. Microcol. Sep. 6 (1994) 515–524.

[52] C. Wu, W.F. Siems, H.H. Hill Jr, Secondary electrospray ionization ion mobility spectrometry - mass spectrometry of illicit drugs, Anal. Chem. 72 (2000) 396–403.

[53] Z. Takats, J.M. Wiseman, B. Gologan, R.G. Cooks, Mass spectrometry sampling under ambient conditions with desorption electrospray ionization, Science 306 (2004) 471–473.

[54] J.M. Koomen, B.T. Ruotolo, K.J. Gillig, J.A. Mclean, D.H. Russell, M.J. Kang, K.R. Dunbar, K. Fuhrer, M. Gonin, J.A. Schultz, Oligonucleotide analysis with MALDI-ion-mobility-TOFMS, Anal. Bioanal. Chem. 373 (2002) 612–617.

[55] C. Wu, H.H. Hill, U.K. Rasulev, E.G. Nazarov, Surface-ionization ion mobility spectrometry, Anal. Chem. 71 (1999) 273–278.

[56] H.C. Bolton, J. Grant, I.G. McWilliam, A.J.C. Nicholson, D.L. Swingler, Ionization in flames. II. Mass-spectrometric and mobility analyses for the flame ionization detector, Proc. R. Soc. London, A: Math. Phys. Eng. Sci. 360 (1978) 265–277.

[57] M.J. Waltman, P. Dwivedi, H.H. Hill, W.C. Blanchard, R.G. Ewing, Characterization of a distributed plasma ionization source (DPIS) for ion mobility spectrometry and mass spectrometry, Talanta 77 (2008) 249–255.

[58] Q. Zhao, M.W. Soyk, G.M. Schieffer, K. Fuhrer, M.M. Gonin, R.S. Houk, E.R. Badman, An ion trap-ion mobility-time of flight mass spectrometer with three ion sources for ion/ion reactions, J. Am. Soc. Mass Spectrom. 20 (2009) 1549–1561.

[59] J. Puton, M. Nousiainen, M. Sillanpää, Ion mobility spectrometers with doped gases, Talanta 76 (2008) 978–987.

[60] P.V. Johnson, L.W. Beegle, H.I. Kim, G.A. Eiceman, I. Kanik, Ion Mobility Spectrometry in Espace Exploration, Int. J. Mass Spectrom. 262 (2007) 1–15.

[61] A.B. Kanu, H.H. Hill Jr, Ion Mobility Spectrometry Detection for Gas

Chromatography, J. Chromatogr., A 1177 (2008) 12–27.

[62] F. Gunzer, 2016. Comparison of Experimental and Calculated Ion Mobilities of Small Molecules in Air. J. Anal. Methods Chem. 6246415.

[63] A.T. Kirk, C.R. Raddatz, S. Zimmermann, Separation of Isotopologues in Ultra-High-Resolution Ion Mobility Spectrometry, Anal. Chem. 89 (2017) 1509–1515.

[64] K.L. Davidson, M.F. Bush, Effects of Drift Gas Selection on the Ambient-Temperature, Ion Mobility Mass Spectrometry Analysis of Amino Acids, Anal. Chem. 89 (2017) 2017-2023.

[65] C. Wu, W.F. Siems, G.R. Asbury, H.H. Hill Jr, Electrospray ionization high-resolution ion mobility spectrometry-mass spectrometry, Anal. Chem. 70 (1998) 4929–4938.

[66] S. Sielemann, J.I. Baumbach, H. Schmidt, P. Pilzecker, Quantitative analysis of benzene, toluene, and m-xylene with the use of a UV-ion mobility spectrometer, Field Anal. Chem. Tech. 4 (2000) 157–169.

[67] D.C. Collins, M.L. Lee, Developments in Ion Mobility Spectrometry-mass Spectrometry, Anal. Bioanal. Chem. 372 (2002) 66–73.

[68] R. Cumeras, E. Figueras, C.E. Davis, J.I. Baumbach, I. Gràcia, Review on ion mobility spectrometry. Part 1: current instrumentation, Analyst 140 (2014) 1376-1390.

[69] M. Hernández-Mesa, D. Ropartz, A.M. García-Campaña, Hélène Rogniaux, G. Dervilly-Pinel, B. Le Bizec, 2019. Ion Mobility Spectrometry in Food Analysis: Principles, Current Applications and Future Trends. Molecules. 24, 2706.

[70] A.A. Shvartsburg, R.D. Smith, Fundamentals of traveling wave ion mobility spectrometry, Anal. Chem. 80 (2008) 9689–9699.

[71] S.D. Pringle, K. Giles, J.L. Wildgoose, J.P. Williams, S.E. Slade, K. Thalassinos, R.H. Bateman, M.T. Bowers, J.H. Scrivens, An investigation of the mobility separation of some peptide and protein ions using a new hybrid quadrupole/traveling wave IMS/oa-TOF instrument, Int. J. Mass Spectrom. 261 (2007) 1–12.

[72] I.A. Buryakov, E.V. Krylov, E.G. Nazarov, U.Kh. Rasulev, A new method of separation of multi-atomic ions by mobility at atmospheric pressure using a high-frequency amplitude-asymmetric strong electric field, Int. J. Mass Spectrom. Ion Proc. 128 (1993) 143–148.

[73] A.L. Rister, E.D. Dodds, 2020. Liquid chromatography-ion mobility spectrometry-mass spectrometry analysis of multiple classes of steroid hormone isomers in a mixture. J. Chromatogr. B. 1137, 121941.

[74] M. Fenclova, M. Stranska-Zachariasova, F. Benes, A. Novakova, P. Jonatova, V. Kren, L. Vitek, J. Hajslova, Liquid chromatography-drift tube ion mobility-mass spectrometry as a new challenging tool for the separation and characterization of

silymarin flavonolignans, Anal. Bioanal. Chem. 412 (2020) 819–832.

[75] M.D. Contreras, N. Jurado-Campos, L. Arce, N. Arroyo-Manzanares, A robustness study of calibration models for olive oil classification: targeted and non-targeted fingerprint approaches based on GC–IMS, Food Chem. 288 (2019) 315–324.

[76] J.I. Baumbach, 2009. Ion mobility spectrometry coupled with multi-capillary columns for metabolic profiling of human breath. J. Breath Res. 3, 034001.

[77] R. Garrido-Delgado, F. Mercader-Trejo, S. Sielemann, W. de Bruyn, L. Arce, M. Valcárcel, Direct classification of olive oils by using two types of ion mobility spectrometers, Anal. Chim. Acta 696 (2011) 108–115.

[78] M. Hernández-Mesa, F. Monteau, B. Le Bizec, G. Dervilly-Pinel, 2019. Potential of ion mobility-mass spectrometry for both targeted and non-targeted analysis of phase II steroid metabolites in urine. Anal. Chim. Acta. 1, 100006.

[79] T.J. Causon, S. Hann, Theoretical evaluation of peak capacity improvements by use of liquid chromatography combined with drift tube ion mobility-mass spectrometry, J. Chromatogr. A 1416 (2015) 47–56.

[80] Q. Wu, J.Y. Wang, D.Q. Han, Z.P. Yao, 2020. Recent advances in differentiation of isomers by ion mobility mass spectrometry. Trac-Trend. Anal. Chem. 124, 115801.

[81] A. Kaufmann, P. Butcher, K. Maden, S. Walker, M. Widmer, Does the ion mobility resolving power as provided by commercially available ion mobility quadrupole time-of-flight mass spectrometry instruments permit the unambiguous identification of small molecules in complex matrices?, Anal. Chim. Acta 1107 (2020) 113–126.

[82] E.W. McDaniel, D.W. Martin, W.S. Barnes, Drift Tube-Mass Spectrometer for Studies of Low-Energy Ion-Molecule Reactions, Rev. Sci. Instrum. 33 (1962) 2–7.

[83] A.B. Kanu, P. Dwivedi, M. Tam, L. Matz, H.H. Hill, Ion mobility–mass spectrometry, J. Mass Spectrom. 43 (2008) 1-22.

[84] A.B. Kanu, C. Wu, H.H. Hill Jr, Rapid preseparation of interferences for ion mobility spectrometry. Anal Chim Acta 610 (2008) 125–34.

[85] U. Chiluwal, G. Lee, M.Y. Rajapakse, T. Willy, S. Lukow, H. Schmidt, G.A. Eiceman, Tandem ion mobility spectrometry at ambient pressure and field decomposition of mobility selected ions of explosives and interferences, Analyst 144 (2019) 2052–2061.

[86] S.I. Merenbloom, S.L. Koeniger, S.J. Valentine, M.D. Plasencia, D.E. Clemmer, IMS- IMS and IMS- IMS- IMS/MS for separating peptide and protein fragment ions, Anal. Chem. 78 (2006) 2802–2809.

[87] R.T. Kurulugama, S.J. Valentine, R.A. Sowell, D.E. Clemmer, Development of a high-throughput IMS--IMS--MS approach for analyzing mixtures of biomolecules, J. Proteomics 71 (2008) 318–331.

[88] H. Shokri, E.G. Nazarov, B.D. Gardner, H.-C. Niu, G. Lee, J.A. Stone, N. Jurado-Campos, G.A. Eiceman, Field Induced Fragmentation (FIF) Spectra of Oxygen Containing Volatile Organic Compounds with Reactive Stage Tandem Ion Mobility Spectrometry and Functional Group Classification by Neural Network Analysis, Anal. Chem. (2020). https://doi.org/10.1021/acs.analchem.9b05651.

[89] T.O. Metz, J.S. Page, E.S. Baker, K. Tang, J. Ding, Y. Shen, R.D. Smith, High-resolution separations and improved ion production and transmission in metabolomics, TrAC-Trends Anal. Chem. 27 (2008) 205–214.

[90] C.L. Crawford, S. Graf, M. Gonin, K. Fuhrer, X. Zhang, H.H. Hill, The novel use of gas chromatography-ion mobility-time of flight mass spectrometry with secondary electrospray ionization for complex mixture analysis, Int. J. Ion Mobil. Spectrom. 14 (2011) 23–30.

[91] P.V. Shliaha, N.J. Bond, L. Gatto, K.S. Lilley, Effects of traveling wave ion mobility separation on data independent acquisition in proteomics studies, J. Proteome Res. 12 (2013) 2323–2339.

[92] S.J. Valentine, X. Liu, M.D. Plasencia, A.E. Hilderbrand, R.T. Kurulugama, S.L. Koeniger, D.E. Clemmer, Developing liquid chromatography ion mobility mass spectometry techniques, Expert Rev. Proteomics. 2 (2005) 553–565.

[93] A. Sorribes-Soriano, M. de la Guardia, F.A. Esteve-Turrillas, S. Armenta, Trace analysis by ion mobility spectrometry: from conventional to smart sample preconcentration methods. A review, Anal. Chim. Acta 1026 (2018) 37–50.

[94] A. Ebrahimi, M.T. Jafari, Negative corona discharge-ion mobility spectrometry as a detection system for low density extraction solvent-based dispersive liquid--liquid microextraction, Talanta 134 (2015) 724–731.

[95] R. Mirzajani, N. Tavaf, Rapid and highly sensitive determination of melamine in different food samples by corona discharge ion mobility spectrometry after dispersive liquid-liquid microextraction, J. Braz. Chem. Soc. 27 (2016) 1657–1666.

[96] M. N. Peiró, S. Armenta, S. Garrigues, M. de la Guardia, Determination of 3, 4-methylenedioxypyrovalerone (MDPV) in oral and nasal fluids by ion mobility spectrometry, Anal. Bioanal. Chem. 408 (2016) 3265–3273.

[97] J. Wang, Z. Zhang, Z. Du, W. Sun, Development of a rapid detection method for seven pesticides in cucumber using hollow fibre liquid phase microextraction and ion mobility spectrometry, Anal. Meth. 5 (2013) 6592–6597.

[98] M.T. Jafari, M. Saraji, H. Sherafatmand, Electrospray ionization-ion mobility spectrometry as a detection system for three-phase hollow fiber microextraction technique and simultaneous determination of trimipramine and desipramine in urine and plasma samples, Anal. Bioanal. Chem. 399 (2011) 3555–3564.

[99] M. Mohammadnejad, M. Farhadpour, V. Mahdavi, M. Tabrizchi, Rapid monitoring and sensitive determination of DDT and its metabolites in water sample using solid-phase extraction followed by ion mobility spectrometry, Int. J.

Mobil. Spectrom. 20 (2017) 23–30.

[100] Y. Lu, R.M. O'Donnell, P.B. Harrington, Detection of cocaine and its metabolites in urine using solid phase extraction-ion mobility spectrometry with alternating least squares, Forensic Sci. Int. 189 (2009) 54–59.

[101] D.J. Cocovi-Solberg, F.A. Esteve-Turrillas, S. Armenta, M. de la Guardia, M. Miró, Towards an automatic lab-on-valve-ion mobility spectrometric system for detection of cocaine abuse, J. Chromatogr. A 1512 (2017) 43–50.

[102] J.X. Wang, X.G. Gao, J. Jia, J.P. Li, X.L. He, Solid phase microextraction-ion mobility spectrometry for rapid determination of trace dichlorovos in tea drinks, Chin. J. Anal. Chem. 43 (2015) 1193–1197.

[103] L. Yang, Q. Han, S. Cao, J. Yang, J. Yang, M. Ding, Portable solid phase micro-extraction coupled with ion mobility spectrometry system for on-site analysis of chemical warfare agents and simulants in water samples, Sensors 14 (2014) 20963–20974.

[104] J.K. Lokhnauth, N.H. Snow, Solid phase micro-extraction coupled with ion mobility spectrometry for the analysis of ephedrine in urine, J. Sep. Sci. 28 (2005) 612–618.

[105] J.K. Lokhnauth, N.H. Snow, Determination of parabens in pharmaceutical formulations by solid-phase microextraction-ion mobility spectrometry, Anal. Chem. 77 (2005) 5938–5946.

[106] M. Nousiainen, S. Holopainen, J. Puton, M. Sillanpää, Fast detection of methyl tert-butyl ether from water using solid phase microextraction and ion mobility spectrometry, Talanta 84 (2011) 738–744.

[107] G. Walendzik, J.I. Baumbach, D. Klockow, Coupling of SPME with MCC/UV-IMS as a tool for rapid on-site detection of groundwater and surface water contamination, Anal. Bioanal. Chem. 382 (2005) 1842–1847.

[108] M.T. Jafari, M.R. Rezayat, M. Mossaddegh, Design and construction of an injection port for coupling stir-bar sorptive extraction with ion mobility spectrometry, Talanta 178 (2018) 369–376.

[109] M.T. Jafari, M. Saraji, S. Yousefi, Negative electrospray ionization ion mobility spectrometry combined with microextraction in packed syringe for direct analysis of phenoxyacid herbicides in environmental waters, J. Chromatogr. A 1249 (2012) 41–47.

[110] E. Szymańska, A.N. Davies, L.M.C. Buydens, Chemometrics for ion mobility spectrometry data: recent advances and future prospects, Analyst 141 (2016) 5689–5708.

[111] P.J. Rauch, P.B. Harrington, D.M. Davis, Near real-time self-modeling mixture analysis, Chemom. Intell. Lab. Syst. 39 (1997) 175–185.

[112] M.L. Ochoa, P.B. Harrington, Detection of methamphetamine in the presence of

nicotine using in situ chemical derivatization and ion mobility spectrometry, Anal. Chem. 76 (2004) 985–991.

[113] V. Pomareda, D. Calvo, A. Pardo, S. Marco, Hard modeling multivariate curve resolution using LASSO: application to ion mobility spectra, Chemom. Intell. Lab. Syst. 104 (2010) 318–332.

[114] V. Pomareda, A. V Guamán, M. Mohammadnejad, D. Calvo, A. Pardo, S. Marco, Multivariate curve resolution of nonlinear ion mobility spectra followed by multivariate nonlinear calibration for quantitative prediction, Chemom. Intell. Lab. Syst. 118 (2012) 219–229.

[115] T. Khayamian, S.M. Sajjadi, S. Mirmahdieh, A. Mardihallaj, Z. Hashemian, Simultaneous analysis of bifenthrin and tetramethrin using corona discharge ion mobility spectrometry and Tucker 3 model, Chemom. Intell. Lab. Syst. 118 (2012) 88–96.

[116] P. Zheng, P. de B. Harrington, D.M. Davis, Quantitative analysis of volatile organic compounds using ion mobility spectrometry and cascade correlation neural networks, Chemom. Intell. Lab. Syst. 33 (1996) 121–132.

[117] F. Ehrentreich, Wavelet transform applications in analytical chemistry, Anal. Bioanal. Chem. 372 (2002) 115–121.

[118] A. Smolinska, A.-C. Hauschild, R.R.R. Fijten, J.W. Dallinga, J. Baumbach, F.J. Van Schooten, Current breathomics-a review on data pre-processing techniques and machine learning in metabolomics breath analysis, J. Breath Res. 8 (2014) 27105.

[119] A.-C. Hauschild, T. Schneider, J. Pauling, K. Rupp, M. Jang, J.I. Baumbach, J. Baumbach, Computational methods for metabolomic data analysis of ion mobility spectrometry data-reviewing the state of the art, Metabolites 2 (2012) 733–755.

[120] W. Cheung, Y. Xu, C.L.P. Thomas, R. Goodacre, Discrimination of bacteria using pyrolysis-gas chromatography-differential mobility spectrometry (Py-GC-DMS) and chemometrics, Analyst 134 (2009) 557–563.

[121] S. Bader, W. Urfer, J.I. Baumbach, Preprocessing of ion mobility spectra by lognormal detailing and wavelet transform, Int. J. Ion Mobil. Spectrom. 11 (2008) 43–49.

[122] E. Szymańska, E. Brodrick, M. Williams, A.N. Davies, H.-J. van Manen, L.M.C. Buydens, Data Size Reduction Strategy for the Classification of Breath and Air Samples Using Multicapillary Column-Ion Mobility Spectrometry, Anal. Chem. 87 (2015) 869–875.

[123] A.A. Urbas, P.B. Harrington, Two-dimensional wavelet compression of ion mobility spectra, Anal. Chim. Acta. 446 (2001) 391–410.

[124] R. Garrido-Delgado, L. Arce, M. Valcárcel, Multi-capillary column-ion mobility spectrometry: a potential screening system to differentiate virgin olive oils, Anal. Bioanal. Chem. 402 (2012) 489–498.

[125] M. Westhoff, P. Litterst, L. Freitag, W. Urfer, S. Bader, J.I. Baumbach, Ion

mobility spectrometry for the detection of volatile organic compounds in exhaled breath of patients with lung cancer: results of a pilot study, Thorax 64 (2009) 744–748.

[126] E. Szymańska, G.H. Tinnevelt, E. Brodrick, M. Williams, A.N. Davies, H.-J. van Manen, L.M.C. Buydens, Increasing conclusiveness of clinical breath analysis by improved baseline correction of multi capillary column--ion mobility spectrometry (MCC-IMS) data, J. Pharm. Biomed. Anal. 127 (2016) 170–175.

[127] G. Kaur-Atwal, G. O'Connor, A.A. Aksenov, V. Bocos-Bintintan, C.L.P. Thomas, C.S. Creaser, Chemical standards for ion mobility spectrometry: a review, Int. J. Ion Mobil. Spectrom. 12 (2009) 1–14.

[128] E. Szymańska, M.J. Markuszewski, X. Capron, A.-M. van Nederkassel, Y. Vander Heyden, M. Markuszewski, K. Krajka, R. Kaliszan, Evaluation of different warping methods for the analysis of CE profiles of urinary nucleosides, Electrophoresis 28 (2007) 2861–2873.

[129] T. Perl, B. Bödeker, M. Jünger, J. Nolte, W. Vautz, Alignment of retention time obtained from multicapillary column gas chromatography used for VOC analysis with ion mobility spectrometry, Anal. Bioanal. Chem. 397 (2010) 2385–2394.

[130] R.A. van den Berg, H.C.J. Hoefsloot, J.A. Westerhuis, A.K. Smilde, M.J. van der Werf, Centering, scaling, and transformations: improving the biological information content of metabolomics data, BMC Genomics 7 (2006) 142.

[131] D. Isailovic, M.D. Plasencia, M.M. Gaye, S.T. Stokes, R.T. Kurulugama, V. Pungpapong, M. Zhang, Z. Kyselova, R. Goldman, Y. Mechref, others, Delineating diseases by IMS-MS profiling of serum N-linked glycans, J. Proteome Res. 11 (2012) 576–585.

[132] L. Zhang, Q. Shuai, P. Li, Q. Zhang, F. Ma, W. Zhang, X. Ding, Ion mobility spectrometry fingerprints: A rapid detection technology for adulteration of sesame oil, Food Chem. 192 (2016) 60–66.

[133] J. Bible, S. Datta, S. Datta, Cluster Analysis: Finding Groups in Data, in: Informatics for Materials Science and Engineering, Elsevier, 2013: pp. 53–70.

[134] M. Calderón-Santiago, Mass spectrometry for the identification and quantitation of metabolomic biomarkers in clinical analysis, Doctoral Thesis, University of Córdoba, Spain, 2014.

[135] E. Szymańska, E. Saccenti, A.K. Smilde, J.A. Westerhuis, Double-check: validation of diagnostic statistics for PLS-DA models in metabolomics studies, Metabolomics 8 (2012) 3–16.

[136] D. Szöllösi, D.L. Dénes, F. Firtha, Z. Kovács, A. Fekete, Comparison of six multiclass classifiers by the use of different classification performance indicators, J. Chemom. 26 (2012) 76–84.

[137] Z. Karpas, Ion Mobility Spectrometry: A tool in the war against terror, Bull. Isr. Chem. Soc. 24 (2009) 26–31.

[138] D. Martinak, A. Rudolph, Explosives detection using an ion mobility spectrometer

for airport security, in: Proc. IEEE 31st Annu. 1997 Int. Carnahan Conf. Secur. Technol., 1997: pp. 188–189.

[139] G.A. Eiceman, M.R. Salazar, M.R. Rodriguez, T.F. Limero, S.W. Beck, J.H. Cross, R. Young, J.T. James, Ion mobility spectrometry of hydrazine, monomethylhydrazine, and ammonia in air with 5-nonanone reagent gas, Anal. Chem. 65 (1993) 1696–1702.

[140] S. Armenta, F.A. Esteve-Turrillas, M. Alcalà, Analysis of hazardous chemicals by "stand alone" drift tube ion mobility spectrometry: a review, Anal. Methods 12 (2020) 1163–1181.

[141] C.K. Hilton, C.A. Krueger, A.J. Midey, M. Osgood, J. Wu, C. Wu, Improved analysis of explosives samples with electrospray ionization-high resolution ion mobility spectrometry (ESI-HRIMS), Int. J. Mass Spectrom. 298 (2010) 64–71.

[142] I.A. Buryakov, 2011. Detection of explosives by ion mobility spectrometry. J. Anal. Chem. 66, 674.

[143] J.R. Verkouteren, J.L. Staymates, Reliability of ion mobility spectrometry for qualitative analysis of complex, multicomponent illicit drug samples, Forensic Sci. Int. 206 (2011) 190–196.

[144] R.G. Ewing, D.A. Atkinson, G.A. Eiceman, G.J. Ewing, A critical review of ion mobility spectrometry for the detection of explosives and explosive related compounds, Talanta 54 (2001) 515–529.

[145] L.L. Danylewych-May, Modifications to the ionization process to enhance the detection of explosives by IMS, Proc. 1st Int. Sym. Explosive Detection Technology, Atlantic City, NJ, 1991, pp. 672–686.

[146] M. Sabo, J. Páleník, M. Kučera, H. Han, H. Wang, Y. Chu and Š. Matejčík, Atmospheric pressure corona discharge ionisation and ion mobility spectrometry/mass spectrometry study of the negative corona discharge in high purity oxygen and oxygen/nitrogen mixtures, Int. J. Mass Spectrom. 293 (2010) 23–27.

[147] F.W. Karasek, H.H. Hill Jr, S.H. Kim, Plasma chromatography of heroin and cocaine with mass-identified mobility spectra, J. Chromatogr. A 117 (1976) 327–336.

[148] S. Armenta, S. Garrigues, M. de la Guardia, J. Brassier, M. Alcalà, M. Blanco, Analysis of ecstasy in oral fluid by ion mobility spectrometry and infrared spectroscopy after liquid--liquid extraction, J. Chromatogr. A 1384 (2015) 1–8.

[149] N. Alizadeh, A. Mohammadi, M. Tabrizchi, Rapid screening of methamphetamines in human serum by headspace solid-phase microextraction using a dodecylsulfate-doped polypyrrole film coupled to ion mobility spectrometry, J. Chromatogr. A 1183 (2008) 21–28.

[150] A. Sorribes-Soriano, R. Arráez-González, F.A. Esteve-Turrillas, S. Armenta, J.M.

Herrero-Martínez, Development of a molecularly imprinted monolithic polymer disk for agitation-extraction of ecgonine methyl ester from environmental water, Talanta 199 (2019) 388–395.

[151] M.M. Contreras, N. Jurado-Campos, C.S.-C. Callado, N. Arroyo-Manzanares, L. Fernández, S. Casano, S. Marco, L. Arce, C. Ferreiro-Vera, Thermal desorption-ion mobility spectrometry: A rapid sensor for the detection of cannabinoids and discrimination of Cannabis sativa L. chemotypes, Sensors Actuators B Chem. 273 (2018) 1413–1424.

[152] I. Márquez-Sillero, E. Aguilera-Herrador, S. Cárdenas, M. Valcárcel, Ion-mobility spectrometry for environmental analysis, TrAC Trends Anal. Chem. 30 (2011) 677–690.

[153] S. Armenta, M. Alcala, M. Blanco, A review of recent, unconventional applications of ion mobility spectrometry (IMS), Anal. Chim. Acta 703 (2011) 114–123.

[154] R. Pozzi, P. Bocchini, F. Pinelli, G.C. Galletti, Rapid analysis of tile industry gaseous emissions by ion mobility spectrometry and comparison with solid phase micro-extraction/gas chromatography/mass spectrometry, J. Environ. Monit. 8 (2006) 1219–1226.

[155] L. Myles, T.P. Meyers, L. Robinson, Atmospheric ammonia measurement with an ion mobility spectrometer, Atmos. Environ. 40 (2006) 5745–5752.

[156] C. Chen, C. Dong, Y. Du, S. Cheng, F. Han, L. Li, W. Wang, K. Hou, H. Li, Bipolar ionization source for ion mobility spectrometry based on vacuum ultraviolet radiation induced photoemission and photoionization, Anal. Chem. 82 (2010) 4151–4157.

[157] L. Criado-Garcia, L. Arce, M. Valcarcel, Membrane set up combined with photoionization-ion mobility spectrometer to improve analytical performance and avoid humidity interference on the determination of aromatics in gaseous samples, J. Chromatogr. A 1431 (2016) 55–63.

[158] L. Criado-Garcia, N. Almofti, L. Arce, Photoionization-ion mobility spectrometer for non-targeted screening analysis or for targeted analysis coupling a Tenax TA column, Sensors Actuat. B Chem. 235 (2016) 370–377.

[159] H. Borsdorf, A. Rämmler, Continuous on-line determination of methyl tert-butyl ether in water samples using ion mobility spectrometry, J. Chromatogr. A 1072 (2005) 45–54.

[160] N. Alizadeh, M. Jafari, A. Mohammadi, Headspace-solid-phase microextraction using a dodecylsulfate-doped polypyrrole film coupled to ion mobility spectrometry for analysis methyl tert-butyl ether in water and gasoline, J. Hazard. Mater. 169 (2009) 861–867.

[161] Y. Du, W. Zhang, W. Whitten, H. Li, D.B. Watson, J. Xu, Membrane-extraction ion mobility spectrometry for in situ detection of chlorinated hydrocarbons in water, Anal. Chem. 82 (2010) 4089–4096.

[162] E. Aguilera-Herrador, R. Lucena, S. Cárdenas, M. Valcárcel, Ionic liquid-based single drop microextraction and room-temperature gas chromatography for on-site ion mobility spectrometric analysis, J. Chromatogr. A 1216 (2009) 5580–5587.

[163] F.K. Tadjimukhamedov, J.A. Stone, D. Papanastasiou, J.E. Rodriguez, W. Mueller, H. Sukumar, G.A. Eiceman, Liquid chromatography/electrospray ionization/ion mobility spectrometry of chlorophenols with full flow from large bore LC columns, Int. J. Ion Mobil. Spectrom. 11 (2008) 51–60.

[164] A. Mohammadi, A. Ameli, N. Alizadeh, Headspace solid-phase microextraction using a dodecylsulfate-doped polypyrrole film coupled to ion mobility spectrometry for the simultaneous determination of atrazine and ametryn in soil and water samples, Talanta 78 (2009) 1107–1114.

[165] M.T. Jafari, Determination and identification of malathion, ethion and dichlorovos using ion mobility spectrometry, Talanta 69 (2006) 1054–1058.

[166] M.T. Jafari, M. Azimi, Analysis of sevin, amitraz, and metalaxyl pesticides using ion mobility spectrometry, Anal. Lett. 39 (2006) 2061–2071.

[167] M. Nousiainen, K. Peräkorpi, M. Sillanpää, Determination of gas-phase produced ethyl parathion and toluene 2, 4-diisocyanate by ion mobility spectrometry, gas chromatography and liquid chromatography, Talanta 72 (2007) 984–990.

[168] A.B. Kanu, H.H. Hill Jr, M.M. Gribb, R.N. Walters, A small subsurface ion mobility spectrometer sensor for detecting environmental soil-gas contaminants, J. Environ. Monit. 9 (2007) 51–60.

[169] D. Sevier, M. Gribb, R. Walters, J. Imonigie, K. Ryan, A. Kanu, H.H. Hill Jr, F. Hong, J. Baker, S.M. Loo, An in-situ ion mobility spectrometer sensor system for detecting gaseous VOCs in unsaturated soils, in: G.A. Miller, C.E. Zapata, S.L. Houston, D.G. Fredlund (Eds), Unsaturated Soils 2006, American Society of Civil Engineers, Reston, 2006, pp. 225–234.

[170] R.R. Kunz, F.L. Leibowitz, D.K. Downs, Ultraviolet photolytic vapor generation from particulate ensembles for detection of malathion residues in aerosols, Anal. Chim. Acta 531 (2005) 267–277.

[171] A.-K. Viitanen, E. Saukko, A. Virtanen, P. Yli-Pirilä, J.N. Smith, J. Joutsensaari, J.M. Mäkelä, Ion Mobility Distributions during the Initial Stages of New Particle Formation by the Ozonolysis of α-Pinene, Environ. Sci. Technol. 44 (2010) 8917–8923.

[172] I. Blaženović, T. Shen, S.S. Mehta, T. Kind, J. Ji, M. Piparo, F. Cacciola, L. Mondello, O. Fiehn, Increasing Compound Identification Rates in Untargeted Lipidomics Research with Liquid Chromatography Drift Time–Ion Mobility Mass Spectrometry, Anal. Chem. 90 (2018) 10758–10764.

[173] C.A. López-Morales, S. Vázquez-Leyva, L. Vallejo-Castillo, G. Carballo-Uicab, L.

Muñoz-García, J.E. Herbert-Pucheta, L.G. Zepeda-Vallejo, M. Velasco-Velázquez, L. Pavón, S.M. Pérez-Tapia, E. Medina-Rivero, Determination of peptide profile consistency and safety of collagen hydrolysates as quality attributes, J. Food Sci. 84 (2019) 430–439.

[174] T.J. Causon, M. Došen, G. Reznicek, S. Hann, Workflow Development for the Analysis of Phenolic Compounds in Wine Using Liquid Chromatography Combined with Drift Tube Ion Mobility-Mass Spectrometry, LC-GC N. Am. 34 (2016) 854–867.

[175] R. Rodríguez-Maecker, E. Vyhmeister, S. Meisen, A.R. Martinez, A. Kuklya, U. Telgheder, Identification of terpenes and essential oils by means of static headspace gas chromatography-ion mobility spectrometry, Anal. Bioanal. Chem. 409 (2017) 6595–6603.

[176] T.O. Alves, C.T.S. D'Almeida, V.C.M. Victorio, G.H.M.F. Souza, L.C. Cameron, M.S.L. Ferreira, Immunogenic and allergenic profile of wheat flours from different technological qualities revealed by ion mobility mass spectrometry, J. Food Compos. Anal. 73 (2018) 67–75.

[177] R. Garrido-Delgado, M. del Mar Dobao-Prieto, L. Arce, M. Valcárcel, Determination of volatile compounds by GC-IMS to assign the quality of virgin olive oil, Food Chem. 187 (2015) 572–579.

[178] Y. Guo, D. Chen, Y. Dong, H. Ju, C. Wu, S. Lin, Characteristic volatiles fingerprints and changes of volatile compounds in fresh and dried Tricholoma matsutake Singer by HS-GC-IMS and HS-SPME-GC--MS, J. Chromatogr. B 1099 (2018) 46–55.

[179] N. Arroyo-Manzanares, A. Martín-Gómez, N. Jurado-Campos, R. Garrido-Delgado, C. Arce, L. Arce, Target vs spectral fingerprint data analysis of Iberian ham samples for avoiding labelling fraud using headspace-gas chromatography-ion mobility spectrometry, Food Chem. 246 (2018) 65–73.

[180] G. Cohen, D.D. Rudnik, M. Laloush, D. Yakir, Z. Karpas, A novel method for determination of histamine in tuna fish by ion mobility spectrometry, Food Anal. Methods 8 (2015) 2376–2382.

[181] S. Cheng, H. Li, D. Jiang, C. Chen, T. Zhang, Y. Li, H. Wang, Q. Zhou, H. Li, M. Tan, Sensitive detection of trimethylamine based on dopant-assisted positive photoionization ion mobility spectrometry, Talanta 162 (2017) 398–402.

[182] Z. Karpas, A. V Guamán, D. Calvo, A. Pardo, S. Marco, The potential of ion mobility spectrometry (IMS) for detection of 2, 4, 6-trichloroanisole (2, 4, 6-TCA) in wine, Talanta 93 (2012) 200–205.

[183] M. Kamalabadi, E. Ghaemi, A. Mohammadi, N. Alizadeh, Determination of furfural and hydroxymethylfurfural from baby formula using headspace solid phase microextraction based on nanostructured polypyrrole fiber coupled with ion mobility spectrometry, Food Chem. 181 (2015) 72–77.

[184] N. Gerhardt, S. Schwolow, S. Rohn, P.R. Pérez-Cacho, H. Galán-Soldevilla, L. Arce, P. Weller, Quality assessment of olive oils based on temperature-ramped HS-GC-IMS and sensory evaluation: comparison of different processing approaches by LDA, kNN, and SVM, Food Chem. 278 (2019) 720–728.

[185] N. Gerhardt, M. Birkenmeier, D. Sanders, S. Rohn, P. Weller, Resolution-optimized headspace gas chromatography-ion mobility spectrometry (HS-GC-IMS) for non-targeted olive oil profiling, Anal. Bioanal. Chem. 409 (2017) 3933–3942.

[186] A. Martín-Gómez, N. Arroyo-Manzanares, V. Rodrñiguez-Estévez, L. Arce, Use of a non-destructive sampling method for characterization of Iberian cured ham breed and feeding regime using GC-IMS, Meat Sci. 152 (2019) 146–154.

[187] R. Garrido-Delgado, L. Arce, A. V Guamán, A. Pardo, S. Marco, M. Valcárcel, Direct coupling of a gas-liquid separator to an ion mobility spectrometer for the classification of different white wines using chemometrics tools, Talanta 84 (2011) 471–479.

[188] N. Gerhardt, M. Birkenmeier, S. Schwolow, S. Rohn, P. Weller, Volatile-compound fingerprinting by headspace-gas-chromatography ion-mobility spectrometry (HS-GC-IMS) as a benchtop alternative to 1H NMR profiling for assessment of the authenticity of honey, Anal. Chem. 90 (2018) 1777–1785.

[189] M. Hernández-Mesa, A. Escourrou, F. Monteau, B. Le Bizec, G. Dervilly-Pinel, Current applications and perspectives of ion mobility spectrometry to answer chemical food safety issues, TrAC Trends Anal. Chem. 94 (2017) 39–53.

[190] W.B. Struwe, C. Baldauf, J. Hofmann, P.M. Rudd, K. Pagel, Ion mobility separation of deprotonated oligosaccharide isomers-evidence for gas-phase charge migration, Chem. Commun. 52 (2016) 12353–12356.

[191] S. Goscinny, L. Joly, E. De Pauw, V. Hanot, G. Eppe, Travelling-wave ion mobility time-of-flight mass spectrometry as an alternative strategy for screening of multi-class pesticides in fruits and vegetables, J. Chromatogr. A 1405 (2015) 85–93.

[192] T.J. Causon, V. Ivanova-Petropulos, D. Petrusheva, E. Bogeva, S. Hann, Fingerprinting of traditionally produced red wines using liquid chromatography combined with drift tube ion mobility-mass spectrometry, Anal. Chim. Acta 1052 (2019) 179–189.

ANALYTICAL TOOLS AND EQUIPMENT

This section of the Thesis Book describes the different analytical tools and equipment used in the experimental part of the Thesis, which are described in more detail in the subsequent chapters.

1. Standards and chemicals

1.1. Analytes

In this part the analytical standards used in the experimental work which are classified by chemical groups are summarized. The standards and analytes used were of high purity and they were stored following advice of the suppliers.

- *Alkanes*: n-octane
- *Alcohols*: Octan-1-ol, heptan-1-ol, hexan-1-ol, pentan-1-ol, butan-1-ol, propan-1-ol, propan-2-ol, butan-2-ol, 2-methyl-propan-1-ol, methanol, ethanol, 1-penten-3-ol, 3-methyl-1-butanol, *cis*-2-penten-1-ol, *trans*-2-hexen-1-ol, 3-hexen-1-ol, 1-octen-3-ol, octan-2-ol and 2-methyl-butan-1-ol.
- *Aldehydes*: Decanal, nonanal, octanal, heptanal, hexanal, pentanal, butanal, propanal, trans-2-pentenal, trans-2-hexen-1-al, trans-2-heptenal, benzaldehyde, trans-2-octenal and trans-2-decenal.
- *Ketones*: Decan-2-one, nonan-2-one, octan-2-one, heptan-2-one, hexan-2-one, pentan-2-one, butanone, acetone, methyl isobutyl ketone, pinacolone, 1-penten-3-ona, 1-octen-3-one and 6-methyl-5-hepten-2-one.
- *Esters*: Butyl acetate, isopentyl acetate, methyl butyrate, pentyl acetate, ethyl acrylate, heptyl acetate, hexyl acetate, isopropyl acetate, propyl acetate, vinyl acetate, isobutyl acetate, nonyl acetate, octyl acetate, sec-butyl acetate, ethyl acetate, ethyl

butanoate, ethyl isovalerate, propyl butanoate and 3-hexenyl-acetate.

- *Ethers*: Dibutyl ether, diethyl ether, dihexyl ether, diisopropyl ether, dipentyl ether and dipropyl ether.
- *Aromatic heterocyclic compounds*: 2,6-di-tert-butyl pyridine
- *Aromatic compounds*: 2,4,6-trinitrotoluene (TNT), benzene, toluene, ethyl benzene, (m-, p- and o-) xylenes, benzoic acid and diethyl phthalate.
- *Cannabinoids*: Deuterated cannabidiol (d3-CBD), cannabidivarin (CBDV), Δ^9-tetrahydrocannabivarin (Δ^9-THCV), cannabidiol (CBD), cannabichromene (CBC), Δ^8-tetrahydrocannabinol (Δ^8-THC), Δ^9-tetrahydrocannabinol (Δ^9-THC), cannabigerol (CBG), cannabinol (CBN), cannabidiolic acid (CBDA), cannabigerolic acid (CBGA) and Δ^9-tetrahydrocannabinolic acid (Δ^9-THCA).
- *Terpenes*: Eucalyptol (synonym: 1,8-cineole), limonene and linalool.
- *Phenolic compounds*: 1-naphthol, 3,4-dihydroxyphenylacetic acid, tyrosol, syringic acid, vanillic acid, p-hydroxybenzoic acid, sinapic acid, ferulic acid, p-coumaric acid, o-coumaric acid, gentisic acid and trans-cinnamic acid.

1.2. Solvents and other chemicals

Solvents (HPLC grade) and other chemicals also used in the experimental work are summarized here:

- Dichloromethane (Alfa Aesar, Ward Hill, MA).
- n-Hexane was obtained from Panreac (Barcelona, Spain).
- Trimethylchlorosilane (TMCS) from Sigma-Aldrich (St. Louis, MO, USA).
- N,O-bis(trimethylsilyl)trifluoro-acetamide (BSTFA) from Sigma-Aldrich (St. Louis, MO, USA).

- Acetonitrile from Sigma-Aldrich (St. Louis, MO, USA).
- Carbon tetrachloride (CCl_4) from Sigma Aldrich Chemical Co. (Milwaukee, WI).
- Methanol from Sigma Aldrich (St Louis, MO, USA).
- Formic acid (Sigma-Aldrich, St. Louis, MO, USA).
- Sodium tetraborate decahydrate (Sigma-Aldrich, St. Louis, MO, USA).
- Sodium hydroxide (Sigma-Aldrich, St. Louis, MO, USA).
- Hydrochloride acid (Sigma-Aldrich, St. Louis, MO, USA).
- Tenax TA porous polymer sorbent (2,6-diphenylene oxide) was purchased from Scientific Instrument Services (Ringoes, New Jersey, USA).
- Diatomaceous earth was obtained from Sigma Aldrich (St Louis, MO, USA).
- Refined oil was provided by Sovena group S.A. (Brenes, Spain).
- Ultrapure water (18.2 MΩ cm-1, Milli–Q Plus system, Millipore Bedford, MA, USA).
- Nitrogen gas 5.0 (purity ≥ 99.999%) was supplied by Abelló Linde (Barcelona, Spain).
- Ultrapure CO_2 (99.9%) in cylinder with a dip tube was supplied by Carburos Metálicos (Barcelona, Spain).
- Helium with 99.99% purity was provided by Air Liquide (Madrid, Spain).

2. Samples

In the experimental work developed in this Thesis, different samples belonging to drugs, environmental and food application areas were analysed:

- *Cannabis* samples: These samples were supplied by Phytoplant Research S.L. (Córdoba, Spain). Plant samples were obtained

from the top of the plant at the optimal harvest point; about 30 cm containing both leaves and flowers (female inflorescences) were sampled for each plant, and then dried. The stems were removed and the dried samples were ground until obtaining a semi-fine powder.

- non-*Cannabis* plants species: Equisetum arvense, Matricaria chamomilla, Calendula officinalis, Papaver rhoeas, Origanum vulgare, as well as tobacco. They were purchased in a local market of the city of Córdoba, Spain. The dry plant materials were ground.
- Soil samples: They were collected from the street. They were sieved in order to homogenize the sample, which means removing pebbles and rocks, and breaking up large soil aggregates.
- Fresh rosemary (*Rosmarinus officinalis* L.) plant: This was purchased in a local market of the city of Córdoba, Spain. The plant was triturated using a stainless-steel grinder.
- Olive oil samples (1): A total of 701 olive oil samples (190 EVOO, 355 VOO and 156 LOO samples) were supplied by the Spanish *Interprofesional del Aceite de Oliva Español*, *Agencia para el Aceite de oliva del Ministerio de Agricultura, Alimentación y Medio Ambiente* and the official control services from the *Consejería de Agricultura, Pesca y Desarrollo Rural de la Junta de Andalucía*. These samples were obtained from olives collected in two different harvest years, 2014-2015 and 2015-2016. A total of 292 samples (98 EVOO, 159 VOO, and 35 LOO samples) were obtained from the harvests of 2014-2015 and analyzed in 2015. The remaining 409 samples (92 EVOO, 196 VOO and 121 LOO) were obtained in 2015-2016 and analyzed in 2016.
- Olive oil samples (2): A total of 120 olive oil samples (40 EVOO, 40 VOO and 40 LOO) were supplied by Sovena group S.A. (Brenes, Spain) belonging to the 2018-2019's harvest.
- Olive oil samples (3): An amount of 83 olive oil samples were

supplied by IFAPA-Cabra (*Instituto de Investigación y Formación Agraria y Pesquera*) located in Cabra (Córdoba, Spain). Each sample was obtained from 2 kg of olives collected from five trees from the same farm using an Abencor analyser (Abengoa S.A., Seville, Spain). The samples were collected and produced in two different harvest: 30 of these samples were from 2018's harvest while the remaining 53 were from 2019's harvest. The samples were also from two olive varieties, *Hojiblanca* and *Picual*, and two production system, organic and conventional.

- Olive samples: A total of 36 olive samples were supplied by IFAPA-Cabra. Each sample was composed for olives of three trees from the same farm. All the samples were from 2019's harvest. The samples were from two olive varieties, *Hojiblanca* and *Picual*, and from two production system, organic and conventional.

3. Systems for sample preparation

The systems used for sample preparation are listed below:

- An ultrasound bath and a centrifuge were used to carry out a solid-liquid extraction of powered plant materials in Chapter III.
- The liquid-liquid extraction of olive oils in Chapters VIII and IX were carried out using 5 mL Eppendorf tubes and a vortex.
- An supercritical fluid extractor from Jasco (Tokyo, Japan) was used to extract samples in Chapters V and VIII. The device included several modules, such as one pump model PU-2080 CO2 Plus used to supply the CO_2, one pump model PU-2080 Plus used to provide the modifier, a BPR model BP-2080 Plus and a CO-2060 Plus oven as extraction chamber into which was placed a stainless-steel extraction cell of 5 mL (Análisis Vínicos, Tomelloso, Spain).

- An Abencor analyser (Abengoa S.A., Seville, Spain) was used to obtain olive oil samples from olives in Chapter IX.

4. Analytical instruments

The methods developed in the experimental part of this Doctoral Thesis have been mainly based on using IMS instruments. Several SISs were used such as HS, TD and SFE; and also different ionization sources were included in the IMS equipments such as ^{3}H, ^{63}Ni and UV. Furthermore, other system to facilitate the separation of analytes such as chromatographic systems were used together with IMS devices. All of them are fully described in this section. In order to compare results obtained with the IMS instruments, other complementary techniques were also employed such as CE-UV and HPLC-UV or FLD that are summarized in this part.

4.1. IMS equipments

From the simplest models to the most complex ones, all IMS instrument employed along this Doctoral Thesis are described here:

UV-IMS

An IMS instrument with an ultraviolet lamp as a photoionization source (10.6 eV) was supplied by G.A.S. Gesellschaft für Analytische Sensorsysteme mbH (Dortmund, Germany). The instrument is 350 × 350 × 150 mm in size and has a weight of 5 kg (see **Figure 1**). The instrument uses a 230 V/50-60 Hz power supply and a constant electrostatic field of 333 V/cm. In addition, the drift tube has a length of 12 cm and operates at room temperature and pressure. Data obtained was processed with GASpector software (version 3.9.9.DSP from G.A.S.). This device was employed in Chapter V and IX.

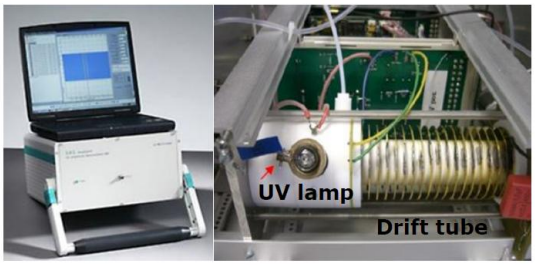

Figure 1. Photo of the UV-IMS and detail of the UV lamp (signaled with an arrow) and the drift tube of the instrument.

TD-IMS

A handheld IMS (Gas Detector Array) with a radiactive source of ^{63}Ni (100 MBq) and TD unit (X-TOOL) (GDA-X) (Airsense Analytics GmbH, Germany) was employed in Chapter III. The TD-IMS consisted of two parts with the following dimensions: IMS device ~395 × 112 × 210 mm and the TD unit ~110 × 64 × 113 mm. For analyzes, samples were deposited on a wipe sampling pad (stainless steel coated with Teflon) and inserted in the tool tray. A photograph of the GDA-X, including the wipe sampling pad, is shown in **Figure 2**. IMS data were acquired in the positive and negative ionization modes using the WinMusterGDA software (version 1.2.6.12) from Airsense Analytics GmbH.

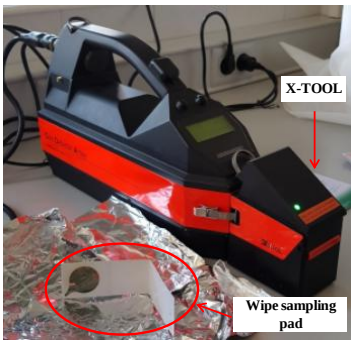

Figure 2. Photograph of the GDA-X device.

TD-tandem IMS with reactive stage

A tandem ion mobility spectrometer (**Figure 3**) was equipped with a thermal desorber as inlet (modified from a Itemizer DX, Rapiscan Systems) using a transfer line of 6 mm OD x 3 mm ID x 40 mm long ceramic tube. The ion source was a 1 cm long x 1 cm OD cylinder of stainless steel with 5 mCi ^{63}Ni. Drift rings were 0.35 mm thick stainless steel with 1.9 cm inner diameter and 3.8 cm outer diameter. The drift rings are held in Teflon supports which are compressed using two aluminum flanges. The drift tube was divided into reaction region, first stage drift region, and second stage drift region with the following distances: reaction region, 6.9 cm; first stage, 4.2 cm; second stage, 6.77 cm. The ion shutters were Bradbury-Nielsen design with tungsten wire 35 μm diameter and 0.5 mm distance between wire centers. Shutters were controlled using in-house electronics where a master clock established a time base for data acquisition and Shutter 1 and Shutter 2 were referenced to this time base. The fragmenter assembly consisted of an auxiliary grid placed 1 cm from the second ion shutter and 3 mm from the two fragmentation grids . The auxiliary grid tungsten wire 35 μm in diameter. Distance between wires was 0.7 mm center to center. Wire diameter in fragmenter grids was 70 μm and distance between wires in a plane was also 0.7 mm center to center. Distance between grids in the fragmenter wire set was 0.65 mm. Voltage on the auxiliary grid was 1.95 kV and on Grid 2 was 1.85 kV, both on a linear voltage gradient of the drift tube. A sinusoidal waveform from a step up transformer built in-house driven by a waveform generator (HP model 754, HP, Palo Alto, CA) was applied to grid 1 at 1.82 MHz. The maximum amplitude of 1300 V (2600 V peak-to-peak) on a DC bias of 1.85 kV provided maximum field strengths of 134 Td. An aperture grid is placed at a distance of 0.2 cm before of the Faraday plate detector. Uniform electric field of 358 V/cm is applied in the drift tube by using negative high voltage power supply. Wide range of uniform temperature inside the drift tube is obtained by placing the drift tube inside the oven. The drift tube was a side-flow design where CCl4 in purified air

was introduced into the source as dopant. All flows were vented through the suction pump. Amplifier and high voltage power supplies were based on in-house designs and acquisition software was the with a PCI 6024E interface card. The signal processing was made using a 6024E interface card (National Instruments, Austin, TX) and Labview-based virtual instrument Linear IMS_1.0. Data processing was referenced to the master clock for operation of both shutter 1 and shutter 2. This device was used in Chapter IV.

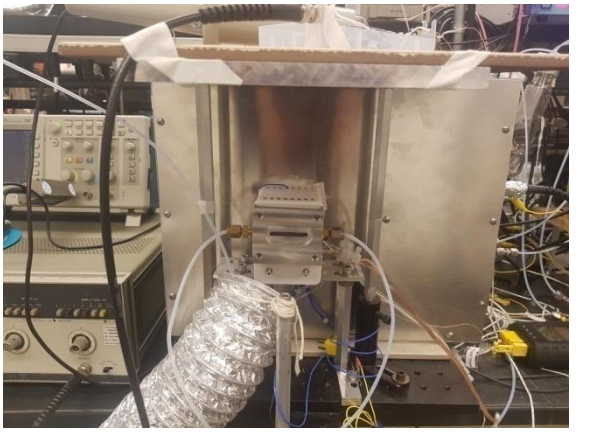

Figure 3. Photo of the TD-tandem IMS with reactive stage.

SFE-IMS

A pioneer on-line hyphenation between a SFE and an IMS detector through a Tenax TA was carried out in Chapter V of this Doctoral Thesis.

All supercritical fluid extractions were performed using a modular Jasco SFE system (Tokyo, Japan), as shown in **Figure 4**, consisting of one pump model PU-2080 Plus used to supply the CO_2, a BPR model BP-2080 Plus, and a CO-2060 Plus oven as extraction chamber to place a stainless-steel extraction cell of 5 mL (Análisis Vínicos, Tomelloso, Spain). The standard configuration of the device was modified using two Rheodyne 7000L valves (Cotati, CA), V1 and V2,

allowing to isolate the extraction cell between analyses, and the use of the static and dynamic extraction mode, respectively. The SFE was controlled by ChromNav software (version 1.19.03).

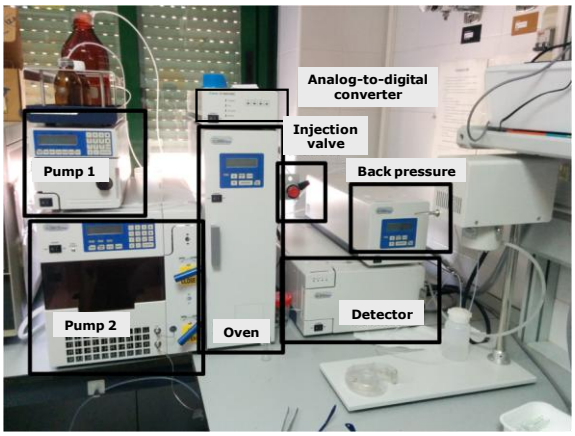

Figure 4. Photo of the SFE device.

Later, a solid trap was used after the SFE module in order to adsorb and desorb the analytes before introducing them into the IMS device. 1-g of solid Tenax TA, as sorbent trap, was placed into a stainless-steel tube of 250 mm length and 6 mm i.d. that was used as column. Glass wool was used in the extremes of the column to avoid the loss of the material. In the experimental set-up, this column was placed in a chromatographic oven model 5890 supplied by HP Hewlett Packard (Minnesota, USA). The inlet part of the column was connected to the restrictor of the SFE device and the outlet part to the IMS detector, through a Rheodyne 6-port switching valve (V3) from Valco (Houston, Texas). All connections were made using 1/16" o.d. x 0.010-inch i.d. stainless steel tubes (Sigma Aldrich). The temperature of the restrictor was controlled using a heat transfer jacket (Ramem, Madrid, Spain) in order to avoid condensation. The IMS instrument was the UV-IMS described above.

GC-IMS

A GC coupled to an IMS equipped with a tritium radioactive ionization source of 6.5 KeV and a drift tube of 5 cm long which operates at a constant electric field strength of 400 V cm^{-1} was used in Chapters I, VII, VIII and IX. This GC-IMS device is a commercial instrument called FlavourSpec® (Gesellschaft für Analytische Sensorsysteme mbH, G.A.S., Dortmund, Germany) (see **Figure 5**). A heated splitless injector (2 mm ID, 6.5 mm OD x 78.5 mm fused quartz glass) enabled direct sampling of the HS by using a 2.5 mL Hamilton syringe furnished with a 51 mm needle. The reproducibility of measurements was improved using an automatic sampler unit (CTC-PAL, CTC Analytics AG, Zwingen, Switzerland).

Two-dimensional GC-IMS data were acquired in positive mode using LAV software (version 2.0.0) from G.A.S. A GC×IMS Library Search software (G.A.S.) was employed to identify VOCs when it was necessary. It comes with a full non restricted version of the NIST2014 Retention Index Database.

Figure 5. Photo of the Flavourspec® used from GAS and internal detail of the instrument.

GC- tandem IMS with reactive stage

A model 5890 series II gas chromatograph (Hewlett-Packard Corp., Avondale, PA) was equipped with a capillary injection port and 10 meters 0.18 mm ID RTX-200 capillary column (Restek Corp, Bellefonte, PA). This column was connected using a Restek VU2 union connector to a 60 cm length of HT5: AQ, 0.32 mm ID capillary column (SGE Analytical Science). The HT5 capillary column passed through a heated stainless steel tube and into the reaction region of the drift tube. Six centimeters of aluminum cladding on the effluent end of this column were removed and the column end was located in the cross section of the drift tube. A tandem ion mobility spectrometer was built in-house with stainless steel drift rings (1.1 mm thick × 14.7 mm ID × 25.6 cm OD) and virgin Teflon insulators (1.9 mm thick × 14.7 mm ID × 25.6 cm OD). The ion source was a planar stainless steel disk (14.4 mm OD) plated with 6 mCi ^{63}Ni. Drift tube dimensions included a 41.8 mm reaction region, a 21.4 mm long first drift region with ion shutter 1 and a 22.0 mm long second drift region with ion shutter 2. Ion shutters were Tyndall Powell type with metal etched grids separated by a 0.05 mm thick Teflon insulator. Each grid was 0.1 mm thick x 13.0 mm ID with wires interdigitated at 0.63 mm between centers. Ion shutters were controlled using in-house electronics where a master clock established a time base for data acquisition and ion shutters 1 and 2 were both referenced to this time base. A uniform electric field of ~293 V/cm in the drift tube was provided by a high voltage supply of ~2.7 kV DC. An aperture grid was located at 0.7 mm from the Faraday plate detector. Electric fields for ion fragmentation were formed between two metal etched grids placed 1.2 mm from ion shutter 2. Ion fragmentation occurred when grid 2 was provided a ~3.4 MHz sinusoidal waveform on a DC voltage of 754 V from a Modular Intelligent Power Sources (MIPS) version 2.0, 2016 (GAA Custom Electronics, LLC, Kennewick, WA). Spectra were acquired using an 18-bit PCI-6281 DAQ interface card (National Instruments, Corp., Austin, TX) and a LabView program developed in-house and termed Linear 2018 version 2.0. This device, which is shown in **Figure 6**, was employed in Chapter II.

Figure 6. Photo of the GC- tandem IMS with reactive stage used in Chapter II.

4.2. Other analytical instruments

A Beckmann P/ACE MDQ CE System (Palo Alto, CA, USA), equipped with a diode array detector and a computer with the Beckmann 32 Karat software, was employed in Chapters VIII and IX.

HPLC-UV and HPLC-FLD analyzes of Chapter VIII were carried out using an Agilent 1100 Series HPLC instrument (Agilent Technologies, Waldbronn, Germany) equipped with a quaternary pump (G1311A) operating at room temperature. An on-line membrane system (G1379A) was included to degas the solvents and a Model 7125-075 Rheodyne injection valve (Rheodyne, Berkeley, CA, USA) was also used to manually inject the samples. Two detection modules, a G1315B diode-array detector and an Agilent FLD (G1321A), were connected in series. Agilent Chemstation software (Rev. A 10.02) was used to record the chromatograms.

Finally, a GC-MS instrument was used in Chapter IX. The instrument was based on a MPS with HS injector (Gerstel, Mülheim, Germany) which was installed in a 8890 gas chromatograph (Agilent Technologies, Santa Clara, CA,

USA) coupled to an Agilent 5977B quadrupole mass selective spectrometer equipped with an inert ion source with extractor. An HP-5MS UI (5% diphenyl–95% dimethylpolysiloxane, Agilent) capillary column (30 m × 0.25 mm I.D., 0.25 μm film thickness) was used. For data processing, MassHunter Workstation Data Acquisition software Qualitative Analysis version 10.0 (Agilent Technologies) was employed.

EXPERIMENTAL PART

BLOCK I

Theoretical study of Ion Mobility Spectrometry

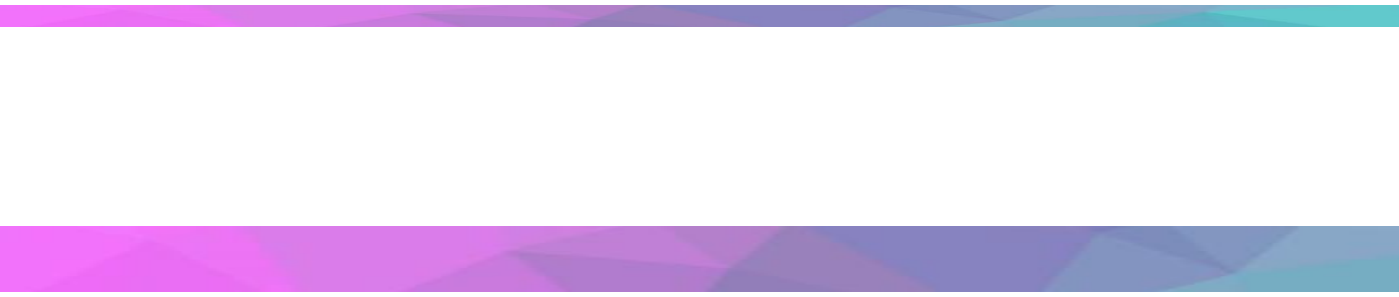

Block I of this PhD Book is devoted to increasing the lack of understanding between analytical IMS measurements and the behaviour of gas ions at ambient pressure to improve the interpretation capacity of the IMS data. Moreover, the possibility of increasing the structural information derived from IMS spectra was explored. This Block was focused on increasing the knowledge on fundamentals and theory of IMS to try to exploit the opportunities of this technique and to enhance its role in qualitative analysis. With these premises, Chapter 1 and 2 were developed.

Chapter I had as objective the study about fundamentals of the formation of product ions from alkyl alcohols, aldehydes and ketones compounds to ease the interpretation of IMS spectra. Also, the modeling of ions stability using ab initio computations to math this results with the spectral patterns and structure of ions was studied.

In Chapter II the use of an additional feature of IMS through the isolation and fragmentation of ions was explored to obtain more information about the structure of compounds detected by IMS. This could enhance the interpretation of IMS data. For that, different tasks were raised: a) to produce field induced fragmentation (FIF) spectra in a reactive stage tandem IMS at ambient pressure for a set of chemicals from alcohols, acetates, aldehydes, ketones and ethers families with known fragmentation pathways, b) to explore the reaction enthalpies for fragmentation, c) to determine rates of categorization of FIF spectra by chemical class using neural networks, and d) to examine trends in performance for neural network classification within each chemical family.

Stability of proton-bound clusters of alkyl alcohols, aldehydes and ketones in Ion Mobility Spectrometry

CHAPTER I

Talanta

185 (2018) 299–308

Stability of proton-bound clusters of alkyl alcohols, aldehydes and ketones in Ion Mobility Spectrometry

Natividad Jurado-Campos[a], Rocío Garrido-Delgado[a], Bruno Martínez-Haya[b], Gary A. Eiceman[c], Lourdes Arce[a]

[a]*Department of Analytical Chemistry, Institute of Fine Chemistry and Nanochemistry, University of Córdoba, Campus de Rabanales, Marie Curie Annex Building, E-14071 Córdoba, Spain*

[b]*Department of Physical, Chemical and Natural Systems, Universidad Pablo de Olavide, E-41013 Sevilla, Spain*

[c]*Department of Chemistry and Biochemistry, New Mexico State University, 1175 North Horseshoe Drive, Las Cruces, NM 88003, USA*

Stability of proton-bound clusters of alkyl alcohols, aldehydes and ketones in Ion Mobility Spectrometry

Natividad Jurado-Campos, Rocío Garrido-Delgado, Bruno Martínez-Haya, Gary A. Eiceman, Lourdes Arce

ABSTRACT

Significant substances in emerging applications of ion mobility spectrometry such as breath analysis for clinical diagnostics and headspace analysis for food purity include low molar mass alcohols, ketones, aldehydes and esters which produce mobility spectra containing protonated monomers and proton-bound dimers. Spectra for all n- alcohols, aldehydes and ketones from carbon number three to eight exhibited protonated monomers and proton-bound dimers with ion drift times of 6.5–13.3 ms at ambient pressure and from 35 to 80 °C in nitrogen. Only n-alcohols from 1-pentanol to 1-octanol produced proton-bound trimers which were sufficiently stable to be observed at these temperatures and drift times of 12.8–16.3 ms. Polar functional groups were protected in compact structures in ab initio models for proton-bound dimers of alcohols, ketones and aldehydes. Only alcohols formed a V-shaped arrangement for proton-bound trimers strengthening ion stability and lifetime. In contrast, models for proton-bound trimers of aldehydes and ketones showed association of the third neutral through weak, non-specific, long-range interactions consistent with ion dissociation in the ion mobility drift tube before arriving at the detector. Collision cross sections derived from reduced mobility coefficients in nitrogen gas atmosphere support the predicted ion structures and approximate degrees of hydration.

Keywords: Proton-bound trimers, aldehydes, n-alcohols, ketones, ion mobility spectrometry, molecular modeling

1. Introduction

Ion mobility spectrometry (IMS) has been central to military preparedness and commercial aviation security for twenty-five years, enabled by relatively simple instrumentation with hand-held or bench-scale portability [1-3]. On-site or in-field applications of IMS were encouraged by low ppb vapor detection limits achieved with ambient pressure chemical ionization and fast response time with mobility analysis in small drift tubes [4,5]. In the past decade, applications have extended into human metabolomics and clinical medicine [6-8], control of food purity [9-11], the quality of atmospheric environments [12,13], breath analysis [14,15], proteomics [16,17] and fundamental gas-phase ion studies [18-22]. This broadened utilization in chemical measurements necessitates a consolidation in the understanding of chemical processes governing the appearance of ions in IMS particularly for substances widely seen in these emerging applications, namely, small polar molecules including alcohols, esters, ketones, and aldehydes. The first step in response to such substances with atmospheric pressure chemical ionization (APCI) based IMS is the formation of ions derived from an analyte (M) in the ion source or reaction region where association of M to a hydrated proton results in displacement of water as shown in Eq. (1):

$$\underset{\text{Analyte}}{M} + \underset{\text{Hydrated proton}}{H^+(H_2O)_n} \rightleftharpoons \underset{\text{Protonated monomer}}{MH^+(H_2O)_{n-x}} + x\,H_2O \quad (1)$$

Levels of moisture and temperature govern the magnitude of n and proton-bound dimers (M_2H^+) may be formed with increased [M] as shown in Eq. (2):

$$\underset{\text{Analyte}}{M} + \underset{\text{Protonated monomer}}{MH^+(H_2O)_m} \rightleftharpoons \underset{\text{Proton-Bound Dimer}}{M_2H^+(H_2O)_{m-y}} + y\,H_2O \quad (2)$$

While proton-bound trimers (M_3H^+) should be produced (Eq. (3)) at the vapor concentrations for M and temperatures used in some commercially available instruments, ion peaks for proton-bound trimers are seldom observed in mobility spectra from such measurements.

$$\underset{\text{Analyte}}{M} + \underset{\text{Proton-Bound Dimer}}{M_2H^+(H_2O)_k} \rightleftharpoons \underset{\text{Proton-Bound Trimer}}{M_3H^+(H_2O)_{k-z}} + z\,H_2O \quad (3)$$

This is understood as a kinetic process where ions are extracted by an electric field from the vapour rich source region for mobility analysis into a drift region containing a purified gas atmosphere forward reactions of Eqs. (1)-(3). The reverse reactions of Eqs. (1)-(3) can occur on time scales faster than residence times for ion swarms in the mobility measurement leading to dissociation of proton bound species. This is widely observed for proton bound trimers of nearly all chemicals and routinely seen with proton bound dimers and depends on interaction enthalpies of the ion at temperatures of 50 °C and above. Dissociation reactions have been observed and characterized for proton-bound dimers of some polar substances including alkyl amines at sub-ambient temperature [23] and organophosphorous compounds at elevated temperatures [24]. Relevant to the current interest with low carbon number oxygen containing substances, proton-bound trimers for n-alcohols in the mobility spectra have also been observed and studied with drift tubes operated from 30 to 50 °C [23,24]. Previously, proton-bound trimers were reported for a substituted alcohol, 2-propanol with distinct peaks ions peaks for M_3H^+ at -20 °C and with lifetimes greater than 5 ms [18]. Intensity of the proton-bound trimer decreased progressively from -20 to 20 °C, which was understood in terms of thermal fragmentation. The appearance of analytical ion mobility spectra is now quantitatively described with refined understandings that ions and proton-bound cluster species formed in the ionization source may undergo fragmentation even at moderately low temperatures around 10 °C [25,26].

In this current study, proton-bound dimers and trimers for n-alcohols, measured experimentally from 35 to 80 °C by IMS, were also modeled for ion stability using *ab initio* computations. Findings were compared to the analogous studies of ketones and aldehydes, two classes of oxygen-containing compound with stable proton-bound dimers and an unstable proton-bound trimer under same conditions. The objective of this study was match spectral patterns with

computed ion stabilities and structures. Findings in this study are intended to contribute to the growing understandings between the appearance of ion mobility spectra in analytical measurements and gas ions at ambient pressure.

2. Experimental

2.1. Reagents

All n-alcohols, n-aldehydes and n-ketones, as well as the 2,6-di-*t*-butylpyridine (2,6-DtBP), the calibrant, were obtained from Sigma-Aldrich (St. Louis, MO, USA). Physicochemical properties of these substances are provided in Table 1. Stock solutions of each compound in concentration 1000 mg L^{-1} in Milli-Q ultrapure water (Millipore, Bedford, MA, USA) were stored at 4 °C. Working solutions were prepared by the appropriate dilution of the stock in Milli-Q ultrapure water. The samples were always analyzed by duplicate.

Table 1. Average values and standard deviations of the retention times obtained in the experiments of this work and physical and chemical properties of analytes measured by HS-GC-^{3}H-IMS.

Family	IUPAC name	Retention time ± standard deviation (s)	Molecular weight (g mol^{-1})	Boiling poing (°C)	Proton affinity** (KJ mol^{-1})	Henry's law constant at 25 °C** (mol (kg bar^{-1}))
Alcohols	*Octan-1-ol*	1753 ± 65	130.2	195.2	799.0	40
	Heptan-1-ol	721 ± 25	116.2	176.5	799.0	52
	Hexan-1-ol	317 ± 9	102.2	157.6	799.0	58
	Pentan-1-ol	156 ± 3	88.1	138.0	795.0	76
	Butan-1-ol	93 ± 2	74.1	117.7	789.2	130
	Propan-1-ol	68 ± 1	60.1	97.2	786.5	130

Ketones	*Octan-2-one*	794 ± 10	128.2	172.5	*	5.3
	Heptan-2-one	348 ± 3	114.2	151.0	*	6.9
	Hexan-2-one	170 ± 3	100.2	127.6	840.0	16
	Pentan-2-one	99 ± 3	86.1	102.3	832.7	16
	Butanone	74 ± 2	72.1	79.6	827.3	20
	Acetone	61 ± 1	58.1	56.0	812.0	25
Aldehydes	*Octanal*	858 ± 9	128.2	171.0	*	2.1
	Heptanal	371 ± 5	114.2	152.8	*	3.3
	Hexanal	178 ± 4	100.2	131.0	796.6	4.9
	Pentanal	102 ± 2	86.1	103.0	792.7	6.4
	Butanal	78 ± 3	72.1	74.8	786.0	9.6
	Propanal	61 ± 1	58.1	48.0	768.5	13

* Data not available.

** Obtained from NIST: http://webbook.nist.gov/chemistry

2.2. Instrument and analytical methodology

Measurements were made with a gas chromatography (GC) coupled to ^{3}H-IMS instrument (FlavourSpec®, G.A.S. Gesellschaft für Analytische Sensorsysteme mbH, Dortmund, Germany), equipped with a heated splitless injector for direct sampling of head space (HS) from sample solutions, as shown in Figure 1. The instrument was coupled to an automatic sampler unit for high reproducibility. Spectra were obtained using parameters given in Table 2.

Sample solutions of 1 mL were placed in a 20 mL vial with a magnetic cap and silicone septum, and thermostated at 60 °C for 20 min. A small volume (200 µL) of headspace was automatically transferred by syringe into the injection port for GC-IMS analysis (both syringe and injector heated to 80 °C).

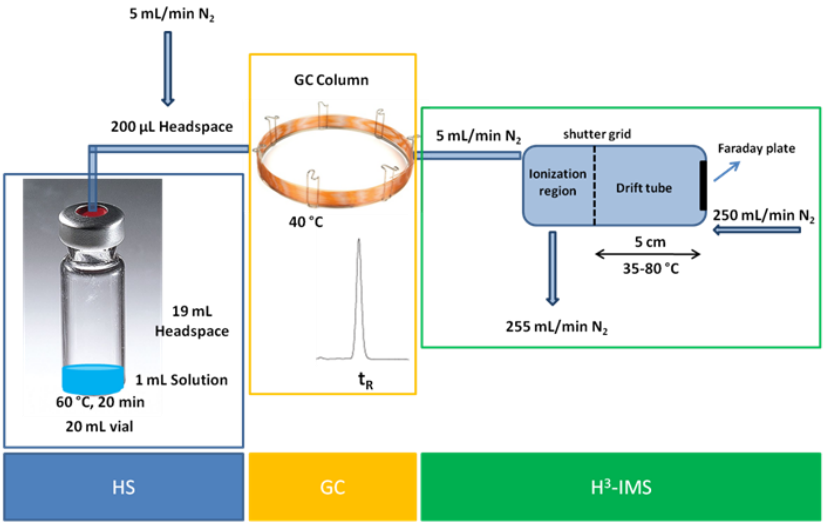

Figure 1. Sketch of the head space (HS), gas chromatography (GC) and ion mobility spectrometry (^{3}H-IMS) stages of the experimental set up employed in the present study.

A 30 m long non-polar capillary column containing methyl, phenyl and vinylsilicone in a 94:5:1 proportion (from CS-Chromatographie Service GmbH, Dürem, Germany), heated at 40 °C, was used to separate the analytes. The GC step precedes the IMS analysis to improve the resolution of signals of ions with similar mass and size, as shown in Table 1. In this study, the coupling of GC and IMS allowed to study samples with mixtures of different compounds (alcohols, ketones or aldehydes) in single runs, thereby reducing the acquisition time and potential systematic errors.

The drift tube was operated in positive polarity with a nominal drift region length of 5 cm and constant electric field strength of 400 V cm^{-1}. Nitrogen (with a purity of 5.0 (≥99.999 %) and moisture ≤ 3 mg L^{-1} supplied by Abello-Linde, Barcelona, Spain) was employed as drift and carrier gas in all the experiments and the temperature of the drift tube was set to a value within 35-80 ºC.

Table 2. Experimental conditions employed in the gas chromatography ion mobility experiments of this work.

Parameters	Values
Sample introduction system	
Sampling	Headspace (200 µL)
Incubation time, min	20
Sample volume, mL	1
Incubation temperature, ºC	60
Injector temperature, ºC	80
Column	
Capillary column	SE-54*
Length of column	30
Column temperature, ºC	40
Run time, min	30/45/50**
IMS	
Ionization source	Tritium (6.5 keV)
Drift voltage polarity	Positive
Electric field, V cm^{-1}	400
Carrier gas flow rate, mL min^{-1}	5
Drift gas flow rate, mL min^{-1}	250
Drift tube length, cm	5
Drift tube temperature, ºC	35-80
Pressure, kPa	Ambient pressure

* SE-54 type of chromatographic column: methyl, phenyl and vinylsilicone (94:5:1).

** Run times required to separate aldehydes, ketones and alcohols mixtures, respectively.

The ion mobility coefficient (K) of a given species is calculated from the drift time measured for the corresponding product ion, and it is given by Eq. (4):

$$K = v_d/E = L/(t_d \cdot E) \quad (4)$$

where E is the electric field strength, v_d is the drift velocity, L is the length of drift region, and t_d is the drift time. Reduced mobility (K_o) is calculated by Eq. (5):

$$K = K_o \cdot (n_o/n) = K_o \cdot (T/T_o) \cdot (P_o/P) \quad (5)$$

where n, T and P are the number density, temperature and pressure of the background gas in the drift region, with standard values of T_o=273.2 K and P_o=101.3 kPa.

The ion mobility is related to molecular parameters, namely to the charge and mass of the sample species and to its collision cross section (CCS) with the background drift gas, through the Revercomb-Mason equation [27]:

$$K = (3/16) \cdot (q/n\Omega) \cdot (2\pi/\mu kT)^{1/2} \quad (6)$$

where k is the Boltzmann constant, q is the analyte ion charge, Ω is the CCS of the ion with the neutral drift gas and μ is the reduced mass of the ion-neutral collision pair.

Inhomogeneity in electric fields and ill-defined length of the drift region require calibration for refined comparison of findings among various drift tubes to obtain CCSs [19, 28-30]. In order to achieve calibration at three significant figures in K_o, 2,6-DtBP was used as the standard. This calibrant was suggested by Eiceman and coworkers [30] based on its stability and reduced tendency for hydration, which leads to a roughly temperature-independent reduced ion mobility constant with a value of 1.42 $cm^2\ V^{-1}\ s^{-1}$. Very recently, this value has been updated to 1.46 $cm^2\ V^{-1}\ s^{-1}$, with slight changes depending on the drift field applied [31]. It can be noted that 2,6-DtBP is particularly appropriate for the

present study since its molecular weight and reduced mobility constant fall within the range of those of the analytes under investigation.

2.3. Quantum computations

Quantum computations based on density functional theory (DFT) at the B3LYP/6-311++G** level were carried out in order to evaluate the conformational constraints involved in the formation of stable proton-bound clusters of the systems under study. Particular efforts were devoted to assessing the energetic stability of the clusters with respect to dissociation in the thermal drift tube of the IM spectrometer. The combination of the B3LYP functional with the 6-311++G** basis set constitutes a consolidated approach that has been shown in many works to perform accurately for the description of a broad range of H-bonded systems and for the prediction of proton affinities [32, 33]. An ensemble of candidate low-energy structures for the protonated monomers and the proton-bound dimers and trimers was built by means of simulated annealing with the universal force field, prior to DFT optimization of the most stable structures for each molecular system. Zero-point corrected energies (ΔE_{ZP}) were determined for each conformer in order to evaluate the stability of the proton-bound dimers and trimers.

The structural calculations were further contrasted with the ion mobility measurements, in terms of the CCSs with the N_2 background gas for the most stable conformation of each type of product ion. For this purpose, we employed the classical trajectory method developed by Jarrold and co-workers [34], and more recently revised by Campuzano and coworkers [35]. Within this method, each of the atoms in the system is treated as an individual scattering center that interacts with N_2 through short-range van der Waals forces and longer-range charge-induced dipole forces. The calculations of the CCS considered a single molecular conformation for each analyte species and were performed at room temperature (28ºC) and at the experimental temperatures (35-80ºC). The Jarrold-Campuzano code has been extensively validated for room temperature N_2

collisions, and it can be expected to be accurate for the present purposes within the temperature range of the experiments. In fact, it will be shown that the variation of the computed cross sections with temperature are roughly consistent with the CCS ~ $T^{-1/5}$ law predicted by Landau-Lifshitz-Schiff collision theory [36]. The effective charges for the atoms were adopted from the Mulliken charges assigned by the DFT computation [35]. The resulting CCSs are in good agreement with the data available from previous studies for the systems under study, in particular for the 2,6-DtBP calibrant and for the (non hydrated) octan-1-ol molecule, as discussed below [30, 37].

3. Results and discussion

3.1. Product ions and effects of concentration and temperature

Ion populations described in Eqs. 1 and 2 depend on vapor concentrations and mobility spectra are shown for octan-2-one in Figure 2a at 40 ºC and vapor concentrations which produced protonated monomer and proton-bound dimer. In Figure 2b, the changes in peak intensities as a function of vapor concentration are shown and are consistent with prior quantiatitve studies. In the absence of the analyte, only RIP (acronym of Reactant Ions Peak; RIP is the peak corresponding to the reactant ions or hydrated proton) is observed and above the limit of detection, the presence of [M] in the ion source results in a decrease in RIP signal intensity via Eq. 1 and the appearance of an ion peak for protonated monomer for octan-2-one (see intensity at 0.0075 mg L^{-1} in Figure 2a). Further increase in vapor concentration results in the proton bound dimer (Eq. 2) with ion peak intensity increasing steadily with increasing vapor concentration.

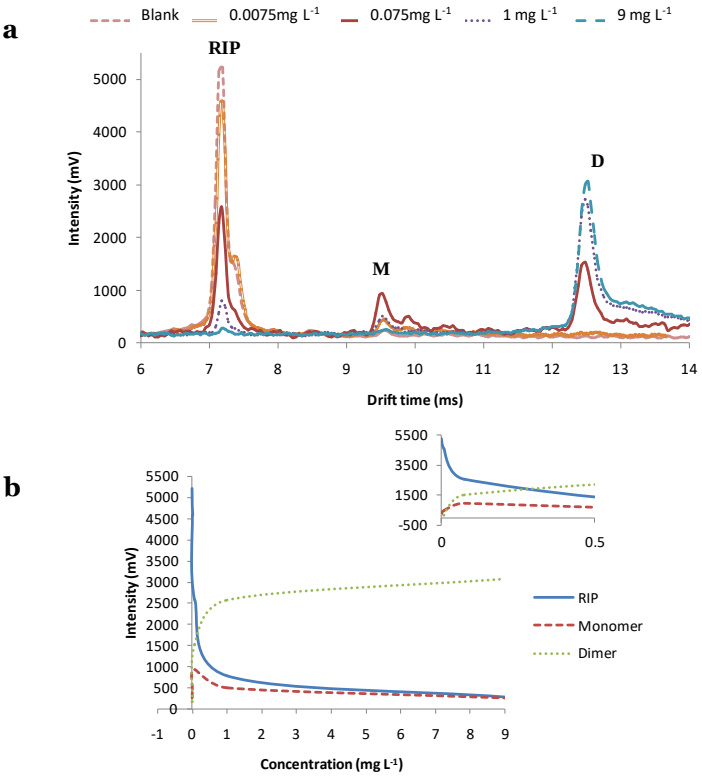

Figure 2. a) Ion mobility spectra at a retention time of 794 s of a blank and octan-2-one at different concentration levels, displaying RIP, protonated monomer (M) and proton-bound dimer (D) ion peaks, b) Plot of the intensity of the three ion peaks vs. sample concentration (the low concentration regime is expanded in the insert for better visualization).

The peak intensity for the protonated monomer levels to a maximum value (at 0.075 mg L^{-1} for the case of octan-2-one) and then decreases with further increases in sample concentration. The upper limit of response for the IMS analyzer is reached at 9 mg L^{-1} (see Figure 2a) where reactant ions ($H^+(H_2O)_n$) are fully depleted and RIP intensity becomes negligible. This qualitative trend of ion peak intensities for the RIP, protonated monomer and proton-bound dimer was observed for all of the analytes studied in this work (ketones, alcohols and

aldehydes) within concentrations in solutions ranging from 0.002 mg L^{-1} up to 12 mg L^{-1}. The analyte concentrations (in gas) in the IM spectrometer are included in Table S1 and a brief summary about how it was calculated is also provided in the Supplementary Information. The findings here demonstrated that the mobility spectrometer exhibited behavior consistent with a separation of ion processes between the reaction region and the drift region, specifically that vapor neutrals of analyte did not significantly enter the drift region.

In addition to the general behavior described above, proton-bound trimers were observed for n-alcohols, only, at concentrations above 0.5 mg L^{-1} and for carbon numbers of 5 and above. As shown in Figure 3 with topographic plots from GC/IMS analysis at 40 °C of mixtures of alcohols, ketones and aldehydes with carbon number of five or more, proton-bound trimers were observed only for alcohols. Ion peaks for protonated monomers and proton-bound dimers with residual intensity for the RIP were also observed.

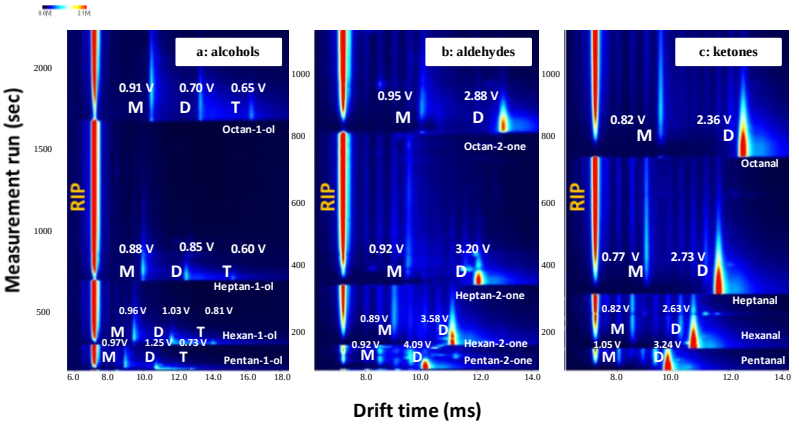

Figure 3. IMS topographic plots of a mixture of C5-C8 (a) 1-substituted alcohols (4 mg L-1), (b) 2-substituted ketones (10 mg L-1) and (c) aldehydes (10 mg L-1). All measurements were performed at a drift tube temperature of 40 °C. M: protonated monomers, D: proton-bound dimers and T: proton-bound trimers.

In contrast, only protonated monomers and proton-bound dimers were observed for the ketones and aldehydes throughout the entire range of concentrations even to the point of saturated response (complete removal of signal for the RIP). Moreover, the proton-bound trimer signal fell below the detection limit of our instrument for the shorter chain alcohols (butan-1-ol and propan-1-ol).

The dependence of ion peak intensities on temperature was investigated from 35 ºC (the lowest drift tube temperature allowed by our equipment) to 80 ºC. Topographic plots in Figure 4 show mobility spectra for four alcohols (pentan-1-ol through octan-1-ol) at three temperatures and the proton-bound dimer is present at appreciable intensity over the entire range of temperatures. This level of thermal stability for proton-bound dimers was observed in our measurements also for the other alcohols and all aldehydes and ketones.

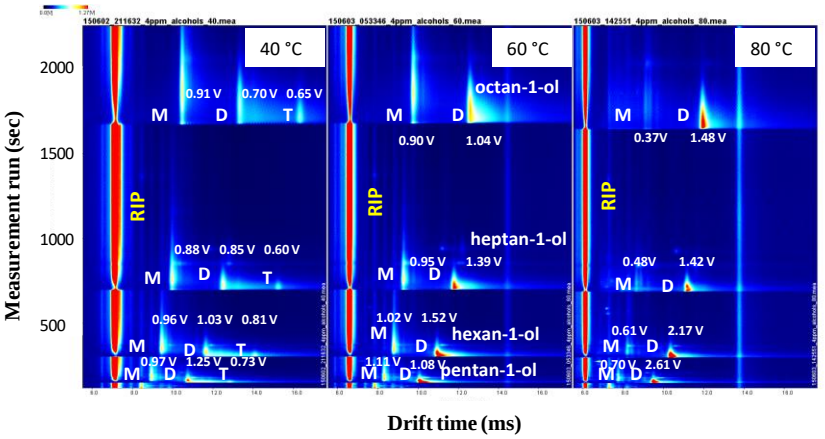

Figure 4. IMS topographic plots of the pentan-1-ol, hexan-1-ol, heptan-1-ol and octan-1-ol (sample concentration 4 mg L-1), measured at drift region temperatures of 40, 60 and 80 oC. M: protonated monomers, D: proton-bound dimers and T: proton-bound trimers.

Interestingly, this finding for the proton-bound dimer is in contrast with the pattern observed for the proton-bound trimer. Ion peaks for the proton-bound trimers were observed only for the alcohols and these decreased rapidly with increased heating, becoming negligible at high temperature. For example, no proton-bound trimer products were detected for any of the alcohols at 50 ºC (Figure 5); at 45 ºC only the longer chain alcohols, heptan-1-ol and octan-1-ol, were observed to form proton-bound trimers sufficiently stable with lifetimes greater than drift time. As discussed below in detail, the proton-bound dimers are formed in particularly compact linear arrangements, whereas the proton-bound trimers adopt more fragile conformations that only for the alcohols involves proton bridges between the three monomeric units.

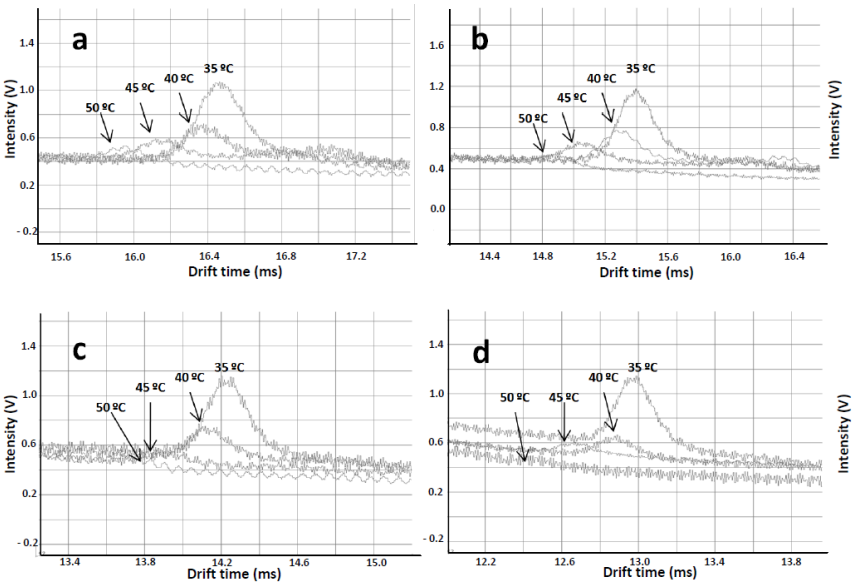

Figure 5. Ion mobility spectra of proton-bound trimers between 35 and 50 ºC a) octan-1-ol, b) heptan-1-ol, c) hexan-1-ol and d) pentan-1-ol.

3.2. Quantum modeling of the proton-bound oligomers

The results of DFT modeling for the lowest energy molecular conformations of the protonated monomers and the proton-bound dimers and trimers of n-alcohols, aldehydes and ketones of this study are illustrated for carbon number eight in Figure 6. It must be remarked that the conformations depicted in Figure 6 are illustrative of an ensemble of low-energy structures with moderate changes in the orientation of the aliphatic chains. Considering all conformations of a given molecule with relative energies within 10 kJ/mol of the most stable one (shown in Figure 6), changes in the CCS of less than 5 Å2 for the dimer and 10 Å2 for the trimer are observed. This scenario is common to all the analytes explored in our experiments, irrespectively of chain length.

The energies required for the dissociation of the most stable conformations of the protonated monomers ($MH^+ \rightarrow MH^+$) and of the proton-bound dimers ($MH^+M \rightarrow MH^+ + M$) and trimers ($MH^+MM \rightarrow MH^+M + M$) of all compounds with eight carbon atoms are listed in Table 3, along with associated CCSs. Protonated monomers with two waters of hydration were also included in the study and are shown in Figure 6a. These were made to assess the mechanism of binding of water, as discussed below.

As shown in Table 3, DFT calculations reproduce correctly the large proton affinities of the three moieties and, hence, the stability of the protonated monomers. Values for ketones were large with respect to those for aldehydes and alcohols. For instance, the computational predictions for the proton affinities of the C5 analytes are ΔE_{ZP}= 830, 788, and 790 kJ mol^{-1} for pentan-2-one, pentanal, and pentan-1-ol, respectively. These were increased slightly to ΔE_{ZP}= 837, 795, and 792 kJ mol^{-1} for octan-2-one, octanal, and octan-2-ol, respectively and were in good agreement with proton affinities values listed in Table 1. This favorable comparison suggests a good level of reliability of the B3LYP/6-311++G** computation.

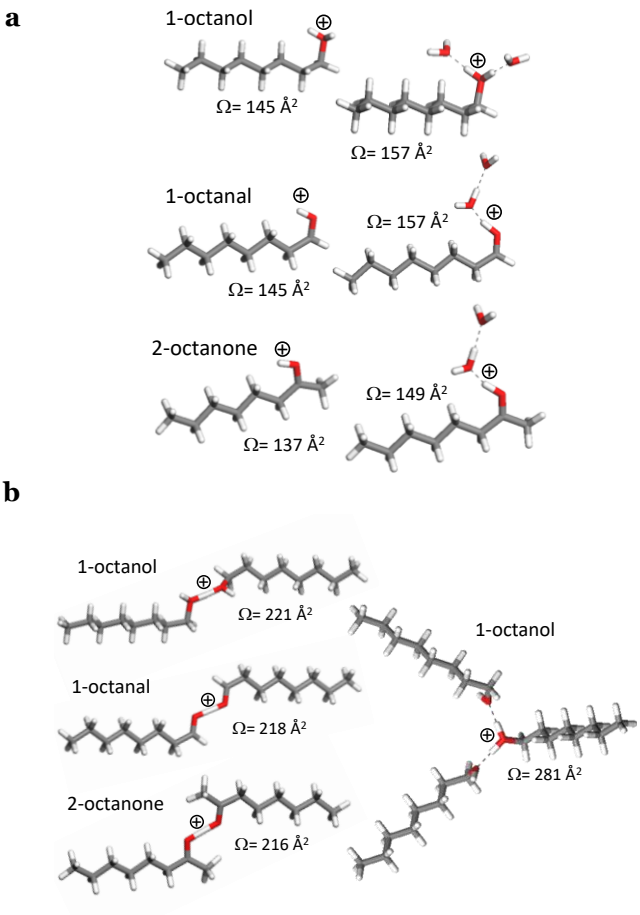

Figure 6. Most stable conformations predicted by the DFT computation for the (a) protonated monomers and (b) the proton-bound dimers and trimers, of the C8 alcohol, aldehyde and ketone included in our study. Hydrated structures are included for the protonated monomers to illustrate the initial stages of water bonding. The computed CCS with background N_2 gas at room temperature (Ω) is indicated next to each structure (see Table 3 for CCS values at higher temperatures). The location of the proton charge in each structure is highlighted with a (+) symbol.

Table 3. Zero-point corrected energies (ΔE_{ZP}), required for the dissociation of the protonated monomers ($MH^+ \rightarrow M+H^+$) and of the proton-bound dimers ($MH^+M \rightarrow MH^+ + M$) and the observed proton-bound trimers ($MH^+MM \rightarrow MH^+M + M$) predicted by the present DFT computation for the C8 alcohol, aldehyde and ketone of our study. The computed N_2 collision CCS (Ω) associated with the predicted conformations of the different adducts (see Figure 6) are indicated for representative temperatures (28, 40 and 80 °C). Energies are in kJ/mol and CCSs are in $Å^2$.

	Octan-1-ol				**Octanal**				**Octan-2-one**			
		Ω				Ω				Ω		
	ΔE_{ZP}	**28**	**40**	**80°C**	ΔE_{ZP}	**28**	**40**	**80°C**	ΔE_{ZP}	**28**	**40**	**80°C**
Monomer	792	145	143	135	795	145	143	134	837	137	134	127
Dimer	139	221	210	200	138	218	216	208	124	216	213	203
Trimer	79	281	278	267								

A remarkable conformational feature in the analysis of the protonated monomers emerges (Figure 6a) which is a V-shape for the two O-H bonds in R-O-H_2^+ with the protonated end group of the alcohols versus the single O-H bonds in the [R=O-H]$^+$ protonated groups of the aldehydes and ketones. In the alcohol, the charge is evenly distributed between the two V-shaped bonds, although both O-H+ bond distances take a similar value of 1.0 Å as in the single bonds of the aldehydes and ketones. Figure 6a also illustrates that such differentiated conformations have a direct influence on the structure of the first hydration shell of the protonated monomers, as the hydration of the alcohols proceeds in a branched-type arrangement sustained by water molecules bound to each of the O-H bonds. In contrast, aldehydes and ketones exhibit only a single H bond and an initially more linear organization of the water molecules. More importantly, the V-shaped arrangement of the terminal R-OH_2^+ group of the protonated alcohols plays a key role in the conformational space available for the subsequent stabilization of the proton-bound clusters.

The proton-bound dimers display similar structures for the three types of molecules, in which the proton charge is located in a linear O··H$^+$··O bond with similar distances (1.2 Å) and also similar bond angles in the C-O··H$^+$ or C=O··H$^+$ groups (120º), see Figure 6b. In all cases, the two aliphatic chains in the proton-bound dimer are oriented to avoid steric overlaps. These dimeric structures are similar to those proposed previously for related systems [38], and lead to quite stable proton-bound complexes, with computed energies similar for the three types of systems under study (e.g., 139, 138 and 124 kJ/mol for octan-1-ol, octanal and octan-2-one, respectively). This finding is in line with previous thermodynamic studies [39, 40] and serves to understand the persistence of the proton-bound dimers of all the alcohols, aldehydes and ketones of this study in the IM spectra recorded over the whole range of temperatures investigated (up to 80 ºC).

There is nevertheless a key conformational difference between the proton-bound dimers of the alcohols with respect to those of the aldehydes and ketones. The proton-bound dimers of alcohols are characterized by two free O-H bonds that have the potential to participate in the formation of stable proton-bound trimers. This differs from the R-C=O··H$^+$··O=C-R moieties of aldehydes and ketones which lack exposed polar groups and result in an overall conformational arrangement impeding the binding of a third monomer. This aspect has been recognized previously for related systems where proton-bound dimers were not as strongly stabilized by carbonyl proton bonds [38, 41, 42].

Figure 6b shows that octan-1-ol forms a stable proton-bound trimer where charge is distributed evenly among two OH bonds (both maintaining a 1.0 Å bond distance) of a central protonated monomer to bind two molecules in a branched configuration with a bond distance of 1.5 Å in each of the two bonds. This same feature was found for the rest of alcohols considered in this work. The DFT predicted stabilization energy is 79 kJ/mol (i.e., the energy required to dissociate it into a neutral monomer and a proton-bound dimer). In contrast to these structural features found for the alcohols, the aldehydes and ketones can only

form the proton-bound trimer through the binding of the third monomer via long range non-specific interactions without significant perturbation of the proton-bound dimer. These latter much weaklier bound trimeric aggregates are not sufficiently stable as to reach the detection stage of the spectrometer at the temperatures of the present experiments.

Significantly, the stabilization energy computed for the proton-bound trimer is essentially constant across the range of alcohols (e.g. ~79 kJ/mol for propan-1-ol and octan-1-ol). This suggests that the lack of proton-bound trimers for the smaller alcohols (propan-1-ol and butan-1-ol) is plausibly related to the kinetics of the formation stage (rather than to dissociation in the drift region). Presumably, only the alcohols with longer chains achieve the dissipation of energy required to stabilize the proton-bound trimer after formation via dimer-monomer collisions.

3.3. Ion mobilities and hydration of the product ions

The experimental calibrated reduced ion mobilities and the corresponding CCSs with the N_2 drift gas for the species included in our study are given in Table 4. For the calculation of the mobilities, eq. (7) was used taking the most recent value of K_o= 1.46 $cm^2\ V^{-1}\ s^{-1}$ for 2,6-DtBP found in the literature [43].

$$K_o\ (unknown) / K_o\ (standard) = t_d\ (standard) / t_d\ (unknown) \qquad (7)$$

In spite of different K_o values can be found in bibliography for the same ion due to inhomogeneities in temperature and electric field or contamination of buffer gas with moisture or other volatile compound [43], the K_o values obtained in this paper (Table 4) are close to some found in other publications. For example, Xie et al. [44] reported a K_o value of 1.560 $cm^2\ V^{-1}\ s^{-1}$ for butanone which is close to the value reported in our case (see Table 4).

As a first general trend, the ion mobilities are found to increase in the order ketones > aldehydes > alcohols. For instance, for the protonated monomers of octan-2-one, octanal and octan-1-ol, the reduced ion mobilities at T= 80 ºC are

K_0^{calib}= 1.259, 1.200 and 1.144 $cm^2\ V^{-1}\ s^{-1}$, and the corresponding CCSs are Ω (N_2)= 167, 175 and 183 $Å^2$, respectively. This is in qualitative agreement with the previous study of Karpas [45], which concluded that the end position of the COH and CHO groups in the 1-alcohols and 1-aldehydes, as compared to the corresponding 2-ketone analogues, lead to stronger interactions with the background gas, and, hence to greater CCSs and smaller ion mobilities.

Table 4. Drift time, $\mathbf{t_d}$ (in ms), calibrated reduced ion mobility, $\mathbf{K_o}$ (in $cm^2\ V^{-1}\ s^{-1}$), and calibrated CCSs, Ω (in $Å^2$), (with 2,6-DtBP as calibrant) derived from the present experiments for all products ions observed at 40, 60 and 80 ºC. Note that proton-bound trimers were only present in the IMS spectra for the heavier alcohols at T= 40 ºC.

		monomers			**dimers**			**trimers**		
	T	$\mathbf{t_d}$	$\mathbf{K_o}$	**Ω**	$\mathbf{t_d}$	$\mathbf{K_o}$	**Ω**	$\mathbf{t_d}$	$\mathbf{K_o}$	**Ω**
Octan-1-ol	40	10.474	1.123	198	13.342	0.881	241	16.350	0.719	291
	60	9.753	1.133	190	12.608	0.877	235	-	-	-
	80	9.115	1.144	183	11.970	0.871	230	-	-	-
Octanal	40	9.958	1.181	189	12.941	0.909	234	-	-	-
	60	9.288	1.190	182	12.216	0.905	228	-	-	-
	80	8.687	1.200	175	11.576	0.901	222	-	-	-
Octan-2-one	40	9.508	1.237	180	12.479	0.942	226	-	-	-
	60	8.881	1.245	174	11.836	0.934	221	-	-	-
	80	8.281	1.259	167	11.261	0.926	216	-	-	-
Heptan-1-ol	40	9.989	1.177	191	12.510	0.940	227	15.24	0.772	272
	60	9.295	1.189	183	11.800	0.936	221	-	-	-
	80	8.668	1.203	176	11.220	0.930	217	-	-	-

Heptanal	40	9.450	1.244	181	11.970	0.982	218	-	-	-
	60	9.288	1.190	184	11.350	0.974	213	-	-	-
	80	8.687	1.200	177	10.730	0.972	207	-	-	-
Heptan-2-one	40	8.989	1.308	172	11.560	1.017	210	-	-	-
	60	8.389	1.318	166	10.990	1.006	206	-	-	-
	80	7.815	1.334	159	10.420	1.001	201	-	-	-
Hexan-1-ol	40	9.470	1.242	183	11.660	1.008	214	14.11	0.834	253
	60	8.793	1.257	176	10.960	1.009	207	-	-	-
	80	8.212	1.270	169	10.370	1.006	202	-	-	-
Hexanal	40	8.950	1.314	174	11.040	1.065	202	-	-	-
	60	8.306	1.331	166	10.450	1.058	198	-	-	-
	80	7.758	1.344	160	9.860	1.058	192	-	-	-
Hexan-2-one	40	8.483	1.386	165	10.680	1.101	196	-	-	-
	60	7.916	1.396	159	10.100	1.094	191	-	-	-
	80	7.382	1.412	152	9.584	1.088	187	-	-	-
Pentan-1-ol	40	8.954	1.313	176	10.760	1.092	199	12.85	0.915	232
	60	8.326	1.328	169	10.090	1.096	192	-	-	-
	80	7.783	1.340	163	9.516	1.096	187	-	-	-
Pentanal	40	8.452	1.391	164	10.060	1.169	184	-	-	-
	60	7.826	1.412	157	9.506	1.163	180	-	-	-
	80	7.273	1.434	150	8.953	1.165	174	-	-	-
Pentan-2-one	40	8.006	1.469	158	9.740	1.207	180	-	-	-
	60	7.472	1.479	152	9.207	1.201	176	-	-	-
	80	6.955	1.499	146	8.723	1.195	172	-	-	-

Butan-1-ol	40	8.453	1.391	170	9.854	1.193	185	-	-	-
	60	7.844	1.409	163	9.197	1.202	178	-	-	-
	80	7.296	1.429	156	8.646	1.206	172	-	-	-
Butanal	40	10.059	1.169	199	9.095	1.293	168	-	-	-
	60	9.506	1.163	194	8.551	1.293	163	-	-	-
	80	8.953	1.165	188	8.044	1.296	158	-	-	-
Butanone	40	7.572	1.553	153	8.873	1.325	167	-	-	-
	60	7.055	1.567	147	8.356	1.323	162	-	-	-
	80	6.571	1.587	141	7.905	1.319	158	-	-	-
Propanol	7.959	1.478	165	8.946	1.315	171	-	-	-	
	7.399	1.494	158	8.332	1.327	164	-	-	-	
	6.886	1.514	152	7.799	1.337	158	-	-	-	
Propanal	7.715	1.524	161	8.009	1.468	153	-	-	-	
	6.974	1.585	150	7.476	1.479	147	-	-	-	
	6.521	1.599	144	7.009	1.488	142	-	-	-	
Acetone*	-	-	-	7.982	1.473	153	-	-	-	
	-	-	-	7.496	1.475	148	-	-	-	
	-	-	-	7.065	1.476	143	-	-	-	

*The signal of the acetone monomer could not be determined as it overlapped with the RIP.

In this context, a key factor that affects the mobility of the product ions is their degree of hydration. It is broadly recognized that analyte ions formed in the ^{3}H ionization region of IM spectrometers are typically hydrated by ambient water and the $H^+(H_2O)_n$ clusters generated in the ion source [18]. Oligomerization occurs then in terms of the water displacement reactions described by Eqs. 1-3

[42]. The degree of hydration of the ions in our experiments was exposed by monitoring the variation of their mobility constants with temperature as derived from the observed drift times [46]. Dehydration is expected to occur as temperature is increased, leading to greater mobility constants. This is consistent with results shown in Table 4, where an appreciable decrease in the CCSs of the product ions occurs with increased temperature from 40 to 80 ºC. The rate of change is similar for the three families of compounds and it is greater for the protonated monomers than for the proton-bound dimers (in the case of C8). In general, the experimentally determined values and their comparison with the computational results (Table 3) suggest that protonated monomers are appreciably more hydrated than proton-bound dimers and also than proton-bound trimers, as discussed below.

The predicted CCS from the trajectory method for the B3LYP molecular structure of protonated 2,6-DtBP at room temperature was Ω (2,6-DtBP) = 144 Å^2. In comparison, a CCS of 145 Å^2 is obtained through Eqs. 4-6, from the latest value of the reduced mobility constant of 2,6-DtBP (K_o= 1.46 cm^2 V^{-1} s^{-1}). Such an excellent concordance between the IMS experiment and the computation for the bare 2,6-DtBP molecule further supports the reliability of the theoretical framework and confirms that the 2,6-DtBP molecule is reluctant to hydration (what constitutes the main reason for its use as calibrant). CCSs derived from our measurements for the protonated monomers are much larger than expected for the non-hydrated species. For instance, for octan-1-ol, octanal and octan-2-one, Ω ranges experimentally between 198 to 183, 189 to 175 and 180 to 167 Å^2 for temperatures from 40 to 80 ºC. These contract with the smaller values predicted by the B3LYP computation, of 143 to 135, 143 to 134, and 134 to 127 Å^2, respectively (see Table 3). The bigger CCSs values obtained from our measurement are indicative of a significant degree of hydration of the protonated sample molecules. As temperature is increased and dehydration occurs, measured CCSs progressively approach the computational values for the un-hydrated protonated monomer. There is nonetheless a difference of ca. 50 Å^2, even at the highest temperature (80 ºC) where measured CCSs are larger than

the corresponding computational values. The inclusion of only two water molecules in the protonated monomer leads to an increase in the CCS of 12 Å^2 (see conformations and CCS values in Figure 6a).

Interestingly, the experimental CCSs observed for the proton-bound dimers are much closer to the quantum predictions; in paticular, a significantly better agreement is found between the experimental and computational values at high temperature. For instance, Table 3 shows that, for the octan-1-ol, octanal and octan-2-one proton-bound dimers, the measured CCSs at 80 ^{0}C are 230, 222 and 216 Å^2, in comparison to the calculated values of 200, 208 and 203 Å^2, respectively. Moreover, for the octan-1-ol proton-bound trimer, the experimental CCS at 40 ^{0}C (291 Å^2) also compares fairly well with the computational one (278 Å^2). Such trend is remarkable and leads to the conclusion that the proton-bound dimers (and correspondingly the observed proton-bound trimers) of the linear alcohols, aldehydes and ketones under study are much less hydrated than the corresponding protonated monomers. The rationalization of this finding can be traced back to the compact structure adopted by the polar groups as the proton bridge is formed in the dimers, which constrains the formation of the hydration shell.

4. Conclusions

The main conclusion from these studies is that ion mobility spectra for low molar mass oxygen-containing molecules contain ion peaks whose presence in the spectrum correlates with ion energies from computational modeling. All substances of alcohols, aldehydes, and ketones with three to eight carbons were predicted to form protonated monomer and also proton-bound dimers of stabilities in excess of 120 to 140 kJ/mol. Such energies provided ion lifetimes for the proton-bound dimers which exceeded resident time of ion swarms in the drift region and appeared as ion peaks in mobility spectra. This was consistent with a compact structure of the linear O··H$^+$··O proton bridge that is similarly formed for the three types of molecules.

In contrast, proton-bound trimers of ketones and aldehydes were insufficiently stable in the 10 to 20 ms time scale and were not observed in spectra. The proton-bound trimer for alcohols of five carbon number and above exhibited lifetimes sufficient to be observed in mobility spectra. While ion lifetimes were not determined, proton-bound trimers of alcohols were near those of residence times in the drift region, as increases in temperature from 35 to 80 ^{o}C resulted in accelerated dissociation of the proton-bound trimer and diminished intensity of the associated ion peaks with full loss of intensity for most above 45 ^{o}C. The stability of M_3H^+ for alcohols was consistent with molecular models where proton-bound trimers are formed from the incorporation of additional monomers to the protonated terminal group [–COH_2]$^+$ of a central monomer in a V-shaped configuration, with a computed stabilization energy of ca. 79 kJ/mol (the energy required for the back dissociation to a neutral monomer and a proton-bound dimer). This structure is impeded in aldehydes and ketones, since the binding of a third monomer to the R-C=O··H$^+$··O=C-R moiety can only take place through non-specific long-range interactions which are too weak to prevent the fragmentation of the proton-bound trimer in the drift region, within the temperature range of the present study.

The effects of vapor concentration were also significant in the appearance of the proton-bound trimer of octan-1-ol, heptan-1-ol, hexan-1-ol and pentan-1-ol and ion peaks were observed only with sample concentrations of 0.5 mg L^{-1} or above. The effects of moisture were also compared between spectra and models where effective collision CCSs with the N_2 drift gas derived from the experiments are considerably larger than the values predicted by the quantum calculations for the bare protonated monomers. Proton-bound dimer and trimer formation results in a significant loss of water molecules bringing values for experimental CCSs to close to the computational ones predicted for the non-hydrated proton-bound dimers. The significant hydration of the protonated monomers plausibly contributes to dynamically stabilize the proton-bound dimers in the ionisation

region through water displacement reactions that account for the removal of the excess of energy required to avoid spontaneous fragmentation.

Conflict of interest

The authors have declared no conflict of interest.

Akcnowledgments

The authors acknowledge support from the Government of Spain (DGICyT Grant CTQ2014-52939R) and from Junta de Andalucia-FEDER (project P12-FQM-4938) for funding this work. We are grateful to I. Campuzano for providing us with the code reported in ref. 35 to compute CCSs.

References

[1] R.G. Ewing, D.A. Atkinson, G.A. Eiceman, G.J. Ewing, A critical review of ion mobility spectrometry for the detection of explosives and explosive related compounds, Talanta 54 (2001) 515-529.

[2] M.A. Mäkinen, O.A. Anttalainen, M.E. Sillanpää, Ion mobility spectrometry and its applications in detection of chemical warfare agents, Anal. Chem. 82 (2010) 9594-600.

[3] G.A. Eiceman, J.A. Stone, Ion mobility spectrometers in national defence, Anal. Chem. 76 (2004) 390A-397A.

[4] H.H. Hill Jr, W.F. Siems, R.H. St. Louis, Ion mobility spectrometry, Anal. Chem. 62 (1990) 1201A-1209A.

[5] G.A. Eiceman, Z. Karpas, H.H. Hill, Jr, Ion Mobility Spectrometry, CRC press, United States, Third Edition, 2013, Chapter 4.

[6] T. Fink, J.I. Baumbach, S. Kreuer, Ion mobility spectrometry in breath research, J. Breath Res. 8 (2014) 027104.

[7] M. Basanta, R.M. Jarvis, Y. Xu, G. Blackburn, R. Tal-Singer, A. Woodcock, D. Singh, R. Goodacre, C.L.P. Thomas, S. J. Fowler, Non-invasive metabolomic analysis of breath using differential mobility spectrometry in patients with chronic

obstructive pulmonary disease and healthy smokers, Analyst 135 (2010) 315-320.

[8] E. Szymańska, E. Brodrick, M. Williams, A. N. Davies, H.J. van Manen, L.M.C. Buydens, Data size reduction strategy for the classification of breath and air samples using multicapillary column-ion mobility spectrometry, Anal. Chem. 87 (2015) 869-875.

[9] W. Vautz, J.I. Baumbach, J. Jung, Beer Fermentation Control Using Ion Mobility Spectrometry-Results of a Pilot Study, J. I. Brewing 112 (2006) 157-164.

[10] R. Garrido-Delgado, M.M. Dobao-Prieto, L. Arce, J. Aguilar, J.L. Cumplido, M. Valcárcel, Ion Mobility Spectrometry versus Classical Physico-chemical Analysis for Assessing the Shelf Life of Extra Virgin Olive Oil According to Container Type and Storage Conditions, J. Agric. Food Chem. 63 (2015) 2179–2188.

[11] M. Camara, N. Gharbi, A. Lenouvel, M. Behr, C. Guignard, P. Orlewski, D. Evers, Detection and quantification of natural contaminants of wine by gas chromatography-differential ion mobility spectrometry (GC-DMS), J. Agric. Food Chem. 61 (2013) 1036-43.

[12] T. Limero, E. Reese, J. Trowbridge, R. Hohman, J.T. James, The volatile organic analyzer (VOA) aboard the international space station, 32nd International Conference on Environmental Systems, SAE Technical Paper 2002-01-2407, San Antonio, Texas, 2002.

[13] T. Limero, E.G. Nazarov, M. Menlyadiev, G.A. Eiceman, Characterization of ion processes in a GC/DMS air quality monitor by integration of the instrument to a mass spectrometer, Analyst 140 (2015) 922-930.

[14] K. Lamote, M. Vynck, J. Van Cleemput, O. Thas, K. Nackaerts, J.P. van Meerbeeck, Detection of malignant pleural mesothelioma in exhaled breath by multicapillary column/ion mobility spectrometry (MCC/IMS), J. Breath Res. 10 (2016) 046001.

[15] L. Peng, L. Hua, E. Li, W. Wang, Q. Zhou, X. Wang, C. Wang, J. Li, H. Li, Dopant titrating ion mobility spectrometry for trace exhaled nitric oxide detection, J. Breath Res. 9 (2015) 016003.

[16] K.E. Burnum-Johnson, S. Nie, C.P. Casei, M.E. Monroe, D.J. Orton, Y.M. Ibrahim, M.A. Gritsenko, T.R. Clauss, A.K. Shukla, R.J. Moore, S.O. Purvine, T. Shi, W. Qian, T. Liu, E.S. Baker, R.D. Smith, Simultaneous Proteomic Discovery and Targeted Monitoring using Liquid Chromatography, Ion Mobility Spectrometry, and Mass Spectrometry, Mol. Cell. Proteomics 15 (2016) 3694-3705.

[17] U. Distler, J. Kuharev, P. Navarro, S. Tenzer, Label-free quantification in ion mobility-enhanced data-independent acquisition proteomics, Nat. Protoc. 11 (2016) 795-812.

[18] R.G. Ewing, G.A. Eiceman, J.A. Stone, Proton-bound cluster ions in ion mobility spectrometry, Int. J. Mass. Spectrom. 193 (1999) 57–68.

[19] G.A. Eiceman, E.G. Nazarov, J.E. Rodriguez, J.F. Bergloff, Positive Reactant Ion Chemistry for Analytical, High Temperature Ion Mobility Spectrometry: Effects of Electric Field of the Drift Tube and Moisture, Temperature, and Flow of the Drift Gas, Int. J. Ion Mobility Spectrom. 1 (1998) 28–37.

[20] M. Mäkinen, M. Sillanpää, A.K. Viitanen, A. Knap, J.M. Mäkela, J. Puton, The effect of humidity on sensitivity of amine detection in ion mobility spectrometry, Talanta 84 (2011) 116-121.

[21] A.K. Viitanen, T. Mattila, J.M. Mäkelä, M. Marjamäki, O. Anttalainen, J. Keskinen, Experimental study of the effect of temperature on ion cluster formation using ion mobility spectrometry, Atmos. Res 90 (2008) 115–124.

[22] H. Borsdorf, R.G. Ewing, Gas phase ion chemistry: what do we know about reactions and ion formation?, Int. J. Ion Mobil. Spec. 18 (2015) 31–32.

[23] R.G. Ewing, Kinetic Decomposition of Proton Bound Dimer Ions with Substituted Amines, PhD dissertation, New Mexico State University, 1996.

[24] R.G. Ewing, G.A. Eiceman, C.S. Harden, J.A. Stone, The kinetics of the decompositions of the proton bound dimers of 1,4-dimethylpyridine and dimethyl methylphosphonate from atmospheric pressure ion mobility spectra, Int. J. Mass Spectrom. 255-256 (2006) 76-85.

[25] M.Y. Rajapakse, J.A. Stone, G.A. Eiceman, Decomposition Kinetics of Nitroglycerine•Cl–(g) in Air at Ambient Pressure with a Tandem Ion Mobility Spectrometer, J. Phys. Chem. A 118 (2014) 2683–2692.

[26] R.M.M.Y. Rajapaksea, G.A. Eiceman, J.A. Stone, An Experimental and Theoretical Study of the Thermal Decomposition of the Ethylene Glycol Dinitrate Chloride Adduct Ion, Int. J. of Mass Spectrom. 371 (2014) 28–35.

[27] H.E Revercomb, E.A. Mason, Theory of plasma chromatography/gaseous electrophoresis. Review, Anal. Chem. 47 (1975) 970-983.

[28] C.L. Crawford, B.C. Hauck, J.A. Tufariello, C.S. Harden, V. McHugh, W.F. Siems, H.H., Jr. Hill, Accurate and reproducible ion mobility measurements for chemical standard evaluation, Talanta 101 (2012) 161–170.

[29] A.K. Viitanen, T. Mauriala, T. Mattila, A. Adamov, C.S. Pedersen, J.M. Mäkelä, M. Marjamäki, A. Sysoev, J. Keskinen, T. Kotiaho, Adjusting mobility scales of ion mobility spectrometers using 2,6-DtBP as a reference compound, Talanta 76 (2008) 1218–1223.

[30] G.A. Eiceman, E.G. Nazarov, J.A. Stone, Chemical standards in ion mobility spectrometry, Anal. Chim. Acta. 493 (2003) 185-194.

[31] B.C. Hauck, W.F. Siems, C.S. Harden, V.M. McHugh, H.H. Hill, Jr., Determination of E/N Influence on Ko Values within the Low Field Region of Ion Mobility Spectrometry, J. Phys. Chem. A 121 (2017) 2274–2281.

[32] N.L. Zakharova, C.L. Crawford, B.C. Hauck, J.K. Quinton, W.F. Seims, H.H., Jr

Hill, A.E. Clark, An assessment of computational methods for obtaining structural information of moderately flexible biomolecules from ion mobility spectrometry, J. Am. Soc. Mass. Spectrom. 23 (2012) 792-805.

[33] A. Taskinen, V. Nieminen, E. Toukoniitty, D.Y. Murzin, M. Hotokka, Proton affinities of ketones, vicinal diketones and α-keto esters: a computational study, Tetrahedron 61 (2005) 8109–8119.

[34] M.F. Mesleh, J.M. Hunter, A.A. Shvartsburg, G.C. Schatz, M.F. Jarrold, Structural Information from Ion Mobility Measurements: Effects of the Long-Range Potential, J. Phys. Chem. 100 (1996) 16082-16086.

[35] I. Campuzano, M.F. Bush, C.V. Robinson, C. Beaumont, K. Richardson, H. Kim, H.I. Kim, Structural characterization of drug-like compounds by ion mobility mass spectrometry: comparison of theoretical and experimentally derived nitrogen collision cross sections, Anal. Chem. 84 (2012) 1026–1033.

[36] L.D. Landau, E.M. Lifshitz, Quantum Mechanics, Non-Relativistic Theory. Pergamon Press, Ltd., London, 1958.

[37] H.Y. Han, H.M. Wang, H.H. Jiang, M. Stano, M. Sabo, S. Matejcik, Y.N. Chu, Corona Discharge Ion Mobility Spectrometry of Ten Alcohols, Chin. J. Chem. Phys. 22 (2009) 605-610.

[38] E.V. Lantsuzskaya, A.V. Krisilov, A.M. Levina, Structure of the cluster ions of ketones in the gas phase according to ion mobility spectrometry and ab initio calculations, Russ. J. Phys. Chem. A 89 (2015) 1838–1842.

[39] Z. Izadi, M. Tabrizchi, H. Farrokhpour, Thermodynamic study of proton-bond dimers formation in atmospheric pressure: An experimental and theoretical study, J. Chem. Thermodyn. 63 (2013) 17–23.

[40] E. Jazan, A.S.G. Khoob, A kinetic study on decomposition of proton-bound dimer using data obtained by ion mobility spectrometry, Chem. Phys. 439 (2014) 30–35.

[41] B.C. Hauck, E.J. Davis, A.E. Clark, W.F. Siems, C.S. Harden, V.M. McHugh, H.H., Jr. Hill, Determining the water content of a drift gas using reduced ion mobility measurements, Int. J. Mass. Spectrom. 368 (2014) 37–44.

[42] Y. Valadbeigi, H. Farrokhpour, M. Tabrizchi, Effect of Hydration on the Kinetics of Proton-Bound Dimer Formation: Experimental and Theoretical Study, J. Phys. Chem. A 118 (2014) 7663–7671.

[43] R. Fernandez-Maestre, C.S. Harden, R.G. Ewing, C.L. Crawford, H.H. Jr Hill, Chemical standards in ion mobility spectrometry, Analyst 135 (2010) 1433–1442.

[44] Z. Xie, S. Sielemann, H. Schmidt, F. Li, J.I. Baumbach, Determination of acetone, 2-butanone, diethyl ketone and BTX using HSCC-UV-IMS, Anal. Bioanal. Chem. 372 (2002) 606–610.

[45] Z. Karpas, The structure and mobility in air of protonated ketones, Int. J. Mass. Spectrom. 107 (1991) 435–440.

[46] H. Borsdorf, T. Mayer, Temperature dependence of ion mobility signals of halogenated compounds, Talanta 101 (2012) 17-23.

Supplementary Information

Table S1. Estimation of the concentration of gas in HS, of the mass injected into the GC column and of the analyte concentration introduced in the ^{3}H-IMS, illustrated for aldehydes at a constant value of solution concentration of 0.5 mg·L$^{-1.}$

Compounds	Henry's law constant at 60 °C (mol (kg bar^{-1}))	Gas concentration in HS (ng mL^{-1})	Injected mass in GC column (pg)	Concentration in IMS (pg mL^{-1})
Octanal	9.7	1.9	373	0.1
Heptanal	9.3	1.9	387	0.2
Hexanal	13.3	1.4	272	0.4
Pentanal	14.2	1.3	254	0.6
Butanal	14.8	1.2	245	0.7
Propanal	17.6	1.0	206	0.8

See text below for details about the estimation method*

*Analyte concentrations in the IM spectrometer

The present paper shows that the distribution of proton-bound oligomers is dependent on the concentration of analyte in the ionization region of the IM spectrometer. To this respect, it is important to take into account that equimolar solutions of different compounds typically lead to different amounts of gas-phase species injected into the IM spectrometer, due to the volatility of each analyte and column retention effects.

The gas concentration introduced in the GC column in our experiments was calculated from Henry's law and the ideal gas equation, considering the concentration of the sample solution and the temperature applied to create the gas compounds in the HS:

$$n_g = PV/(RT) = (C_S V)/(RTK_H) \quad (1)$$

where n_g is the number of moles of analyte in the gas phase, C_S is the concentration of analyte in the solution, K_H is Henry's constant, P is the gas pressure in the HS, R is ideal gas constant, T is temperature of the HS (60 ºC) and V is the volume available in the vial (19 mL). The final concentration of each compound introduced in the IMS ionization region is calculated from the expression:

$$[C]_{IMS} = \frac{Mass\ flux\ (pg \cdot s^{-1})}{Drift\ flow\ (mL \cdot s^{-1})} = \frac{\frac{injected\ \ mass\ (pg)}{retention\ \ time\ (s)}}{4.2\ mL \cdot s^{-1}} \quad (1)$$

where the drift gas flow was of 4.2 mL s^{-1} in our experiments, and the mass flux is calculated as the ratio of the injected mass over the retention time of the analyte in the GC column.

Table S1 shows the estimate total masses (calculated using Eqs. 1 and 2) that enter the GC stage and the IMS spectrometer for the aldehydes of the present study (note that, Henry's constants for the alcohols and ketones at 60 ºC are not available), considering that only 200 µL of the gas created in the vial were injected into the GC column. It can be observed that the gas-phase mass in the HS is consistently higher for the compounds with a lower Henry's constant, corresponding to a longer hydrocarbon chain. However, the concentration in the IMS ionization stage is smaller for those compounds due to their longer retention times in the GC column (see values in Table 1). Furthermore, comparing the values of Henry's constant at 25 ºC (Table 1), and the GC retention times (Table 1) for the compounds included in this study, it can be noticed that alcohols plausibly lead to smaller concentrations in the IMS drift tube than ketones and aldehydes, under similar operating conditions. Therefore, the limit of detection (LOD) for alcohols is comparably higher. As an example, the minimum sample concentration detected for octan-2-one and octanal was 25 µg L^{-1}, while for octan-

1-ol it was 75 μg L^{-1}. To compensate this fact, the sample solutions prepared and analyzed for alcohols were more concentrated throughout this work.

Field Induced Fragmentation (FIF) Spectra of Oxygen Containing Volatile Organic Compounds with Reactive Stage Tandem Ion Mobility Spectrometry and Functional Group Classification by Neural Network Analysis

CHAPTER II

ACS Publications

Analytical Chemistry

92 (2020) 5862–5870

Field Induced Fragmentation (FIF) Spectra of Oxygen Containing Volatile Organic Compounds with Reactive Stage Tandem Ion Mobility Spectrometry and Functional Group Classification by Neural Network Analysis

Hossein Shokri[1], Erkinjon G. Nazarov[1], Ben D. Gardner[2], Hsein-Chi Niu[2], Gyoungil Lee[1], John A. Stone[3], Natividad Jurado-Campos[4], and Gary A. Eiceman[1]

[1]*Department of Chemistry and Biochemistry, New Mexico State University, Las Cruces, New Mexico 88003, United States.*

[2]*Collins Aerospace, San Dimas, California 91773, United States.*

[3]*Department of Chemistry, Queens University, Kingston, Ontario Canada K7L 3N6.*

[4]*Department of Analytical Chemistry, University of Córdoba 14071 Córdoba, Spain.*

Field Induced Fragmentation (FIF) Spectra of Oxygen Containing Volatile Organic Compounds with Reactive Stage Tandem Ion Mobility Spectrometry and Functional Group Classification by Neural Network Analysis

Hossein Shokri, Erkinjon G. Nazarov, Ben D. Gardner, Hsein-Chi Niu, Gyoungil Lee, John A. Stone, Natividad Jurado-Campos, and Gary A. Eiceman

ABSTRACT

Mobility isolated spectra were obtained for protonated monomers of 42 volatile oxygen containing organic compounds at ambient pressure using a tandem ion mobility spectrometer with a reactive stage between drift regions. Fragment ions of protonated monomers of alcohols, acetates, aldehydes, ketones and ethers were produced in the middle reactive stage using a 3.3 MHz symmetrical sinusoidal waveform with an amplitude of 1.4 kV and mobility analyzed in a 19 mm long drift region. The resultant Field Induced Fragmentation (FIF) spectra included residual intensities for protonated monomers and fragment ions with characteristic drift times and peak intensities, associated with ion mass and chemical class. High efficiency of fragmentation was observed with single bond cleavage of alcohols and in six-member ring rearrangements of acetates. Fragmentation was not observed, or seen weakly, with aldehydes, ethers, and ketones due to their strained four-member ring transition states. Neural networks were trained to categorize spectra by chemical class and tested with FIF spectra of both familiar and unfamiliar compounds. Rates of categorization were class dependent with best performance for alcohols and acetates, moderate performance for ketones, and worst performance for ethers and aldehydes. Trends in the rates of categorization within a chemical family can be understood as a combination of steric influences influencing the

energy of activation for ion fragmentation. Electric fields greater than 129 Td or new designs of reactive stages with improved efficiency of fragmentation will be needed to extend the practice of reactive stage tandem IMS to an expanded selection of volatile organic compounds.

Keywords: Field induced fragmentation (FIF) spectra, mobility-selected, protonated monomers, neural networks, categorization, chemical class

Introduction

Small hand-held or bench-top instruments based on ion mobility spectrometry (IMS) at ambient pressure have emerged today in clinical research for breath analysis,[1-3] quality control in food production,[4-7] and environmental monitoring of airborne vapors.[8-10] These build upon the historic uses of IMS for chemical measurements in human spaceflight,[11-13] commercial aviation security,[14] and military preparedness.[15-17] The functional component in these analyzers, regardless of model or manufacturer, is a drift tube comprised of an ion source and a drift region where ions pass as swarms through a voltage gradient of a set distance. Selectivity of response is provided in mobility spectra from the preferential ionization of sample and from the drift times of sample-derived ions. While some characteristics of ion shape and size can be extracted[18,19] from mobility spectra using models well-developed for ions in non-clustering atmospheres,[20] understandings for ions in polar, clustering gases (e.g., air) are incomplete, even for carefully controlled experimental conditions.[21,22] As a consequence, interpretations of mobility spectra at ambient pressure are impeded by the approximations in linking ion mobility coefficients with chemical identity through ion size and mass.[23]

Another significant shortcoming with molecular identifications in such IMS analyzers today is the absence of structural information as provided, for example, with fragment ions in electron impact mass spectrometry.[24] In contrast, IMS spectra obtained at ambient pressure usually contain one or two product ion

peaks, often protonated monomers and/or proton bound dimers. While peaks for fragment ions are not routinely observed in mobility spectra, the decomposition of ions at elevated temperatures has been described for butyl acetates[25] and lately for nitro-esters of explosives.[26-28] Ions at ambient pressure can also undergo fragmentation in electric fields >100 Td (or ~14,000 V/cm) as demonstrated in differential mobility spectrometry with ions of aromatic compounds,[29] acetates,[30] organophosphorous compounds,[31] and alcohols.[32,33] Recently, fragments of ions were generated in tandem mobility analyzers from precursor ions that were mobility isolated in a first mobility drift tube, fragmented using a reactive (middle) stage of electric fields[34,35] or thermal fragmenters,[36,37] and mobility analyzed in a second drift tube. Fragment ions derived from these three steps, if specific to a chemical class or functional group, could introduce structural information into mobility spectra and enable molecular identification.

This possibility was suggested first from findings with neural networks where spectra of familiar and unfamiliar compounds were categorized by chemical class.[38-40] Success at spectral classification with unfamiliar chemicals was attributed to a region of drift times between the reactant ion peak ($H^+(H_2O)_n$) and the protonated monomer ($MH^+(H_2O)_y$), where ions of high mobility (or low mass) could be extracted from spectral baselines. Ions with high significance for classification by neural networks were attributed to fragments formed through in-source decomposition possibly from reactions with high-energy reactant ion intermediates such as $N_2^{+\cdot}$ or $H_2O^{+\cdot}$.[41] Some spectral detail could arise also from thermal decomposition, though little progress was made further in exploring the significance of structure information in spectra in the absence of mass analysis of ions. Other concerns included limitations in the resolving power of small drift tubes and inadequate technology to control fragmentation reactions, now possible with wire grid assemblies.[34,35]

The mobility spectra derived from the three steps in reactive stage tandem IMS are termed field induced fragmentation (FIF) spectra similar to the term collision induced dissociation (CID) in tandem mass spectrometry. The benefits

of reactive stage tandem IMS methods are found in the chemical simplicity in fragmenting only a specific ion and in spectral clarity where fragment ions appear on a baseline free of ions from matrix or analyte with other drift times. In a preliminary study of alcohols from propanol to nonanol with this concept, hydrates of protonated monomers of alcohols were dehydrated through the loss of water adducts and finally fragmented to a carbocation.[35] Unlike proton transfer reaction mass spectrometry (PTR-MS) with several successive fragmentations to even smaller mass fragments with increased E/N[42] or multiple fragments with high kinetic energy IMS at 19 torr,[43] only a single fragment ion was observed in the FIF spectra with a fixed (and relatively low) E/N for ion fragmentation.[35] Nonetheless, preliminary results suggested, in plots of drift times for the fragment ions and protonated monomers for alkanes, acetates, and aldehydes, that structural information might be available in the FIF spectra.

The objectives of this work were: A) to produce FIF spectra in a reactive stage tandem IMS at ambient pressure for a set of chemicals with known fragmentation pathways, B) to explore the reaction enthalpies for fragmentation, C) to determine rates of categorization of FIF spectra by chemical class using neural networks, and D) to examine trends in performance for neural network classification within each chemical family. The goals were to benchmark performance of a small reactive stage tandem IMS analyzer with drift region lengths of ~20 mm, to clarify understandings of ion fragmentation in electric fields at ambient pressure, and to disclose the presence of structural information in FIF spectra through neural network categorization of familiar and unfamiliar compounds.

Experimental

Instrumentation

A model 5890 series II gas chromatograph (Hewlett-Packard Corp., Avondale, PA) was equipped with a capillary injection port and 10 meters 0.18

mm ID RTX-200 capillary column (Restek Corp, Bellefonte, PA). This column was connected using a Restek VU2 union connector to a 60 cm length of HT5: AQ, 0.32 mm ID capillary column (SGE Analytical Science). The HT5 capillary column passed through a heated (190°C) stainless steel tube and into the reaction region of the drift tube. Six centimeters of aluminum cladding on the effluent end of this column were removed and the column end was located in the cross section of the drift tube. The drift tube as a reactive stage tandem mobility spectrometer described in detail[35] and used without modification (see schematic in Figure S1 in Supporting Information). The pulse widths of both ion shutters were 200 μs, generated using an in-house shutter controller where a master clock established a time base for data acquisition and the time base for ion shutters 1 and 2. Electric fields in the wire grid fragmenter were supplied using a Modular Intelligent Power Sources (MIPS) version 2.0, 2016 (GAA Custom Electronics, LLC, Kennewick, WA) with a 3.3 MHz sinusoidal amplitude of 1.4 kV applied to one grid of the wire-grid assembly. Wires were interdigitated at 0.63 mm between centers (0.5 mm between planes) with capacitance of 10.9±2 pF. Spectra were acquired using an 18-bit PCI-6281 DAQ interface card (National Instruments, Corp., Austin, TX) and a LabView program developed in-house and termed Linear 2018 version 2.0. Data were acquired at 166.7 kHz for a 20 ms spectrum with resolution of 6 μs. Twenty scans were averaged per spectrum which contained 3333 points per spectrum.

Chemicals and Solutions

Substances included butyl acetate, isopentyl acetate, methyl butyrate, pentyl acetate, ethyl acrylate, heptyl acetate, hexyl acetate, isopropyl acetate, propyl acetate, vinyl acetate, isobutyl acetate, nonyl acetate, octyl acetate, sec-butyl acetate, dibutyl ether, diethyl ether, dihexyl ether, diisopropyl ether, dipentyl ether, dipropyl ether, 2-hexanone, 2-pentanone, 2-decanone, 2-heptanone, 2-nonanone, 2-octanone, methyl isobutyl ketone, pinacolone, butanal, pentanal, hexanal, heptanal, octanal, nonanal, 1-butanol, 1-hexanol, 1-

heptanol, 1-pentanol, 1-propanol, 2-propanol, 2-butanol, 2-methyl-1-propanaol, and 2,6-di-tert-butyl pyridine. These were obtained at highest purity from Sigma-Aldrich (St. Louis, MO). Standard solutions of individual substances at 100 ng/µl were prepared using HPLC grade dichloromethane (Alfa Aesar, Ward Hill, MA). Vapor concentrations ranged from near detection limits to nearly source saturation.

Procedures

Consistency in drift tube performance, including purity and moisture in the drift gas, was monitored daily using reduced mobility coefficients of the reactant ion peak (RIP) and of the protonated monomer for 2,6-di-tert-butyl pyridine. Variations in K_o of these were no more than ±0.002 cm^2/Vs in this study. The oven program for the chromatograph was: initial temperature, 40°C; final temperature, 200°C; and temperature ramp, 10°C/min. Spectral libraries of whole, mobility-selected, and FIF spectra were prepared using individual solutions of 14 acetates, 8 alcohols, 8 ketones, 6 aldehydes, and 6 ethers. Injection volumes were 1 µl for each solution with split-splitless injection times of 30 s. Spectra were acquired continuously throughout the chromatographic elution of a substance providing a range of vapor concentrations inside the drift tube. Mobility-selected spectra were acquired using a delay in ion shutter 2, adjusted for the drift times of protonated monomers of each compound. Field induced fragmentation (FIF) spectra were generated using these same procedures with the 1.4 kV amplitude and 3.3 MHz sinusoidal waveform applied to the wire grid assembly during chromatographic elution of a substance.

Computational studies

Neural Networks

General. All mobility-selected and FIF spectra were pre-processed identically in EXCEL, and MATLAB by removing excess drift times at spectral extremes. The region of drift times between ion shutter 1 and the delay with ion shutter 2 were removed establishing t_d=0 for ion shutter 2. In addition, 0.6 ms from the beginning of each mobility selected or FIF spectrum was removed due to a spectral artifact from the pulse of ion shutter 2. Each spectrum contained 450 drift time bins (2.7 ms) and included the full peak for the slowest protonated monomer. Whole spectra were pre-processed similarly with 1200 drift time bins from 3.33 to 10.52 ms. Only spectra with product ion intensity 3x baseline noise were included in the library and these were baseline corrected and smoothed using a Savitzky–Golay method with polynomial order=2 and points of window=51. The neural network software was NeuralWorks Professional II/Plus version 5.52 (NEURALWARE, Carnegie PA). Parameters for the Back-Propagation network included potential energies (PEs) or input layer elements, 1200 (whole spectra) and 450 (mobility selected and FIF spectra); hidden layers, 1 with 15 PEs; Learn Rule, External Delta-Bar-Delta; Transfer, Tangent Hyperbolic; validation method, root mean square error; convergence criterion, threshold of 0.0010.

Familiar Chemicals. When networks were trained and tested using Familiar Chemicals, every fourth spectrum produced during the chromatographic elution of a substance was removed and added to a test file; all remaining spectra were used in the training step. In general, five to seven spectra per chemical were placed into the test file. Thus, an average of 240 spectra (4 to 8 spectra per chemical) were used for the testing step and an average of 790 spectra (8 to 25 spectra per chemical) were used for the training step.

Unfamiliar Chemicals. When studies were made using unfamiliar chemicals, all spectra from each of five compounds in the spectral library were isolated as the test set (i.e., unfamiliar chemicals); those remaining were used in the training step. Nine unique combinations of training and test sets were made

to allow each compounds to be unfamiliar in one combination with ~700 spectra in the training set and ~330 spectra in the test set.

Findings from Neural Networks and Graphic Presentation. The scores or adjusted average values (AAV) from neural networks can be fractional (e.g., 0.800 or 0.853) for each of five output layers (or chemical class) ranging from an assignment to the correct class (1.000) to complete misassignment for the specific chemical class (0.000). The overall quantitative performance of test spectra can be displayed graphically when AAVs are sorted by magnitude for each spectrum, numbered (N), and plotted as AAV vs. N/Nmax (where Nmax is total number of spectra in the test file). The resulting plot permits convenient quantitative comparisons of performance for multiple train/test studies.[44]

Gaussian Calculations-Enthalpies for reactions corresponding to dehydrations of $MH^+(H_2O)_n$ (n=3) and ion transformation of protonated monomers into fragment ions of the chemical families were calculated using both *Gaussian 09* (Gaussian, Inc., Wallingford CT, 2009) and *Spartan 10* (v.1.1.0, Wave function, Inc., Irving, CA) using DFT density functional B3LYP with the 6-311+G(d,p) basis set. Fragment ions for different chemicals were chosen according to the most abundant fragment ions in spectra from literature references, principally studies using chemical ionization mass spectrometry.[48,49]

Results and discussion

Mobility Selection and Fragmentation of Protonated Monomers, $MH^+(H_2O)_n$

Mobility-selected spectra shown in Figure 1 (dotted line) were obtained by reactive stage tandem ion mobility spectrometry[34,35] where dual ion shutters were used to select protonated monomers by drift time in the first drift region for subsequent mobility analysis in the second drift region. Reactant ions (4.07 ms) and proton bound dimers (5.26 to 9.56 ms) were excluded in mobility-selected

spectra leaving a single peak on a baseline without other discernable peaks. All compounds in the library of oxygen containing compounds with proton affinities from 786 to 850 kJ/mol exhibited intense peaks for protonated monomers (0.4 to 1.2 V at 2.5 x 10^8 V/A gain) with baseline noise of 15 mV and average signal-to-noise of 77. Absolute mass of ~100 ng delivered on column produced vapor concentrations for substances (e.g., 1-propanol) of ~160 mg/m^3 in the ion source and reaction region. Protonated monomers and fragment ions, described below, were mass-analyzed using a wire grid assembly in a drift tube interfaced to a mass spectrometer to confirm identities.

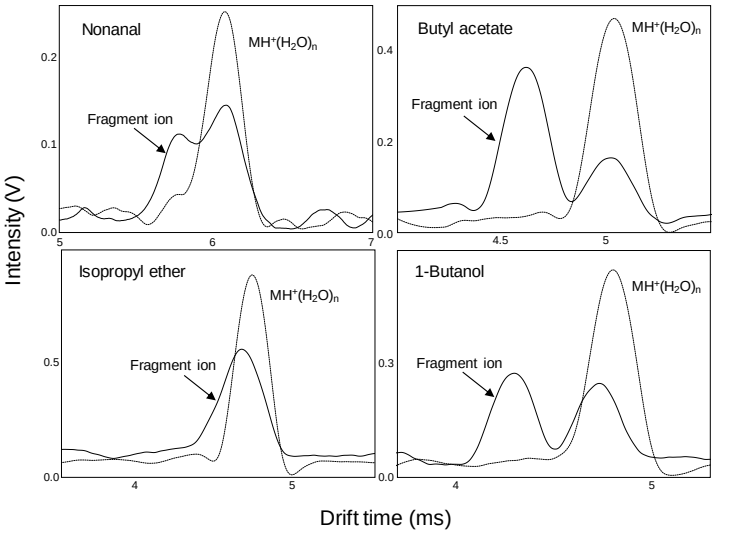

Figure 1. Mobility spectra for mobility isolated protonated monomers of nonanal, butyl acetate, di-isopropyl ether, and 1-butanol, with (solid line) and without (dashed line) ion heating by E/N at 129 Td at 93 °C. Reduced mobility coefficients (cm^2/Vs) for fragment ions and protonated monomers were: 1-butanol 1.88, 2.01 (two fragment ions), 1.79; di-isopropyl ether, 1.98, 1.83; nonanal, 1.78, 1.42; and butyl acetate 2.13, 1.72.

Field induced fragmentation (FIF) spectra were produced using the 1.4 kV amplitude, 3.3 MHz, sinusoidal waveform with calculated average fields (at waveform maximum) in the wire grid assembly of 22.4 kV/cm or 129 Td. In such fields, the average translational kinetic energies for gas ions will include terms from thermal energy and electric fields as described in Equation 1, originally for atomic ion and atomic neutral collisions:[45,46]

$$KE_{ion} = 3/2\ k_B T + 1/2\ m_{ion} V_d^2 + 1/2\ m_b v_d^2 \quad (1)$$

Thermal source Field energy Collision energy

where terms are k_B, Boltzmann constant (1.381×10^{-23} J K^{-1}); T, temperature (K); mb, molecular mass of supporting gas atmosphere (4.81×10^{-26} kg for air), and m_{ion}, mass of ion, here $MH^+(H_2O)_n$. Mayhew and Ellis developed Equation 1 into center-of-mass kinetic energy (KE_{CM}, Eq. 2) for ions in PTR-MS:[47]

$$KE_{CM} = [m_b/(m_{ion} + m_b)] \cdot (KE_{ion} - 3/2k_BT) + 3/2k_BT \quad (2)$$

This equation was used to calculate approximate energies, e.g., 157 Da for 1-hexanol as a six carbon oxygen containing compound) returning thermal energies (J/molecule) of 6.65×10^{-21} at 48 ºC and 7.58×10^{-21} at 93 ºC. When an electric field (129 Td) is included, KE_{CM} (J/molecule) is increased to 1.22×10^{-20} at 48 ºC and 1.48×10^{-20} at 93 ºC, ion energy is doubled over thermal alone. Fragment ions appeared in FIF spectra for some members of each chemical class, as shown in Figure 1, where FIF spectra (solid line) are overlaid with the original mobility selected spectra. Fragment ions can be seen at drift times lower than those for the protonated monomers on a baseline free of other spectral detail. While fragment ions were observed for a large number of compounds (Table 1), fragmentation was not observed for all members within a chemical class or for all chemical classes. Fragmentation efficiency at 93 ºC and 129 Td was 57 to 78.9 % for alcohols, 14.6 to 72.2 % for acetates with three at 0 %, 11.5 to 49.1 % for aldehydes with two at 0 %, all 0 % for ethers apart from 15.6 % for di-propyl ether, and all 0 % for ketones.

Table 1. Intensities protonated monomer peaks in mobility-selected spectra, KE_{CM}, enthalpies for fragmentation and percent fragmentation from FIF spectra at 93°C for normal compounds or homologous series. Spectra were selected at maximum vapor concentration in the gas chromatographic elution profile (see Table S2 in Supporting Information for K_o values for protonated monomers and fragment ions). Lists for branched and unsaturated compounds are given in Table S3 (Supporting Information).

Compounds	Peak intensity (V) $MH^+(H_2O)_n$	Peak intensity (V) Fragment Ion	Percent fragmentation	KE_{CM} (kJmol^{-1})	Enthalphy of fragmentation reaction (kJmol^{-1})	MH^+ Heat Capacity, Cv (J/K-mol)*
Alcohols						
1-propanol	0.52	0.74	58.7	8.09	97.05	85.74
1-butanol	0.24	0.32	57	7.58	85.94	106.53
1-pentanol	0.07	0.24	76.9	7.13	81.56	127.60
1-hexanol	0.05	0.20	78.9	6.74	76.46	146.79
1-heptanol	0.05	0.10	66.4	6.45	78.06	167.75
Acetates						
Propyl acetate	0.47	0.12	20.1	7.61	104.76	129.18
Butyl acetate	0.15	0.39	72.2	7.28	107.38	148.94
Pentyl acetate	0.42	0.08	15.5	6.77	114.01	170.15
Hexyl acetate	0.37	0.06	14.6	6.45	108.69	190.44
Heptyl acetate	0.35	0.00	0.0	6.18	107.08	211.52
Octyl acetate	0.34	0.00	0.0	5.91	106.39	214.94
Nonyl acetate	0.29	0.00	0.0	5.73	105.71	251.99
Aldehydes						
Butanal	0.58	0.00	0.0	8.08	57.00	91.70
Pentanal	0.49	0.06	11.5	7.57	54.72	111.56
Hexanal	0.46	0.00	0.0	7.11	54.59	132.49
Heptanal	0.32	0.12	28.0	6.74	51.86	152.63

Octanal	0.25	0.17	40.5	6.42	49.12	172.91
Nonanal	0.14	0.13	49.1	6.14	50.58	193.72
Ketones						
2-pentanone	0.63	0.00	0.0	7.91	149.58	115.07
2-hexanone	0.56	0.00	0.0	7.43	156.03	135.54
2-heptanone	0.58	0.00	0.0	7.02	166.67	155.07
2-octanone	0.56	0.00	0.0	6.68	159.95	176.13
2-nonanone	0.46	0.00	0.0	6.38	165.90	195.92
2-decanone	0.32	0.00	0.0	5.72	175.03	217.29
Ethers						
Diethyl ether	0.53	0.00	0.0	8.44	102.55	104.44
Dipropyl ether	0.56	0.10	15.6	7.46	91.62	144.87
Dibutyl ether	0.48	0.00	0.0	6.81	100.00	186.05
Dipentyl ether	0.40	0.00	0.0	6.27	103.09	226.42
Dihexyl ether	0.29	0.00	0.0	5.87	104.24	267.25

* Cv is the contribution to heat capacity due to vibrational motion at 298.15 K from *Gaussian* calculations.

Calculated Reaction Enthalpies and Extent of Fragmentation

Reaction enthalpies are shown in Figure 2 for the fragmentation of protonated monomers of normal compounds or homologous series through one of three pathways: alcohols and aldehydes underwent loss of H_2O with the formation of a carbocation,[35,42,49] ketones and ethers lost an alkene to form a carbocation,[48,49] and acetates rearranged to protonated acetic acid and an alkene.[30,49,50] Patterns of reaction enthalpies as a function of carbon number can be seen to have significant differences between chemical families ranging from average high of 160 kJ/mole for ketones to average low of 54 kJ/mole for aldehydes. Protonated monomers of alcohols and acetates were abundantly fragmented with average enthalpies of 108 and 84 kJ/mole respectively, yet

ethers averaged 100 kJ/mole and aldehydes averaged 54 kJ/mole with comparatively low levels of fragmentation.

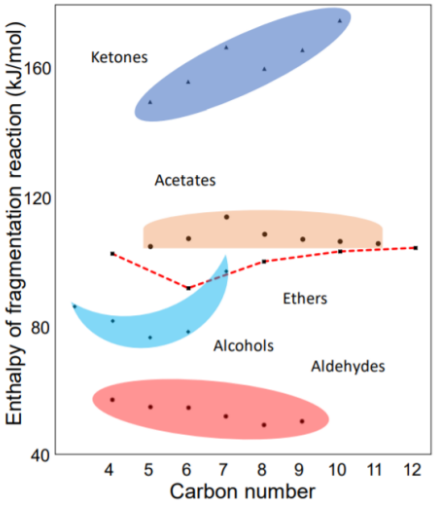

Figure 2. Plot of Reaction Enthalpy calculated for fragmentation of protonated monomer of normal or homologous oxygen containing volatile organic compounds.

Of the five classes of these oxygen-containing volatile organic compounds, three chemical classes (ketones, aldehydes, and ethers) are known to undergo fragmentation via rearrangements through a strained four-member ring transition states[48-49] as shown here:

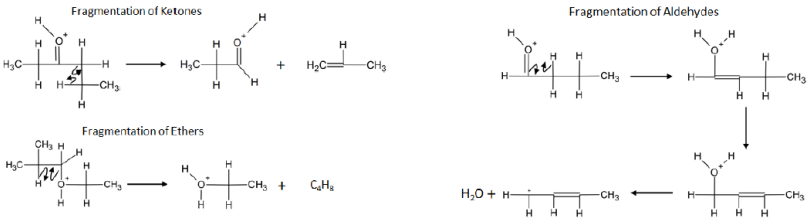

These four-member ring transition states are strained in bond angles with comparatively large energies of activation for the fragmentation from protonated monomers. This common pattern matched experimental finding (Table 1) where the extent of fragmentation for aldehydes was minor despite favorable reaction enthalpies (Fig. 2) and where fragmentation ethers and ketone could not be observed (apart from di-propyl ether). In contrast, protonated monomers of alcohols fragment through the cleavage of a single bond with a loss of water and fragmentation was observed significantly for all alcohols. Protonated monomers of acetates fragment via rearrangement reactions with a five or six member ring transition states and fragmentation was observed for acetates with carbon number 5 to 8 (see below). While heat capacities have been considered relevant to increasing ion effective temperature and the on-set of fragmentation,30 there was no general pattern seen (Table 1, Table S3) with the extent of fragmentation in FIF spectra, although the data sets may be insufficient for general interpretations.

Classification of Mobility Selected Spectra of Protonated Monomers, $MH^+(H_2O)_n$

Results from classification of mobility-selected spectra by chemical class are shown *for familiar compounds* in adjusted average values for ~1050 individual spectra (Figure 3A) and in Table 2. At 93 ºC, 47.0 % of all test spectra are classified perfectly by chemical class, 21.8 % of test spectra were classified below AAV of 0.500, and 8.1% were completely misclassified (i.e., AAV=0.000). Overall adjusted average values (AAVs) increased slightly from 0.724 to 0.768 (Table 2) between 48 to 930C and this was consistent broadly with a minor increase in thermal decomposition of ions. This was however chemical class dependent as shown in Table 3 where protonated monomers for alcohols exhibited significant improvements in AAV plots consistent with the prior experience of thermal fragmentation of protonated monomers of alcohols.[51]

Table 2. Results from testing Neural Networks with *classification using familiar spectra*

	Mobility Selected Spectra			FIF Spectra*			Whole Spectra		
	48 ºC	**70 ºC**	**93 ºC**	**48 ºC**	**70 ºC**	**93 ºC**	**48 ºC**	**70 ºC**	**93 ºC**
Overall AAV	0.724	0.757	0.768	0.762	0.887	0.953	0.977	0.988	0.973
% of spectra AAV=1.000	46.0	47.3	47.0	50.8	59.1	62.7	66.4	66.7	73.4
% of spectra AAV>0.900	64.6	69.1	70.1	70.3	84.6	93.0	95.1	97.0	95.4
% of spectra AAV<0.500	28.8	22.8	21.8	20.9	14.0	6.4	4.9	3.0	4.6
% of spectra AAV=0.900	9.6	8.1	8.1	8.8	1.4	0.6	0.0	0.0	0.0

*Field Induced Fragmentation Spectra. Electric fields with a fixed amplitude of 1.4 kV, in Townsend (Td) were 113 (48˚C), 120 (70°C) and 129 (93˚C). These are approximate values since the fields have complex distributions within the wire grid assembly and at 3.3 MHz.

Spectra at temperatures greater than 100 ºC could not be used since fragmentation was extensive and peak intensities were too low to pass criteria for spectral pre-processing. The influence with other chemical classes was minor or unexplainable at present (ketones); nonetheless, even in the absence of thermal fragmentation of ions, temperature can benefit the process of field induced fragmentation since increased temperatures for gas ions lower the on-set of fragmentation in electric fields.[30] Consequently, 93 ºC was chosen as a temperature to heighten field induced fragmentation at 129 Td and all subsequent studies with *unfamiliar compounds* were completed only at 93 ºC.

The process of mobility isolating protonated monomers (and removing other regions of drift times in whole mobility spectra) decreased the overall

classification rates in reference to the performance observed with whole spectra, for both familiar (Table 2) and unfamiliar compounds (Table 3).

Table 3. Adjusted average values from neural network classification of whole, mobility selected, and Field Induced Fragmentation spectra.

Mobility Selected Spectra					
Temperature °C	Alcohols (59)*	Acetates (88)*	Ketones (55)*	Aldehydes (37)*	Ethers (34)*
Familiar Chemicals					
48	0.819	0.773	0.698	0.808	0.787
70	0.778	0.819	0.820	0.829	0.684
93	0.922	0.765	0.848	0.784	0.839
Unfamiliar Chemicals					
93	0.145	0.387	0.109	0.008	0.000
Field Induced Fragmentation Spectra					
Temperature °C	Alcohols (57)*	Acetates (80)*	Ketones (54)*	Aldehydes (35)*	Ethers (31)*
Familiar Chemicals					
48	0.905	0.838	0.734	0.963	0.788
70	0.994	0.917	0.795	0.939	0.852
93	0.969	0.934	0.883	0.944	0.992
Unfamiliar Chemicals					
93	0.587	0.379	0.343	0.042	0.000

Whole Spectra					
Temperature °C	Alcohols (72)*	Acetates (98)*	Ketones (58)*	Aldehydes (43)*	Ethers (37)*
Familiar Chemicals					
48	0.987	0.963	0.973	0.996	0.990
70	0.993	0.992	0.996	0.952	0.995
93	0.964	0.960	0.990	0.987	0.982
Unfamiliar Chemicals					
93	0.559	0.577	0.158	0.100	0.058

*Average number of spectra in tests shown in parentheses.

The decrease in AAVs for all chemical families suggested that some, perhaps significant, amounts of structural information in whole spectra were removed and the classification by chemical family was worsened. This was observed for all chemical families (Table 3) and can be attributed the removal of ions that are formed through in-source fragmentation. These ions were located in whole spectra between the reactant ion peak and the protonated monomer and were understood to provide structural information recognized by neural networks.[38-40]

Results for *unfamiliar compounds* provide a rigorous test of network learning, in contrast to familiar compounds where memorization could influence performance with test spectra. Mobility selected spectra (at 93 °C) for unfamiliar compounds exhibited AAVs ranging from 0.387 for acetates to 0.000 for ethers (Table 3 and Figure 3B). Since neural network performance with unfamiliar compounds is wholly dependent on learning structural information, the weak performance is consistent with the finding above, that is structural information was removed by mobility selection. Since such structural information could arise by thermal energies (3/2 k_BT) of ions in mobility-selected spectra, thermal

heating of ions did not appreciably exceed thresholds for fragmentation at 930 ºC with a 20 mm long drift region; nor should thermal fragmentation be considered a significant aspect in studies below with FIF spectra.

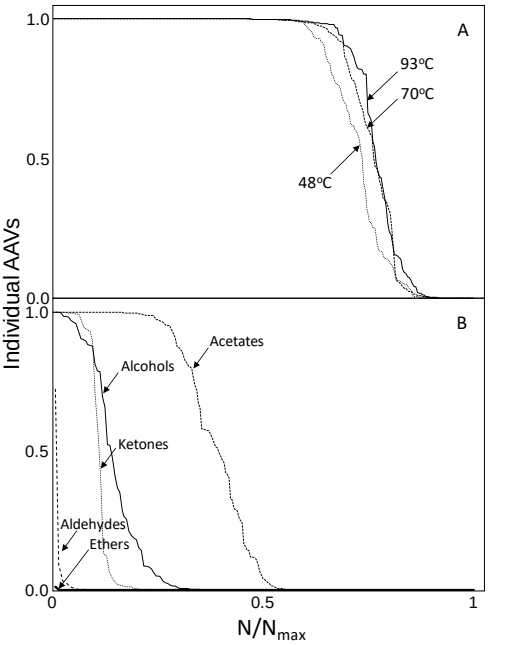

Figure 3. Neutral network classification of mobility selected spectra by chemical class for A. familiar compounds at 48, 70, and 93 ºC and B) unfamiliar compounds by chemical class.

Classification of Field Induced Fragmentation (FIF) Spectra of Protonated Monomers

Performance by neural networks with FIF spectra, i.e., protonated monomers heated with an E/N of ~129 Td, is shown in Figure 4A and Table 2 *for familiar compounds*. As with temperature effects with mobility selected spectra, AAVs for these familiar compounds increased with temperature from 0.762 to 0.953 (93 ºC). This improvement, in comparison only to mobility-selected

spectra, is understood to arise from the addition of electric field heating with thermal heating of ions. The additional energy promoted the formation of structural information in FIF spectra by increasing ion energies beyond thresholds for fragmentation. At 93 ºC with unfamiliar compounds, the performance in categorization of FIF spectra was dependent on chemical family as shown in Table 3 and Figure 4B and differed from mobility selected spectra of Figure 3B. Classification was improved significantly for alcohols and ketones, improved moderately for acetates, and improved slightly for aldehydes. There was no improvement in classification observed with ethers.

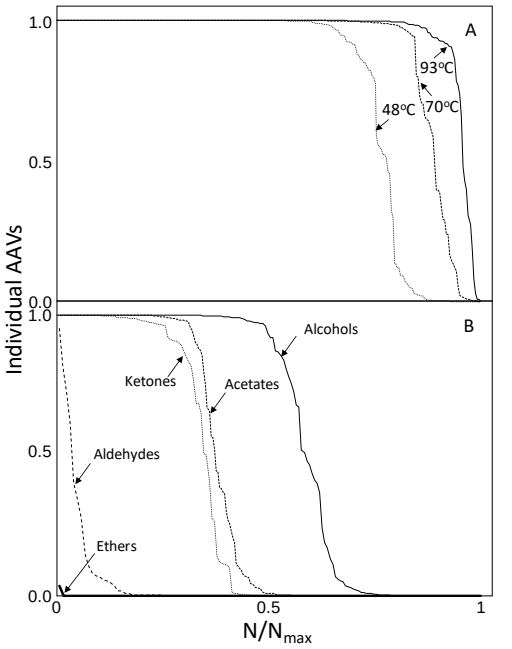

Figure 4. Neutral network classification of fragment ion spectra by chemical class for A). unfamiliar compounds at 48, 70, and 93 ºC and B) unfamiliar compounds plotted by chemical class.

Reaction enthalpies for alcohols were comparatively low across the whole range of carbon number (Fig. 2) suggesting that favorable fragmentation and classification for all alcohols, if reaction enthalpy (average of 85 kJ/mole for alcohols) was the controlling variable. Yet classification for 3 and 4 carbon alcohols was significantly greater than for 5 to 7 carbon number alcohols. A similar pattern of decreased performance with increase carbon number was observed with acetates (average enthalpy of 105 kJ/mole). At the other extreme of performance, fragmentation of ethers was hindered by steric demands of a four-member ring transition state. No FIF spectrum exhibited fragmentation for any ether (apart from dipropyl ether at 16 %, Table 1) and no spectrum for these normal ethers was classified correctly (Figure 5, Table 3).

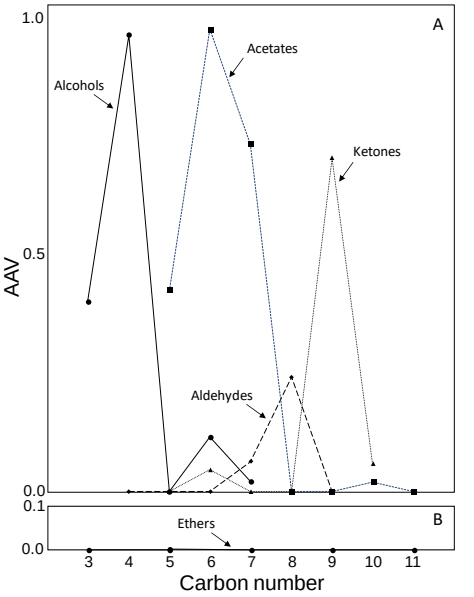

Figure 5. Plots of AAV for FIF spectra for unfamiliar compounds by chemical class of normal or homologous oxygen containing volatile organic compounds.

Patterns of AAVs for ketones and aldehydes contain one or a few compounds at larger carbon number where fragmentation occurred and classification was observed. This may be evidence of a rearrangement with a larger ring size and is pending further study. The limited or minor improvement in neural network classification with FIF spectra of aldehydes, ethers, and ketones is understood as insufficient electric field strength in the reactive stage of the tandem IMS drift tube. Energies of ions were too low to exceed activation barriers in their strained transition states and the process is under kinetic control. Acetates exhibited AAVs of ~0.780 for low carbon numbers of 4 to 5 where ring sizes would be five or six atoms and thermal fragmentation can occur at temperatures above 90 ^{o}C; thus, even mobility selected spectra must have contained sufficient structural information which was not improved appreciably in FIF spectra. Misclassifications of mobility-selected and FIF spectra could be organized by chemical classes receiving the false scores for AAVs (Table S1 in Supporting Information). Acetates and ketone received the bulk of misclassification though no interpretation suitably explained these trends.

Branched Isomers of and other Oxygen Containing Compounds

A limited number of branched or unsaturated isomers or compounds lacking a homologous series from the oxygen containing compounds above was also included in training and testing of neural networks and findings are shown in Figure S2 and Table S3 (Supporting Information). While some rates of classification by chemical class were relatively strong e.g., 0.816, 2-propanol; 1.000, 2-butanol; 0.954, 2-methylpropanol; 0.789, isopropyl acetate; 0.999, sec-butyl acetate; 0.944, isopentyl acetate; 0.909, methyl isobutyl ketone; and 0.853, pinacolone (Figure S2 in Supporting Information), several compounds showed AAVs at or near 0.000, e.g., isobutyl acetate and di-isopropyl ether.

Although the number of compounds in this section is limited and few conclusions can be made broadly on structure, a few compounds contain trends in structures. One series is iso-propyl, iso-butyl-, and iso-pentylacetates where

the iso-group is displaced by one additional methylene in the three member series ($CH_3CO(CH_2)_nC_3H_7$ where n = 0, 1, 2, respectively. Each of these can form six center rings for rearrangement reaction in the transition state and enthalpies of reactions are comparable; however, the iso-butylacetate will have in the transition state will have steric hindrance from two methyl groups for the proton on the tertiary carbon. This results in fragmentation with loss of $C_4H_9^+$ and acetic acid unlike other acetates which decompose to protonated acetic acid.[30,50] Consequently, unfamiliar spectra for isopropyl acetate and iso-pentyl acetate exhibited favorable classification with AAVs of 0.789 and 0.944 (Fig. S2), respectively and isobutyl acetate was completed misclassified using neural networks from this limited training set. Other possible structural trends could not be drawn from these other oxygen containing compounds with too few members for evaluation.

Generally, the reaction enthalpies for fragmentation of protonated monomers of these other oxygen containing compounds ranged from a low of 43.9 kJ/mol for 2-methylpropanol to a high of 211.1 kJ/mol for methyl butyrate and were not unlike that of normal compounds. Unlike the fragmentation with normal-acetates (below 20 % except for n-butyl acetate), fragmentation with branched acetates (Table S3) was relatively strong between 25 and 70 %.

A significant number (8 of 13) of these other compounds exhibited AAVs of 0.7 or greater as unfamiliar FIF spectra (Fig. S3) suggesting these compounds contained transition states with low activation energies. As with normal ketones, pinacolone and methyl isobutyl ketone did not exhibit fragments and yet were classify by chemical family though yet uncertain explanations. May fragment through a five and six member rings, respectively significantly lowering activation energies.

Although an exploration with systematic changes in branched or unsaturated groups is necessary for future advances with tandem IMS and FIF spectra, the immediately priority is for improved control and strength of electric fields in the reactive stage.

Conclusions

Findings shown above on the formation of FIF spectra are the first results toward introducing structural information in mobility spectra in ways that are analogous to mass spectra from collision induced dissociation in reactive stage tandem MS. The results from spectral analysis using neural networks suggest that the concept of mobility isolation, fragmentation, and mobility analysis of ions at ambient pressure can generate spectral detail permitting assignment by chemical class with *unfamiliar chemicals* even in a 20 mm long drift region. This capability is governed significantly by kinetics of ion fragmentation, rather than reaction enthalpies, and the field strength of 129 Td is insufficient for fragmentation of protonated ketones, ethers and low carbon number of aldehydes. Advances in technology are needed to improve fragmentation efficiency for further development of reactive stage tandem IMS as an analytical method with application to these and an expanded range of substances.

Akcnowledgments

This research was funded in part by Collins Aerospace and in part by the Office of the Director of National Intelligence (ODNI), Intelligence Advanced Research Projects Activity (IARPA), through an AFRL contract. All statements of fact, opinion or conclusions contained herein are those of the authors and should not be construed as representing the official views or policies of IARPA, the ODNI, or the U.S. Government. The Government is authorized to reproduce and distribute reprints for Governmental purposes notwithstanding any copyright annotation thereon.

References

[1] Brodrick, E.; Davies, A.; Neill, P.; Hanna, L.; Williams, E. M. Breath Analysis: Translation into Clinical Practice. *J. Breath Res.* **2015**, *9* (2), 27109.

[2] Ha, H.; Usuba, A.; Maddula, S.; Baumbach, J. I.; Mineshita, M.; Miyazawa, T. Exhaled Breath Analysis for Lung Cancer Detection Using Ion Mobility Spectrometry. PLoS One **2014**, 9 (12), 1–13.

[3] Bannier, M.; Van De Kant, K.; Baumbach, J.; Jobsis, Q., Dompeling, E. Exhaled breath analysis by ion mobility spectrometry in children with asthma and cystic fibrosis, European Respiratory Journal **2018** 52: PA4613.

[4] Zhang, L.; Shuai, Q.; Li, P.; Zhang, Q.; Ma, F.; Zhang, W.; Ding, X. Ion Mobility Spectrometry Fingerprints: A Rapid Detection Technology for Adulteration of Sesame Oil. Food Chem. **2016**, 192, 60–66.

[5] Gerhardt, N.; Birkenmeier, M.; Schwolow, S.; Rohn, S.; Weller, P. Volatile-Compound Fingerprinting by Headspace-Gas-Chromatography Ion-Mobility Spectrometry (HS-GC-IMS) as a Benchtop Alternative to 1H NMR Profiling for Assessment of the Authenticity of Honey. Anal. Chem. **2018**, 90 (3), 1777–1785.

[6] Hernández-Mesa, M.; Ropartz, D.; García-Campaña, A. M.; Rogniaux, H.; Dervilly-Pinel, G.; Le Bizec, B. Ion Mobility Spectrometry in Food Analysis: Principles, Current Applications and Future Trends. Molecules **2019**, 24 (15), 1–28.

[7] Garrido-Delgado, R.; Dobao-Prieto, M. D. M.; Arce, L.; Valcárcel, M. Determination of Volatile Compounds by GC-IMS to Assign the Quality of Virgin Olive Oil. Food Chem. **2015**, 187, 572–579.

[8] Roehl, J. E. Environmental and Process Applications for Ion Mobility Spectrometry. Appl. Spectrosc. Rev. **1991**, 26 (1–2), 1–57.

[9] Márquez-Sillero, I; Aguilera-Herrador, E.; Cárdenas, S.; Valcárcel, M. Ion-mobility spectrometry for environmental analysis, Trends in Analytical Chemistry **2011**, 30, 677-690

[10] Huang, W.; Wang, W.; Chen, C.; Li, Y.; Wang, Z.; Li, Q.; Li, M.; Hou, K. Real-Time Monitoring Traces of SF6 in near-Source Ambient Air by Ion Mobility Spectrometry. Int. J. Environ. Anal. Chem. **2019**, 99 (9), 868–877.

[11] Limero, T. Revalidation of the Volatile Organic Analyzer Following a Major On-Orbit Maintenance Activity, SAE Transactions, Journal of Aerospace **2007**, 116, Section 1: 426-432.

[12] Wallace, W.T.; Limero, T.F.; Lho, L.J.; Mudgett, P.D.; Gazda, D.B.

Monitoring of the Atmosphere on the International Space Station with the Air Quality Monitor, No. ICES-2017-103, Proceedings of 47th International Conference on Environmental Systems, Charleston, South Carolina, 16-20 July 2017.

[13] Eiceman, G. A.; Salazar, M. R.; Rodriguez, M. R.; Limero, T. F.; Beck, S. W.; Cross, J. H.; Young, R.; James, J. T. Ion Mobility Spectrometry of Hydrazine, Monomethylhydrazine, and Ammonia in Air with 5-Nonanone Reagent Gas. Anal. Chem. **1993**, 65 (13), 1696–1702.

[14] Martinak, D.; Rudolph, A. Explosives Detection Using an Ion Mobility Spectrometer for Airport Security. Proc. - Int. Carnahan Conf. Secur. Technol. **1997**, 188–189.

[15] Karpas, Z. Ion Mobility Spectrometry: A Tool in the War against Terror. Bull. Isr. Chem. Soc. **2009**, No. 24, 26–31.

[16] Puton, J.; Namieśnik, J. Ion Mobility Spectrometry: Current Status and Application for Chemical Warfare Agents Detection. TrAC - Trends Anal. Chem. **2016**, 85 (June), 10–20.

[17] Satoh, T.; Kishi, S.; Nagashima, H.; Tachikawa, M.; Kanamori-Kataoka, M.; Nakagawa, T.; Kitagawa, N.; Tokita, K.; Yamamoto, S.; Seto, Y. Ion Mobility Spectrometric Analysis of Vaporous Chemical Warfare Agents by the Instrument with Corona Discharge Ionization Ammonia Dopant Ambient Temperature Operation. Anal. Chim. Acta **2015**, 865 (1), 39–52.

[18] Lai, R.; Dodds, E. D.; Li, H. Molecular Dynamics Simulation of Ion Mobility in Gases. J. Chem. Phys. **2018**, 148 (6), 064109-1.

[19] Mason, E. A.; Schamp, H. W. Mobility of Gaseous Lons in Weak Electric Fields. Ann. Phys. (N. Y). **1958**, 4 (3), 233–270.

[20] Viehland, L. A.; Chang, Y. Beyond the Monchick-Mason Approximation: The Mobility of Li^+ Ions in H_2. Mol. Phys. **2012**, 110 (5), 259–266.

[21] Karpas, Z.; Berant, Z.; Shahal, O. Effect of Temperature on the Mobility of Ions. J. Am. Chem. Soc. **1989**, 111 (16), 6015–6018.

[22] Karpas, Z. Ion Mobility Spectrometry of Aliphatic and Aromatic Amines. Anal. Chem. **1989**, 61 (7), 684–689.

[23] McLafferty, F. W.; Turecek, F. Interpretation of mass spectra. Mill Valley, California: University Science Books, 1993.

[24] Pedersen, C. S.; Lauritsen, F. R.; Sysoev, A.; Viitanen, A. K.; Mäkelä, J. M.; Adamov, A.; Laakia, J.; Mauriala, T.; Kotiaho, T. Characterization of

Proton-Bound Acetate Dimers in Ion Mobility Spectrometry. J. Am. Soc. Mass Spectrom. **2008**, 19 (9), 1361–1366.

[25] Eiceman, G. A.; Shoff, D. B.; Harden, C. S.; Snyder, A. P. Fragmentation of Butyl Acetate Isomers in the Drift Region of an Ion Mobility Spectrometer. Int. J. Mass Spectrom. Ion Process. **1988**, 85 (3), 265–275.

[26] Rajapakse, M. Y.; Stone, J. A.; Eiceman, G. A. Decomposition Kinetics of Nitroglycerine·Cl^-(g) in Air at Ambient Pressure with a Tandem Ion Mobility Spectrometer. J. Phys. Chem. A **2014**, 118 (15), 2683–2692.

[27] Rajapakse, R. M. M. Y.; Stone, J. A.; Eiceman, G. A. An Ion Mobility and Theoretical Study of the Thermal Decomposition of the Adduct Formed between Ethylene Glycol Dinitrate and Chloride. Int. J. Mass Spectrom. **2014**, 371 (3), 28–35.

[28] Rajapakse, M. Y.; Fowler, P. E.; Eiceman, G. A.; Stone, J. A. Dissociation Enthalpies of Chloride Adducts of Nitrate and Nitrite Explosives Determined by Ion Mobility Spectrometry. J. Phys. Chem. A **2016**, 120 (5), 690–698.

[29] Kendler, S.; Lambertus, G. R.; Dunietz, B. D.; Coy, S. L.; Nazarov, E. G.; Miller, R. A.; Sacks, R. D. Fragmentation Pathways and Mechanisms of Aromatic Compounds in Atmospheric Pressure Studied by GC-DMS and DMS-MS. Int. J. Mass Spectrom. **2007**, 263 (2–3), 137–147.

[30] An, X.; Stone, J.A.; Eiceman, G. A. Gas Phase Fragmentation of Protonated Esters in Air at Ambient Pressure through Ion Heating by Electric field in Differential Mobility Spectrometry and by Thermal bath in Ion Mobility Spectrometry, Int. J. Mass Spectrom. **2011**, 303 (2-3), 181-190.

[31] Maziejuk, M.; Puton, J.; Szyposzyńska, M.; Witkiewicz, Z. Fragmentation of Molecular Ions in Differential Mobility Spectrometry as a Method for Identification of Chemical Warfare Agents. Talanta **2015**, 144, 1201–1206.

[32] Ruszkiewicz, D. M.; Thomas, C. L. P.; Eiceman, G. A. Fragmentation, Auto-Modification and Post Ionisation Proton Bound Dimer Ion Formation: The Differential Mobility Spectrometry of Low Molecular Weight Alcohols. Analyst **2016**, 141 (15), 4587–4598.

[33] Bohnhorst, A.; Kirk, A. T.; Yin, Y.; Zimmermann, S. Ion Fragmentation and Filtering by Alpha Function in Ion Mobility Spectrometry for Improved Compound Differentiation. Anal. Chem. **2019**, 91 (14), 8941–8947.

[34] Chiluwal, U.; Lee, G.; Rajapakse, M. Y.; Willy, T.; Lukow, S.; Schmidt, H.; Eiceman, G. A. Tandem Ion Mobility Spectrometry at Ambient Pressure and Field Decomposition of Mobility Selected Ions of Explosives and Interferences. Analyst **2019**, 144 (6), 2052–2061.

[35] Shokri, H.; Vuki, M.; Gardner, B. D.; Niu, H. C.; Chiluwal, U.; Gurung, B. K.; Emery, D. B.; Eiceman, G. A. Reactive Tandem Ion Mobility Spectrometry with Electric Field Fragmentation of Alcohols at Ambient Pressure. Anal. Chem. **2019**, 91 (9), 6281–6287.

[36] Fernández de la Mora, J.; Amo-González, M.; Delgado, R.; Eiceman, G. A.; Pérez, S.; Carnicero, I.; Fernández de la Mora, G. Ion Mobility Spectrometer-Fragmenter-Ion Mobility Spectrometer Analogue of a Triple Quadrupole for High-Resolution Ion Analysis at Atmospheric Pressure. Anal. Chem. **2018**, 90 (11), 6885–6892.

[37] Amo-González, M.; Pérez, S.; Delgado, R.; Arranz, G.; Carnicero, I. Tandem Ion Mobility Spectrometry for the Detection of Traces of Explosives in Cargo at Concentrations of Parts per Quadrillion. Anal. Chem. **2019**, 91 (21), 14009–14018.

[38] Bell, S.; Nazarov, E.; Wang, Y. F.; Rodriguez, J. E.; Eiceman, G. A. Neural Network Recognition of Chemical Class Information in Mobility Spectra Obtained at High Temperatures. Anal. Chem. **2000**, 72 (6), 1192–1198.

[39] Bell, S. E., Nazarov, E. G., Wang, Y. F., Eiceman, G. A., Classification of Ion Mobility Spectra by Chemical Moiety Using Neural Networks with Whole Spectra at Various Concentrations, Anal. Chim. Acta **1999**, 394, 121-133.

[40] Eiceman, G. A.; Nazarov, E. G.; Rodriguez, J. E. Chemical Class Information in Ion Mobility Spectra at Low and Elevated Temperatures. Anal. Chim. Acta **2001**, 433 (1), 53–70.

[41] Good, A.; Durden, D. A.; Kebarle, P. Ion–Molecule Reactions in Pure Nitrogen and Nitrogen Containing Traces of Water at Total Pressures 0.5–4 torr. Kinetics of Clustering Reactions Forming $H^+(H_2O)_n$, J. Chem. Phys. **1970**, 52, 212-221.

[42] Brown, P.; Watts, P.; Märk, T. D.; Mayhew, C. A. Proton Transfer Reaction Mass Spectrometry Investigations on the Effects of Reduced Electric Field and Reagent Ion Internal Energy on Product Ion Branching Ratios for a Series of Saturated Alcohols. Int. J. Mass Spectrom. **2010**, 294 (2–3), 103–111.

[43] Langejuergen J.; Allers M.; Oermann J.; Kirk A.; Zimmermann A. High

Kinetic Energy Ion Mobility Spectrometer: Quantitative Analysis of Gas Mixtures with Ion Mobility Spectrometry Anal. Chem. **2014**, 86, 14, 7023-7032

[44] Nazarov E. G.; Eiceman G. A.; Bell S. E. Quantitative Assessment for the Training of Neural Networks with Large Libraries of Ion Mobility Spectra, Int. J. Ion Mobility Spectrom. **1999**, 2, 45-60.

[45] Wannier, G. H. On the Motion of Gaseous Ions in a Strong Electric Field. I, Physical Review, **1951**, 83, 281-289.

[46] Wannier, G. H. Motion of Gaseous Ions in a Strong Electric Field. II, Physical Review, **1952**, 87, 795-798.

[47] Ellis, A. M.; Mayhew, C. A. Proton Transfer Reaction Mass Spectrometry: Principles and Applications; Wiley: New York, **2014**, pp. 71-72.

[48] Sigsby, M. L.; Day, R. J.; Cooks, R. G. Fragmentation of Even Electron Ions. Protonated Ketones and Ethers. Org. Mass Spectrom. **2005**, 14 (5), 273–280.

[49] Hawthorne, S. B.; Miller, D. J. Water Chemical Ionization Mass Spectrometry of Aldehydes, Ketones, Esters, and Carboxylic Acids. Appl. Spectrosc. **1986**, 40 (8), 1200–1211.

[50] Herman, J. A.; Harrison, A. G. Energetics and Structural Effects in the Fragmentation of Protonated Esters in the Gas Phase. Can. J. Chem. **1981**, 59 (14), 2133–2145.

[51] Safaei, S.; Willy, T.J.; Eiceman, G.A.; Stone, J.A.; Sillanpää, M., Quantitative Response in Ion Mobility Spectrometry with Atmospheric Pressure Chemical Ionization in Positive Polarity as a Function of Moisture and Temperature, Anal. Chem. Acta **2019**, 1092, 144-150

Supplementary Information

Figure S1. Schematic of Tandem IMS drift tube.

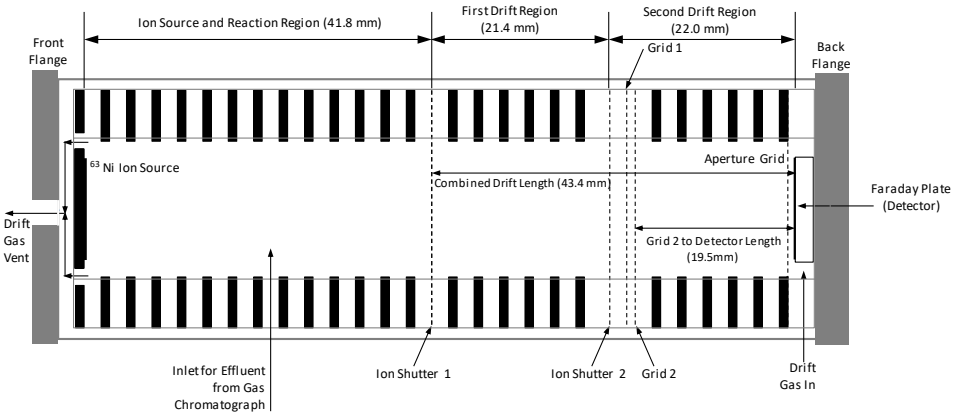

Figure S2. Classification AAVs for unfamilar compounds of other oxygen containing compounds vs. carbon number.

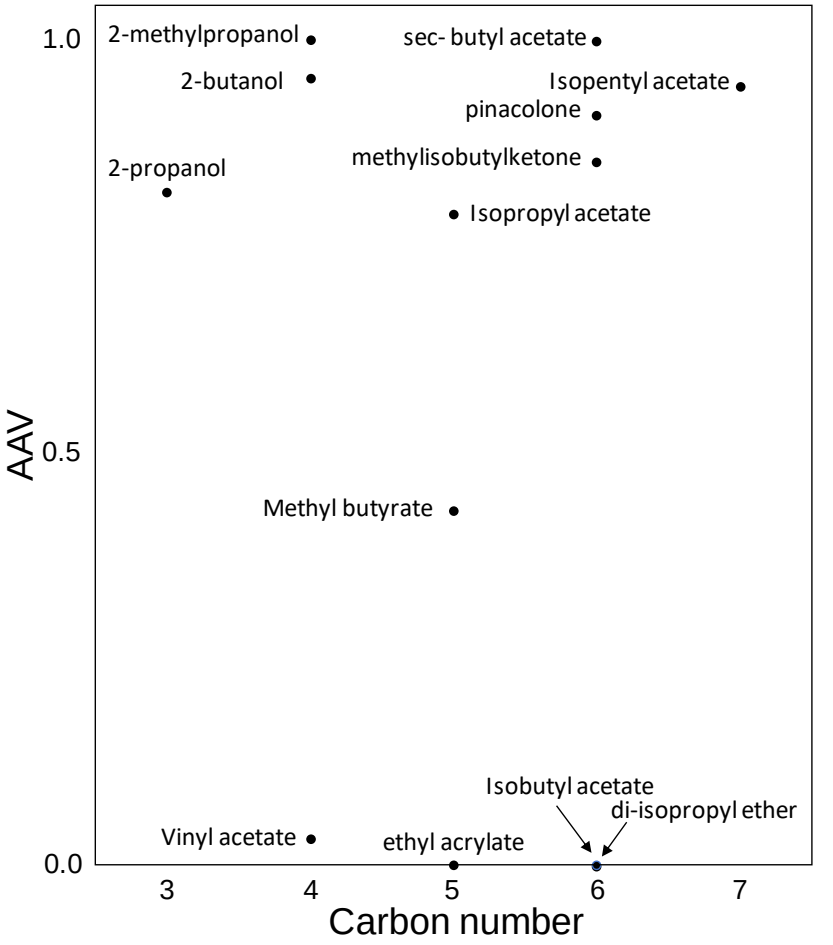

Figure S3. Enthalpies of the fragmentation reaction for oxygen containing compounds vs. carbon number.

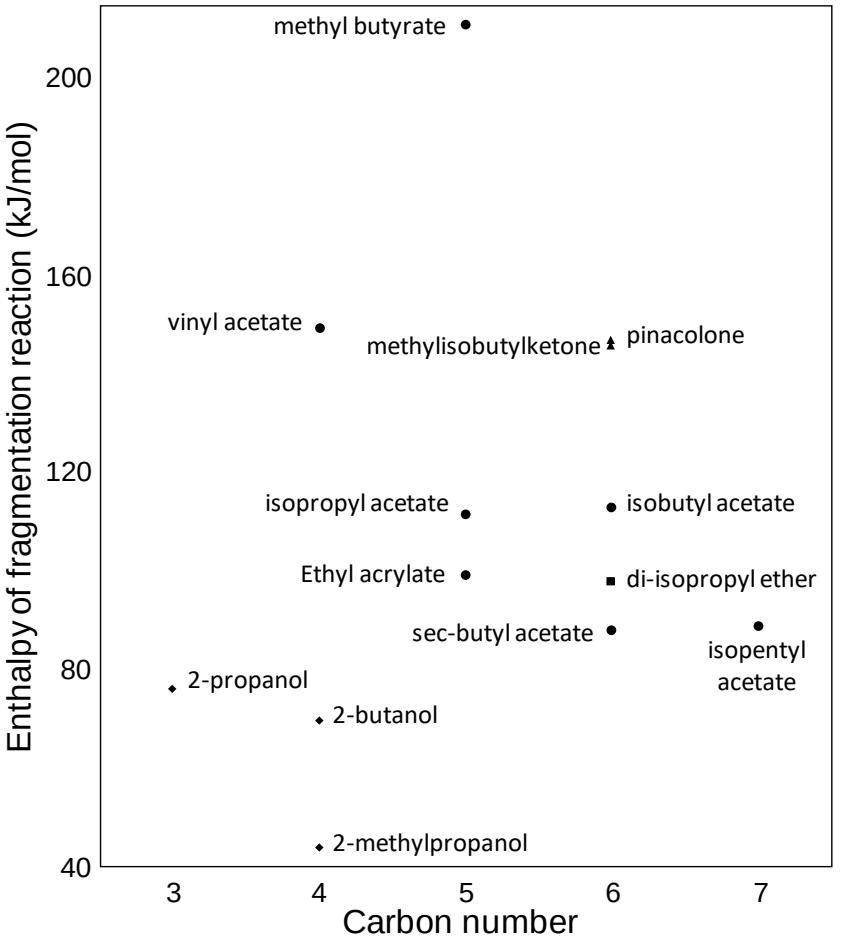

Table S1. Normalized summation of misclassified AAVs in each chemical family.

Misclassified as:	mobility isolated monomer	mobility isolated monomer with ion heating
	alcohols	
acetates	0.121	0.231
ketones	0.258	0
ethers	0.082	0.12
aldehydes	0.362	0.088
	acetates	
alcohols	0.03	0.017
ketones	0.207	0.252
ethers	0.207	0.242
aldehydes	0.165	0.066
	ketones	
alcohols	0.105	0
acetates	0.511	0.296
ethers	0.106	0.208
aldehydes	0.136	0.151
	ethers	
alcohols	0.017	0
acetates	0.534	0.515
ketones	0.281	0.394
aldehydes	0.122	0.057
	aldehydes	
alcohols	0.253	0.12
acetates	0.366	0.154
ketones	0.083	0.398
ethers	0.084	0.182

Table S2. Reduced mobilities ($cm^2/V{\cdot}s$) of hydrated protonated monomer ($MH^+(H_2O)_n$) and Fragment ion (M^+) in FIF spectra.

Normal compounds

SUBSTANCE	K_o of $MH^+(H_2O)_3$	K_o of M^+
Acetates		
propyl acetate	1.8	2.12
butyl acetate	1.72	2.13
pentyl acetate	1.59	2.13
hexyl acetate	1.5	2.2
heptyl acetate	1.43	
octyl acetate	1.35	
nonyl acetate	1.29	
Alcohols		
1-propanol	1.9	1.96
1-butanol	1.79	2.01, 1.88
1-pentanol	1.68	2.23
1-hexanol	1.58	2.1
1-heptanol	1.51	1.98
Aldehydes		
butanal	1.9	
pentanal	1.79	
hexanal	1.68	2.19
heptanal	1.58	2.13
octanal	1.5	1.9
nonanal	1.42	1.78
Ketones		
2-pentanone	1.86	
2-hexanone	1.76	
2-heptanone	1.66	
2-octanone	1.57	
2-nonanone	1.48	
2-decanone	1.29	
Ethers		
diethyl ether	1.98	
dipropyl ether	1.76	1.89
dibutyl ether	1.6	1.78

dipentyl ether	1.45	1.6
dihexyl ether	1.34	

Irregular compounds

SUBSTANCE	K_o of $MH^+(H_2O)_3$	K_o of M^+
Acetates		
vinyl acetate	1.95	
ethyl acrylate	1.87	
methyl butyrate	1.83	
isopropyl acetate	1.8	2.09
isobutyl acetate	1.69	2.44, 2.11
sec-butyl acetate	1.7	2.09
isopentyl acetate	1.62	2.25
Alcohols		
2-propanol	1.94	1.95
2-butanol	1.87	2.33
2-methyl-1-propanol	1.87	2.33
Ketones		
methyl isobutyl ketone	1.78	
pinacolone	1.34	
Ethers		
diisopropyl ether	1.83	1.98

Table S3. Intensities for protonated monomer peaks in mobility-selected spectra and for fragment ions in FIF spectra, KE_{CM}, and enthalpy of fragmentation of irregular compounds at 93°C. Spectra were selected at maximum vapor concentration in the gas chromatographic elution profile.

compound	Peak Intensity (V) of $MH^+(H_2O)_n$	Peak Intensity (V) of fragment ion	Percent fragmentation	KE_{CM} (kJmol^{-1})	Enthalpy of fragmentation (kJmol^{-1})	MH^+ Heat Capacity, Cv (J/K-mol)*
Alcohols						
2-propanol	0.55	0.65	54.2	8.26	76	90.38
2-butanol	0.17	0.2	54	7.92	69.5	110.48
2-methylpropanol	0.15	0.34	69.7	7.95	43.9	109.02
Acetates						
vinyl acetate	0.68	0	0	8.3	149.4	99.94
ethyl acrylate	0.73	0	0	7.92	99.3	120.09
methyl butyrate	0.71	0	0	7.74	211.1	127.97
isopropyl acetate	0.23	0.39	63	7.63	111.4	133.04
isobutyl acetate	0.32	0.15	31.4	7.18	88.1	152.63
sec-butyl acetate	0.17	0.4	69.7	7.22	113	153.4
isopentyl acetate	0.39	0.13	24.6	6.86	89	172.77
Ketones						
methyl isobutylketone	0.58	0	0	7.54	145.7	137.59
pinacolone	0.64	0	0	5.89	146.8	141.62
Ethers						
diisopropyl ether	0.48	0.39	45.1	7.77	97.9	152.58

*Cv is the contribution to heat capacity due to vibrational motion at 298.15 K from *Gaussian* calculations

BLOCK II

Applied study of Ion Mobility Spectrometry

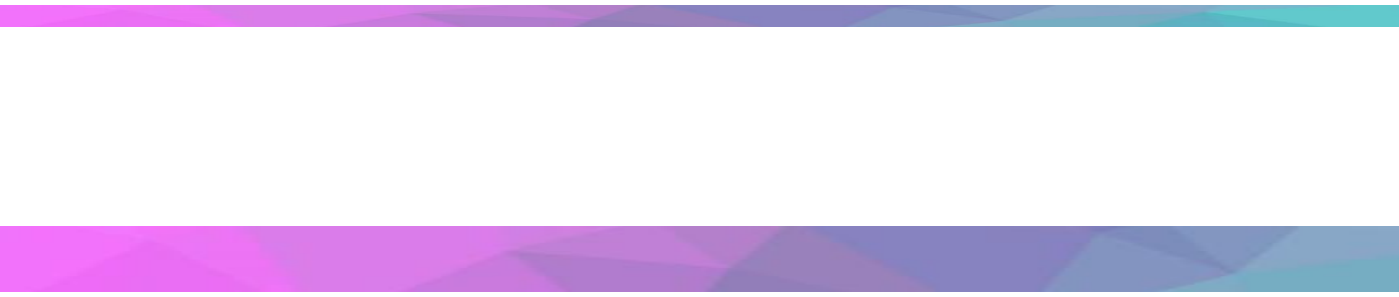

Block II of this PhD Book is devoted to improving analytical properties of IMS such as selectivity or sensitivity over the whole analytical process. For that, the development of new strategies or the use of existing alternative throughout different steps of the analytical process were applied to improve the detection and identification capacity in IMS analysis. These enhancements on IMS analytical properties were demostrated on different field of application in Chapter III, IV and V.

In Chapter III, a TD-IMS was used to properly detect cannabinoids with relative high boiling points in Cannabis plants. Spectral fingerprints of Cannabis herbal samples, with and without pretreatment, in the positive and negative ionization modes were recorded. PCA and LDA were used as chemometric strategies to perform the chemotyping of different Cannabis varieties to demonstrate the potential of TD-IMS for the screening of cannabinoids.

The selectivity detection of TNT using a tandem IMS with reactive stage as detection system was the aim of Chapter IV. For that, an Interferent B was removal through its isolation and fragmentation.

Finally, an innovative coupling of a SFE system with an IMS device was developed using a column filled with Tenax TA material as sorbent trap in Chapter V. The main objective which encouraged the design of this pioneer system was to improve analytical properties such as sensitivity and selectivity of future IMS methods. In this case, benzene and toluene were analyzed in soil samples using this coupling. Additionally, the extraction of eucalyptol as a model bioactive compound in rosemary plant was carried out to highlight the utility of the new hyphenation to solve a real problem on an industrial scale.

Thermal desorption–ion mobility spectrometry: A rapid sensor for the detection of cannabinoids and discrimination of *Cannabis* sativa L. chemotypes

CHAPTER III

Sensor & Actuator B: Chemical

273 (2018) 1413–1424

Thermal desorption–ion mobility spectrometry: A rapid sensor for the detection of cannabinoids and discrimination of *Cannabis* sativa L. chemotypes

María del Mar Contreras[a#], Natividad Jurado-Campos[a#], Carolina Sánchez-Carnerero Callado[b], Natalia Arroyo-Manzanares[a], Luis Fernández[c,d], Salvatore Casano[b], Santiago Marco[c,d], Lourdes Arce[a] and Carlos Ferreiro-Vera[b]

[a]*Department of Analytical Chemistry, University of Córdoba, 14071 Córdoba, Spain.*

[b]*Phytoplant Research S.L., The Science and Technology Park of Córdoba-Rabanales 21, 14014, Córdoba, Spain.*

[c]*Department of Electronics and Biomedical Engineering, Universitat de Barcelona, 08028, Barcelona, Spain.*

[d]*Signal and Information Processing for Sensing Systems, The Barcelona Institute of Science and Technology, 08028, Barcelona, Spain.*

[#]*Both authors contribute equally*

Thermal desorption–ion mobility spectrometry: A rapid sensor for the detection of cannabinoids and discrimination of *Cannabis* sativa L. chemotypes

María del Mar Contreras, Natividad Jurado-Campos, Carolina Sánchez-Carnerero Callado, Natalia Arroyo-Manzanares, Luis Fernández, Salvatore Casano, Santiago Marco, Lourdes Arce and Carlos Ferreiro-Vera

ABSTRACT

Existing analytical techniques used for the determination of cannabinoids in *Cannabis sativa* L. (*Cannabis*) plants mostly rely on chromatography-based methods. As a rapid alternative for the direct analysis of them, thermal desorption (TD)-ion mobility spectrometry (IMS) was used for obtaining spectral fingerprints of single cannabinoids from *Cannabis* plant extracts and from plant residues on hands after their manipulation. The ionization source was ^{63}Ni, with automatic switchable polarity. Although in both ionization modes there were signals in the TD-IMS spectra of the plant extracts and residues that could be assigned to concrete cannabinoids and chemotypes, most of them could not be clearly distinguished. Alternatively, the global spectral data of the plant extracts and residues were pre-processed and then, using principal component analysis (PCA)-linear discriminant analysis (LDA), grouped in function of their chemotype in a more feasible way. Using this approach, the possibility of false positive responses was also studied analyzing other non-*Cannabis* plants and tobacco, which were clustered in a different group to those of *Cannabis*. Therefore, TD-IMS, as analytical tool, and PCA-LDA, as a strategy for data reduction and pattern recognition, can be applied for on-site chemotaxonomic discrimination of *Cannabis* varieties and detection of illegal marijuana since the IMS equipment is portable and the analysis time is highly short.

Keywords: *Cannabis sativa* L.; cannabinoids; chemometrics; chemotype; ion mobility spectrometry

1. Introduction

Cannabis sativa L. (*Cannabis*) (family *Cannabaceae*) is one of the most ancient domesticated crops. In some zones of the world, *Cannabis* has been mainly cultivated as fibre and grains source, while in other zones this plant have been also used as spiritual and recreational drug [1,2]. The vast majority of modern industrial hemp varieties are characterized by a low content of Δ^9-tetrahydrocannabinol (Δ^9-THC), the main psychoactive cannabinoid, and having cannabidiol (CBD), a non-psychoactive isomer of Δ^9-THC, as predominant cannabinoid. Based on the peaks ratio of Δ^9-THC, CBD and cannabinol (CBN), an oxidation product of Δ^9-THC, *Cannabis* has been generically subdivided into: fibre-type when ([Δ^9-THC]+[CBN])/[CBD] is <1 and drug-type (i.e. marijuana, marihuana, herbal *Cannabis* or *Cannabis*) when ([Δ^9-THC]+[CBN])/[CBD] is >1 [1]. However, this formula cannot be used for legal purposes while the content of Δ^9-THC is used for the discrimination of fibre and drug-types, being regulated on a national level and ranging from 0.2% in European Union countries to 1.0% in countries such as Switzerland, Uruguay and Colombia. Additionally, in last decades medicinal *Cannabis* varieties with different chemotypes have been selected [3], and some of these chemotypes are characterized for having different cannabinoids, such as cannabigerol (CBG), cannabidivarin (CBDV), and Δ^9-tetrahydrocannabivarin (Δ^9-THCV), than the ones considered in the previous formula. It is possible that in such cases the formula does not perfectly fit with the generic subdivision into fibre and drug-types. The scientific interest in both types of *Cannabis* (fibre-type and drug-type), as well as on chemotypes of medicinal varieties, is constantly growing, explained by the fact that: i) *Cannabis* is still the most widely cultivated, produced, trafficked and consumed drug worldwide, with approximately 183 million consumers in 2014 [4], ii) since 1990 the crop of hemp has been introduced or reintroduced in several countries to

obtain fibre and grains [2,5], and iii) it is increasingly being explored for medicinal applications and therapies, together with one of its main cannabinoids, CBD [2,6].

Cannabinoids are characteristic of the *Cannabis* genus. These compounds are produced biosynthetically as their carboxylic acid forms (cannabinoid acids), which are degraded into their neutral forms, including Δ^9-THC, CBD and CBG, during storage through interaction with heat and light or when smoking [7,8]. For the analysis of *Cannabis* samples and cannabinoids, forensic laboratories use colorimetric tests, but in some cases they can lead to false positive results in the presence of other plants [7]. Chromatographic techniques are commonly applied for this purpose, including thin layer chromatography (TLC), gas chromatography (GC) and liquid chromatography (LC) [1, 8–10]. In particular, GC coupled to flame ionization detector (FID) or mass spectrometry (MS) are highly selective, but acidic forms of cannabinoids are decarboxylated into their neutral counterparts due to heating and the thermo-degradation (oxidation and isomerization) of Δ^9-THC may also occur in the injector [1, 9–11]. Thus, a derivatization step, normally by silylation, is required to avoid the conversion of Δ^9-THCA into Δ^9-THC, making the analysis time longer. However, several reference methods for the determination of Δ^9-THC and the ratio [Δ^9-THC+CBN]/[CBD] were based on GC analysis [1,12]. These inconveniences could be solved using LC-MS. Nevertheless, GC- and LC-MS provide very reliable identification and selectivity, but they cannot readily be made portable for in-field measurements. Bear in mind, moreover, that the samples should be pretreated before being injected into the chromatographic system which is time-consuming and usually an error source. In this context, it seems plausible to apply sensors that enable the rapid screening and distinction of *Cannabis* types (fibre-type and drug-type) and chemotypes of medicinal varieties for both on-site drug control and quality control of vegetal raw material used by the pharmaceutical industry.

Ion mobility spectrometry (IMS) is a potential alternative because of its rapid analysis time, simplicity, sensitivity, and portability [13]. IMS has been used as a sensor to analyze drugs. Its use to detect Δ^9-THC in the positive ionization mode seems promising, while what happens in the negative ion mode is not known. However, some drawbacks were reported, such as poor selectivity and the existence of false-positive responses [13–15]. Moreover, most of these methods were tested using standards and no real samples [15–18]. The use of IMS in combination with time-of-flight mass spectrometry (TOF-MS) was also reported as a rapid screening method for drugs [19]. However, TOF-MS is not a portable device and increases analysis costs.

Therefore, in this work a thermal-desorption (TD)-IMS was selected to obtain spectral fingerprints of *Cannabis* herbal samples, with and without pretreatment, in the positive and negative ionization modes. A chemometric strategy based on principal component analysis (PCA)-linear discriminant analysis (LDA) was then performed for the chemotyping of different *Cannabis* varieties to demonstrate the potential of TD-IMS for the screening of cannabinoids.

2. Material and methods

2.1. Plant material

A total of 33 *Cannabis* samples were used. Some of these samples were taken from plants of asexually propagated medicinal varieties registered by Phytoplant in the Community Plant Variety Office (CPVO) (http://cpvo.europa.eu/en) and identified with denomination proposals, while other samples were taken from plants of genotypes and hybrids, obtained as a result of an internal breeding program and identied with codes, and from plants of modern industrial hemp varieties identified with their denominations. The information about *Cannabis* plant materials is shown in Table 1.

Table 1. Summary of the *Cannabis sativa* L. varieties studied and non-*Cannabis* plants. Based on GC-MS analysis, *Cannabis* plants were grouped according to the ratio ([Δ9-THC]+[CBN])/[CBD]) and the main cannabinoids found, whose amount is also described.

Variety/Hybrid	Nº of samples	([Δ9-THC]+[CBN])/ [CBD]	Chemotype (pychoactivity)[a]	Main cannabinoids groups	Amount (%, dry weight)	Chemotype (main cannabinoids)[b]
C. sativa						
Theresa	1	0.04	3'	CBD+CBDA/CBDV+CBDVA	4.71/0.92	2
	2	0.05	3'	CBD+CBDA/CBDV+CBDVA	5.11/1.27	2
Pilar	1	0.07	3'	CBD+CBDA	2.11	1
	2	0.04	3'	CBD+CBDA	10.09	1
Aida	1	0.20	3'	CBG+CBGA	1.78	4
Sara	1	0.05	3'	CBD+CBDA	7.77	1
	2	0.04	3'	CBD+CBDA	11.71	1
Juani	1	0.32	3'	CBG+CBGA	1.27	4
	2	0.32	3'	CBG+CBGA	1.83	4
Octavia	1	0.23	3'	CBG+CBGA	2.10	4
Mati	1	0.69	2'	CBD+CBDA/Δ9-THC+Δ9-THCA	7.20/5.00	6
Moniek	1	ND[d]	1'	Δ9-THC+Δ9-THCA	23.50	5
Carma	1	0.17	3'	CBG+CBGA	1.24	4
Futura 75	1	0.05	3'	CBD+CBDA	3.42	1
	2	0.06	3'	CBD+CBDA	1.93	1
Santhica 27	1	0.25	3'	CBG+CBGA	0.93	4
Divina	1	0.05	3'	CBD+CBDA	5.04	1
Beatriz	1	0.60	2'	CBD+CBDA/Δ9-THC+ Δ9-THCA	7.58/4.52	6
Magda	1	415.29	1'	Δ9-THC+Δ9-THCA	12.05	5
H6	1	0.09	3'	CBD+CBDA/CBG+CBGA	1.04/3.07	3
H53	1	0.18	3'	CBG+CBGA	1.22	4
H6	1	0.05	3'	CBD+CBDA	6.55	1
H7	1	0.06	3'	CBD+CBDA	4.54	1
H17_p5	1	0.04	3'	CBD+CBDA/CBDV+CBDVA	5.94/1.41	2
H17_p7	1	0.04	3'	CBD+CBDA/CBDV+CBDVA	6.51/1.53	2
H17_p8	1	0.05	3'	CBD+CBDA/CBDV+CBDVA	4.52/1.11	2
H14	1	0.09	3'	CBG+CBGA	2.59	4
27/7	1	ND[d]	1'	Δ9-THC+Δ9-THCA	9.37	5
1 26.3/2	1	ND[d]	1'	Δ9-THC+Δ9-THCA	5.10	5
2 26.3/2	1	ND[d]	1'	Δ9-THC+ Δ9-THCA	5.55	5
H19	1	ND[d]	1'	CBG+CBGA	2.77	4
3 26.3/2	1	ND[d]	1'	Δ9-THC+Δ9-THCA	5.80	5
26.2/4	1	ND[d]	1'	Δ9-THC+Δ9-THCA	2.63	5

Other samples[c]					
Horsetail, aerial parts (*Equisetum arvense)*	ND[e]	-	-	-	-
Sweet chamomile, flowers (*Matricaria chamomilla*)	ND[e]	-	-	-	-
Calendula, flowers (*Calendula officinalis*)	ND[e]	-	-	-	-
Poppy, aerial parts (*Papaver rhoeas*)	ND[e]	-	-	-	-
Origanum, leaves (*Origanum vulgare*)	ND[e]	-	-	-	-
Tobacco, brand 1	ND[e]	-	-	-	-
Tobacco, brand 2	ND[e]	-	-	-	-
Aromatic pipe tobacco	ND[e]	-	-	-	-

[a]According to the following ratio ([Δ9-THC]+[CBN])/[CBD]: 1', (Δ9-THC]+[CBN])>[CBD]; 2', ([Δ9-THC]+[CBN]) ≈ [CBD]; 3', ([Δ9-THC]+[CBN])<[CBD]; where [Δ9-THC] is the sum of Δ9-THCA and Δ9-THC, CBD is the sum of CBDA and CBD.

[b]According to the most abundant cannabinoid groups: 1, CBD+CBDA; 2, CBD+CBDA/CBDV+CBDVA; 3, CBD+CBDA/CBG+CBGA; 4, CBG+CBGA; 5, Δ9-THC+Δ9-THCA; 6, CBD+CBDA/Δ9-THC+Δ9-THCA.

[c]Horsetail, *Equisetum arvense*; sweet chamomile, *Matricaria chamomilla*; Calendula, *Calendula officinalis*; Poppy, *Papaver rhoeas*; Origanum, *Origanum vulgare*.

[d]ND, not determined because the amount of CBD+CBDA was 0%.

[e]These plants did not present cannabinoids (-) and so the ratio ([Δ9-THC]+[CBN])/[CBD] was not determined (ND).

Plant samples were obtained from the top of the plant at the optimal harvest point; about 30 cm containing both leaves and flowers (female inflorescences) were sampled for each plant, and then dried at 40 ºC for 72 hours in a forced ventilation oven (J. P. Selecta model Conterm 2000210, Barcelona, Spain). The stems were removed and the dried samples were ground until obtaining a semi-fine powder (passing through a 1 mm mesh sieve). A portion of approximately 1 g was placed into heat sealed pouches and stored at 4 ºC until analysis.

In order to evaluate potential interferences, five different kinds of non-*Cannabis* species (*Equisetum arvense*, *Matricaria chamomilla*, *Calendula officinalis*, *Papaver rhoeas*, and *Origanum vulgare*), as well as tobacco from two

commercial different brands and aromatic pipe tobacco were purchased from local shops (Table 1). The dry plant materials were ground and stored as before.

2.2. Reagents

Cannabinoids standard compounds, deuterated cannabidiol (d3-CBD), CBDV, Δ^9-THCV, CBD, cannabichromene (CBC), Δ^8-tetrahydrocannabinol (Δ^8-THC), Δ^9-THC, CBG and CBN, were purchased from THCPharm (Frankfurt, Germany). Their acidic forms, cannabidiolic acid (CBDA), cannabigerolic acid (CBGA) and Δ^9-tetrahydrocannabinolic acid (Δ^9-THCA) were purchased from Cerilliant (Round Rock, Texas, USA). All standards were commercially acquired as solution in methanol at 1000 mg L^{-1}. Table S1 summarizes some physicochemical parameters of these compounds and their chemical structures.

HPLC grade *n*-hexane was obtained from Panreac (Barcelona, Spain), and trimethylchlorosilane (TMCS) as well as N,O-bis(trimethylsilyl)trifluoro-acetamide (BSTFA) reagents from Sigma-Aldrich (St. Louis, MO, USA). Purified nitrogen (N_2, 5.0) was supplied by Abelló Linde (Barcelona, Spain).

Stock and working solutions were stored at -18 °C. Working solutions were also prepared in hexane at different concentrations before analysis.

2.3. Plant extracts

Powdered plant materials (100 mg) were extracted with 5 mL of *n*-hexane, placed in an ultrasound bath for 20 min, and centrifuged for 5 min at 3000 rpm. Then, the supernatant containing cannabinoids was collected and stored at -18 ºC until analysis.

2.4. Instrumentation and software

2.4.1. IMS device

A handheld IMS (Gas Detector Array) with a thermal desorption (TD) unit (X-TOOL) (GDA-X) (Airsense Analytics GmbH, Germany) was employed. The TD-IMS consisted of two parts with the following dimensions: IMS device ~395 × 112 × 210 mm and the TD unit ~110 × 64 × 113 mm. For analyzes, samples were deposited on a wipe sampling pad (stainless steel coated with Teflon) and inserted in the tool tray. A photograph of the GDA-X, including the wipe sampling pad, is shown in Figure S1a. IMS data were acquired in the positive and negative ionization modes using the WinMusterGDA software (version 1.2.6.12) (Figure S1b) from Airsense Analytics GmbH.

2.4.2. GC-MS equipment

An Agilent GC 7890B series (Agilent Technologies Inc, Santa Clara, CA, USA) equipped with a 7693 autosampler and a 5877B mass detector was used. The instrument was equipped with a Rxi-35Sil MS capillary column (15 m length, 0.25 mm internal diameter, film thicknes 0.25 μm) (Resteck, Bellefonte, PA, USA). The device was controlled by the software Agilent GC MassHunter Workstation 7.0 version.

2.5. TD-IMS analysis

For standards and plant extracts measurements, 6-24 μL (0.6-2.4 μg) of sample was carefully deposited on the centre of the wipe sampling pad, avoiding the diffusion of the liquid towards the peripheral zones of the fibre. Then, samples were heated at 60 °C for 4 min to eliminate the solvent. After this time, the wipe sampling pad was placed into the X-TOOL, and when it reached a temperature of 240 °C, the data were measured in both modes for about 20 seconds. Thus, once the analytes were desorbed, they were driven into the

ionization chamber with atmospheric air (400 mL min^{-1}). In this module, the compounds were ionized by a ^{63}Ni source, and the generated ions passed into the drift tube (6.29 cm length) through the shutter grid, which was open for 200 μs and operated at a constant temperature (60 °C) and at atmospheric pressure. The drift gas (clean air) flow was set at 200 mL min^{-1}. All these parameters are summarized in Table 2.

Table 2. Main design and operating parameters of the commercial IMS device used in this study.

	GDA-X
Type	Handheld
Ion source	^{63}Ni (100 MBq)
Standard inlet	Gas/vapours; thermal desorption (solids/liquids)
Drift tube temperature (ºC)	60
Standard flow of sample (mL min^{-1})	400
Drift gas flow (mL min^{-1})	200
Shutter grid type	Bradbury-Nielson
Grid pulse width/Opening time (μs)	200
Drift length (cm)	6.29
Pressure	Ambient
Inlet type	Membrane

Electric field (V cm^{-1})	289

For the direct analysis of plant materials, the plant residues on fingers of laboratory staff were also analyzed. For that, they passed one finger over the inner surface of the pouches, where the plants were stored, for 20 s. Consecutively, the fingers were rubbed on the surface of the wipe sampling pad in a circular manner for 20 s. Then, the measurements were carried out as before.

2.6. Plant material

The content of cannabinoids was evaluated by GC-MS analysis. For the simultaneous measure of neutral and acidic cannabinoids a derivatization process was carried out. Thus, a representative portion of the hexane extract mentioned in section 2.3 was transferred to a clean tube, evaporated to dryness and then derivatized with BSTFA:TMCS (98:2, v/v) at 37 ºC for 60 min. After cooling to room temperature, the samples were transferred to GC vials, which were recapped. The trimethylsilyl (TMS) derivatives were analyzed by GC-MS. The injector temperature was 250 ºC, with an injection volume of 1 µL in splitless mode and a carrier gas (He) flow rate of 2.5 mL/min. The temperature gradient started at 150 ºC, maintained 1 min and linearly increased at a rate of 50 ºC/min until 170 ºC, then it was linearly increased at 1 ºC/min until 177 ºC, increased again at 25 ºC/min until 230 ºC, and finally at 120 ºC/min until 300 ºC, which was held for 3 min. The MS interface temperature was set to 330 ºC. The internal standard employed was d3-CBD.

2.7. Chemometric analysis of the IMS data

As commented before, the GDA-X operated with automatic switchable polarity, obtaining ion mobility spectra in the positive and negative ionization

modes (see Figure S1b). A spectrum was recorded every 1.5 s, approximately (including positive and negative polarity). The drift time and sample frequency were 30 ms and 30 kHz, respectively. Each measuse is registered as two data file in format *.scm and *.nos. The signals were pre-processed and a multivariate analysis was performed using the statistical software MATLAB (The Mathworks Inc., Natick, MA, USA, 2007) and PLS Toolbox 5.5 (Eigenvector Research, Inc., Manson, WA, USA).

The pre-processing of both positive and negative IMS data for each sample was performed individually by using the IMS data file registered in format *.nos. As an example, Figure S2 summarizes the main steps carried out using MATLAB. For each sample, firstly a baseline correction was performed along the drift time axis. Basically, the baseline was removed by using a fourth order polynomial fitted using the drift range [1:150,600:895], since no peaks were found in this region (see Figure S2). Then, the spectra were smoothed using a second order Savitzky-Golay filter, with a window width of 9. Afterwards, the first spectra were removed to select the relevant spectral data, which contain the analytical signals. For this, sample data was plotted to visualize the scan (y axis in the plot) where the signals of a sample began to appear (see Figure S2). This enables us to limit the region of analysis, since no peaks were found out of this region. Next, the first six spectra of the y axis were taken to match the size of all the samples and the reactant ion peak (RIP) was removed by selecting points from 270 to the end of the x axis (drift time axis). This resulted in a data matrix of 6 × 626. Once then, the data was transposed to convert rows to columns and vice versa, and finally all the spectra of sample were concatenated in a single row to generate a feature vector. The dimensions of the concatenated data for each sample were 1 × 3756.

Once the pre-processing was performed, each concatenated spectrum was arranged consecutively to obtain the data matrices and to build the chemometric models. The samples and classes, according to their psychoactivity and chemotype, included in the models are in Table 1. Firstly, in order to detect

outliers, individual PCAs using auto-scaled data were carried out for each group of samples. A statistical confidence region provided by the software was used as an aid in the detection of outliers. This confidence region is based on Hotelling's T^2-test, which is a multivariate version of Student's t-test. The confidence limit was 95%. Later, a non-supervised PCA analysis using auto-scaled data was employed for dimensionality reduction and extraction of the most relevant information. In all cases, the number of selected principal components correspond to a cumulative variance of 90%. Finally, LDA was used to incorporate class information into the model and find directions to maximize the class separation [20].

3. Results and discussion

3.1. Analysis by GC-MS

As commented before, GC is usually applied in several reference methods for the determination of cannabinoids. In this work, GC-MS was firstly used to determine the ratio of ([Δ^9-THC]+[CBN])/[CBD] in the plant samples. Moreover, the rest of cannabinoids, Δ^9-THCA, CBDA, CBGA, CBG, Δ^9-THCV, CBDV, Δ^8-THC, and CBC, were also determined to group in chemotypes the varieties of plants according to the major ones. This information is summarized in Table 1.

3.2. Optimization of the IMS methodology

A TD-IMS with a ^{63}Ni ionization source was tested for the detection of cannabinoids standards. Firstly, the influence of the solvent (hexane) was evaluated immediately after smearing on the surface of the wipe sampling pad. Although hexane (672.5 kJ/mol) has a lower proton affinity than water (691.0 kJ/mol) [21], several signals that may interfere with the compounds of interest were detected. An example is shown in Figure S3, and as it can be seen, using

hexane the CBC signal was not observed and only hexane signals were seen. However, CBC signals appear in the absence of hexane. Thus, hexane was removed to avoid a loss of sensitivity and contamination of the detector. Derivation agents were also avoided for the same reasons. Moreover, the influence of the sample volume (6, 12, and 24 μL) deposited on the pad was studied using cannabinoids standards at 100 mg L^{-1}. Not surprisingly, a volume of 12 μL was chosen, achieving more intense signals than that obtained when using 6 μL. However, a larger sample volume was not used due to the difficulty getting a centered drop in the wipe pad, which affects to the volatilization efficiency, and so the detected signal. In the case of the analysis of cannabinoids residues on fingers, a contact during 20 s with the pad was employed to ensure that the compounds were homogeneously retained.

Once the analytical methodology was well established, all the commercial cannabinoids standards were analyzed. Table 3 lists the reduced mobilities values (K_o) of the main signals (markers) detected for each compound in the positive and negative ionization modes during the analysis (drift time scans). The K_o values of some of these peak signals agreed well with those previously reported in literature, i.e. the protonated monomer of CBD (1.08 ± 0.02 $cm^2 V^{-1} s^{-1}$) [16] and Δ^9-THC (1.05 ± 0.0004 and 1.06 $cm^2 V^{-1} s^{-1}$) [13,16,17]. In these previous studies, only the K_o value of the most intense peak was pointed out in a drift time measurement using TD-IMS [13], while other used electrospray ionization, a soft volatilization/ionization source [16]. Moreover, nicotinamide (with a high proton affinity, 918.3 kJ/mol) was employed as an internal calibrant using TD-IMS in the positive ionization mode [13,17]. This means that only molecules with higher proton affinity in the vapor phase were protonated and detected, increasing the selectivity of the analysis [13], but it reduces the number of the markers detected compared to those found in the present work. Thus, it should be noted that the markers reported in the Table 3 enrich the literature with new data about the studied cannabinoids in both positive and negative ionization modes.

Table 3. Summary of peak signals of cannabinoids standards at 100 mg L^{-1} (12 µL) detected by TD-IMS**.**

Compound	Positive mode		Negative mode	
	K_0 (cm^2 V^{-1} s^{-1})[a]	Height (a.u.)	K_0 (cm^2 V^{-1} s^{-1})[a]	Height (a.u.)
Δ⁹-THCA	1.842 ± 0.003	55 ± 0.4	**1.009 ± 0.003**	**16 ± 1**
	1.579 ± 0.006	14 ± 1		
	1.412 ± 0.000	13 ± 3		
	1.079 ± 0.004	**27 ± 3**		
Δ⁹-THC	1.834 ± 0.004	44 ± 8	**1.008 ± 0.004**	**46 ± 8**
	1.568 ± 0.000	28 ±1		
	1.405 ± 0.003	20 ± 8		
	1.076 ± 0.004[b]	**98 ± 16**		
CBDA	**1.419 ± 0.007**	**325 ± 48**	**1.015 ± 0.000**	**23 ± 0.4**
	1.091 ± 0.008	**40 ± 9**		
CBD	**1.709 ± 0.011**	**64 ± 12**		
	1.662 ± 0.004	47 ± 3	**1.533 ± 0.004**	**86 ± 13**
	1.584 ± 0.006	40 ± 14	1.403 ± 0.018	22 ± 9
	1.432 ± 0.008	39 ± 2	**1.019 ± 0.006**	**38 ± 16**
	1.092 ± 0.005[b]	77 ± 42		
CBGA	**1.682 ± 0.001**	**150 ± 16**		
	1.395(s)/1.420 ± 0.007/0.001	**48 ± 5[c]**	**1.274 ± 0.006**	**17 ± 9**
			1.119 ± 0.001	**10 ± 4**
	1.096 ± 0.001	**16 ± 1**	1.010 ± 0.003	14 ± 1
	1.044 ± 0.004	**18 ± 2**		
CBG	**1.924 ± 0.015**	**94 ± 15**		
	1.688(s)/1.737 ± 0.012/0.013	**119 ± 11[c]**	**1.744 ± 0.005**	**18 ± 0.1**
			1.533 ± 0.008	**136 ± 29**
	1.410 ± 0.009	**46 ± 7**	1.401 ± 0.004	30 ± 9
	1.102 ± 0.010	**9 ± 2**	**1.301 ± 0.006**	**56 ± 9**
	1.048 ± 0.007	**18 ± 1**		
Δ⁹-THCV	1.845 ± 0.004	42 ± 4		
	1.576 ± 0.002	28 ± 3	**1.072 ± 0.001**	**89 ± 20**
	1.400 ± 0.004	18 ± 2	**0.767 ± 0.001**	**20 ± 16**
	1.162 ± 0.001	**198 ± 89**		
CBDV			1.883 ± 0.016	15 ± 1
			1.732 ± 0.010	**73 ± 12**
	1.714 ±0.005	**39 ± 10**	1.589 ± 0.006	27 ± 5
	1.582 ± 0.007	43 ± 12	1.415 ± 0.007	16 ± 2
	1.429 ± 0.005	25 ± 2	**1.133 ± 0.003**	**77 ± 2**
	1.182 ± 0.001	**248 ± 14**	**1.083 ± 0.001**	**88 ± 1**
			1.033 ± 0.001	**24 ± 3**
			0.772 ± 0.001	**32 ± 3**
Others				
CBN	1.831 ± 0.009	69 ± 7	**1.016 ± 0.004**	**34 ± 8**
	1.568 ± 0.001	28 ± 1		
	1.404 ± 0.001	20 ± 8		
	1.090 ± 0.004	72 ± 29		
Δ⁸-THC	1.825 ± 0.006	52 ± 21		
	1.565 ± 0.009	23 ± 3	**1.004 ± 0.001**	**59 ± 4**
	1.375 ± 0.021	15 ± 3	**0.721 ± 0.002**	**13 ± 2**
	1.075 ± 0.000	102 ± 11		

CBC	1.848 ± 0.004	42 ± 10	**1.025 ± 0.000**	**28 ± 1**
	1.422 ± 0.001	14 ±1	**0.996 ± 0.003**	**19 ± 5**
	1.096 ± 0.002	88 ± 14		

[a]Bold letter indicates more intense peaks (K_o) and/or characteristic, which may be used for differentiating them from others. (s) means shield.

[b]K_o previously reported in literature: CBD, 1.08 $cm^2\ V^{-1}\ s^{-1}$; Δ^9-THC, 1.05-1.06 $cm^2\ V^{-1}\ s^{-1}$.

[c]Height for peak maximum.

The mobility spectra profiles obtained for each cannabinoid prepared at the same concentration (100 mg L^{-1}) in the positive and negative ionization modes during the analysis are depicted in Figure S4 and S5, respectively. In the positive mode, the profiles of some compounds presented different signals, which enable their differentiation, e.g., CBDA (only two signals appear at 1.09 and 1.42 $cm^2\ V^{-1}\ s^{-1}$), CBG (signal at 1.92 $cm^2\ V^{-1}\ s^{-1}$), Δ^9-THCV (signal at 1.16 $cm^2\ V^{-1}\ s^{-1}$), CBDV (signals at 1.18 and 1.71 $cm^2\ V^{-1}\ s^{-1}$) and CBGA (the signals at 1.92 or 1.16/1.18 $cm^2\ V^{-1}\ s^{-1}$ does not appear). However, Δ^9-THCA, Δ^8-THC, Δ^9-THC, CBD, CBC, and CBN gave similar profiles, sharing a signal with K_o 1.08 $cm^2\ V^{-1}\ s^{-1}$ (Δ^9-THCA, Δ^8-THC and Δ^9-THC) and 1.09 $cm^2\ V^{-1}\ s^{-1}$ (CBD, CBC and CBN), but with changes in intensity. In negative mode, some of the studied compounds can be also differentiated visually based on their fingerprints, e.g., CBD, CBG, THCV, CBDV, CBGA and CBC. However, Δ^9-THCA, Δ^9-THC, CBDA, Δ^8-THC and CBN presented a signal closer to K_o 1.01/1.02 $cm^2\ V^{-1}\ s^{-1}$ whose intensity varied depending on the compound. The above suggests that the direct differentiation of the cannabinoids through their TD-IMS fingerprints is possible, however, it is a difficult task especially for those aforementioned compounds that shares some common signals. Then, before the analysis of more complex samples, i.e. *Cannabis* extracts and plant materials, a chemometric study of the global spectra of the cannabinoids standards was carried out employing positive and negative data recorded by TD-IMS as well as the positive and negative data arranged together. For that, the aforementioned data of the cannabinoids were pre-processed following the steps summarized in Material and Methods, and a PCA was performed to assess the applicability of the strategy. The cumulative

percentage of the PCA in the positive, negative, and positive + negative ionization modes were 91.03% (five components), 92.85% (six components), and 90.95% (six components) for an input dataset of 22 samples, i.e. two measurements of each individual cannabinoid standard. As an example, Figure 1 shows the most representative score plots of the PCAs, respectively.

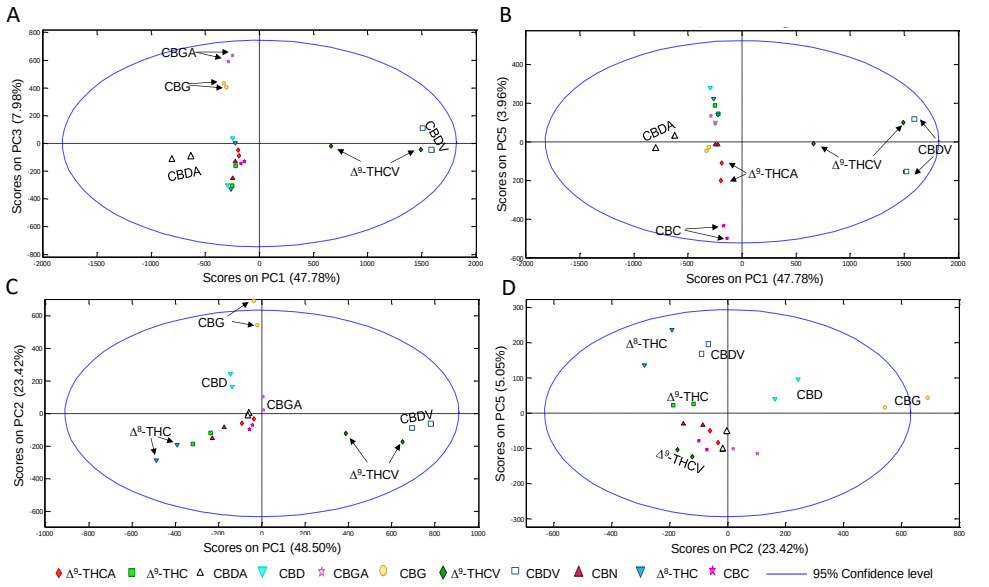

Figure 1. Representative PCAs score plots of the cannabinoids fingerprints: (A and B) positive, (C and D) negative modes.

In the positive mode, with three components, Δ9-THCV, CBDV, CBDA, CBGA and CBG were clustered separately (see Figure 1A). Additionally, with five components (PC1 *vs* PC5), CBC could be also separated, while Δ9-THCA was slightly separated from Δ9-THC (see Figure 1B). However, it is difficult to differentiate CBC from Δ9-THCA, Δ9-THC or Δ8-THC, by simply visual inspection (see Figure S4). So, the need of chemometric data treatment can be highlighted with this example. In the negative mode, Δ9-THCV, CBDV, CBD and CBG were grouped separately in the first two components (see Figure 1C), while Δ8-THC

appeared in an extreme of the plot and separated using five components (see Figure 1D). Notice that CBD was not well separated in the positive ionization mode. So, the analysis in the positive ionization mode, which is the commonest mode used in IMS, can be complemented with the negative one. The PCA of the combined data positive + negative needed more components, with similar results than the PCAs of the individual IMS polarities. Anyway, this strategy could be useful if the analysis using individual positive or negative data fail in clustering some compounds.

3.3. Plant extracts

3.3.1. Evaluation of the TD-IMS spectra

A common solid-liquid extraction method using *n*-hexane was applied to extract the cannabinoids (see section 2.3). The extracts were firstly analyzed by GC-MS to define *Cannabis* chemotypes based on their psychoactivity and the major cannabinoids groups present in the plants (Table 1), as commented before.

Secondly, the extracts were checked by TD-IMS to correlate all the information. Figure 2 depicts examples of TD-IMS spectra of the different *Cannabis* chemotypes in the positive and negative ionization modes. In the positive ionization mode, the spectra of the extracts showed different profiles, but shared some common signals, e.g., at K_o 1.38-1.39 $cm^2\ V^{-1}\ s^{-1}$ (see Figures 2A1-A6). Some signals could be assigned to the presence of concrete cannabinoids by visual inspection of the spectra. As an example, peaks with K_o close to 1.09 (e.g., chemotype 1), 1.18 (e.g., chemotype 2), 1.08 (e.g., chemotype 5) and 1.16 $cm^2\ V^{-1}\ s^{-1}$ are related to CBD/CBDA, CBDV, Δ^9-THC/Δ^9-THCA and Δ^9-THCV, respectively. In addition, the appearance of two peaks at K_o 1.05 and 1.10 $cm^2\ V^{-1}\ s^{-1}$ indicated the presence of CBGA and/or CBG. Nevertheless, the differentiation of the chemotypes using the positive ionization mode in this way is a difficult task due to the low peak resolution provided by the TD-IMS. As an example, there were peaks with shoulders not clearly resolved and wide peaks, which could be

formed by several similar signals (e.g. at K_0 1.72, 1.68, 1.38 cm^2 V^{-1} s^{-1}). Moreover, chemotype 1 and chemotype 6 shared the main peaks signals.

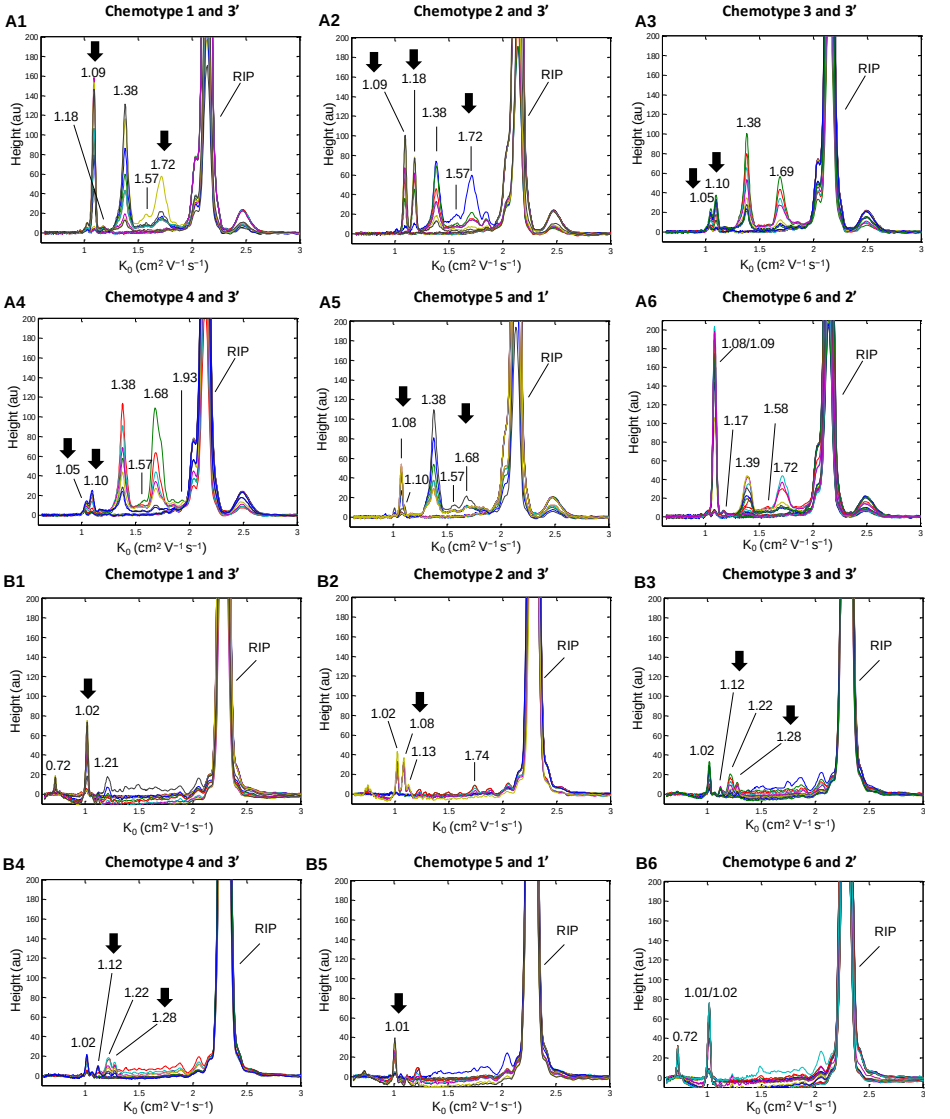

Figure 2. Spectra of *Cannabis sativa* L. plants extracts obtained by TD-IMS in the positive (A1-A6) and negative (B1-B6) ionization modes. The chemotypes are defined in Table 1. The arrows highlight the main characteristic signals of the chemotypes.

Generally, in the negative ionization mode the signal peaks showed lower intensities (see Figures 2B1-B6) than those obtained in the positive ionization mode (see Figures 2A1-A6). Similarly, the studied chemotypes gave different TD-IMS profiles and some peaks could be assigned to concrete cannabinoids.

To evaluate the possibility of obtaining false positive results, other plant materials were extracted with hexane and analyzed by TD-IMS: *Equisetum arvense* (*Equisetaceae*), *Matricaria chamomilla* (*Asteraceae*), *Calendula officinalis* (*Asteraceae*), *Papaver rhoeas* (*Papaveraceae*), and *Origanum vulgare* (*Lamiaceae*). Neither of these species contains cannabinoids. On the contrary, some of them contain terpenes, such as α-pinene, β-pinene, myrcene and limonene [22–24], which are also present in *Cannabis* [25]. These volatiles have K_o values between 1.26 and 1.28 ($cm^2\ V^{-1}\ s^{-1}$) [25,26]. Moreover, tobacco is usually smoked mixed with *Cannabis* in Europe [13]. Therefore, tobacco was also extracted and analyzed in order to evaluate the potential inferences of nicotine (K_o, 1.54 $cm^2\ V^{-1}\ s^{-1}$, [27]) and other components. The IMS spectra of these plants (Figure S6) and tobacco (Figure 3) were clearly different from both standards and *Cannabis* plants extracts. Although there were some common signals between these extracts, *Cannabis* plants extracts and/or cannabinoids standards, the characteristic signal of Δ^9-THC/Δ^9-THCA at K_o 1.08 $cm^2\ V^{-1}\ s^{-1}$ (positive ionization mode) were not found after subtraction of the blanks. In the negative ionization mode, the extracts of these plants presented TD-IMS profiles with low intensity signals, except *M. chamomilla*, and they were clearly different to those of *Cannabis*. There was also no presence of a signal at K_o 1.01 $cm^2\ V^{-1}\ s^{-1}$, characteristic of Δ^9-THC/Δ^9-THCA; reaffirming the results obtained in the positive ionization mode.

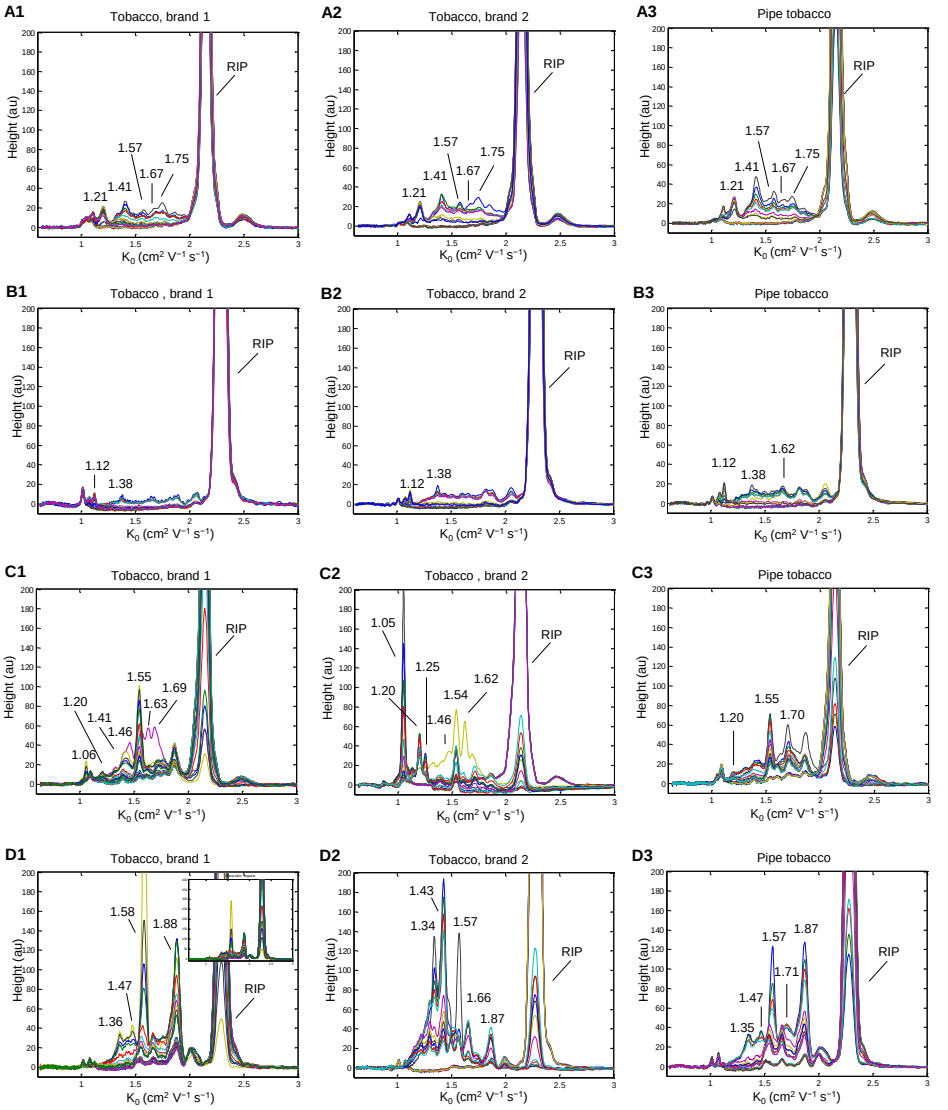

Figure 3. Spectra of tobacco extracts in the positive (A1-A3) and negative ionization modes (B1-B3), and spectra of tobacco residues on fingers in the positive (C1-C3) and negative ionization modes (D1-D3).

3.3.2. Multivariate data analysis

Due to the difficulty to differentiate *Cannabis* chemotypes by the visual inspection of the TD-IMS spectra, a chemometric study based on PCA-LDA [20] was performed after the pre-processing of the spectral fingerprint data, as for standards.

Our results showed that the extracts were grouped properly in different clusters according to the previous defined chemotypes, psychoactivity and major cannabinoids groups, in each ionization mode. Some examples are illustrated in Figure 4 for psychoactivity (A1) and major cannabinoids (B2) chemotypes, for positive (A1) and negative (B2) mode.

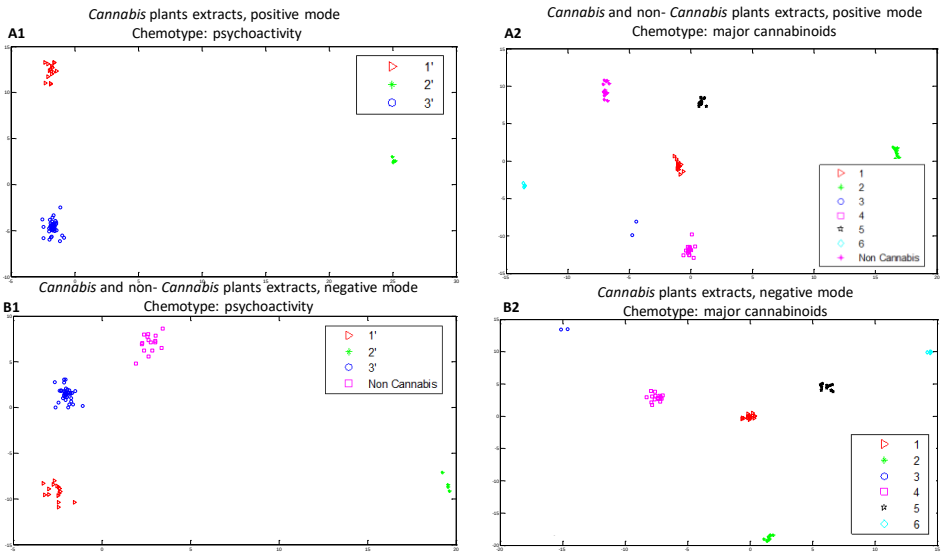

Figure 4. PCA-LDA plots for positive (A1-A2) and negative (B1-B2) spectra of *Cannabis sativa* L. and non-*Cannabis* plants extracts. The chemotypes are defined in Table 1.

Moreover, the aforementioned plants and tobacco were also extracted and analyzed by TD-IMS and PCA-LDA was used to check the potential of the methodology for *Cannabis* discrimination. In this way, non-*Cannabis* plants (including tobacco) were clustered in a different group (see some examples in Figures 4A2 and 4B1). Compared to other IMS methodologies, Sonnberg et al. [13] found that some compounds from non-cannabinoids plants could be misinterpreted as Δ^9-THC because of a partial peak overlapping of signals at a similar drift time. These authors used an algorithm based on the inverse of the second derivative to minimize the low selectivity of the TD-IMS. When using ESI-IMS, Kanu et al. [16] used the conditional reduced mobility (combination of reduced mobility and the width-at-half-height of a peak) to differentiate between real drugs peaks from those of false-positive peaks with similar K_o values. Another study applied GC-FID to determine terpenoids and cannabinoids in ethanolic extracts of *Cannabis* plants and PCA for chemotaxonomic purposes, but the medium Δ^9-THC varieties were not well separated [8]. So, the methodology presented here can be used as a faster screening tool to complement GC-MS analysis, being able to discriminate *Cannabis* varieties from other plant species, including tobacco.

3.4. Residues of plants on fingers

3.4.1. Evaluation of the TD-IMS spectra

The direct measurement of plants residues on fingers, after being in contact with *Cannabis* plants, was also evaluated since this strategy is faster and can be applied on-site, not only for chemotyping but also for drug control. In fact, the most common way of *Cannabis* consumption is smoking, marijuana and hashish being manipulated to make cigarettes.

In the positive ionization mode, the spectra obtained show similar characteristic signals to those for hexane extracts, with some slight shifts, and a higher intensity (Figures 5A1-A6).

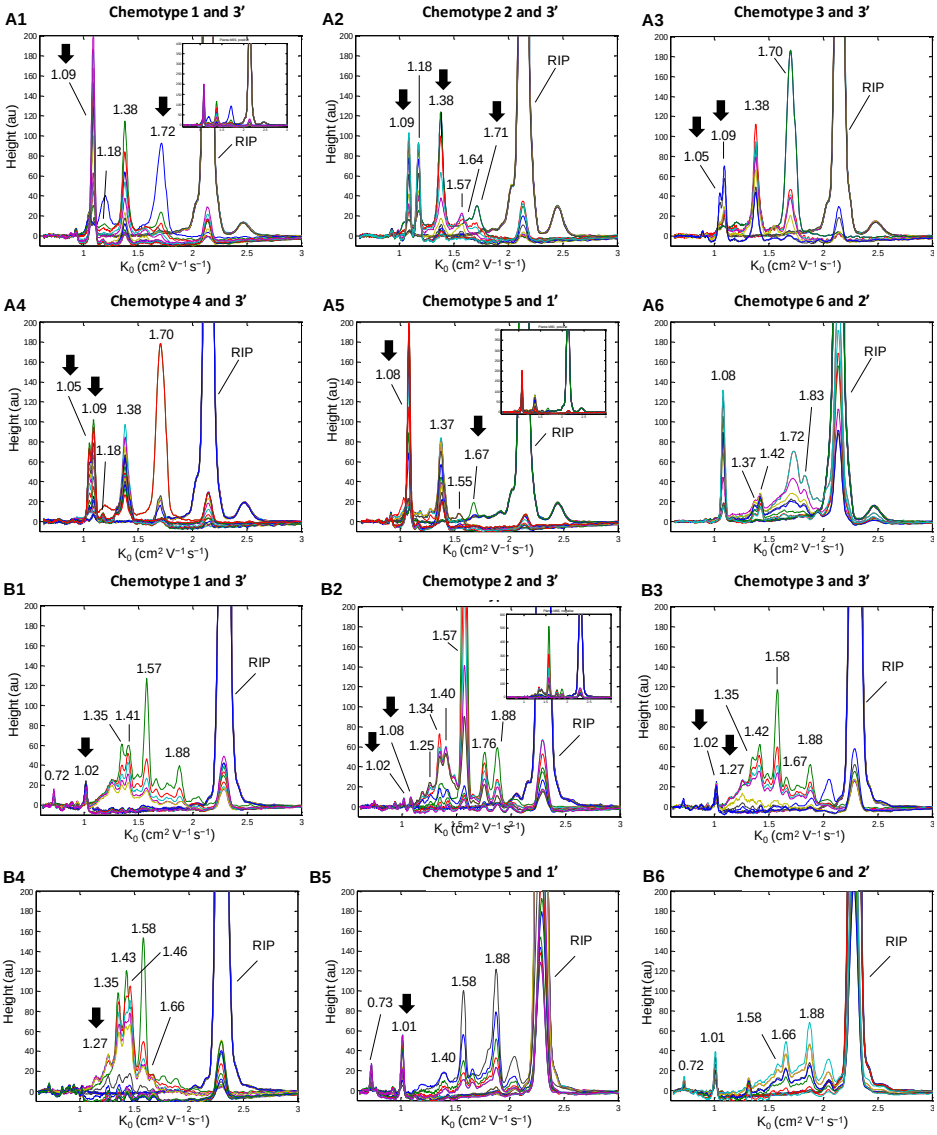

Figure 5. Spectra of *Cannabis sativa* L. plants residues on fingers obtained by thermal desorption-ion mobility spectrometry in the positive (A1-A6) and negative (B1-B6) ionization modes. The chemotypes are defined in Table 1. The arrows highlight the main characteristic signals of the chemotypes.

On the contrary, in the negative ionization mode the spectra of the plants were more complex (see Figures 5B1-B6) than those observed after extraction with *n*-hexane, indicating the potential detection of other polar phytochemicals. This could be explained by the fact that *n*-hexane is a non-polar solvent. In these spectra, peaks with K_o values at 1.01, 1.02, 1.08, and 1.27 $cm^2\ V^{-1}\ s^{-1}$ could be related to the presence of Δ^9-THCA and Δ^9-THC, CBDA and CBD, CBDV, as well as CBGA, respectively (Figure 5 and Table 3).

When non-*Cannabis* plants (Figure S7) and tobacco (Figure 3) were evaluated, the TD-IMS spectra in both modes were clearly different from those of cannabinoids standards and *Cannabis* plants as before. As observed for *Cannabis* plants, the spectral fingerprints were more complex than those of the hexane extracts. Moreover, in the positive ionization mode a peak with K_o close to 1.54 $cm^2\ V^{-1}\ s^{-1}$ was detected in tobacco samples (Figure 3), which could be assigned to nicotine according to literature [27].

Despite the conclusions obtained throught the direct inspection of spectra, a deeper and objective chemometric data treatment is necessary for the proper chemotyping of the plants using TD-IMS.

3.4.2. Multivariate data analysis

A second strategy consisted of using PCA-LDA to discriminate *Cannabis* chemotypes based on the direct measurement of the plant material by TD-IMS. Figure 6 summarizes some examples of the groups clustered in each ionization mode using PCA-LDA; i.e. the plants could be separated in three and five groups according to the pre-established chemotypes, i.e. psychoactivity (Figures 6A1) and major cannabinoids groups (Figures 6B2), respectively. Moreover, when non-*Cannabis* plants were analyzed, they were grouped in a separated cluster (Figures 6A2 and 6B1). However, using the positive TD-IMS fingerprints, a

partial overlapping of the chemotypes 2 (CBD+CBDA/CBDV+CBDVA) and 5 (Δ^9-THC+Δ^9-THCA) was observed (Figure 6A2). Anyway, these strategies can be used for the detection of cannabinoids and the discrimination of *Cannabis* chemotypes, without the requirement of a pre-extraction method and so in a faster way than other methodologies, e.g., GC-FID [8], ESI coupled to Fourier transform ion cyclotron resonance MS [7], nuclear magnetic resonance and high performance TLC [28,29].

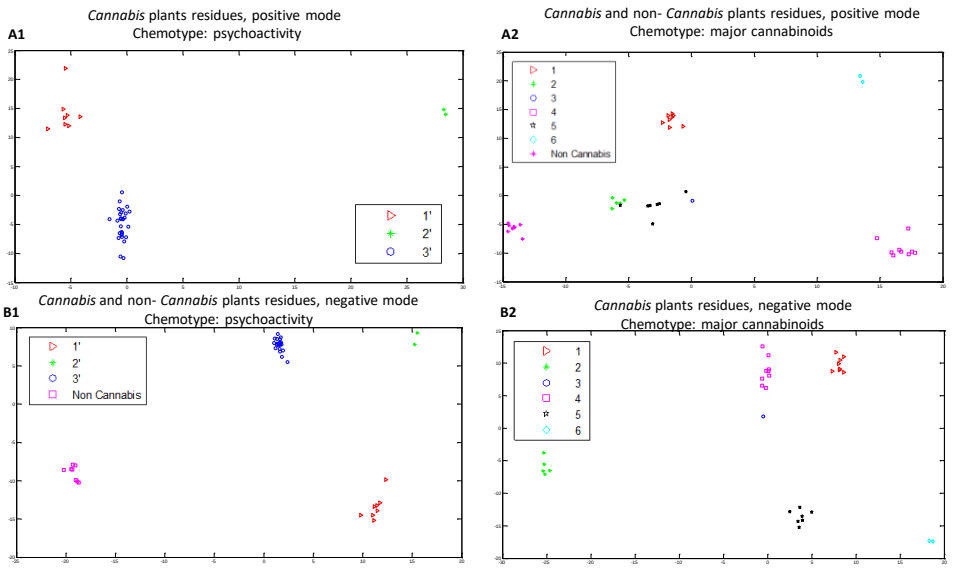

Figure 6. PCA-LDA plots for positive (A1-A2) and negative (B1-B2) spectra of *Cannabis sativa* L. and non-*Cannabis* plants residues on fingers. The chemotypes are defined in Table 1.

4. Conclusions

On the basis of these results, the methodology based on TD-IMS can be used to detect cannabinoids in the positive and negative ionization modes. These data combined with PCA-LDA as chemometric strategy was useful for the

discrimination of *Cannabis* chemotypes after hexane extraction. Moreover, samples of different *Cannabis* plants could be also clustered in different chemotypes after the direct measurement of plant material as residue on fingers, making the analysis faster (< 2 min) and with applicability for on-site measurements, making this technical tool particularly attractive for *Cannabis* breeders. Potentially interfering non-*Cannabis* plants were measured, showing different TD-IMS fingerprint profiles than those of *Cannabis* plants, being clustered in a different group when using PCA-LDA. Thus, further studies are required to test the methodology on site for illegal marijuana handling through the detection of residues on hands of consumers.

Akcnowledgments

The authors acknowledge support from the Government of Spain (DGICyT Project CTQ2014-52939R). N.A.M. thanks the Ministry of Economy and Competitiveness (MINECO) of the Spanish Government for a Juan de la Cierva post-doctoral contract (FJCI-2014-20321). N.J.C. wishes to thank the Spanish Ministry of Education, Culture and Sport for award of a FPU pre-doctoral grant.

References

[1] United Nations Office on Drugs and Crime, Recommended methods for the identification and analysis of cannabis and cannabis products, United Nations, New York, 2009.

[2] J. Cherney, E. Small, Industrial hemp in North America: Production, Politics and Potential, Agronomy 6 (2016) 58.

[3] E. P. M. de Meijer, K. M. Hammond, The inheritance of chemical phenotype in *Cannabis sativa* L. (V): regulation of the propyl-/pentyl cannabinoid ratio, completion of a genetic model, Euphytica 210 (2016) 291–307.

[4] United Nations Office on drugs and crime, World Drug Report 2016. Cannabis, 2016.

[5] K. Tang, P.C. Struik, X. Yin, C. Thouminot, M. Bjelková, V. Stramkale, et al., Comparing hemp (*Cannabis sativa* L.) cultivars for dual-purpose production under contrasting environments, Ind. Crops Prod. 87 (2016) 33–44.

[6] J. Fike, Industrial Hemp: renewed opportunities for an ancient crop, CRC. Crit. Rev. Plant Sci. 35 (2016) 406–424.

[7] I.R. Nascimento, H.B. Costa, L.M. Souza, L.C. Soprani, B.B. Merlo, W. Romão, Chemical identification of cannabinoids in street marijuana samples using electrospray ionization FT-ICR mass spectrometry, Anal. Methods. 7 (2015) 1415–1424.

[8] J.T. Fischedick, A. Hazekamp, T. Erkelens, Y.H. Choi, R. Verpoorte, Metabolic fingerprinting of *Cannabis sativa* L., cannabinoids and terpenoids for chemotaxonomic and drug standardization purposes, Phytochemistry 71 (2010) 2058–2073.

[9] B. De Backer, B. Debrus, P. Lebrun, L. Theunis, N. Dubois, L. Decock, et al., Innovative development and validation of an HPLC/DAD method for the qualitative and quantitative determination of major cannabinoids in cannabis plant material, J. Chromatogr. B Anal. Technol. Biomed. Life Sci. 877 (2009) 4115–4124.

[10] A. Hazekamp, A. Peltenburg, R. Verpoorte, C. Giroud, Chromatographic and spectroscopic data of cannabinoids from *Cannabis sativa* L., J. Liq. Chromatogr. Relat. Technol. 28 (2005) 2361–2382.

[11] J. Mazina, A. Spiljova, M. Vaher, M. Kaljurand, M. Kulp, A rapid capillary electrophoresis method with LED-induced native fluorescence detection for the analysis of cannabinoids in oral fluid, Anal. Methods. 7 (2015) 7741–7747.

[12] Commission Regulation (EEC) No 421/86 of 25 February 1986 amending Regulation (EEC) No 771/74 and Regulation (EEC) No 2188/84 by prescribing a Community method for the quantitative determination of tetrahydrocannabinol in hemp.

[13] S. Sonnberg, S. Armenta, S. Garrigues, M. de la Guardia, Detection of tetrahydrocannabinol residues on hands by ion-mobility spectrometry (IMS). Correlation of IMS data with saliva analysis, Anal. Bioanal. Chem. 407 (2015) 5999–6008.

[14] C. Fuche, A. Gond, D. Collot, C. Faget, The use of IMS and GC/IMS for analysis of saliva, IJIMS. (2001) 20–25.

[15] A.B. Kanu, H.H. Hill, Identity confirmation of drugs and explosives in ion mobility spectrometry using a secondary drift gas, Talanta 73 (2007) 692–699.

[16] A.B. Kanu, A. Leal, Identity efficiency for high-performance ambient pressure ion mobility spectrometry, Anal. Chem. 88 (2016) 3058–3066.

[17] J.R. Verkouteren, J.L. Staymates, Reliability of ion mobility spectrometry for qualitative analysis of complex, multicomponent illicit drug samples, Forensic Sci. Int. 206 (2011) 190–196.

[18] Y. Mohsen, N. Gharbi, A. Lenouvel, C. Guignard, Detection of d9-tetrahydrocannabinol, methamphetamine and amphetamine in air at low ppb level using a field asymmetric ion mobility spectrometry microchip sensor, Procedia Eng. 87 (2014) 536–539.

[19] R. Lian, Z. Wu, X. Lv, Y. Rao, H. Li, J. Li, R. Wang, C. Ni, Y. Zhang, Rapid screening of abused drugs by direct analysis in real time (DART) coupled to time–of–flight mass spectrometry (TOF–MS) combined with ion mobility spectrometry (IMS), Forensic Sci. Int. 279 (2017) 268–280.

[20] R. Garrido-Delgado, L. Arce, A. V. Guamán, A. Pardo, S. Marco, M. Valcárcel, Direct coupling of a gas–liquid separator to an ion mobility spectrometer for the classification of different white wines using chemometrics tools, Talanta 84 (2011) 471–479.

[21] N. Sato, K. Sekimoto, M. Takayama, Ionization capabilities of hydronium ions and high electric fields produced by atmospheric pressure corona discharge, Mass Spectrom. 5 (2017) S0067–S0067.

[22] A.J. Karamanos, D.E.K. Sotiropoulou, Field studies of nitrogen application on Greek oregano (*Origanum vulgare* ssp. hirtum (Link) Ietswaart) essential oil during two cultivation seasons, Ind. Crops Prod. 46 (2013) 246–252.

[23] O.O. Okoh, A.P. Sadimenko, O.T. Asekun, A.J. Afolayan, The effects of drying on the chemical components of essential oils of *Calendula officinalis* L., African J. Biotechnol. 7 (2008) 1500–1502.

[24] M.H.H. Roby, M.A. Sarhan, K.A.H. Selim, K.I. Khalel, Antioxidant and antimicrobial activities of essential oil and extracts of fennel (*Foeniculum vulgare* L.) and chamomile (M*atricaria chamomilla* L.), Ind. Crops Prod. 44 (2013) 437–445.

[25] H. Lai, P. Guerra, M. Joshi, J.R. Almirall, Analysis of volatile components of drugs and explosives by solid phase microextraction-ion mobility spectrometry, J. Sep. Sci. 31 (2008) 402–412.

[26] H. Lai, I. Corbin, J.R. Almirall, Headspace sampling and detection of cocaine, MDMA, and marijuana via volatile markers in the presence of potential interferences by solid phase microextraction-ion mobility spectrometry (SPME-IMS), Anal. Bioanal. Chem. 392 (2008) 105–113.

[27] M.L. Ochoa, P.B. Harrington, Detection of methamphetamine in the presence of nicotine using in situ chemical derivatization and ion mobility spectrometry, Anal. Chem. 76 (2004) 985–991.

[28] C. Citti, D. Braghiroli, M.A. Vandelli, G. Cannazza, Pharmaceutical and biomedical analysis of cannabinoids: A critical review, J. Pharm. Biomed. Anal. 147 (2018) 565–579.

[29] F. Fowler, B. Voyer, M. Marino, J. Finzel, M. Veltri, N.M. Wachter, et al., Rapid screening and quantification of synthetic cannabinoids in herbal products with NMR spectroscopic methods, Anal. Methods. 7 (2015) 7907–7916.

Supplementary Information

Table S1. Physico-chemical parameters of the studied cannabinoids and their chemical structures.

Compound[a]	Molecular formula[b]	Molecular Weight (Da)[b]	Experimental boiling temperature[c,d] (°C)	Theoretical boiling temperature[b] (°C)	Gas phase ion energetics data[d,e]	Experimental K_o[f] ($cm^2 V^{-1} s^{-1}$)	Chemical structure[b]
Δ^9-THCA	$C_{22}H_{30}O_4$	358.471	ND	530.8 ± 50.0	ND	ND	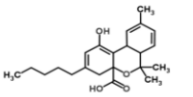
Δ^9-THC	$C_{21}H_{30}O_2$	314.462	200 (at 0.02 mmHg)	390.4 ± 42.0	ND	1.0500 ± 0.0004; 1.06	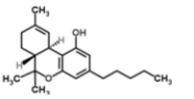
CBDA	$C_{22}H_{30}O_4$	358.471	ND	530.8 ± 50.0	ND	ND	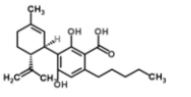
CBD	$C_{21}H_{30}O_2$	314.462	188.5	463.9 ± 45.0	ND	1.08±0.02 (monomer); 0.94 ± 0.01 (dimer)	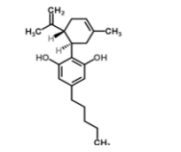
CBGA	$C_{22}H_{32}O_4$	360.487	ND	535.7 ± 50.0	ND	ND	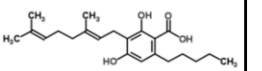
CBG	$C_{21}H_{32}O_2$	316.478	ND	470.4 ± 40.0	ND	ND	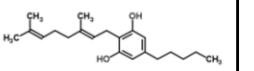
Δ^9-THCV	$C_{19}H_{26}O_2$	286.409	ND	360.6 ± 42.0	ND	ND	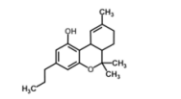
CBDV	$C_{19}H_{26}O_2$	286.409	ND	439.4 ± 45.0	ND	ND	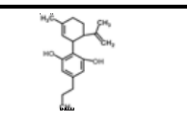

Others							
CBN	$C_{21}H_{26}O_2$	310.193	160-161 (at 0.02 mmHg)	476.5 ± 34.0	ND	ND	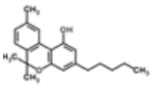
Δ^8-THC	$C_{21}H_{30}O_2$	314.462	ND	NA	ND	ND	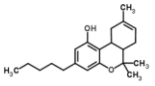
CBC	$C_{21}H_{30}O_2$	314.462	ND	428.7 ± 45.0	ND	ND	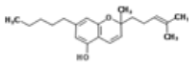

[a]Δ^9-THCA, Δ^9-tetrahydrocannabinolic acid; Δ^9-THC, Δ^9-tetrahydrocannabinol; CBDA, cannabidiolic acid; CBD, cannabidiol; CBGA, cannabigerolic acid; CBG, cannabigerol; Δ^9-THCV, Δ^9-tetrahydrocannabivarin; CBDV, cannabidivarin; CBN, cannabinol; Δ^8-THC, Δ^8-tetrahydrocannabinol; CBC, cannabichromene.
[b]ChemSpider database (http://www.chemspider.com/).
[c]SciFinder database (https://scifinder.cas.org/scifinder/).
[d]ND, not described.
[e]Ionization energy (eV), proton affinity (kJ/mol), and electron affinity (eV) (http://webbook.nist.gov/chemistry/).
[f]These values has been previously reported by [1–4].

References

[1] A.B. Kanu, H.H. Hill, Identity confirmation of drugs and explosives in ion mobility spectrometry using a secondary drift gas, Talanta 73 (2007) 692–699.

[2] A.B. Kanu, A. Leal, Identity Efficiency for High-Performance Ambient Pressure Ion Mobility Spectrometry, Anal. Chem. 88 (2016) 3058–3066.

[3] S. Sonnberg, S. Armenta, S. Garrigues, M. de la Guardia, Detection of tetrahydrocannabinol residues on hands by ion-mobility spectrometry (IMS). Correlation of IMS data with saliva analysis, Anal. Bioanal. Chem. 407 (2015) 5999–6008.

[4] J.R. Verkouteren, J.L. Staymates, Reliability of ion mobility spectrometry for qualitative analysis of complex, multicomponent illicit drug samples, Forensic Sci. Int. 206 (2011) 190–196.

Figure S1. (a) Photograph of the GDA-X device and (b) acquisition view of the cannabinoid Δ^9-tetrahydrocannabinolic acid (Δ^9-THCA) at the scan 52 (70 s) using WinMusterGDA software.

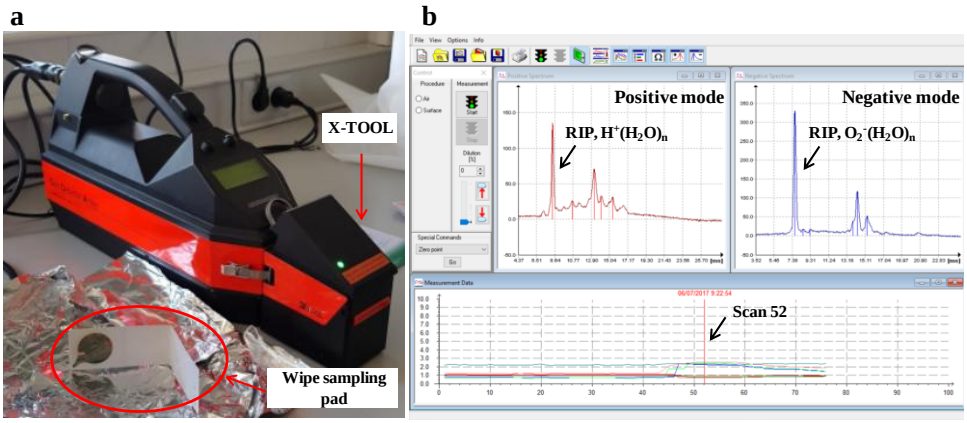

Figure S2. Summary of the main steps followed for the preprocessing of the ion mobility spectrometry data using MATLAB software.

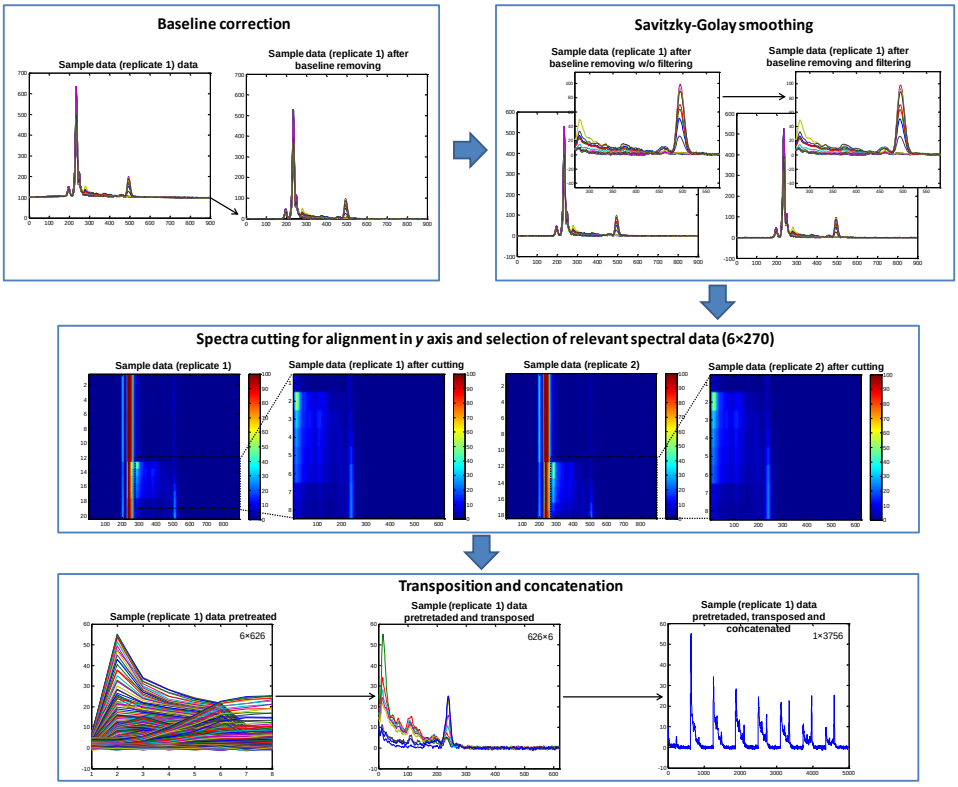

Figure S3. Topographic views obtained by thermal desorption-ion mobility spectrometry: a blank, hexane, cannabichromene (CBC) (100 mg L^{-1}) in hexane, and CBC (100 mg L^{-1}) after removing of the hexane.

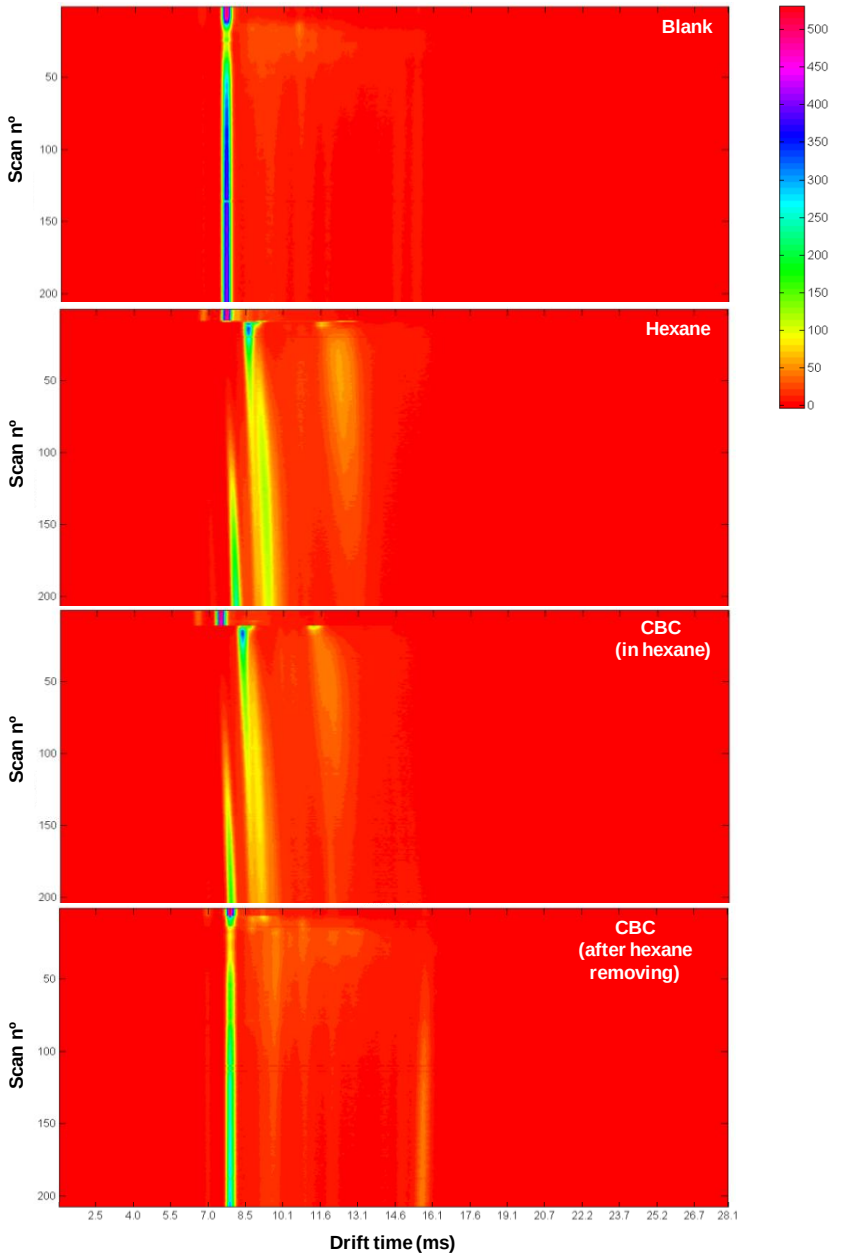

Figure S4. Spectra of the cannabinoids of interest obtained by thermal desorption-ion mobility spectrometry in the positive ionization mode.

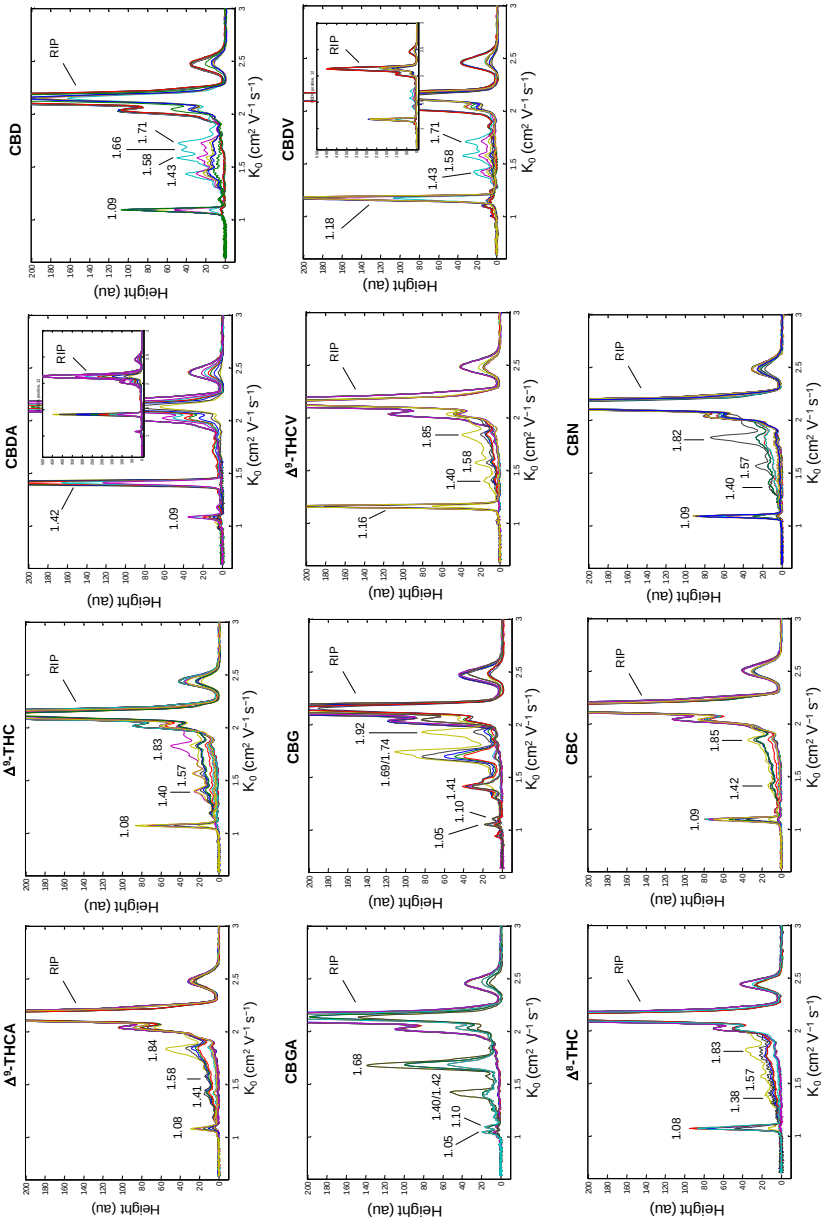

Figure S5. Spectra of the cannabinoids of interest obtained by thermal desorption-ion mobility spectrometry in the negative ionization mode

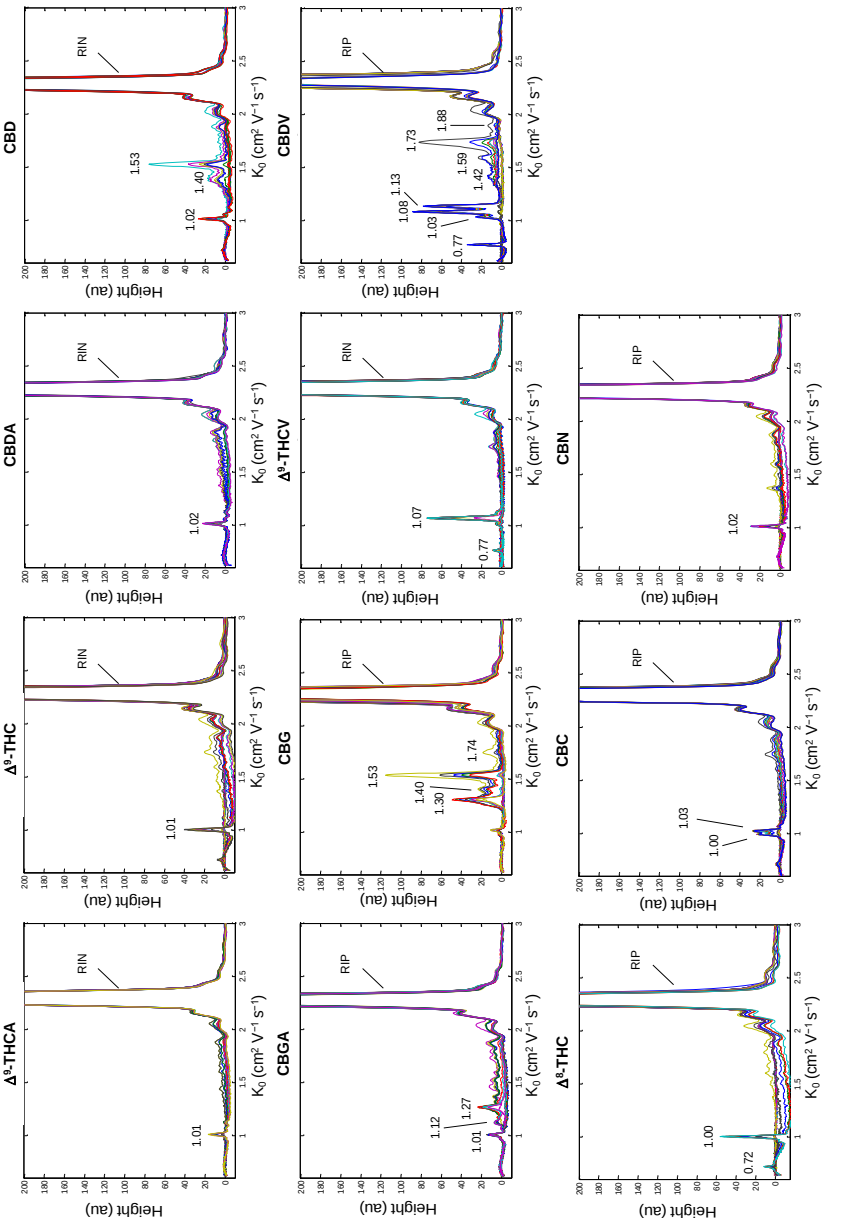

Figure S6. Spectra of non-*Cannabis* plant materials extracted with hexane and determined by thermal desorption-ion mobility spectrometry in the (a) positive and (b) negative ionization modes.

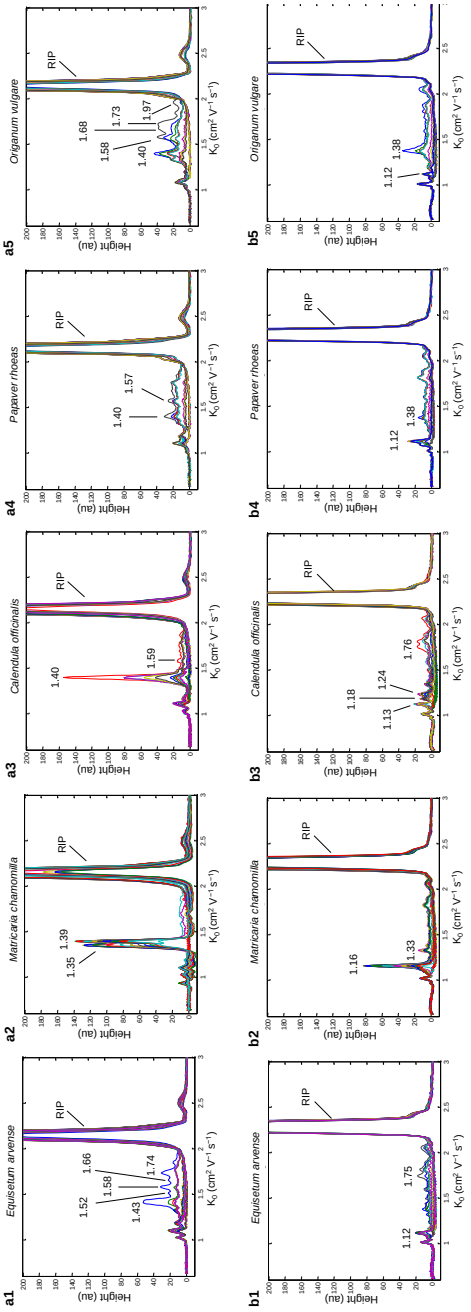

Figure S7. Spectra of non-*Cannabis* plants residues on fingers determined by thermal desorption-ion mobility spectrometry in the (a) positive and (b) negative ionization modes.

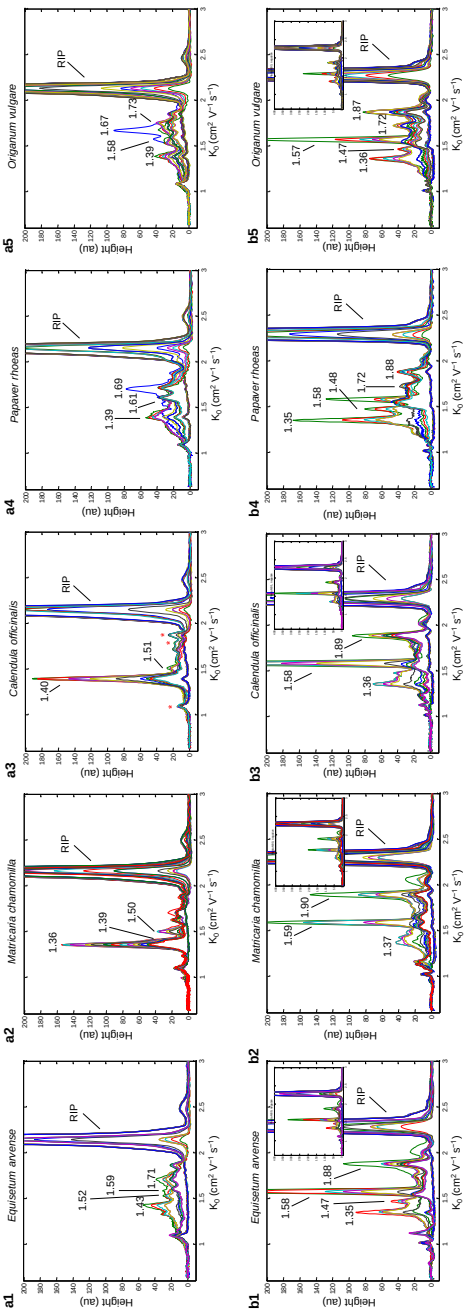

Improved selectivity for the determination of trinitrotoluene through reactive stage tandem ion mobility spectrometry and a quantitative measure of source-based suppression of ionization

CHAPTER IV

To send

Improved selectivity for the determination of trinitrotoluene through reactive stage tandem ion mobility spectrometry and a quantitative measure of source-based suppression of ionization

Natividad Jurado-Campos[1], Umesh Chiluwal[2], Gary A. Eiceman[2]

[1]*Department of Analytical Chemistry, University of Córdoba 14071 Córdoba, Spain.*

[2]*Department of Chemistry and Biochemistry, New Mexico State University, Las Cruces, New Mexico 88003, United States.*

Improved selectivity for the determination of trinitrotoluene through reactive stage tandem ion mobility spectrometry and a quantitative measure of source-based suppression of ionization

Natividad Jurado-Campos, Umesh Chiluwal, Gary A. Eiceman

ABSTRACT

A tandem ion mobility spectrometer was used to mobility isolate ions at the drift time for trinitrotoluene (TNT) in a first mobility stage, remove an interfering compound by ion decomposition in a middle reactive stage, and mobility characterize the remaining TNT ions in a second mobility stage. This sequential processing of ions provided decisive detection of TNT in the presence of an interfering peak differing from TNT in reduced mobility coefficient (K_o) by only 0.02 cm^2/Vs. Even though ions of TNT (as $M-1)^-$ and the interfering compound was more than 90% convolved, TNT could be selectively detected with more than 95% decomposition of the interferent at 123 Td to an ion now separated by ΔK_o of 0.2 cm^2/Vs from TNT. Ions for TNT were not decomposed in these electric fields though transmission efficiency was decreased by 20% through a wire grid assembly (the reactive stage). The concept of reactive stage tandem ion mobility spectrometry does not avert the suppression of ionization of interferences in the ion source and was determined as 30% with 1 ng of TNT and 200 ng of interference on a sample trap.

Keywords: Trinitrotoluene (TNT), Tandem Ion Mobility Spectrometry, Reactive Stage, Selective, Quantitative.

Innovative coupling of Supercritical Fluid Extraction with Ion Mobility Spectrometry

CHAPTER V

Talanta

188 (2018) 637–643

Innovative coupling of Supercritical Fluid Extraction with Ion Mobility Spectrometry

Natividad Jurado-Campos[1$], Azahara Carpio[1$], Mohammed Zougagh[2], Lourdes Arce[1] and Natalia Arroyo-Manzanares[3]

[1]*Department of Analytical Chemistry. Institute of Fine Chemistry and Nanochemistry. Marie Curie Annex Building. Campus de Rabanales, 14071 Córdoba (Spain)*

[2]*Regional Institute for Applied Chemistry Research, IRICA, Av. Camilo José Cela 10, E-13004 Ciudad Real, Spain. Castilla-La Mancha Science and Technology Park, E-02006 Albacete, Spain*

[3]*Department of Analytical Chemistry, Faculty of Chemistry, Regional Campus of International Excellence "Campus Mare-Nostrum", University of Murcia, E-30100 Murcia, Spain*

[$]*These authors contributed equally to this work*

Innovative coupling of Supercritical Fluid Extraction with Ion Mobility Spectrometry

Natividad Jurado-Campos, Azahara Carpio, Mohammed Zougagh, Lourdes Arce and Natalia Arroyo-Manzanares

ABSTRACT

This paper describes a pioneer on-line hyphenation between a supercritical fluid extraction (SFE) and an ion mobility spectrometry (IMS) detector through a Tenax TA sorbent trap as retention interface. By means of a simple design, taking advantage of both techniques, this new coupling allows us to extract and preconcentrate analytes and in a second step to determine them. As result, an increase in the accuracy of the analytical process was achieved by elimination of sample transfer from one device to another. In addition, this new coupling reduces the time needed for the optimization of a new SFE method, since the detector can monitor on-line the efficiency of the extraction.

The parameters affecting the coupling and its success have been studied in detail via the extraction of benzene and toluene from soil samples. Finally, the suitability of IMS as on-line detector to monitor compounds of industrial interest extracted by SFE was evaluated taking as a model, the extraction and detection of 1,8-cineole (eucalyptol) in rosemary aromatic plants, which could be extrapolated on an industrial scale.

Keywords: Ion Mobility Spectrometer, Supercritical Fluid Extraction, Coupling, BTEX, Eucalyptol (1,8-Cineole), Rosemary

1. Introduction

The Supercritical Fluid Extraction (SFE) technique offers advantages as a separation technique due to the non-toxic nature of the most used fluid CO_2. Moreover, SFE is a versatile technique that allows the extraction of non-polar compounds due to the solvent properties of CO_2, which can be modified by the addition of a polar solvent such as methanol, ethanol and others. When a new SFE method is developed, the obtained extracts are usually recovered in a liquid solvent or in a solid trap. A solid-liquid phase collection or empty vessel trap collection may also be used [1]. Later, the extracts are usually analysed off-line with Gas Chromatography (GC), Liquid Chromatography (LC) or spectroscopic methods for quantification of the leaching yield. However, the analyte collection following SFE remains an important area for improvement due to problems related to collection temperature, fluid flow rate, extraction time, analyte volatility and so on, which hamper -and slow down the optimization of a good extraction method of SFE. In this situation, the direct monitoring of the extracts in real time by coupling the supercritical fluid extractor with the analytical detector provide advantages such as: improvement of the recovery or extraction yield, reduction of sample manipulation avoiding errors related to this step [1], automatization and integration of sample pre-treatment step, reduction of risk of loss of thermolabile analytes which is beneficial for trace analysis, decrease of optimization and analysis times, costs and human participation. For all these benefits, the SFE device has already been on-line coupled to different analytical instrumentation [2-4]. Considering liquid phase separations, the SFE has been mainly coupled to LC [5-8]. In addition, the efficiency of on-line coupling with other techniques, such as Capillary Electrophoresis [9,10], or Supercritical Fluid Chromatography [11-13], has also been successfully tested. In most cases, the coupling of SFE to the different instruments have been accomplished using laboratory-made programmable arm [9], continuous flow system [10], valves [13] or sorbent traps [11-12]. Furthermore, GC have also been on-line coupled to SFE [14] being the most common to connect the restrictor from the SFE directly with

the inlet liner of the GC [14, 15-17]. Additionally, the hyphenation of SFE-GC has been carried out using a sorbent trap and valve systems [18].

As a gas detector, ion Mobility Spectrometry (IMS) is emerging in the analytical chemistry field due to its potential to detect and monitor trace levels of volatile and semivolatile chemical compounds. This inexpensive tool is also characterized by its portability, ease of use and operation at atmospheric pressure, among other advantages [19]. One of the known bottlenecks of this technique is how to introduce volatile compounds. Until now, multiple strategies have been designed to overcome this problem, such as the use of permeation tubes, thermal desorption units or headspace samplers [20]. But their main disadvantage is that most of them must be handled manually, and this may imply a loss of robustness of the proposed analytical method.

In this article the advantages of SFE as a sample introduction system and the advantages of IMS as a powerful detector to monitor some target analytes extracted by SFE has been combined and studied for the first time. A successful environmentally-friendly hyphenation between both instruments, SFE and IMS, was carried out using a column filled with Tenax TA material as a sorbent trap to couple both devices. The proper and reliable functioning of the present new coupling was successfully demonstrated by analyzing toluene and benzene from soil sample, characterizing the methodology in terms of precision and sensitivity. Additionally, the utility of this new hyphenation to solve a real problem on an industrial scale was studied. The extraction of eucalyptol as a model bioactive compound [21] was chosen to demonstrate the usefulness of the coupling due to its beneficial properties [22, 23]. Eucalyptol has also been previously extracted by SFE in plants or essential oils such as lavender, eucalyptus, tansy and coriander [24-26]. However, eucalyptol has been rarely determined by IMS, and its determination has been focused on breath [27]. In this work, rosemary plant was selected as an interesting sample due to its high content of eucalyptol [28, 29].

2. Material and methods

2.1. Reagents, chemicals and samples

Benzene, toluene, ethylbenzene, (m-, p- and o-) xylenes (BTEX), eucalyptol (synonym: 1,8-cineole) and methanol used for standard preparations were obtained from Sigma Aldrich (St Louis, MO, USA). The Tenax TA porous polymer sorbent (2,6-diphenylene oxide) was purchased from Scientific Instrument Services (Ringoes, New Jersey, USA). Diatomaceous earth was obtained from Sigma Aldrich (St Louis, MO, USA). Purified nitrogen (N_2, 5.0) was provided by Abelló Linde (Barcelona, Spain). Ultrapure CO_2 (99.9%) in cylinder with a dip tube was supplied by Carburos Metálicos (Barcelona, Spain).

Soil samples were collected from the street. They were sieved in order to homogenize the sample, which means removing pebbles and rocks, and breaking up large soil aggregates.

Fresh rosemary (*Rosmarinus officinalis* L.) was purchased in a local market of the city of Córdoba, Spain. The plant was triturated using a stainless-steel grinder.

2.2. Instrumentation

2.2.1. Supercritical fluid extractor

All supercritical fluid extractions were performed using a modular Jasco SFE system (Tokyo, Japan) consisting of one pump model PU-2080 Plus used to supply the CO_2, a backpressure regulator (BPR) model BP-2080 Plus, and a CO-2060 Plus oven as extraction chamber to place a stainless-steel extraction cell of 5 mL (Análisis Vínicos, Tomelloso, Spain). Depending on the final purpose, a configuration for solid or liquid samples could be used.

The standard configuration of the device was modified using two Rheodyne 7000L valves (Cotati, CA), V1 and V2, allowing to isolate the extraction cell between analyses, and the use of the static and dynamic extraction mode, respectively. The whole scheme is shown in Figure 1. As a supercritical fluid, CO_2 pure was used. The SFE was controlled by ChromNav software (version 1.19.03).

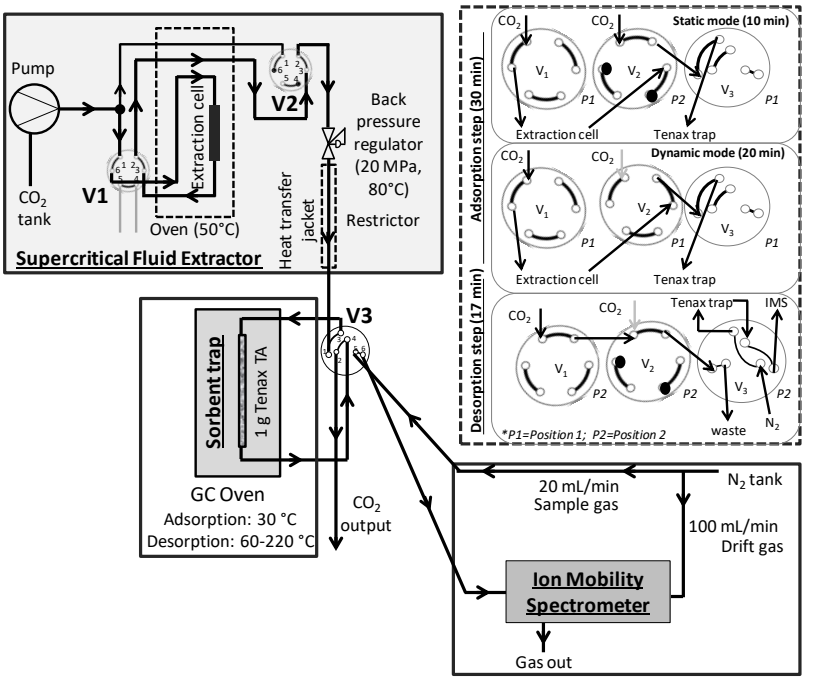

Figure 1. Scheme of the hyphenation SFE-IMS proposed including the conditions of the methodology described in section 3.2. A flow diagram of the two positions of valves 1, 2 and 3 throughout the entire procedure is included.

2.2.2. Interface description

A direct SFE-IMS coupling was not possible for the following reasons: if the IMS device had been hyphenated before the BPR of the SFE, the high

pressure originated in the SFE system could damage the drift tube of the IMS device. Moreover, if IMS detector had been coupled after BPR, instability of baseline would have been observed in the spectra. For these reasons, it was necessary to use a solid trap in order to adsorb and desorb the analytes before introducing them into the IMS device. Figure 1 shows the interface (sorbent trap) designed for SFE-IMS, meeting this requirement.

1-g of solid Tenax TA, as sorbent trap, was placed into a stainless-steel tube of 250 mm length and 6 mm i.d. that was used as column, in order to adsorb and desorb the analytes. Glass wool was used in the extremes of the column to avoid the loss of the material. Before being used, the Tenax TA sorbent was activated in an oven at 250 ºC by passing N_2 gas at a flow rate of 100 mL/min for 4 hours [30].

In the experimental set-up, this column was placed in a chromatographic oven model 5890 supplied by HP Hewlett Packard (Minnesota, USA). The inlet part of the column was connected to the restrictor of the SFE device and the outlet part to the IMS detector (see Figure 1), through a Rheodyne 6-port switching valve (V3) from Valco (Houston, Texas). All connections were made using 1/16" o.d. x 0.010-inch i.d. stainless steel tubes (Sigma Aldrich). The temperature of the restrictor was controlled using a heat transfer jacket (Ramem, Madrid, Spain) in order to avoid condensation.

2.2.3. Ion mobility spectrometer

The IMS instrument with an ultraviolet lamp as a photoionization source was supplied by G.A.S. Gesellschaft für Analytische Sensorsysteme mbH (Dortmund, Germany). The instrument uses a 230 V/50-60 Hz power supply and a constant electrostatic field of 333 V/cm. In addition, the drift tube has a length of 12 cm and operates at room temperature and pressure. Purified nitrogen was used as sample and drift gas. Data obtained was processed with GASpector

software (version 3.9.9.DSP from G.A.S.). The IMS method to detect a mixture of BTEX was previously described [30] and all spectra were recorded in the positive ion mode. The IMS operational parameters are summarized in Table 1. This same method was employed to detect eucalyptol.

Table 1. IMS operational parameters.

Parameter	Value
Number of spectra	315
Average	64
Trigger delay (ms)	0.4
Spectra length (points)	1024
Grid pulse width (μs)	100
Repetition rate (ms)	50
Sampling frequency (Hz)	30000

2.3. Overall manifold and working procedure

The procedure to extract and determine analytes using SFE-IMS (Figure 1) was divided into two steps: first the analytes were selectively extracted using SFE and adsorbed onto the sorbent trap, and as a second step. Thermal desorption and measurement by the IMS were carried out consecutively.

The sample was homogenised and placed in a 5 mL stainless steel extraction cell. Once the operational conditions of pressure and temperature were reached, CO_2 was passed through the system with a constant flow rate.

Under these conditions, the extraction of the analytes and the adsorption on the sorbent column was started (Figure 1). At this point, the sample was extracted in the static mode during a certain time. Then valve V2 was switched to extract the analytes in the dynamic extraction mode until the extraction was completed. During this step, valve V3 allowed the analytes to reach the column placed in the oven set to a specific temperature, while N_2 was passing through the IMS device. The heat transfer jacket that covers the restrictor was also set at a certain temperature.

After the adsorption step, valve V3 was switched to desorption position to thermally desorb the analytes from the column enabling their simultaneous detection on the IMS. At the same time the extraction cell of SFE device was depressurized. The direction of the desorption of the analytes was the same as the direction in which they were adsorbed on the sorbent trap.

3. Results and discussion

3.1. On-line hyphenation SFE-IMS

The standard configuration of the SFE system used in this work does not allow its direct coupling to the IMS, so a modification of the initial set up of the extractor was carried out. Firstly, the liquid injection valve present in the instrument, which is necessary in SFC mode, was reused as V2 to select between static and dynamic extraction. In static mode the outlet of the extraction cell is closed using V2, consequently the cell is pressurized with the fluid and the sample is extracted with no outflow of the supercritical fluid. This mode allows a better penetration of the fluid in the matrix sample. In the dynamic mode, the outlet of the extraction cell is open. In this step, the sample is continually swept

with fresh supercritical fluid, transferring the extraction effluent into the Tenax trap to retain the analytes. A combination of both modes is used to achieve quantitative extractions.

Furthermore, a valve (V1) was added to the system connecting the pump and the extraction cell that enabled the reactor to be isolated, which is necessary to decompress it between analyses and change it to place a new sample.

The following step was to design a suitable interface to couple the SFE to an IMS detector, which is one of the most crucial aspects for success in this coupling. It is important to take into account that SFE system operates at high pressures to achieve the supercritical conditions for the CO_2. When CO_2 reaches the BPR (the final module of the SFE instrument), the supercritical fluid begins its depressurization changing its state to gas and expanding in the restrictor and therefore, the outlet gas flow is not constant. For this reason, this would cause that, the analytes are not introduced into the IMS detector in a gaseous state at atmospheric pressure swept by a sample gas. In addition, the direct connection of SFE to IMS would not allow a constant flow into the IMS resulting in an irreproducible measurements. Hence, the idea of trapping the analytes using a solid trap as an interface between the SFE and the IMS was considered as best option. In addition, the use of this solid trap could also improve the selectivity of the IMS method. This novel hyphenation (SFE-solid trap-IMS) was tested using a BTEX mixture. For retaining them, the sorbent Tenax TA was selected as a sorbent trap due to it having been previously tested successfully [30] and because it has been specifically designed for the trapping of volatiles and semi-volatiles from air or which have been purged from liquid or solid sample matrices. In order to carry out the adsorption and desorption steps of the analytes into the solid trap and coupling the SFE to IMS correctly, a new valve (V3) was included in the system which allowed switching between both steps as previously mentioned. Moreover, this automation of the whole system provides a quantitative transfer of the extracted analytes to the IMS detector because no sample manipulation is required.

The last modification carried out in the commercial device was to change the external polytetrafluoroethylene tube at room temperature of the BPR where CO_2 gas starts to expand. It was replaced by a 10 cm stainless-steel tube of 1/16" o.d. heated using a heat transfer jacket to compensate for the temperature drop in the CO_2 and to minimize the possibility of condensation (preventing freezing and deposition of analytes in the restrictor), and the extracted analytes could be more efficiently transferred to the trap. The temperature of BPR is commercially limited at 80 ºC, therefore the heat transfer jacket was set at this maximum temperature. Finally, to reduce the vibration caused by the SFE system decompression and the fan vibration of the oven that could interfere in the reproducibility of the results, a vibration absorbing material was placed under the IMS device.

3.2. Assessment of the SFE-IMS coupling

3.2.1. Optimization of an SFE-IMS method to extract BTEX from soil samples

In order to study the good-functioning of the SFE-IMS coupling, a method to detect BTEX in soil samples was used [30]. Therefore, only variables related to SFE were optimized taking into account its possible effect on the proposed coupling. The initial analyses were performed using a dynamic extraction of 30 min with a constant CO_2 flow rate of 1.5 mL/min, 60 ºC of temperature, and the system was pressurized at 30 MPa, based on previous studies [31, 32]. However, these conditions were re-optimized in order to obtain the maximum signal from the extraction of the analytes. For this purpose, 0.5 g of soil spiked with 100 µL of a standard mixture of BTEX at 5 mg/kg was inserted into the extraction cell, and the optimization of the signal was based on the peak intensity obtained in the ion mobility spectrum. First, preliminary experiments were carried out to study the duration of static mode in order to achieve a good penetration of the supercritical fluid into the soil matrix, and consequently a better extraction. More than 10 min of static mode did not improve the signal. This value was therefore chosen. Then, different dynamic extraction times were tested from 5 to 20 min, and after 20

min the signal remained constant. Thus, 10 min of static extraction followed by 20 min of dynamic extraction were used in the subsequent analyses.

The influence of oven temperature in the SFE system was studied in a range between 40 to 80 ºC. When higher temperatures were tested, more interference appeared in the IMS spectra corresponding to undesirable compounds extracted from the soil samples. The higher extraction temperatures also affect the response of the Tenax sorbent negatively and a depth cleaning of the sorbent is required between analyses, which implies a more time-consuming method. For these reasons, 50ºC was the optimum extraction temperature to obtain the highest signal for the benzene and toluene extracted from soil sample.

The pressure of the SFE system was varied between 10 and 30 MPa. This last value is the maximum working pressure recommended by the manufacturer. Using this value, the conditions were not totally reproducible because the pressure was not constant during the whole extraction step. Additionally, no increase in the peak intensity was obtained with values higher than 20 MPa, hence this value was chosen as optimal.

Finally, the effect of the CO_2 flow rate (between 0.5 and 2.5 mL/min) was also studied. It was observed that using the lowest flow rate value, the high pressure used in the extraction (20 MPa) could not be achieved successfully, and for this reason such a low value was discarded for further experiments. Moreover, values higher than 2.5 mL/min caused less intensity on the peaks, possibly due to a lower interaction of the CO_2 with the soil in the reactor. Even when using 2.5 mL/min the extraction was not very reproducible. The highest peak intensities for toluene and benzene were achieved using 1.5 mL/min and this value was selected for further experiments. It should be highlighted that due to the non-polar character of the target analytes no organic modifier was added to the CO_2 stream to extract them from the soil.

The temperature ramp in the chromatographic oven to desorb the analytes from the Tenax was as follows: initial temperature 60 ºC for 1 min, a temperature

ramp of 15 ºC/min up to 220 ºC held for 2 min [30], while the adsorption step of the analytes onto the Tenax was developed at 30 ºC.

After many analyses using the Tenax sorbent, some interference can appear in the IMS spectra corresponding to compounds strongly retained in the column. Thus, in order to eliminate them, once a week the Tenax trap was cleaned with N_2 flow and a high temperature, while never exceeding the temperature limit of 350 ºC recommended by the manufacturer, until the disappearance of such signals. Figure 2 shows a topographic map obtained from a soil sample spiked with BTEX at 5 mg/kg demonstrating the success of the developed hyphenation.

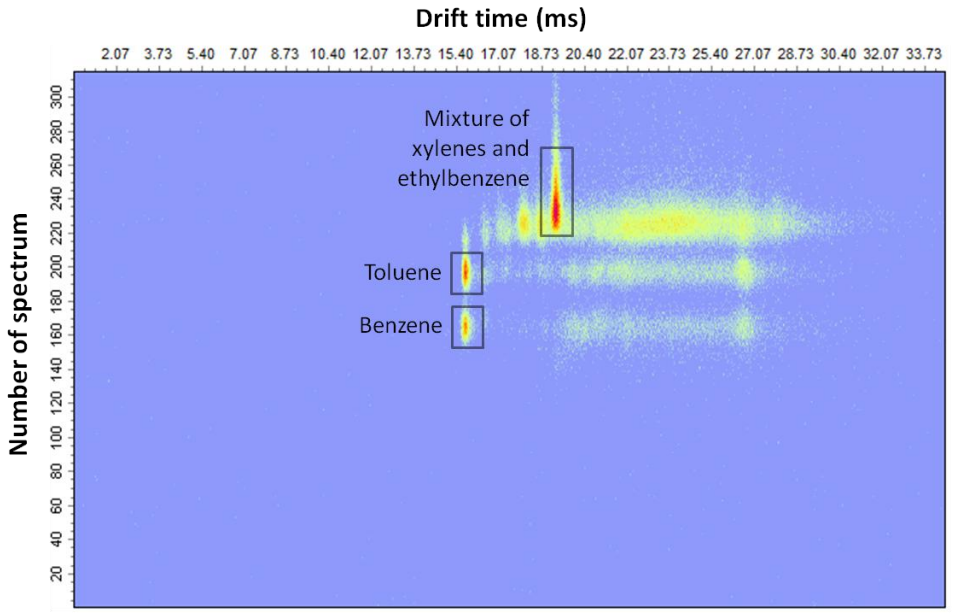

Figure 2. Topographic plot obtained from a spiked soil sample with BTEX at 5 mg/kg submitting to the proposed methodology SFE-IMS described in section 3.2.

A topographic map collects all the spectra recorded during the measurement, specifically 315 spectra were recorded in this work, which correspond to 17 min. The individual signals that form each spectrum are characterized by its intensity in volts and drift time in milliseconds (the necessary time for ions to cross the IMS drift tube and to reach the detector).

3.2.2. Characterization of the proposed SFE-IMS method

The novel hyphenation was assessed in terms of linearity and precision, using soil samples spiked with a benzene and toluene mixture. Notice that only these two analytes were taken into account in the characterization of the method due to the fact that they were individually identified in the ion mobility spectra.

Matrix-matched calibration curves were obtained using soil samples at different concentration levels (ranging from 1 to 50 mg/kg). Each concentration level was analysed once a day for five consecutive days, considering the peak intensity as the analytical signal. Calibration curves were calculated by least-square regression, and the determination coefficients (>0.93) confirmed that the analytical responses from benzene and toluene were linear over the range studied. This demonstrates the efficiency of the whole system, it being able to extract and detect the analytes in a range concentration up to one order of magnitude of difference.

Additionally, limit of detection (LOD) and quantification (LOQ) were calculated based on the signal to noise of peak height, as 3×S/N ratio and 10×S/N ratio, respectively. The same LODs and LOQs (0.2 and 0.8 mg/kg respectively) for benzene and toluene were found using the SFE-IMS method. Thus, making use of this on-line approach, analytes at trace levels in complex samples could be successfully analyzed.

Moreover, the precision of the SFE-IMS method was evaluated in terms of intra-day and inter-day precision calculating the relative standard deviation (RSD) of peak intensity, which is of great importance in coupled techniques to assure reproducible analysis. The intra-day precision of the assay was estimated by application of the whole procedure on the same day to five soil samples containing benzene and toluene spiked at three different concentration levels (1, 10 and 50 mg/kg). Inter-day precision was determined by the analysis of three spiked soil samples with benzene and toluene at the same concentration levels on three consecutive days. In all cases RSD was lower than 10.5%, showing the good precision of the proposed coupling (see values in Table 2).

Table 2. Precision study as % RSD of peak intensity obtained for benzene and toluene in soil samples.

	Level 1 (1 mg/kg)		**Level 2 (10 mg/kg)**		**Level 3 (50 mg/kg)**	
	Intra-day	**Inter-day**	**Intra-day**	**Inter-day**	**Intra-day**	**Inter-day**
Benzene	2.4	3.9	4.3	7.9	2.7	4.8
Toluene	4.9	6.7	4.9	10.5	3.2	5.9

3.3. Application of SFE-IMS coupling to monitor extracts of industrial interest

3.3.1. SFE-IMS method to extract eucalyptol from rosemary plant

Once the effectiveness of the SFE-IMS was demonstrated, the potential of this coupling was studied proposing a methodology to extract and detect on-line a compound with high value added such as eucalyptol from a complex matrix such as rosemary, an aromatic plant.

The first step to tackle this problem was to optimize the variables related to the SFE system. For this purpose, we based it on a previous method which employed SFE to extract some volatile compounds from aromatic plants and the extracts were measured by using Tenax TA trap to retain them before the analysis by GC-MS [33]. Then the initial analyses were performed using a dynamic extraction of 5 min with a constant CO_2 flow rate of 1 mL/min, 35 ºC of temperature, and the system was pressurized at 13.5 MPa. To adapt this methodology to our device, 0.25 g of an inert solid, diatomaceous earth, was spiked with 100 µL of the standard eucalyptol at 100 mg/kg. Firstly, the CO_2 flow rate had to be increased at 2 mL/min due to the fact that the previous value did not allow reaching the working pressure. Then, the dynamic extraction time was extended until 25 min for a higher extraction to be achieved. A previous static extraction step was introduced for the same reason. Five minutes of static extraction was enough time to reach the maximum intensity signal of eucalyptol. The temperature of the BPR, which was not specified in the reference work, was fixed at 80 ºC to avoid the condensation of volatile compounds at the end of the SFE system.

In respect of the variables related to Tenax TA trap, the same temperature used by Omar et al. [33] was employed to adsorb the eucalyptol (30 ºC). However, the final temperature and the temperature ramp of the desorption step were modified. The final temperature was reduced to 270 ºC to avoid further deterioration of the filling, thus avoiding the cleaning step with N_2. And the temperature ramp used was 60 ºC/min instead of 150 ºC/min due to the limitation of the oven where the Tenax TA column was placed. Then, the final

conditions used in the chromatographic oven where the sorbent trap was placed to desorb the analytes were: initial temperature 30 ºC for 1 min, a temperature ramp of 60 ºC/min up to 270 ºC held for 10 min.

To demonstrate the usefulness of this methodology, a real rosemary plant sample was extracted using the procedure. Figure 3 shows the topographic map obtained from the analysis of this extract, and the signal that appears at 19.93 ms corresponds to eucalyptol. Therefore, the success in the extraction and detection of the analyte from a real and complex matrix, such as a rosemary plant, was proved.

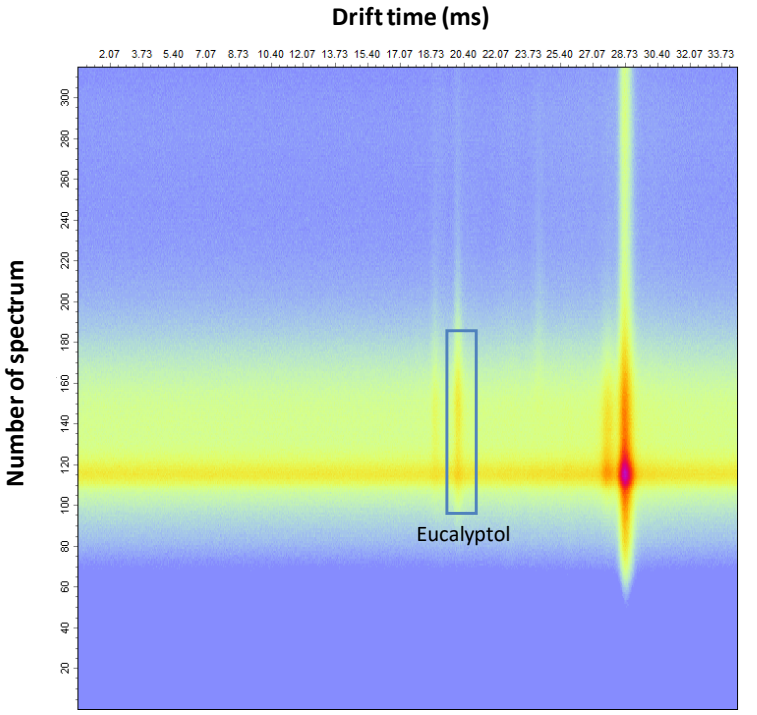

Figure 3. Topographic plot obtained from rosemary plant through the developed methodology included in the section 3.3.

3.3.2. Characterization of the developed method

The methodology was evaluated in terms of linearity, precision and recovery using diatomaceous earth spiked with eucalyptol. Moreover, the matrix effect (ME) was studied through the standard addition method.

Calibration curve for eucalyptol was obtained analyzing different concentration levels (ranging from 500 to 1200 mg/kg). The peak intensity was considered as the analytical signal and least-square regression was used to calculate the calibration curve. The determination coefficient was 0.95, confirming that the analytical response was linear over the range studied. Moreover, LOD and LOQ were calculated based on the signal to noise of peak height, as 3×S/N ratio and 10×S/N ratio, respectively. The LODs and LOQs values were 140 and 470 mg/kg, respectively, for eucalyptol by using this SFE-IMS method.

Additionally, the precision of the SFE-IMS method was evaluated in terms of intra-day and inter-day precision and were expressed as RSD of peak intensity. The intra-day precision of the assay was estimated by application of the whole procedure on the same day to six diatomaceous earth samples spiked with eucalyptol at 1000 mg/kg. Inter-day precision was determined by the analysis of three diatomaceous earth samples spiked with eucalyptol at the same concentration level on three consecutive days. RSD values were 15% for intra-day precision and 15.9% for inter-day precision. All in all, the RSD values were lower than 20%, which means the methodology under study showed a good precision.

In order to check the trueness of the proposed methodology, recovery result experiments were carried out in two diatomaceous earth samples spiked with eucalyptol at 500 mg/kg. The recovery value was 85.1%.

Finally, the ME was studied for rosemary plants using the standard addition method. The ME is defined as the influence of one or more matrix constituents on the detection and/or determination of an analytical parameter. This effect can be evaluated through the difference of sensitivity of a method when the calibration is prepared in a solvent or inert matrix against one that is prepared in the same environment of the sample. If the value of matrix/solvent (or inert matrix) slope ratio ranged from 0.9 to 1.1, the ME could not be considered. In this case, the calibration curve in the matrix, rosemary plant, was built spiking 0.25 g of the sample from 0 to 300 mg/kg with the eucalyptol standard (determination coefficient = 0.98). Note that when the eucalyptol standard had not yet been added, the recorded IMS signal value was above that obtained for the concentration corresponding to the LOQ. The result of the slopes ratio was 1.7, therefore it was apparent that the ME exists and must be taken into account for quantitative purposes.

4. Conclusions

The coupling of the SFE system to the IMS detector was successfully evaluated determining benzene and toluene present in soil as an example for testing the performances of the whole system, in which the extraction, collection and transfer of analytes were automated by using different valves and a sorbent trap. This new coupling has the advantages of SFE, considered as an environmentally-friendly sample treatment, and IMS, an inexpensive and fast detector that operates at atmospheric pressure, able to determine a wide range of volatile analytes. Signal intensity of benzene and toluene correlated linearly to sample concentration and good precision values were obtained. Moreover, the extraction power of SFE for the extraction of eucalyptol from rosemary plant on a laboratory scale was also demonstrated by using IMS as an innovative sensor coupled on-line. Results from the validation suggested that this methodology is suitable for the extraction and determination of eucalyptol in rosemary samples,

but the effect of the matrix for quantitative purpose should be taken into account. In view of these results, it was concluded that the employment of IMS as a detector to monitor, on-line, some target analytes extracted by SFE on an industrial scale is proper.

Therefore, considering that: 1) different modalities of SFE can be applied, 2) a wide range of sorbents can be used as a sorbent trap, and 3) the same hyphenation can be applied to other types of IMS. Then, the proposed new hyphenation can have a strong impact on extracting and detecting different volatile analytes from complex matrices, expanding the scope of the present technique to other research areas or even in different industrial applications.

Notes

The authors declare no conflict of interest.

Akcnowledgments

The authors wish to thank the Spanish Ministry of Innovation and Science for the funding project CTQ2014-52939R. N.J.C. wishes to thank the Spanish Ministry of Education, Culture and Sport for award of a pre-doctoral grant (FPU15/00639).

References

[1] M. Zougagh, M. Valcarcel, A. Rios, Supercritical fluid extraction: a critical review of its analytical usefulness, Trac-Trend Anal. Chem. 23 (2004) 399-405.

[2] M. D. Burford, K. D. Bartle, S. B. Hawthorne, Directly coupled (on-line) SFE-GC: Instrumentation and applications, Adv. Chromatogr. 37 (1997) 163-204.

[3] A. D. Sánchez-Camargo, F. Parada-Alfonso, E. Ibáñez, A. Cifuentes, On-line

coupling of supercritical fluid extraction and chromatographic techniques, J. Sep. Sci. 40 (2016) 213-227.

[4] R. W. Vannoort, J. P. Chervet, H. Lingeman, G. J. Dejong, U. A. T. Brinkman, Coupling of supercritical fluid extraction with chromatographic techniques, J. Chromatogr. 505 (1990) 45-77.

[5] K. K. Unger, P. Roumeliotis, Online high-pressure extraction high-performance liquid-chromatography: Equipment design and operation variables, J. Chromatogr. 282 (1983) 519-526.

[6] Z. Y. Wang, M. Ashraf-Khorassani, L. T. Taylor, Feasibility study of online supercritical fluid extraction-liquid chromatography-UV absorbance-mass spectrometry for the determination of proanthocyanidins in grape seeds, J. Chromatogr. Sci. 43 (2005) 109-115.

[7] Z. Y. Wang, M. Ashraf-Khorassani, L. T. Taylor, Air/light-free hyphenated extraction/analysis system: Supercitical fluid extraction on-line coupled with liquid chormatography-UV absorbance/electrospray mass spectrometry for the determination of hyperforin and its degradation products in Hypericum pertoratum, Anal. Chem. 76 (2004) 6771-6776.

[8] R. Batlle, H. Carlsson, E. Holmgren, A. Colmsjö, C. Crescenzi, On-line coupling of supercritical fluid extraction with high-performance liquid chromatography for the determination of explosives in vapour phases, J. Chromatogr. A 963 (2002) 73-82.

[9] C. Mardones, A. Rios, M. Valcarcel, Automatic on-line coupling of supercritical fluid extraction and capillary electrophoresis, Anal. Chem. 72 (2000) 5736-5739.

[10] M. Zougagh, A. Rios, Supercritical fluid extraction as an on-line clean-up technique for determination of riboflavin vitamins in food samples by capillary electrophoresis with fluorimetric detection, Electrophoresis 29 (2008) 3213-3219.

[11] E. Ibáñez, J. Palacios, G. Reglero, Analysis of tocopherols by on-line coupling supercritical fluid extraction-supercritical fluid chromatography, J. Microcolumn Sep. 11 (1999) 605-611.

[12] K. Suto, S. Kakinuma, Y. Ito, K. Sagara, H. Iwasaki, H. Itokawa, Determination of atractylon in Atractylodes rhizome using supercritical fluid chromatography on-line coupled with supercritical fluid extraction by the direct induction method, J. Chromatogr. A. 810 (1998) 252-255.

[13] D. Okamoto, Y. Hirata, Development of supercritical fluid extraction coupled to comprehensive two-dimensional supercritical fluid chromatography (SFE-SFCxSFC), Anal. Sci. 22 (2006) 1437-1440.

[14] J. M. Levy, A. C. Rosselli, Quantitative supercritical fluid extraction coupled to capillary gas-chromatography, Chromatographia 28 (1989) 613-616.

[15] G. C. Slack, H. M. McNair, S. B. Hawthorn, D. J. Miller, Coupled solid-phase

extraction supercritical-fluid extraction online gas-chromatography of explosives from water, Hrc-J. High Res. Chrom. 16 (1993) 473-478.

[16] G. P. Blanch, G. Reglero, M. Herraiz, Analysis of wine aroma by off-line and online supercritical-fluid extraction gas-chromatography, J. Agr. Food Chem. 43 (1995) 1251-1257.

[17] T. Hyotylainen, M. L. Riekkola, Approaches for on-line coupling of extraction and chromatography, Anal. Bioanal. Chem. 378 (2004) 1962-1981.

[18] R. Fuoco, A. Ceccarini, M. Onor, S. Lottici, Supercritical fluid extraction combined on-line with cold-trap gas chromatography mass spectrometry, Anal. Chim. Acta 346 (1997) 81-86.

[19] S. Hajialigol, S. A. Ghorashi, A. H. Alinoori, A. Torabpour, M. Azimi, Thermal Solid Sample Introduction-Fast Gas Chromatography-Low Flow Ion Mobility Spectrometry as a field screening detection system, J. Chromatogr. A 1268 (2012) 123-129.

[20] L. Arce, M. Menendez, R. Garrido-Delgado, M. Valcarcel, Sample-introduction systems coupled to ion-mobility spectrometry equipment for determining compounds present in gaseous, liquid and solid samples, Trac-Trend Anal. Chem. 27 (2008) 139-150.

[21] R. P. F. F. da Silva, T. A. P. Rocha-Santos, A. C. Duarte, Supercritical fluid extraction of bioactive compounds, Trac-Trend Anal. Chem. 76 (2016) 40-51.

[22] A. E. Sadlon, D. W. Lamson, Immune-modifying and antimicrobial effects of eucalyptus oil and simple inhalation, Altern. Med. Rev. 15 (2010) 33-47.

[23] H. Worth, C. Schacher, U. Dethlefsen, Concomitant therapy with Cineole (Eucalyptole) reduces exacerbations in COPD: A placebo-controlled double-blind trial, Respir. Res. 10 (2009) 69.

[24] Z. Zekovic, B. Pavlic, A. Cvetanovic, S. Durovic, Supercritical fluid extraction of coriander seeds: Process optimization, chemical profile and antioxidant activity of lipid extracts, Ind. Crop. Prod. 94 (2016) 353-362.

[25] A. Piras, D. Falconieri, E. Bagdonaite, A. Maxia, M. J. Goncalves, C. Cavaleiro, L. Salgueiro, S. Porcedda, Chemical composition and antifungal activity of supercritical extract and essential oil of Tanacetum vulgare growing wild in Lithuania, Nat. Prod. Res. 28 (2014) 1906-1909.

[26] N. Herzi, J. Bouajila, S. Camy, S. Cazaux, M. Romdhane, J. S. Condoret, Comparison between Supercritical CO2 Extraction and Hydrodistillation for Two Species of Eucalyptus: Yield, Chemical Composition, and Antioxidant Activity, J. Food. Sci. 78 (2013) C667-C672.

[27] V. Ruzsanyi, Ion mobility spectrometry for pharmacokinetic studies—exemplary application, J. Breath. Res. 7 (2013) 046008.

[28] L. A. Conde-Hernandez, J. R. Espinosa-Victoria, A. Trejo, J. A. Guerrero-Beltran,

CO2-supercritical extraction, hydrodistillation and steam distillation of essential oil of rosemary (Rosmarinus officinalis), J. Food. Eng. 200 (2017) 81-86.

[29] J. Omar, A. Sarmiento, M. Olivares, I. Alonso, N. Etxebarria,Quantitative analysis of essential oils from rosemary in virgin olive oil using Raman spectroscopy and chemometrics, J. Raman. Spectrosc. 43 (2012) 1151-1156.

[30] L. Criado-Garcia, N. Almofti, L. Arce, Photoionization-ion mobility spectrometer for non-targeted screening analysis or for targeted analysis coupling a Tenax TA column, Sensors Actuators B-Chem. 235 (2016) 370-377.

[31] S. E. Eckerttilotta, S. B. Hawthorne, D. J. Miller, Supercritical-fluid extraction with carbon-dioxide for the determination of total petroleum-hydrocarbons in soil, Fuel 72 (1993) 1015-1023.

[32] L. Lojkova, J. Sedlakova, V. Kuban, A solvent recirculation trapping device for supercritical fluid extraction of polyaromatic hydrocarbons, J. Sep. Sci. 28 (2005) 1188-1194.

[33] J. Omar, M. Olivares, I. Alonso, A. Vallejo, O. Aizpurua-Olaizola, N. Etxebarria, Quantitative analysis of bioactive compounds from aromatic plants by means of dynamic headspace extraction and multiple headspace extraction-gas chromatography-mass spectrometry, J. Food Sci. 81 (2016) C867-C873.

BLOCK III

Applied study of Gas Chromatography coupled to Ion Mobility Spectrometry

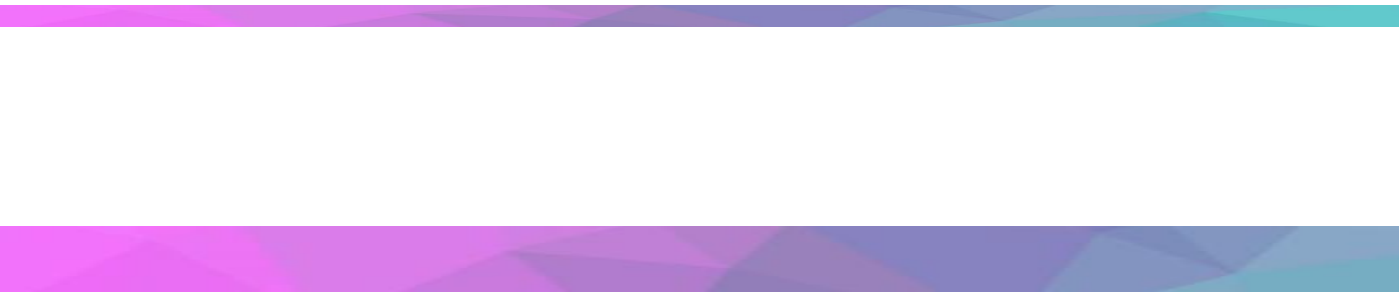

Block III of this PhD Book was mainly focused on using a pre-separation step, concretely a GC column prior IMS to improve both sensitivity, by avoiding or reducing competitive ionization effects, and selectivity by providing a dual separation to the IMS methods. This allowed to explore the possibilities of this technique to authenticate complex food samples such as olive oils and olives according to their quality or production system based on untargeted analysis methods.

Firstly, a bibliographical study which gather and critically discuss recent publications related to distinguish olive oils according to their quality as extra virgin (EVOO), virgin (VOO) or lampante (LOO) was carried out in Chapter VI. This enabled to know more about the role of IMS and other techniques in this field.

In Chapter VII, two different chemometric approaches for olive oil classification as EVOO, VOO or LOO were investigated and compared using GC-IMS in an attempt to get the most robust model over time. One approach was based on non-targeted fingerprinting while the other method was based on the selection of significant markers. In addition, the study of characteristic and stable GC-IMS markers and their characterization was carried out.

The use of orthogonal techniques to be combined with GC-IMS was explored in Chapter VIII to differentiate olive oils samples according to their quality as EVOO, VOO or LOO. The idea was to imitate the expert panels when using both the flavour components perceived in the mouth and the aroma compounds in the nose. The explored complementary techniques were CE-UV and HPLC coupled to UV or FLD.

Finally, in Chapter IX, the authentication of olive and olive oil samples according with their production system to categorize them as organic or conventional was carried out. UV-IMS, GC-IMS and/or CE-UV were explored as

analytical techniques using untargeted fingerprinting approaches together with chemometrics, concretely, OPLS-DA models. Results of percentages of classification success for the volatile fraction of olive and olive oils were contracted with GC-MS data since this technique is considered as a more implemented technique in analytical laboratories. Also, the identification of some volatile compounds was carried out with GC-MS.

Instrumental techniques to classification Olive oils according to their quality

CHAPTER VI

To send

Instrumental techniques to classification Olive oils according to their quality

Natividad Jurado-Campos[a], Rocío Rodríguez-Gómez[a], Natalia Arroyo-Manzanares[b], Lourdes Arce[a]

[a]*Department of Analytical Chemistry, University of Córdoba. Institute of Fine Chemistry and Nanochemistry. International Agrifood Campus of Excellence (ceiA3), Marie Curie Annex Building. Campus de Rabanales. 14071 Córdoba (Spain).*

[b]*Department of Analytical Chemistry, Faculty of Chemistry, Regional Campus of International Excellence "Campus Mare-Nostrum", University of Murcia, E-30100, Murcia, Spain*

Instrumental techniques to classification Olive oils according to their quality

Natividad Jurado-Campos, Rocío Rodríguez-Gómez, Natalia Arroyo-Manzanares, Lourdes Arce

ABSTRACT

This review includes an update of the publications on quality classification of olive oils into extra, virgin or lampante olive oil categories. Nowadays, official methods to carry out this classification are time-consuming and, sometimes, they are not systematic and/or objective. These methods are based on conventional physicochemical analysis and on a sensorial tasting of olive oils carried out by a panel test of experts.

The aim of this revision was to explore and give value to the possibilities reported in bibliography to complement the current official methods established for that classification of olive oils. Specifically, non-separation and separation analytical techniques which could contributed to correctly classify olive oils according with their physicochemical and/or sensorial characteristics were considered. A deep description was carried out about that methods and the main advantages and disadvantages of the proposed procedures and techniques were highlighted. Great importance was given to those methods that analyzed samples from the three categories with the main objective of differentiating them since they could be a real and close in time option to complement or even substitute some of the official methods.

Finally, general trends and detected difficulties found in this context were discussed along the work.

Keywords: Quality, Ion Mobility Spectrometry, Mass Spectrometry, Capillary Electrophoresis, Electronic Devices, Lampante Olive Oil

A robustness study of calibration models for olive oil classification: targeted and non-targeted fingerprint approaches based on GC-IMS

CHAPTER VII

Food Chemistry

288 (2019) 315–324

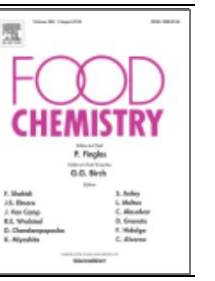

A robustness study of calibration models for olive oil classification: targeted and non-targeted fingerprint approaches based on GC-IMS

María del Mar Contreras[ab#], Natividad Jurado-Campos[a#], Lourdes Arce[a], Natalia Arroyo-Manzanares[ac]

[a]*Department of Analytical Chemistry. Institute of Fine Chemistry and Nanochemistry, University of Córdoba, Campus de Rabanales, Marie Curie Annex Building, E-14071 Córdoba, Spain.*

[b]*Present address: Department of Chemical, Environmental and Materials Engineering , Universidad de Jaén, Campus Las Lagunillas, 23071 Jaén, Spain.*

[c]*Department of Analytical Chemistry, Faculty of Chemistry, Regional Campus of International Excellence "Campus Mare-Nostrum", University of Murcia, E-30100 Murcia, Spain.*

[#]*These authors contributed equally to this work*

A robustness study of calibration models for olive oil classification: targeted and non-targeted fingerprint approaches based on GC-IMS

María del Mar Contreras, Natividad Jurado-Campos, Lourdes Arce, Natalia Arroyo-Manzanares

ABSTRACT

The dual separation in gas chromatography-ion mobility spectrometry generates a complex multi-dimensional data whose interpretation is a challenge. In this work, two chemometric approaches for olive oil classification are compared to get the most robust model over time: i) an non-targeted fingerprinting analysis, in which the overall GC-IMS data was processed and ii) a targeted approach based on peak-region features (markers). A total of 701 olive samples from two harvests (2014-2015 and 2015-2016) were analyses and processed by both approaches. The models built with data samples of 2014-2015 showed that both approaches were suitable for samples classification (success > 74%). However, when these models were applied for classifying samples from 2015-2016, better values were obtained using markers. The combination of data from the two harvests to build the chemometric models improved the percentages of success (> 90%). These results confirm the potential of GC-IMS based approaches for olive oil classification.

Keywords: chemometric models, olive oil classification, spectral fingerprint, markers, gas chromatography, ion mobility spectrometry

1. Introduction

Olive oil, extra virgin olive oil (EVOO) and virgin olive oil (VOO), is a unique fat because of its composition (Contreras Gámez, Rodriguez Pérez, García Salas, & Segura Carretero, 2014), so that this product is normally sold at a higher price than other vegetable oils and subjected to fraudulent practices. One of the most important aspects for quality olive oil assessment involves the standardized sensory analysis according to the 'panel test' method (European Commission Regulation (EEC), 1991). Olives contain a complex system of endogenous enzymes that, according to agronomical parameters and processing conditions in an oil mill, produce olive oils with different compositions of organic volatile organic compounds (VOCs), which are the main factors responsible for their sensory characteristics (Alcalá et al., 2017, Fortini, Migliorini, Cherubini, Cecchi, & Calamai, 2017). For these reasons, the determination of VOCs, which contribute to the positive attributes and off-flavors, seems a good strategy for classifying olive oils (Garrido-Delgado, Dobao-Prieto, Arce & Valcárcel, 2015a, Dierkes, Bongartz, Guth, & Hayen, 2012). Thus, reliable analytical methodologies combined with multivariate statistical techniques able to differentiate EVOO from other olive oil categories and/or unmask adulteration are highly demanded. Reviewing the literature it can be confirmed that several analytical strategies have been previously proposed for olive oil grading combining: metal oxide sensors (MOS) and artificial neural networks (ANN) (García-González & Aparicio, 2003); synchronous fluorescence spectroscopy, hierarchical cluster analysis and principal component analysis (PCA) (Poulli, Mousdis, & Georgiou, 2005); mass spectrometry (MS), mid-infrared (MIR) and UV–visible spectroscopy with partial least-squares discriminant analysis (PLS-DA) (Borràs et al., 2016a); gas chromatography (GC)-MS and PLS-DA (Dierkes et al., 2012) or its modification: orthogonal partial least-squares discriminant analysis (OPLS-DA) (Sales et al., 2017). However, there are some controversial aspects that have not been properly taken into account, such as the evaluation of the robustness of a calibration/prediction chemometric model over time within a large sample set involving several harvesting/production years, or whether models require further

recalibration. It should be noted that in some cases only relatively small numbers of samples were examined, while in other cases the calibration models were not validated with blind samples, which reduces the reliability of the results.

As an alternative analytical choice, GC coupled to ion mobility spectrometry (IMS) has emerged as a powerful separation technique for in-depth investigations of VOCs in food (Garrido-Delgado et al., 2015a, Garrido-Delgado et al., 2015b, Gallegos, Garrido-Delgado, Arce, & Medina, 2015, Gerhardt, Birkenmeier, Sanders, Rohn, & Weller, 2017). GC-IMS has been proposed for olive oil fingerprinting combined with chemometric tools for reducing this data complexity (Garrido-Delgado et al., 2015b, Garrido-Delgado, Arce, & Valcárcel, 2012). In GC-IMS, a dual separation of VOCs occurs in a GC column and in the ion mobility spectrometer. So, each VOC is characterized by two parameters, retention time and drift time, which is defined as the time needed for ions to traverse the distance between the ion shutter and detector. Drift time is usually reported indirectly as normalized to electric field, temperature and pressure as a reduced ion mobility coefficient (K_o) or its inverse $1/K_o$ (Szymanska, Davies, & Buydens, 2016). Therefore, the combination in a single analytical platform of automated sampling (e.g. headspace (HS) autosampler), GC separation and IMS deliver highly efficient and robust VOCs profiling and fingerprinting of food samples. However, each analytical run generates dense and multi-dimensional data, whose comparison by direct image analysis is difficult and overall interpretation a challenge.

For all these reasons, the objective of this study was to investigate and compare two different chemometric approaches for olive oil classification in an attempt to get the most robust model over time: i) an non-targeted fingerprinting, accordingly to previous works (Garrido-Delgado et al., 2015b; Gerhardt et al., 2019), and ii) a targeted approach based on the selection of significant markers (Arroyo-Manzanares et al., 2018). As an added value, these work-flows were applied to a large number of samples (701 olive oil samples) of the categories EVOO, VOO and lampante olive oil (LOO), from two different olive

oil harvests (2014-2015 and 2015-2016) and the robustness of the proposed calibration models over time was evaluated. In addition, several characteristic and stable GC-IMS markers are proposed and some of them characterized (see section 3.5.).

2. Materials and methods

2.1. Chemicals and reagents

All the reagents used in this work were of analytical grade. Nonan-2-one, octan-2-one, hexan-2-one, pentan-2-one, and butan-2-one were supplied by Sigma-Aldrich (St. Louis, MO, USA). Stock solutions at 1000 mg L^{-1} for each compound were prepared by dissolving the appropriate volume of each compound in Milli-Q ultrapure water and they were stored at 4 °C. Intermediate solutions at 10 mg L^{-1} were prepared by dilution with Milli-Q water of stock solution. Finally, working solutions at concentration of 0.5 mg L^{-1} were prepared by dilution with Milli-Q water of intermediate solution for precision studies.

Besides the latter ketones, 34 analytical standards were also supplied by Sigma-Aldrich (St. Louis, MO, USA) and diluted in refined olive oil for identification purposes (0.5-40 mg kg^{-1}): methanol, ethanol, ethyl acetate, 1-penten-3-ol, 1-penten-3-one, 3-methyl-1-butanol, 2-methyl-1-butanol, *trans*-2-pentenal, 1-pentanol, *cis*-2-penten-1-ol, ethyl butanoate, hexanal, ethyl isovalerate, *trans*-2-hexen-1-al, *trans*-2-hexen-1-ol, 3-hexen-1-ol, heptan-2-one, heptanal, 2-heptenal, propyl butanoate, benzaldehyde, 1-octen-3-one, 1-octen-3-ol, octanal, hexyl acetate, 2-octenal, nonanal, decanal, 1-hexanol, 1-octanol, 2-octanol, limonene, linalool and *trans*-2-decenal. Refined olive oil was used since it is an analogue matrix to the studied olive oil types. This oil is obtained from non-edible olive oils by refining methods, which do not lead to alterations in the initial glyceridic structure. In this process, the volatile fraction is eliminated and it was confirmed by its previous analysis by GC-IMS.

Ultrapure water (18.2 MΩ cm^{-1}, Milli–Q Plus system, Millipore Bedford, MA, USA) was used throughout the work. Nitrogen gas 5.0 (purity ≥ 99.999%) was supplied by Abelló Linde (Barcelona, Spain).

2.2. Olive oil samples

A total of 701 olive oil samples (190 EVOO, 355 VOO and 156 LOO samples) were supplied by the Spanish *Interprofesional del Aceite de Oliva Español*, *Agencia para el Aceite de oliva del Ministerio de Agricultura, Alimentación y Medio Ambiente* and the official control services from the *Consejería de Agricultura, Pesca y Desarrollo Rural de la Junta de Andalucía*. These samples were obtained from olives collected in two different harvest years, 2014-2015 and 2015-2016. A total of 292 samples (98 EVOO, 159 VOO, and 35 LOO samples) were obtained from the harvests of 2014-2015 and analyzed in 2015. The remaining 409 samples (92 EVOO, 196 VOO and 121 LOO) were obtained in 2015-2016 and analyzed in 2016. All samples were stored at 4ºC until their analysis.

The olive oil samples were from several cultivars, geographical origins, fruit ripeness, processing practices and storage, so that the heterogeneity of this sample group is guaranteed to provide universal chemometric models as much as possible. Moreover, the physicochemical and sensory characteristics of the samples were assessed by Spanish official laboratories (*Laboratorio Arbitral Agroalimentario del Ministerio de Agricultura y Pesca, Alimentación y Medio Ambiente, Laboratorio Agroalimentario de Córdoba* and *Laboratorios Agroalimentarios Atarfe de la Junta de Andalucía*) according to the European Union regulation (European Commission Regulation (EEC), 1991) and amendments.

2.3. Instrumentation and software

Analyses of olive oil samples were performed on an IMS commercial instrument (FlavourSpec®) equipped with a tritium radioactive ionisation source of 6.5 KeV and a drift tube of 5 cm long (Gesellschaft für Analytische Sensorsysteme mbH, G.A.S., Dortmund, Germany). A heated splitless injector (2 mm ID, 6.5 mm OD x 78.5 mm fused quartz glass) enabled direct sampling of the HS by using a 2.5 mL Hamilton syringe furnished with a 51 mm needle. The reproducibility of measurements was improved using an automatic sampler unit (CTC-PAL, CTC Analytics AG, Zwingen, Switzerland). In addition, a non-polar column consisting of 94% methyl-5% phenyl- 1% vinylsilicone with 30 m of length, an internal diameter of 0.32 mm and 0.25 μm of film thickness (SE-54-CB of CS-Chromatographie Service GmbH, Dürem, Germany) was coupled to an IMS device in order to provide a dual separation. This means that GC separates VOCs depending on their interaction with the column stationary phase, and IMS separates charged species under the influence of an electrical field which depends on their drift behaviour in a carrier gas atmosphere.

Two-dimensional GC-IMS data were acquired in positive mode using LAV software (version 2.0.0) from G.A.S. GC×IMS Library Search software (G.A.S.) was employed to identify VOCs. It comes with a full non restricted version of the NIST2014 Retention Index Database. MATLAB software (The Mathworks Inc., Natick, MA, USA, 2007), PLS Toolbox 5.5 (Eigenvector Research, Inc., Manson, WA, USA) and SIMCA software version 14.1 (MKS Umetrics, Umeå, Sweden) were used for data processing.

One-way analysis of variance (ANOVA) test and LSD multiple range test at the 0.05 significance level were performed using Statgraphics Centurion 16.2.04 software (StatPoint Technologies, Inc., Warrenton, VA, USA).

2.4. GC-IMS analysis

The GC-IMS method used for olive oil analysis was based on a previous method developed in our laboratory (Garrido-Delgado et al., 2015a) modifying the drift tube temperature from 45 to 55 °C. 1 g of sample was placed into a 20 mL vial and closed with magnetic caps and silicone septum. This amount is adequate to guarantee reproducibility during weighing. The sample was incubated at 60 °C for 8 min and 200 µL of headspace was automatically injected by means of a heated syringe (80 °C) into the heated injector (80 °C). The carrier gas (nitrogen gas with inlet pressure of 4 bar) at 5 mL min^{-1} passed through the GC-IMS injector inserting the sample into the GC column the first 6 minutes and then it increased up to 25 mL min^{-1} during the remaining 17 minutes. The analytes were separated in isocratic mode at 55 ºC and they were introduced into an ionization chamber of IMS. There, the tritium source (6.5 Kev) ionised the compounds eluted from GC column and the ions reach the drift tube of the IMS through the shutter grid. The drift tube was maintained at a constant temperature and voltage of 55 °C and 400 V cm^{-1}, respectively. The gas flow rate of nitrogen introduced in the opposite direction of the sample into IMS (drift gas) was of 250 mL min^{-1}. The acquisition of the data was made in the positive ion mode and the values of different IMS´s parameters were set at: 32 for averages of scan for each spectrum acquired, 100 µs for grid pulse width, 21 ms for repetition rate and 150 kHz for sampling frequency.

2.5. Data analysis

After data acquisition, peak alignment in retention and drift time scales was applied to each measurement using the position of the reactant ion peak (RIP) (see Figure S1) as reference in LAV software and also using a sample reference. The RIP corresponds to the reactant ions or hydrated protons, which are generated in the ion source of the employed IMS device. The analytes interact

with the RIP to generate protonated species by displacement of water (Jurado-Campos, Garrido-Delgado, Martínez-Haya, Eiceman, & Arce, 2018).

Moreover, two chemometric approaches were applied. The first approach was based on the use of the whole spectral fingerprint of the olive oils, and the second approach was based on the selection of specific olive oil markers (Figure S1). In both strategies and for each category, data were randomly divided into two different sets: a training set containing around the 80% of the analyzed samples to build the calibration models and a validation set including the remaining 20%, approximately. The calibration models were ternaries and binaries (Figure S1). In the former type, three olive oil categories were compared as different classes (EVOO, VOO and LOO). Alternatively, in the latter type, two classes were compared, EVOO *vs.* non-EVOO (VOO and LOO) and LOO *vs.* non-LOO (EVOO and VOO), being able to differentiate non-defective (EVOO) and defective (VOO and LOO) and also edible (EVOO and VOO) and non-edible (LOO) olive oils.

2.5.1. Spectral fingerprint chemometric approach

In the first approach raw data were converted to *.csv format using LAV software and MATLAB and PLS Toolbox software were used for processing data. The chemometric models were built after a pre-treatment of the data consisting of the normalization of data using the RIP intensity value (as an internal standard) taken before the injection of each sample, where no analytical signals appeared. Then a smoothing procedure based on second order Savitzky-Golay filtering and a baseline correction were applied. The baseline from each spectrum was corrected by subtracting the mean value of a region with a lack of peaks (between 0 to 1 ms). After that the area of the topographic plot containing the majority of the analytical signals (see Figure S2A) was selected for data treatment (retention time from 54.7 to 325.8 s and drift time from 7.9 to 11.4 ms), enabling the reduction of the dimensions of the data matrix to 392×522. Finally, the data was transposed to convert rows to columns and vice versa, and all the spectra of a

sample were concatenated (arranged consecutively) in a single row to generate a feature vector of 1×204624. Once the pre-processing was performed, the concatenated data for each sample were included in a row of the dataset matrix and then the chemometric processing was performed. Briefly, it consisted of a non-supervised PCA (auto-scaled) in order to reduce dimensionality and extract the most relevant information, with a minimum cumulative variance of 99%. Subsequently, a linear discriminant analysis (LDA) was built to incorporate the class information into the model. Finally, k-nearest neighbour method (kNN), using k=3, was applied for samples classification.

2.5.2. Markers chemometric approach

The second strategy was based on the selection of individual signals (markers) from the topographic plots of the olive oil samples (Figure S2B). A total of 113 markers were selected by visual exploration of the topographic plots of all the samples analyzed. The intensity values of these markers over the baseline were automatically obtained using the LAV – quantitation module tool. They were normalized with respect to RIP height intensity value in each measurement which was also automatically provided by the latter software for each sample. In this case, the feature vector for each sample was 1×113. Then a dataset matrix was built including the total number of olive oil samples and the normalized intensity for the selected markers. In this strategy the data was transformed logarithmically, and no further pre-processing was carried out. Using the software SIMCA, two binaries and a ternary OPLS-DA models (see section 2.5.) were firstly built for the 113 markers. Then, significant markers were selected by comparing the two-in-two classes (EVOO *vs*. VOO, EVOO *vs*. LOO and VOO *vs*. LOO) with the S-Plot™ utility obtained from the OPLS-DA models, according to Sales et al. (2017). Note that only binary models can be used in order to apply the S-plot to find relevant markers. The binaries and ternary OPLS-DA models were rebuilt with the selected markers (see section 2.5. and Figure S1).

The R2Y(cum) and Q2(cum) parameters, which express the cumulative percentage of the variation of the dependent variable explained by the model and a measure of the predictive ability, respectively, were provided by the software and taking into account in this data reduction approach and to select the best models. Values closer to 1 indicate a perfect fit of the model (Contreras, Arroyo-Manzanares, Arce, & Arce, 2019). For that, automatic cross-validation (7-fold cross-validation) was performed.

3. Results and discussion

3.1. Assessment of the precision of the GC-IMS method

Precision was evaluated using a quality control consisted of butan-2-one, pentan-2-one, 2-hexan-2-one, octan-2-one, and 2-nonan-2-one at 0.5 mg L^{-1}. These compounds were chosen since they cover the HS-GC-IMS spectrum region, in terms of both retention time and drift time, where olive oil VOCs appeared. Stock solutions of these compounds were stable at 4ºC (data not shown) and can be used in long-term studies.

In this way, precision was assayed by 5 analyses of the standard solution on the same day (repeatability) and through 58 analysis (intermediate precision) spanning a time period of 3 months, approximately. In the latter case, two different analysts carried out the analyses. The values were expressed as relative standard deviation (RSD, %) of peak intensity, normalized peak intensity, retention time and drift time. In addition, the precision values for the RIP signal (intensity and drift time) were also determined (Table 1). It should be noted that in this IMS type each compound can generate several ionic species depending on the concentration, mainly, monomers and dimers.

In general, repeatability values were acceptable and lower than 8.2%; achieving the best results for drift time (RSD < 0.3%). The normalization of the peak intensity, with respect to the RIP height intensity value automatically

provided by the GC-IMS software, improved the repeatability values. Furthermore, intermediate precision values were lower than 10%, except for the peak intensity of butan-2-one monomer and nonan-2-one dimer.

Table 1. Precision study for butan-2-one, pentan-2-one, hexan-2-one, octan-2-one and nonan-2-one using HS-GC-IMS. The values were expressed as relative standard deviation (RSD).

	Repeatability[a]				**Intermediate precision[b]**			
Compound	Peak height (RSD, %)	Normalized peak height (RSD, %)	Retention time (RSD, %)	Drift time (RSD, %)	Peak height (RSD, %)	Normalized peak height (RSD, %)	Retention time (RSD, %)	Drift time (RSD, %)
RIP	4.4			0.3	0.3			8.4
Butan-2-one M	4.2	0.5	5.7	0.2	21.8	19.7	9.5	1.0
Butan-2-one D	5.6	2.4	6.0	0.2	8.0	9.8	2.6	0.2
Pentan-2-one M	4.8	1.0	5.8	0.2	9.6	9.3	4.8	0.3
Pentan-2-one D	4.3	1.9	4.3	0.2	4.0	6.1	2.2	0.2
Hexan-2-one M	2.6	4.1	2.7	0.2	8.7	5.1	6.4	0.4
Hexan-2-one D	3.9	2.0	2.4	0.2	3.9	6.5	1.3	0.2
Octan-2-one M	6.3	2.3	1.8	0.2	8.0	3.9	1.9	0.3
Octan-2-one D	2.7	1.7	0.4	0.2	3.7	6.2	0.4	0.2
Nonan-2-one M	8.2	4.4	1.0	0.2	8.0	4.1	1.5	0.3
Nonan-2-one D	6.6	8.1	0.6	0.3	14.9	13.7	0.6	0.3

[a] n = 5, same day and performed by one analyst; [b] n = 58, different days and performed by two analysts. M = monomer; D = dimer.

In the case of butan-2-one monomer, the cause could be the presence of other signals appearing in this same area of the topographic plot, including in blank samples. The lower solubility of nonan-2-one in water could be the reason for the high RSD value obtained, especially for the dimer of this analyte. Again, the minimum variation was obtained for drift time, while the maximum variation corresponded to peak intensity. These results suggest that the analytical method was highly robust for the analysis of most of VOCs in long-time studies.

3.2. Construction of chemometric models for olive oil classification using samples from the production year of 2014-2015

In the production year 2014-2015, a total of 292 samples were procured. The chemometric models were built using 80% of these samples (a total of 234 olive oil samples, of which 75 were EVOO, 130 VOO and 29 LOO). The remaining 20% was used for further validation (23 EVOO, 29 VOO and 6 LOO). Specifically, three types of chemometric models were built as commented before: two binary models and one ternary model. The first binary model allowed differentiation between EVOO and non-EVOO samples, the second binary model discriminated between LOO and non-LOO samples, and the ternary model classified samples in EVOO, VOO and LOO. These models were obtained applying two different data processing approaches in an attempt to obtain the best model to classify olive oil samples (detailed in section 2.5.): (i) a chemometric approach using the spectral fingerprint, PCA-LDA and kNN and (ii) a chemometric approach based on specific markers and OPLS-DA.

In the first strategy, a dataset matrix was built with all pre-processed samples of the training set with a final dimension of 234 × 204624. Subsequently, PCA-LDA binary and ternary models were built. For that, the number of components used was 58. As an example, Figures 1A and 1B show the EVOO/non-EVOO model and the LOO/non-LOO model, respectively, where the classes could be clustered adequately, but with some intermingled samples. Therefore, these models were applied to classify the training set using the kNN method with percentages of success of 94.7% and 96.0% for the latter models, respectively (Table 2). Then, the validation set was also classified and the percentages of success were 74.6% in the model EVOO/non-EVOO and 88.1% in the model LOO/non-LOO (Table 2). These values were in the range of previous studies using MOS, spectroscopy and chromatography techniques combined with linear and non-linear classification methods, including ANN, PLS-DA and OPLS-DA (Dierkes et al., 2012, García-González & Aparicio, 2003, Poulli, Mousdis, & Georgiou, 2005, Borràs et al., 2016a, Sales et al., 2017). Therefore, this demonstrates the suitability of PCA-LDA combined with kNN to classify samples within the same harvest.

Table 2. Percentages of success in classification (or training) and validation of the models built with olive oil samples from 2014-2015 and percentages of success in validation to predict samples of the production year of 2015-2016.

		Spectral fingerprint		**Specific markers**	
	Models	Classification or training (% of success)	Validation (% of success)	Classification or training (% of success)	Validation (% of success)
Model built with olive oil samples from 2014-2015	EVOO/VOO/LOO	90.22[a]	67.80[b]	81.00[a]	56.90[b]
	EVOO/non EVOO	94.67[a]	74.58[b]	88.24[a]	74.13[b]
	LOO/non LOO	96.00[a]	88.14[b]	89.14[a]	89.66[b]
Prediction of olive oil samples from 2015-2016	EVOO/VOO/LOO	-	36.03[c]	-	51.60[c]
	EVOO/non-EVOO	-	41.42[c]	-	67.75[c]
	LOO/non-LOO	-	69.61[c]	-	85.25[c]

[a]The model was built with 234 samples (75 EVOO, 130 VOO and 29 LOO).

[b]The model was validated with 58 blind samples (23 EVOO, 29 VOO and 6 LOO).

[c]A total of 409 blind samples (92 EVOO, 196 VOO and 121 LOO) from the production year of 2015-2016 were predicted.

The ternary model (Figure 1C) also shows grouping of the olive oil samples according to the categories EVOO, VOO and LOO in the PCA-LDA plot. In this case, the percentages of classification and validation were 90.2 and 67.8%, respectively; slightly less successful than that obtained using the binary models (see Table 2). This could be explained by the fact that the models were unbalanced and this could cause the specificity, which is the ability to correctly recognize positive samples in the class with fewer samples (Borràs et al., 2016a).

Due to the large amount of data handled with this strategy, added to the fact that it requires a tedious pre-treatment of the data, a second chemometric strategy was investigated. In this case, a selection of individual signals from the topographic plot obtained by GC-IMS was carried out. These signals were selected by visual exploration of all the topographic maps of the olive oil samples analyzed. This means that all these signals were not found in each of the olive oil samples explored, but any signal that was observed in a sample was considered as

a potential marker of interest. In this way, a total of 113 markers were selected (see Figures S1B) and their location on the topographic plot was defined by their upper and lower retention time and their drift time (see Table S1). Then, a dataset matrix was built with the normalized values of intensity of the 234 training set samples analyzed and the 113 markers selected (234 × 113). PCA was firstly applied over the training set to visualise any possible grouping of samples, but it was not enough to discriminate the categories. Hence, tentative binaries and ternary OPLS-DA models were constructed with all markers. Afterwards, the S-plot tool was used to reduce the number of markers needed to obtain the best models and providing the highest R2(cum) and Q2(cum) values (see section 2.5.2.). The ideal markers, whose intensity data should be included in the models, are those with smaller risk for spurious correlations. Referring to S-plot graphics, the selected markers should be placed at the extremes of the graphic with p-corr values close to |1|. As a result of using this statistical tool, a total of 94 markers were selected to rebuild the binary and ternary models (Table S1). Hence, these final OPLS-DA models were selected for classification purposes (Figure 1D-F). Classification percentages between 88.2 and 89.1% were found for the two binary models (EVOO/non-EVOO and LOO/non-LOO) while the validation percentages were between 74.1 and 89.7%. In the same way as in the first strategy, worse results of both classification (81.0%) and validation (56.9%) were obtained through the ternary model (EVOO/VOO/LOO).

In summary, based on the results obtained after analyzing 292 olive oil samples of the same harvest (2014-2015), both chemometric approaches were appropriate for the classification of olive oil samples in the categories EVOO and non-EVOO (defective samples) as well as LOO (non-edible samples) and non-LOO (edible samples). In fact, the validation rates using these binary models were similar for both strategies. However, the best option seems to be the spectral fingerprint approach (with more data per sample) using binary chemometric models since the classification rates were higher and it also procured a higher validation percentage for the ternary model.

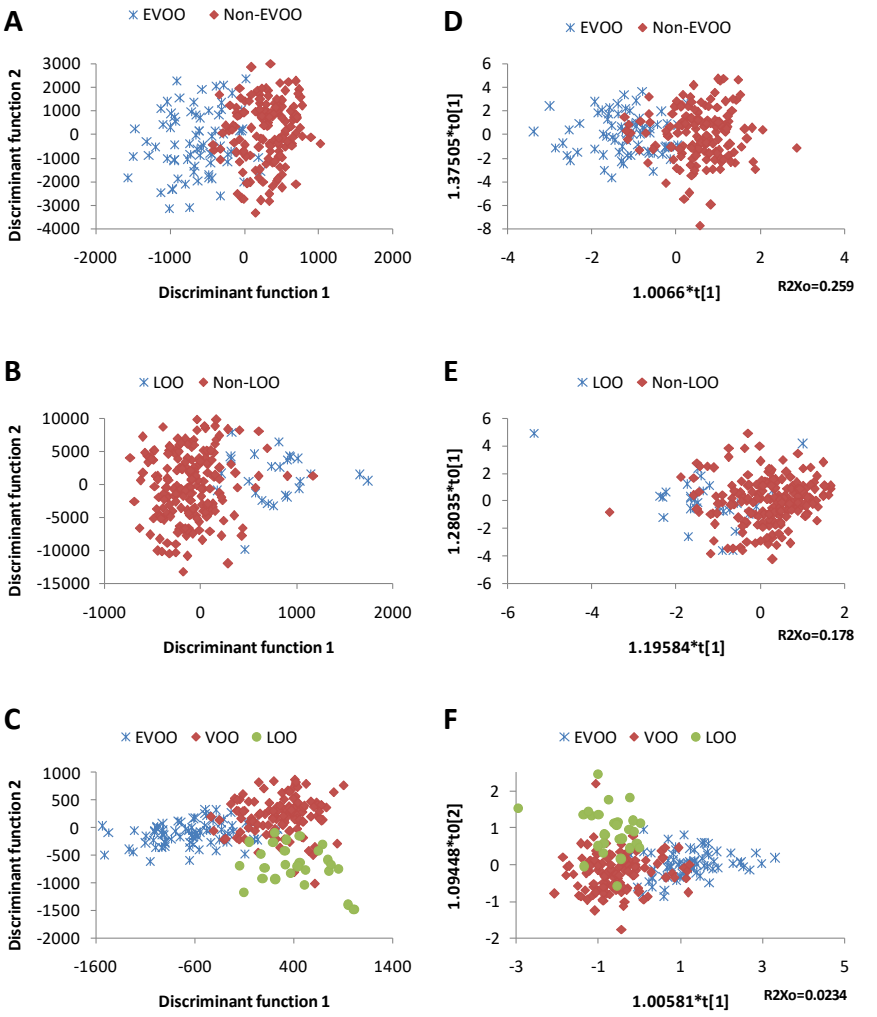

Figure 1. PCA-LDA A) EVOO/non-EVOO binary model, B) LOO/non-LOO binary model and C) ternary model; and OPLS-DA D) EVOO/non-EVOO binary model, E) LOO/non-LOO binary model and F) ternary model built using olive oil samples from 2014-2015 harvest.

3.3. Use of the chemometric models for classification of olive oil samples from a new production year

In 2016, 409 olive oil samples (92 EVOO, 196 VOO and 121 LOO) were analyzed from the production year of 2015-2016. Then, the chemometric models built with samples analyzed in 2015 from the production year of 2014-2015 (section 3.2.) were applied to classify these samples, in order to evaluate their robustness and prediction capacity over time. The results are shown in Table 2.

Binary models (EVOO/non-EVOO and LOO/non-LOO) by both chemometric strategies (41.42-85.25%) showed better results than ternary models (36.0% and 51.6% for spectral fingerprint and markers approaches, respectively). The validation percentage value is especially low in the case of the ternary model for the fingerprint strategy (36%). It could be explained by the fact that a ternary model is more demanding than a binary model since the number of discriminated olive oil classes is higher. And also, without feeding the chemometric models, the prediction of the category of samples from a different harvest/production year seems a more difficult task, resulting in this low value. In particular, the best success of classification was obtained with the binary model LOO/non-LOO (above 85.3%). As can be seen, the percentages of success obtained using the markers approach were better than those obtained with the spectral fingerprint approach in all cases. However, these values were worse that those obtained before with samples from the same harvest of 2014-2015. In any case, using markers, the percentages of success in the validation set of 2015-2016 were only slightly lower than those obtained in the validation set of 2014-2015 with the calibration models of 2014-2015, between 4.4 and 6.4% lower.

Therefore, this suggests that the chemometric models had a loss of stability and sensitivity between production years, when models built with samples analyzed in 2015 were applied to predict samples analyzed in 2016. Although the characteristics of the olive oil samples, including the content of VOCs, may vary between the production years according to other studies (Romero, Saavedra, Tapia, Sepúlveda, & Aparicio, 2016, D'Imperio et al., 2010), the variability of the

instrument conditions, such as deterioration of the chromatographic column, could be also the cause of these results, making the first strategy more prone to fail over time.

3.4. Recalibration of chemometrics models with samples from new production years

In order to improve the success of classification and to evaluate the need of recalibrating the models each olive oil harvest/production year, new chemometric models were built using samples from two successive periods (2014-2015 and 2015-2016), which were analyzed in the years 2015 and 2016, respectively. Precisely, 234 and 327 samples from the harvests of 2014-2015 and 2015-2016, respectively, were selected for the training of the models. It corresponded to the 80% of the total samples analyzed from each harvest, with a total of 149 EVOOs, 286 VOOs and 126 LOOs. Again, for the construction of the binary and ternary models both data analysis strategies, spectral fingerprint and markers, were used.

Figure 2 shows the recalibrated chemometrics models by both strategies. In the case of using the spectral fingerprint, PCA-LDA analysis were performed and the results are plotted in Figure 2A for the model EVOO/non-EVOO, Figure 2B for the model LOO/non-LOO, and Figure 2C for the ternary model. These plots show a good visual separation of the olive oil categories. In addition, after applying PCA-LDA (with 114 components) and kNN to the training set, the classification percentages were above 91.5% for all the models (Table 3). In order to validate the models, a validation set consisted of 140 olive oil samples (58 and 82 from the harvests of 2014-2015 and 2015-2016, respectively) was studied, i.e. 41 EVOOs, 69 VOOs and 30 LOOs. The validation percentage results were between 79.4% and 92.9% for the three models. In this case, the ternary model showed again the worst percentage of success compared to the binary models. This was also observed by Sales et al. (2017) using GC-MS data and PLS-DA/OPLS-DA. Nevertheless, these classification and validation values were

higher than those obtained for the models from the harvest of 2014-2015. Probably, it is explained by the fact that these models included more variability due to the analysis of more samples and from two different harvests and production years.

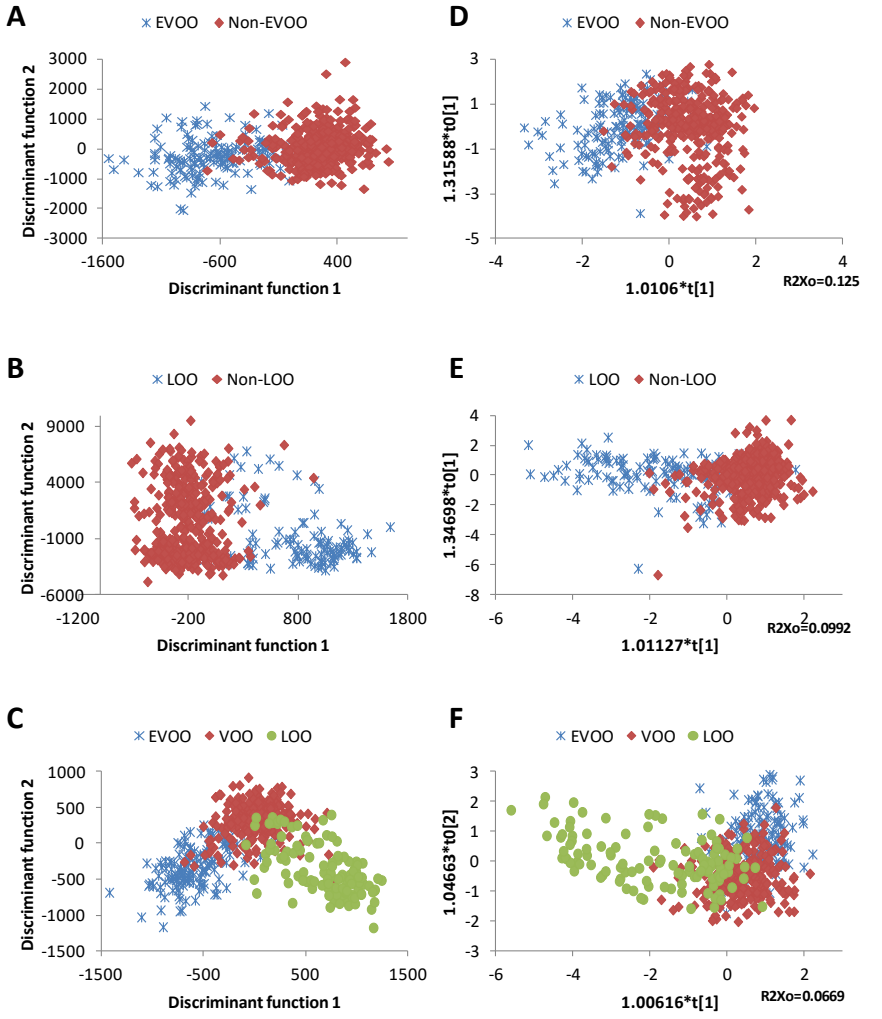

Figure 2. PCA-LDA A) EVOO/non-EVOO binary model, B) LOO/non-LOO binary model and C) ternary model; and OPLS-DA D) EVOO/non-EVOO binary model, E) LOO/non-LOO binary model and F) ternary model built using olive oil samples from 2014-2015 + 2015-2016 harvests.

Likewise, the data treatment was also carried out using the strategy based on employing specific markers. In this case, a total of 81 markers were selected from the 113 total markers using S-plot tool as before (Table S1). The obtained OPLS-DA models are represented in Figure 2D-F, which showed a good clustering of the categories in two or three groups depending on the model. The classification and validation percentages were 89.6% and 85.7% for the binary model EVOO/non-EVOO as well as 90.3% and 90.7% for the binary model LOO/non-LOO (see Table 3), respectively. Similarly, as in previous cases, these percentages were lower for the ternary model, showing a success of 74.3% in classification and validation.

Table 3. Percentages of success in classification (or training) and validation of the models built with olive oil samples from 2014-2015 + 2015-2016 and percentages of success in validation to predict samples of the production year of 2015-2016.

		Spectral fingerprint		**Specific markers**	
	Models	Classification or training (% of success)	Validation (% of success)	Classification or training (% of success)	Validation (% of success)
Model built with olive oil samples from 2014-2015 + 2015-2016	EVOO/VOO/LOO	91.53[a]	79.40[b]	74.30[a]	74.29[b]
	EVOO/non-EVOO	95.95[a]	85.10[b]	89.57[a]	85.72[b]
	LOO/non-LOO	95.58[a]	92.90[b]	90.32[a]	90.71[b]
Prediction of olive oil samples from 2015-2016	EVOO/VOO/LOO	-	86.59[c]	-	82.93[c]
	EVOO/non-EVOO	-	90.24[c]	-	91.46[c]
	LOO/non-LOO	-	93.90[c]	-	91.46[c]

[a]The model was built with 561 samples: 234 from the production year of 2014-2015 (75 EVOO, 130 VOO and 29 LOO) and 327 from the production year of 2015-2016 (74 EVOO, 156 VOO and 97 LOO).

[b]The model was validated with 140 blind samples: 58 from the production year of 2014-2015 (23 EVOO, 29 VOO and 6 LOO) and 82 from the production year of 2015-2016 (18 EVOO, 40 VOO and 24 LOO).

[c]A total of 82 blind samples (18 EVOO, 40 VOO and 24 LOO) from the production year of 2015-2016 were predicted.

Summarizing, when models were recalibrated with samples from a new production year, better classification percentages were reached by using the spectral fingerprint approach in comparison with the strategy based on specific markers (Table 3). Alternatively, the percentages of success in validation were only slightly higher in the first case, suggesting that both strategies can be applied for olive oil grading, especially the binary models with percentages of success higher than 85%. This means that the calibration models provided better results when a greater number of samples were used, including more LOOs, and procured from two harvest/production periods. Indeed, when the chemometric models were constructed with samples from the two harvests, the most significant improvements (from 1 to 17.4%) were in validation applying both strategies.

Otherwise, the chemometric models resulting from data fusion of two successive harvests (2014-2015 and 2015-2016) were used to predict samples of the latter harvest (Table 3). These results were compared with those obtained with the models built only with samples from the production year of 2014-2015 (Table 2). An enhancement of the prediction percentages was observed using both chemometric approaches; between 24.3 and 50.6% for the spectral fingerprint approach and between 6.2 and 31.3% for the markers approach. In this context, previous studies have shown a large inter-annual variability of olive oil samples by PCA (Romero et al., 2016, Cajka et al., 2010, Borràs et al., 2016b). In one of them, the prediction ability to differentiate the geographical origin of olive oil samples analyzed by GC-MS were improved using ANN with multilayer perceptrons and LDA models with three-year sampling data (Cajka et al., 2010). In another work, to minimize this effect using MS and MIR, each dataset was orthogonalized against the production year using the scores on the first principal component for the prediction of sensory descriptors of olive oil with PLS (Borràs et al., 2016b). In our case, the present results demonstrate that using either spectral fingerprint or markers data processing strategies for olive oil grading, the prediction abilities were enhanced recalibrating the models with samples from a new harvest.

In this context, other targeted approaches, combining chromatographic and non-chromatographic methods with chemometrics, have been also developed to classify olive oils according to their quality using binary and/or ternary models, with percentages of success between 70-100% (Dierkes et al., 2012, Fragaki et al., 2005, Sales et al., 2017, Zhou, Lib, Wenga, Fangc, & Gud, 2016). Some of these analytical methods are faster, e.g. those based on NMR, but others required sample pretreatment and sophisticated equipment. In these studies, the number of studied samples was generally low and no attention was paid to their robustness along different olive oil campaigns. Therefore, this study supports that GC-IMS using the markers approach is suitable to be implemented in the olive oil industry, with adequate percentages of success and data that can be easily handled. However, further work is required through inter-laboratory studies to generate classification models with performance independent from the operator and the GC-IMS instrumentation used (Piccinonna et al., 2016).

3.5. Characterization of the markers

A total of 39 VOCs standards were analyzed for identification purposes. These compounds were previously reported in olive oil samples from different cultivars, qualities and geographical origins (Garrido-Delgado et al., 2015a, Dierkes et al., 2012, Romero et al., 2016, Magagna et al., 2016, Morales, Luna, & Aparicio, 2005; Procida, Cichelli, Lagazio, & Conte, 2016, Peres, Jeleń, Majcher, Arraias, Martins, & Ferreira-Dias, 2013, Kesen, Kelebek, & Selli, 2013). Initially, a putative identification of markers was carried out using a commercial GC-IMS library (see section 2.3.). The identification of 20 compounds could be confirmed by injecting real standards on the basis of both their retention time and drift time, i.e. ethanol, ethyl acetate, pentan-2-one, 1-penten-3-one, 3-methyl-1-butanol, 2-methyl-1-butanol, *trans*-2-pentenal, 2-hexanone, ethyl butanoate, hexanal, *trans*-2-hexen-1-al, *trans*-2-hexen-1-ol, octanal, hexyl acetate, nonanal, 1-hexanol, 2-heptenal, 2-octanol, 3-hexen-1-ol, and limonene. These VOCs corresponded to 21 markers (monomers and/or dimers), whose coordinates (drift

and retention time) in the topographic maps are detailed in Table S1. Some of the species coeluted and thus some markers could correspond to one and/or two compounds, e.g. the dimers of 2- and 3-methyl-1-butanol, hexanal and ethyl butanoate, as well as *trans*-2-hexen-1-ol and 3-hexen-1-ol.

Interestingly, 15 of these markers were selected as important class markers by the S-plot tool when samples from one harvest (2014-2015) and two harvests (2014-2015 + 2015 and 2016) were compared. One way ANOVA was performed to evaluate the differences between the categories and the multiple range test LSD was used as a multiple comparison procedure to compare the means (see section 2.3.). Depending on the compound, a significant difference was found between three or two categories according to their normalized intensity (Figure 3). The markers 2 (ethyl butanoate and/or hexanal dimer), 3 (3- and/or 2-methyl-1-butanol dimer) and 76 (2-heptenal monomer) showed a higher normalized intensity in LOO samples. In this sense, other studies have suggested that the presence of hexanal in olive oils was associated to both positive and negative attributes depending on its concentration (Dierkes et al., 2012). Alternatively, 2-heptenal was found to be a good marker of rancidity and oxidation (Garrido-Delgado et al., 2015b) and it also contributed to mustiness–humidity (Morales et al., 2005). The compounds 2-/3-methyl-1-butanol can contribute to off-flavors of fustiness, winey–vinegary, mustiness–humidity (Dierkes et al., 2012, Morales et al., 2005, Angerosa, Lanza, & Marsilio, 1996). However, the presence of these compounds in some EVOO samples could indicate that the detection limit of the GC-IMS device is lower than their limit of recognition.

Furthermore, in the category EVOO the ANOVA showed a higher normalized intensity of the following markers: 4 (*trans*-2-hexen-1-al monomer), 34 (1-hexanol dimer), 49 (*trans*-2-pentenal dimer), 61 (1-penten-3-one dimer), 67 (pentan-2-one dimer), 72 (*trans*-2-hexen-1-ol/ 3-hexen-1-ol dimer), and 73 (*trans*-2-hexen-1-al dimer).

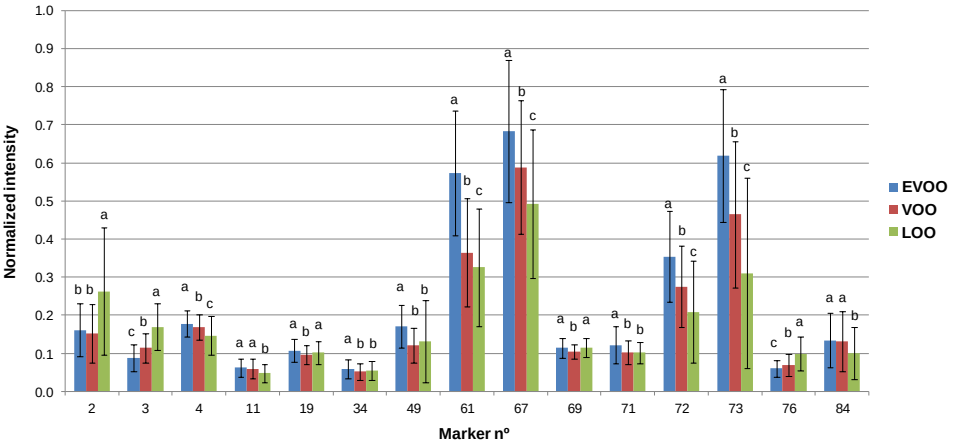

Figure 3. Bar graph showing the normalized intensity (mean ± standard deviation) of markers identified in olive oil samples and relevant for the models built with samples from one harvest (2014-2015) and two harvests (2014-2015 + 2015-2016). Different letters indicate statistically significant differences between groups, $p < 0.05$. Markers: 2 (ethyl butanoate and/or hexanal dimer), 3 (3- and/or 2-methyl-1-butanol dimer), 4 (*trans*-2-hexen-1-al monomer), 11 (hexyl acetate monomer), 19 (1-hexanol monomer), 34 (1-hexanol dimer), 49 (*trans*-2-pentenal dimer), 61 (1-penten-3-one dimer), 67 (pentan-2-one dimer), 69 (ethyl butanoate monomer), 71 (hexan-2-one monomer), 72 (*trans*-2-hexen-1-ol/ 3-hexen-1-ol dimer), 73 (*trans*-2-hexen-1-al dimer), 76 (2-heptenal monomer), and 84 (2-octanol dimer).

These compounds are related to positive attributes (green, grass, banana, apple, bitter almond, etc.) (Garrido-Delgado et al., 2015a, Magagna et al., 2016, Morales et al., 2005, Procida et al., 2016, Kesen et al., 2013). In particular, 1-penten-3-one, 2-hexenal and 2-pentenal were suggested to be markers EVOO quality in other studies (Garrido-Delgado et al., 2015b, Procida et al., 2016), agreeing with our results. In the case of the marker 71 (hexan-2-one monomer), although this compound has been associated to oxidation (Procida et al., 2016), its signal was generally higher in EVOO samples. This could be explained due to a

charge competition effect with compounds with higher proton affinity in samples with defects in this chromatographic region.

Nevertheless, the observed normalized intensity trend for each marker between the categories is general and a high variation within each category was observed (Figure 3); differentiating all samples of a category was not possible based on an individual marker. As noted above, a high number of olive oil samples were compared and from two harvest periods with different agro-climatic conditions and productions, which can affect the content of VOCs. VOOs and LOOs could present more than one defect at different levels (Angerosa et al., 1996, Souayah et al., 2017), and the presence of singular samples should not be ruled out. Moreover, samples were characterized by Official Panels concerning its category with a maximum robust coefficient of variation established of 20.0% (International Olive Council, 2018). All these facts could contribute to explain these deviation values. In any case, some of the aforementioned markers could be useful to predict a category when a very high and, on the contrary, a very low normalized intensity of some of the aforementioned markers is observed, and to assess the reproducibility of the methodology between laboratories.

4. Conclusions

Our results showed that the spectral fingerprint chemometric approach provides better classification and validation results of olive oil samples than the use of specific markers approach when both chemometric models were fed with olive oil samples from a single harvest and for those fed with samples from two harvests. However, when these models were applied to predict samples from a new harvest, the lowest success percentages were obtained by the former approach (section 3.3.). It could be associated to small variations of the instrument, such as column deterioration. In addition, the spectral fingerprint approach is laborious and time consuming, as well as generates large-size data files, which requires the use of powerful computers. While, the second strategy

based on the selection of markers handles much less data per sample, which would facilitate their implementation in the olive oil industry. For this reason, this strategy is a suitable approach to be implemented for olive oil grading.

Moreover, independently of the chemometric strategy used, the best percentages of success in both training and validation sets were obtained using the binary models built with either 2014-2015 olive oil samples or with fusion of 2014-2015 + 2015-2016 samples.

Furthermore, focusing on the robustness of the proposed calibration models over time, those built by combining data from different production years (2014-2015 + 2015-2016) provided better results to classify unknown olive oil samples based on their category. Probably, the greater heterogeneity of the samples improved the prediction ability using models able to collect the variation from different harvest/production years, including different meteorological conditions. Hence, the recalibration of the models with samples from at least two different harvests is recommended. It would be even better if the chemometric approaches proposed in this work are enriched with samples from every new production year.

Abbreviations used

GC: Gas Chromatography

IMS: Ion mobility Spectrometry

VOCs: Volatile Organic Compounds

EVOO: Extra Virgin Olive Oil

VOO: Virgin Olive Oil

LOO: *Lampante* Olive Oil

PCA: Principal Component Analysis

LDA: Linear Discriminant Analysis

kNN: k-Nearest Neighbour

PLS-DA: Partial Least-Squares-Discriminant Analysis

OPLS-DA: Orthogonal Partial Least-Squares-Discriminant Analysis

MS: Mass Spectrometry

HS: Headspace

RIP: Reactant Ion Peak

RSD: Relative Standard Deviation

Akcnowledgments

The authors acknowledge financial support from the Government of Spain (DGICyT Project CTQ2014-52939R) and from *Interprofesional del aceite de oliva español*. N.J.C. wishes to thank the Spanish Ministry of Education, Culture and Sport for awarding a FPU pre-doctoral grant. M.d.M Contreras are grateful for the postdoctoral grant funded by the "Acción 6 del Plan de Apoyo a la Investigación de la Universidad de Jaén, 2017-2019".

References

Alcalá, S., Ocaña, M. T., Cárdenas, J. R., Miquel, M. A., Vilar, J., Espinola, F. et al. (2016). Alkyl esters content and other quality parameters in oil mill: A response surface methodology study. European *Journal of Lipid Science and Technology, 119*, 1600026 (1–10).

Angerosa, F., Lanza, B., & Marsilio, V. (1996). Biogenesis of «fusty» defect in virgin olive oils. *Grasas y Aceites, 47*, 142–150.

Arroyo-Manzanares, N., Martín-Gómez, A., Jurado-Campos, N., Garrido-Delgado, R., Arce, C., & Arce, L. (2018). Target vs spectral fingerprint data analysis of Iberian ham samples for avoiding labelling fraud using headspace – gas chromatography–ion mobility spectrometry. *Food Chemistry, 246*, 65–73.

Borràs, E., Ferré, J., Boqué, R., Mestres, M., Aceña, L., Calvo, A. et al. (2016a) Olive oil sensory defects classification with data fusion of instrumental techniques and multivariate analysis (PLS-DA). *Food Chemistry, 203*, 314–322.

Borràs, E., Ferré, J., Boqué, R., Mestres, M., Aceña, L., Calvo, A. et al. (2016b). Prediction of olive oil sensory descriptors using instrumental data fusion and partial least squares (PLS) regression. *Talanta, 155*, 116–123.

Cajka, T., Riddellova, K., Klimankova, E., Cerna, M., Pudil, F., & Hajslova, J. (2010). Traceability of olive oil based on volatiles pattern and multivariate analysis. *Food Chemistry, 121*, 282–289.

Contreras, M. d. M., Arroyo-Manzanares, N., Arce, C., & Arce, L. (2019). HS-GC-IMS and chemometric data treatment for food authenticity assessment: Olive oil mapping and classification through two different devices as an example. *Food Control, 98,* 82–93.

Contreras Gámez, M. M., Rodríguez Pérez, C., García Salas, P., & Segura Carretero, A. (2014). Polyphenols from the Mediterranean Diet: Structure, Analysis and Health Evidence. In N. Motohashi (Ed.), *Occurrences, structure, biosynthesis, and health benefits based on their evidences of medicinal phytochemicals in vegetables and fruits*, (pp. 141–209). New York: Nova Science Publishers, Inc.

Dierkes, G., Bongartz, A., Guth, H., & Hayen, H. (2012). Quality evaluation of olive oil by statistical analysis of multicomponent stable isotope dilution assay data of aroma active compounds. *Journal of Agricultural and Food Chemistry, 60,* 394–401.

D'Imperio, M., Gobbino, M., Picanza, A., Costanzo, S., Della Corte, A., & Mannina, L. (2010). Influence of harvest method and period on olive oil composition: an NMR and statistical study. *Journal of Agricultural and Food Chemistry,* 58, 11043-11051.

European Commission Regulation (EEC) (1991). European Commission Regulation EEC/2568/91 of 11 July on the characteristics of olive and pomace oils and on their analytical methods. *Official Journal of the European Union, L248(640)*, 1–82.

Fortini, M., Migliorini, M., Cherubini, C., Cecchi, L., & Calamai, L. (2017). Multiple internal standard normalization for improving HS-SPME-GC-MS quantitation in virgin olive oil volatile organic compounds (VOO-VOCs) profile. *Talanta, 165,* 641–652.

Fragaki, G., Spyros, A., Siragakis, G., Salivaras, E., & Dais, P. (2005). Detection of extra virgin olive oil adulteration with lampante olive oil and refined olive oil using nuclear magnetic resonance spectroscopy and multivariate statistical analysis. *Journal of Agricultural and Food Chemistry, 53,* 2810–2816.

García-González, D. L., & Aparicio, R. (2003). Virgin olive oil quality classification combining neural network and MOS sensors. *Journal of Agricultural and Food Chemistry, 51 (12),* 3515–3519.

Gallegos, J., Garrido-Delgado, R., Arce, L., & Medina, L. M. (2015). Volatile metabolites of goat cheeses determined by ion mobility spectrometry. potential applications in quality control. *Food Analytical Methods, 8 (7),* 1699–1709.

Garrido-Delgado, R., Arce, L., & Valcárcel, M. (2012). Multi-capillary column-ion mobility spectrometry: A potential screening system to differentiate virgin olive oils. *Analytical and Bioanalytical Chemistry, 402 (1),* 489–498.

Garrido-Delgado, R., Dobao-Prieto, M. D. M., Arce, L., & Valcárcel, M. (2015a). Determination of volatile compounds by GC-IMS to assign the quality of virgin olive oil. *Food Chemistry, 187,* 572–579.

Garrido-Delgado, R., Dobao-Prieto, M. M., Arce, L., Aguilar, J., Cumplido, J. L., & Valcárcel, M. (2015b). Ion mobility spectrometry versus classical physico-chemical analysis for assessing the shelf life of extra virgin olive oil according to container type and storage conditions. J*ournal of Agricultural and Food Chemistry, 63 (8),* 2179–2188.

Gerhardt, N., Birkenmeier, M., Sanders, D., Rohn, S., & Weller, P. (2017). Resolution-optimized headspace gas chromatography-ion mobility spectrometry (HS-GC-IMS) for non-targeted olive oil profiling. *Analytical and Bionalytical Chemistry, 409,* 3933–3942.

Gerhardt, N., Schwolow, S., Rohn, S., Pérez-Cacho, P. R., Galán-Soldevilla, H., Arce, L., & Weller, P. (2019). Quality assessment of olive oils based on temperature-ramped HS-GC-IMS and sensory evaluation: Comparison of different processing approaches by LDA, kNN, and SVM. *Food Chemistry, 278,* 720-728.

International Olive Council (2018). Sensory analysis of olive oil. Method for the organoleptic assessment of virgin olive oil. COI/T.20/Doc. No 15/Rev. 10.

Jurado-Campos, N., Garrido-Delgado, R., Martínez-Haya, B., Eiceman, G. A., & Arce, L. (2018). Stability of proton-bound clusters of alkyl alcohols, aldehydes and ketones in Ion Mobility Spectrometry. *Talanta, 185,* 299–308.

Kesen, S., Kelebek, H., & Selli, S. (2013). Characterization of the volatile, phenolic and antioxidant properties of monovarietal olive oil obtained from cv. Halhali. *Journal of the American Oil Chemists' Society, 90 (11),* 1685–1696.

Magagna, F., Valverde-Som, L., Ruíz-Samblás, C., Cuadros-Rodríguez, L., Reichenbach, S. E., Bicchi, C., et al. (2016). Combined untargeted and targeted fingerprinting with comprehensive two-dimensional chromatography for volatiles and ripening indicators in olive oil. *Analytica Chimica Acta, 936,* 245–258.

Morales, M. T., Luna, G., & Aparicio, R. (2005). Comparative study of virgin olive oil sensory defects. *Food Chemistry, 91,* 293–301.

Peres, F., Jeleń, H. H., Majcher, M. M., Arraias, M., Martins, L. L., & Ferreira-Dias, S. (2013). Characterization of aroma compounds in Portuguese extra virgin olive oils from Galega Vulgar and Cobrançosa cultivars using GC-O and GC×GC-ToFMS. *Food Research Internatinal, 54,* 1979–1986.

Piccinonna, S., Ragone, R., Stocchero, M., Del Coco, L., De Pascali, S. A., Schena, F. P., & Fanizzi, F. P. (2016). Robustness of NMR-based metabolomics to generate comparable data sets for olive oil cultivar classification. An inter-laboratory study on Apulian olive oils. *Food Chemistry, 199,* 675-683.

Poulli, K. I., Mousdis, G. A., & Georgiou, C. A. (2005). Classification of edible and lampante virgin olive oil based on synchronous fluorescence and total luminescence spectroscopy. *Analytica Chimica Acta, 542 (2),* 151–156.

Procida, G., Cichelli, A., Lagazio, C., & Conte, L. S. (2016). Relationships between volatile compounds and sensory characteristics in virgin olive oil by analytical and chemometric approaches. *Journal of the Science of Food and Agriculture, 96,* 311–318.

Romero, N., Saavedra, J., Tapia, F., Sepúlveda, B., & Aparicio, R. (2016). Influence of agroclimatic parameters on phenolic and volatile compounds of Chilean virgin olive oils and characterization based on geographical origin, cultivar and ripening stage. *Journal of the Science of Food and Agriculture, 96,* 583–592.

Sales, C., Cervera, M. I., Gil, R., Portolés, T., Pitarch, E., & Beltran, J. (2017). Quality classification of Spanish olive oils by untargeted gas chromatography coupled to hybrid quadrupole-time of flight mass spectrometry with atmospheric pressure chemical ionization and metabolomics-based statistical approach. *Food Chemistry, 216,* 365–373.

Souayah, F., Rodrigues, N., Veloso, A. C. A., Dias, L. G., Pereira, J. A., Oueslati, S., & Peres, A. M. (2017). Discrimination of olive oil by cultivar, geographical origin and quality using potentiometric electronic tongue fingerprints. *Journal of the American Oil Chemists' Society, 94,* 1417–1429.

Szymanska, E., Davies, A., & Buydens, L. (2016). Chemometrics for ion mobility spectrometry data: recent advances and future prospects. *Analyst, 141,* 5689–5708.

Zhou, L. L., Lib, C., Wenga, X. C., Fangc, X. M., & Gud, Z. H. (2016). 19F NMR method for the determination of quality of virgin olive oil. *Grasas y Aceites, 67,* e126.

Supplementary Information

Table S1. Drift time (DT) (ms), reduced ion mobility (K_o) ($cm^2 \cdot V^{-1} \cdot s^{-1}$), upper and lower retention time (RT) of the selected markers from GC-IMS topographic plots of olive oil samples.

Marker number	DT (ms)	Lower RT [c] (s)	Upper RT[c] (s)	Corresponding compound ion species[d]	Ref.[d]
1[a,b]	11.214	201	216		
2[a,b]	10.616	162	185	Ethyl butanoate and/or hexanal d	Dierkes et al. (2012), Garrido-Delgado et al. (2015a)
3[a,b]	10.092	118	134	3- and/or 2-Methyl-1-butanol d	Dierkes et al. (2012), Garrido-Delgado et al. (2015a), Morales et al. (2005)
4[a,b]	7.978	249	272	*Trans*-2-hexen-1-al m	Magagna et al. (2016)
5[a,b]	9.259	161	186		
6[a]	11.353	554	595		
7[a,b]	8.287	647	683		
8[b]	9.451	531	559		
9[a]	9.035	406	479		
10[a,b]	9.035	514	538		
11[a,b]	9.43	574	602	Hexyl acetate m	Peres et al. (2013)
12	12.357	536	553	Octanal d	Morales et al. (2005)
13[b]	10.252	528	554		
14[a,b]	10.733	394	444		
15[a,b]	8.96	349	367		
16[a,b]	9.622	346	373		
17[b]	8.523	325	351		
18[a,b]	9.216	328	347		
19[a,b]	8.917	295	326	1-Hexanol m	Garrido-Delgado et al. (2015a), Kesen et al. (2013)
20	9.451	297	326		
21[a,b]	8.907	267	290		
22[a,b]	8.811	199	225		
23[a,b]	9.377	200	224		

24[a]	9.868	197	216		
25[a]	10.733	198	211		
26[b]	12.506	201	220		
27[a,b]	7.625	209	257		
28[a,b]	7.593	174	207		
29[a]	7.582	130	172	*Trans*-2-Pentenal m	Morales et al. (2005), Procida et al. (2016)
30[a]	8.17	107	123		
31[a,b]	11.085	327	347		
32[a,b]	11.513	351	365		
33[a,b]	12.474	331	347		
34[a,b]	11.107	301	317	1-Hexanol d	Garrido-Delgado et al. (2015a), Kesen et al. (2013)
35[a,b]	12.389	298	322		
36[a,b]	12.036	265	281		
37[a,b]	12.485	249	267		
38	8.864	121	141		
39[a]	7.583	396	424		
40[a,b]	8.614	82	92		
41[a]	9.075	71	86	Ethyl acetate d	Dierkes et al. (2012), Garrido-Delgado et al. (2015a), Magagna et al. (2016)
42[a,b]	7.636	88	96		
43[b]	7.658	53	62	Ethanol d	Dierkes et al. (2012), Magagna et al. (2016), Morales et al. (2005)
44[a]	7.858	60	67		
45[a,b]	8.136	60	71		
46[a,b]	14.546	556	578		
47[a,b]	11.492	299	317		
48[a,b]	11.962	299	314		
49[a,b]	9.279	132	139	*Trans*-2-Pentenal d	Garrido-Delgado et al. (2015a), Procida et al. (2016)
50[a,b]	9.285	123	131		

51[a,b]	9.674	123	130		
52[a,b]	9.937	168	177		
53[a,b]	7.629	98	125		
54[b]	7.662	76	86		
55[a,b]	8.49	66	73		
56[a,b]	8.81	69	77		
57[b]	9.577	82	90		
58[a,b]	7.644	85	92		
59[b]	9.479	71	80		
60	8.203	75	85		
61[a,b]	8.92	89	99	1-Penten-3-one d	Garrido-Delgado et al. (2015a)
62[a,b]	9.779	146	161		
63[a,b]	10.054	146	161		
64[a,b]	9.503	146	161		
65[a,b]	11.138	146	161		
66[a,b]	7.611	62	73		
67[a,b]	9.272	93	105	2-Pentanone d	
68[a,b]	7.666	107	124		
69[a,b]	8.526	161	186	Ethyl butanoate m	Dierkes et al. (2012), Garrido-Delgado et al. (2015a)
70[a,b]	8.844	161	186		
71[a,b]	8.177	165	173	Hexan-2-one monomer	Procida et al. (2016)
72[a,b]	10.366	262	281	*Trans*-2-hexen-1-ol/ 3-hexen-1-ol d	Garrido-Delgado et al. (2015a), Morales et al. (2005)
73[a,b]	10.389	243	262	*Trans*-2-hexen-1-al d	Magagna et al. (2016)
74[a,b]	8.755	249	264		
75[a,b]	8.972	264	282		
76[a,b]	8.578	452	471	2-Heptenal m	Garrido-Delgado et al. (2015a)
77[a,b]	8.283	462	485		
78[a,b]	8.061	504	528		
79[a,b]	8.405	510	533		
80[b]	8.272	552	575	Limonene m	Magagna et al. (2016)
81[b]	8.783	552	575		
82[a]	11.389	557	581		

83[b]	9.962	910	978	Nonanal m	Magagna et al. (2016), Morales et al. (2005)
84[a,b]	12.381	538	584	2-Octanol d	Garrido-Delgado et al. (2015a)
85[a]	8.873	877	925		
86[a]	9.474	807	863		
87[a]	11.278	894	953		
88[a]	12.23	870	925		
89[a]	9.363	940	999		
90	7.955	708	791		
91	8.449	570	605		
92[a,b]	8.329	231	305		
93[a]	11.383	71	106		
94[a]	8.188	1661	1734		
95[a]	10.087	786	863		
96[a]	8.171	870	953		
97[a]	12.767	927	985		
98	9.006	746	825		
99[a]	11.912	753	805		
100[a,b]	12.107	414	522		
101[a,b]	9.865	384	496		
102	8.232	620	644		
103[a]	9.003	617	654		
104[a]	10.744	98	120		
105[a,b]	10.528	131	144		
106[a,b]	11.196	240	257		
107[a,b]	10.51	935	997		
108[a,b]	8.694	1004	1071		
109[a,b]	9.777	556	579		
110[a,b]	9.666	263	286		
111[a]	8.055	414	429		
112[a,b]	8.806	416	428		
113[a,b]	10.557	302	326		

[a]Selected markers in the strategy based on employing specific markers to build chemometric models of olive oil samples from the campaign of 2014-2015.

[b]Selected markers in the strategy based on employing specific markers to build chemometric models of olive oil samples from the campaigns 2014-2015 + 2015-2016.

[c]The signal of each markers was taken automatically at the maximum intensity between the upper and lower retention time.

[d]Monomer (m); dimer (d); ref. (reference).

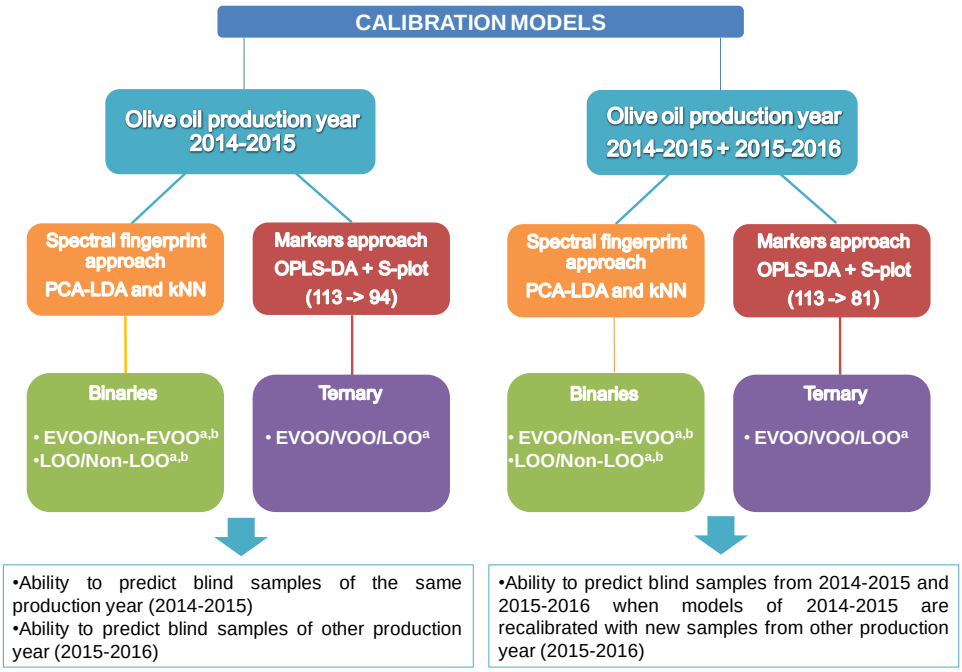

[a]EVOO, extra virgin olive oil; LOO, lampante olive oil; VOO, virgin olive oil
[b]Non-EVOO is comprised of VOO and LOO samples; Non-LOO is comprised of EVOO and VOO samples

Figure S1. Scheme summarizing the chemometric strategies and calibration models built to classify olive oil samples.

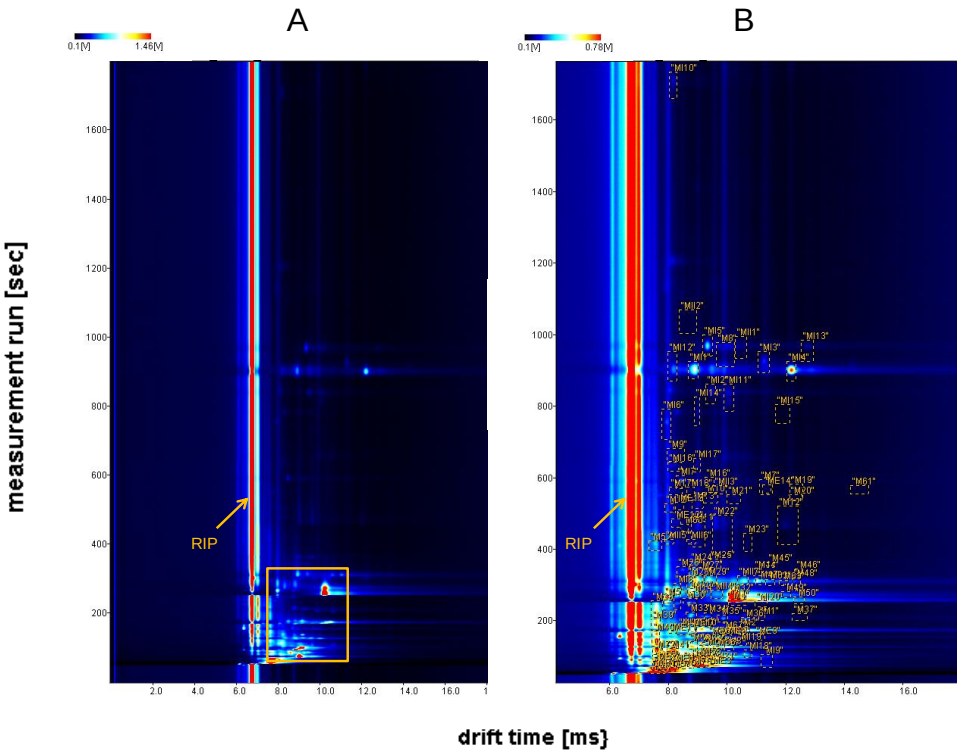

Figure S2. GC-IMS topographic maps of an olive oil sample: A) highlighting the selected area for spectral fingerprint chemometric strategy and B) including the 113 markers initially selected, which are represented by boxes. RIP, reactant ion peak.

Quality authentication of Virgin Olive Oils using Orthogonal Techniques and Chemometrics based on individual and high-level data fusion information

CHAPTER VIII

Talanta

Vol. 219, 1 November 2020, 121260

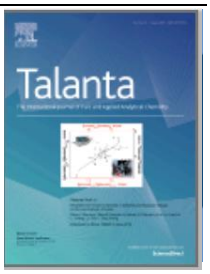

Quality authentication of Virgin Olive Oils using Orthogonal Techniques and Chemometrics based on individual and high-level data fusion information

Natividad Jurado-Campos[a], Natalia Arroyo-Manzanares[b], Pilar Viñas[b], Lourdes Arce[a]

[a]*Department of Analytical Chemistry, University of Córdoba. Institute of Fine Chemistry and Nanochemistry. International Agrifood Campus of Excellence (ceiA3), Marie Curie Annex Building. Campus de Rabanales. 14071 Córdoba, Spain.*

[b]*Department of Analytical Chemistry, Faculty of Chemistry, Regional Campus of International Excellence "Campus Mare-Nostrum", University of Murcia, E-30100, Murcia, Spain.*

Quality authentication of Virgin Olive Oils using Orthogonal Techniques and Chemometrics based on individual and high-level data fusion information

Natividad Jurado-Campos, Natalia Arroyo-Manzanares, Pilar Viñas, Lourdes Arce

ABSTRACT

Currently, extra virgin olive oil, virgin olive oil and lampante olive oil are classified using physical-chemical analyses and a sensory analysis of fruitiness and defects, which is carried out by expert panels. This manual analysis is nowadays considered to be controversial and therefore analytical methodologies, which may be automated to classify these samples, are needed. In this work, we propose using an analytical platform based on two orthogonal techniques to determine the flavour components perceived in the mouth and the components contributing to the olive oils (OOs) aroma, respectively. For the former, capillary electrophoresis with ultraviolet detector (CE-UV) and high-performance liquid chromatography with UV or fluorescence detection were explored. The CE-UV analysis provided better results with the developed chemometric models (principal component analysis, linear discriminant analysis and k-nearest neighbors method). While for the latter, headspace (HS) - gas chromatography coupling with ion mobility spectrometry (GC-IMS) was selected due to the easy applicability of this technique to classify OOs. Then both techniques, CE-UV and GC-IMS, were selected to be integrated into one analytical platform. The potential of using both complementary/orthogonal techniques was demonstrated using high-level data fusion of CE-UV and GC-IMS data.

Keywords: Ion Mobility Spectrometry, Capillary Electrophoresis, High-Performance Liquid Chromatography, volatile and polar fraction

1. Introduction

The official method for analysing extra virgin olive oil (EVOO), virgin olive oil (VOO) and lampante olive oil (LOO) samples is based on several physical-chemical analyses methods as well as a sensory assessment carried out by trained panelists [1]. The olive oils (OOs)' flavour is described by the perception of positive attributes (fruity, bitter and spicy) and defects (fusty, mould, winey, muddy sediment, metallic, rancid, and others). The flavour of higher quality OOs, EVOO, is usually characterised by a pleasant balanced flavour of green and fruity sensory characteristics and being free of defects. However, the sensory assessment methodology is slow, expensive and not free of error – sometimes more than 25 % of samples are judged to have been misclassified, causing serious economic loss for both producers and retailers [2]. As such, the sensorial analysis carried out by non-official panels is being questioned by numerous sectors.

For all these reasons, several analytical methods have been under study in recent years to differentiate the three categories of OOs and to guarantee their authenticity. Based on our experience, we can confirm that there are no chemical standards to calibrate the instrumental methods. At this point it is very important to mention that only the OO samples tested by two official tasting panels whose results match are those that ideally should be used to calibrate the instrumental techniques needed to evaluate the final category of OOs. If this procedure is not followed, the error of sensorial analysis will be transferred to the analytical methodologies. For these reasons, notice that the results shown in this paper are not intended to prove the non-utility of the sensorial analysis. In fact, as has been mentioned, the instrumental methodologies must be calibrated with OOs labeled by official sensorial analysis. So, the analytical instruments could be seen as a screening system which allows the OOs industry to classify OOs samples with a faster tool, and only those sitting on the border of two groups (e.g. EVOO-VOO or VOO-LOO) will be tested by sensorial analysis.

Some of the developed analytical methodologies are based on information related to the taste of OOs to classify them [3-6] as, for example, information

related to polyphenols, since they are the main compounds which have an influence on bitter and spicy taste [7]. Note that in [4] and [6] only VOO/LOO and EVOO/LOO samples were employed, respectively, while recently other authors have given more weight to the volatile fraction of OOs [8-12], mainly consisting of aldehydes, esters, alcohols and ketones [13]. Only Cecchi et al. (2019) [11] solely employed EVOO and VOO samples instead of the three possible categories.

Nevertheless, most of the studies published addressing the quality authentication of OOs have not combined the use of two or more techniques to imitate the procedure followed by a panelist. Note that the expert panels classify a sample using both the flavour components perceived in the mouth and the aroma compounds in the nose. Until now, to the best of our knowledge, only Borrás et al. [14] have combined the data of three techniques, headspace-mass spectrometry (HS-MS), mid-infrared spectroscopy (MIR) and UV–visible spectrophotometry (UV–vis), to classify OO samples, although the group of samples employed was not balanced by categories. Recently, one company searched the potential of electrospray ionisation (ESI)-differential mobility analysis (DMA)-mass spectrometry (MS) for the analysis of OOs based on the information obtained from the chemical fingerprint (nontargeted analyses) [15]. Since ESI is a soft and wide-ranging ionisation technique, volatile and non-volatile compounds present in the sample (compounds perceived by the panel test in the nose and mouth, respectively) were used to differentiate OO categories according to their quality (EVOO, VOO, and LOO). Promising results were obtained but the cost of the technology is not competitive to be affordable for a routine lab.

In this work, the main objective evaluated has been whether the combination of the results of two orthogonal instrumental techniques which provide complementary information about sensorial description may be more suitable to differentiate OOs as the tasters do through data fusion. Firstly, two different separation techniques which evaluate compounds related to OOs taste,

capillary electrophoresis with ultraviolet detector (CE-UV) and high-performance liquid chromatography with UV (HPLC-UV) or with fluorescence detector (HPLC-FLD) were explored. And one technique which allows the separation and detection of volatile compounds detected in the nose by the panelist - gas chromatography coupled with ion mobility spectrometry (GC-IMS) - was used with the same set of OOs samples. Later, the instrumental data were treated using principal component analysis (PCA), linear discriminant analysis (LDA) and k-nearest neighbors method (kNN), to end up with individual chemometric models and percentages of success in classification and validation of samples according to their quality as EVOO, VOO or LOO. Thus, GC-IMS to determine compounds related to aroma and CE-UV to determine compounds related to taste were found to be the best techniques together with chemometric data treatment to demonstrate the potential of using data fusion of both techniques to classify OOs.

2. Materials and methods

2.1. Chemicals and reagents

All the reagents used in this work were of analytical grade and solvents were HPLC-grade.

For CE-UV analysis, sodium tetraborate and sodium hydroxide were obtained from Sigma-Aldrich (St. Louis, MO, USA). Solutions of 0.1 M NaOH and 45 mM of sodium tetraborate buffer at pH 9.0 were used to condition the capillary. These reagents were filtered through a Nylon membrane of 0.45 μm pore size (Analysis Vinicos S.L, San Juan, Spain) before analysis.

Methanol (Scharlau, Gato Perez, Spain) and formic acid (Sigma-Aldrich, St. Louis, MO, USA) were employed for the HPLC mobile phase and this methanol was also employed for the supercritical fluid extraction (SFE) procedure. Hexane from Sigma-Aldrich (St. Louis, MO, USA) was used to carry out liquid-liquid extraction (LLE) of samples.

The analytical standards used to characterise CE-UV and HPLC-UV or HPLC-FLD methods were also supplied by Sigma-Aldrich (St. Louis, MO, USA): 1-naphthol (internal standard (IS) for HPLC methods), benzoic acid (IS for CE-UV analysis), 3,4-dihydroxyphenylacetic acid, tyrosol, syringic acid, vanillic acid, p-hydroxybenzoic acid, sinapic acid, ferulic acid, p-coumaric acid, o-coumaric acid, gentisic acid and trans-cinnamic acid. Stock solutions of 1 mg mL^{-1} were prepared using a mixture of purified water/methanol (1:1 v/v).

Nitrogen gas with a purity of 5.0 was supplied by Abelló Linde (Barcelona, Spain) to be used as drift and sample gas for the GC-IMS device.

Ultrapure CO_2 (99.9%) in cylinder with a dip tube was supplied by *Carburos Metálicos* (Barcelona, Spain) for SFE device.

Ultrapure water (18.2 MΩ cm^{-1}, Milli–Q Plus system, Millipore Bedford, MA, USA) was used throughout the work.

2.2. Olive oil samples

A total of 120 OO samples (40 EVOO, 40 VOO and 40 LOO) were supplied by Sovena group S.A. (Brenes, Spain) belonging to the 2018-2019 harvest. The samples were stored in bottles at - 4 °C, the analyses were carried out within about a month and at the same period (between June and September 2019) with all the devices used in this work.

2.3. Instrumentation and software

SFE extraction was carried out using Jasco SFE system (Tokyo, Japan). The device included several modules, such as one pump model PU-2080 CO_2 Plus used to supply the CO_2, one pump model PU-2080 Plus used to provide the modifier, a backpressure regulator (BPR) model BP-2080 Plus and a CO-2060

Plus oven as extraction chamber into which was placed a stainless-steel extraction cell of 5 mL (*Análisis Vínicos, Tomelloso*, Spain).

A Beckmann P/ACE MDQ Capillary Electrophoresis System (Palo Alto, CA, USA), equipped with a diode array detector and a computer with the Beckmann 32 Karat software, was employed to obtain the electrophoretic fingerprints.

HPLC-UV and FLD analysis was carried out using an Agilent 1100 Series HPLC instrument (Agilent Technologies, Waldbronn, Germany) equipped with a quaternary pump (G1311A) operating at room temperature. The solvents were degassed using an on-line membrane system (G1379A) and samples were manually injected using a Model 7125-075 Rheodyne injection valve (Rheodyne, Berkeley, CA, USA). Two detection modules, a G1315B diode-array detector and an Agilent FLD (G1321A), were connected in series. Agilent ChemStation software (Rev. A 10.02) to record the chromatograms was used.

GC-IMS analysis was performed on a commercial instrument (FlavourSpec®) from G.A.S. (Dortmund, Germany) coupled with an automatic sampler unit (CTC-PAL, CTC Analytics AG, Zwingen, Switzerland) as a sample introduction system. The sampler unit included an oven for HS vials, a tray with capacity for 32 vials and a 2.5 mL Hamilton syringe furnished with a 51 mm needle which enabled direct injection of the HS into the GC-IMS equipment. A non-polar column (94% methyl-5% phenyl- 1% vinylsilicone) with 30 m of length, an internal diameter of 0.32 mm and 0.25 μm of film thickness (SE-54-CB of CS-Chromatographie Service GmbH, Dürem, Germany) was used for GC separation. IMS device was equipped with a tritium radioactive ionisation source (6.5 KeV) and a drift tube of 5 cm long (Gesellschaft für Analytische Sensorsysteme mbH, G.A.S., Dortmund, Germany) to provide a dual separation. Two-dimensional data were acquired and exported as excel files using LAV software (version 2.0.0) from G.A.S. (Dortmund, Germany).

In addition, a pH-meter with a resolution of ±0.01 pH unit (Crison model pH 2000, Barcelona, Spain) was employed to prepare the CE separation buffer,

and a vortex from Heidolph (Schwabach, Germany) was used during the LLE extraction procedure.

Data processing was carried out using MATLAB software (The Mathworks Inc., Natick, MA, USA, 2007) and PLS Toolbox 5.5 (Eigenvector Research, Inc., Manson, WA, USA).

2.4. Analytical methods

2.4.1. Analysis of polar fraction

The extraction of polar fraction from 1 g of OO samples was based on LLE, which was described in detail in [3]. Basically, the extraction was carried out in 5 mL Eppendorf tube by addition of 1 mL of hexane to separate fats, 900 μL of a mixture of methanol/water (1:1, v/v) as extraction solvent and 50 μL of each of the ISs, 1-naphthol (400 μg mL^{-1}) and benzoic acid (400 μg mL^{-1}) in methanol/water (1:1 v/v). After mixing by hand (10 times), by vortexing (30 s) and again by hand (10 times), the separation of the phases, oil/hexane and methanol/water, was completed at 15 min. Then the upper phase was removed with a micropipette and discarded, while the methanol/water phase, 300 μL approx., was placed into a vial with insert to carry out the CE analysis or into a glass vial to develop the HPLC measurements.

At the same time, SFE was tested to extract the samples prior to their analysis by CE-UV. The SFE procedure had to be previously optimised using an experimental design (a Box-Behnken design, involving 15 run). Three factors were considered, and they were studied in the following ranges: percentage of methanol (5-20 %) used as modifier of polarity of supercritical CO_2, time of extraction (15-45 min) and pressure (10-20 MPa). The optimum conditions were found at 5% of methanol, 30 min as time of extraction and 20 MPa as working pressure. A volume of 300 μL of oil fortified with ferulic and vanillic acid as ISs at 400 mg L^{-1} was placed over a filter paper. The filter paper was placed into a

sample vessel to carry out the extraction procedure. The extract was collected in a 500 μL methanol/water (1:1, v/v) liquid trap.

The CE-UV method was previously optimised in our research group [3]. Separations were performed on a fused-silica capillary (Beckman Coulter) of 75 μm inner diameter, a total length of 50.2 cm and an effective separation length of 40 cm. Measurements were carried out at 20 kV and 25 ºC. UV data were recorded at 200 nm.

Chromatographic separation was carried out in reversed-phase mode at room temperature by using a Zorbax Bonus-RP column (150 × 4.6 mm i.d., 5 μm particle size) provided by Agilent Technologies. Formic acid (0.25 %, v/v) aqueous solution (solvent A) and methanol (solvent B) were used as mobile phase to establish the gradient elution as follows: 0–2 min at 10% B (initial conditions); 2–22 min linear gradient from 10% B to 90% B; 22–24 min at 90% B; 24–26 min back to initial conditions at 10% B; and 26–30 min at 10% B for column equilibration. A mobile phase flow-rate of 1 mL min^{-1} was employed and 20 μL of liquid-liquid extracts were injected manually. UV detection at 200 nm was performed. Also, FLD detection operated at 280 nm and 350 nm as excitation and emission wavelengths, respectively.

2.4.2. Analysis of volatile fraction

The GC-IMS method used was previously developed and updated for our research group [9]. Summarising, 1 g of sample was heated 60 °C for 8 min to generate the headspace. The heating temperature of the injector, GC column and drift tube were fixed at 80, 55 and 55 °C, respectively. At the beginning of the measurement, sample and drift flows were 5 mL min^{-1} and 250 mL min^{-1}, respectively. The carrier gas flow was increased up to 25 mL min^{-1} during the last 17 min. The electric field of the IMS module was 400 V cm^{-1}.

2.5. Chemometric data treatment

Different data pre-treatments were carried out with the data obtained through the different instruments employed throughout this study. Later, the pre-treated data were submitted to the same chemometric tools specified below.

For the techniques employed to analyse the polar extracts of OOs, HPLC-UV or FLD and CE-UV, the whole chromatographic or electrophoretic profiles, respectively, were used as input data (one-dimensional data). With regards to preprocessing of data, CE raw data were pre-treated as detailed in Arroyo-Manzanares et al. [3]. This procedure was based on electropherogram alignment, using the ISs 1-naphthol and benzoic acid to carry it out, and baseline correction, resulting in a final feature vector of 1×5703 for each sample. Similarly, a baseline correction was carried out with raw HPLC data. The final vectors were 1×2402 and 1×2773 for each sample for HPLC-UV and HPLC-FLD, respectively.

However, for GC-IMS, unknown markers (one-dimension data) selected from the global topographic map (two-dimension data) were the input data. This strategy was used in a previous work of our research group [9] instead of using the global fingerprint of each sample. The pre-treatment of GC-IMS data was specified in Contreras et al. [9] for markers chemometric approach. As a result, a final vector with dimensions of 1×113 was obtained for each sample.

Once the data were pre-treated, the final dataset matrices for each technique were built separately, including the vectors of the total number of OOs analysed (120 samples). These matrices were then split into two subsets: 80 % to build chemometric models (training set) and 20 % for their further validation (validation set). This splitting procedure was repeated five times, thus avoiding results depending on a particular split. The samples were randomly included in training or validation sets but maintaining an equilibrate distribution of them by category (EVOO, VOO and LOO) into each set. Note that the same samples were selected to be included in the validation sets for CE, HPLC and GC-IMS data, to

compare the conclusions at the same conditions, which consisted of success rates in both calibration and validation expressed as an average value for each technique. The chemometric models built for the classification of OOs according to their quality were based on PCA, LDA and kNN in all cases, to be able to compare between techniques as detailed in [3].

3. Results and discussion

3.1. Meta-analysis from classification of olive oil samples

A bibliographic analysis about results published for the classification of OOs as EVOO, VOO or LOO using IMS technology or CE-UV was carried out to highlight the need of further studies to find a final methodology which could be used to classify OO samples using these technologies. Only seven works [8-10, 15, 17, 18, 19] were published to address this issue with IMS instruments and only one research [3] was found related to CE-UV technology. Despite the low number of published scientific articles related to the potential of analytical methods to classify OO, the industry is already paying attention to the results provided by GC-IMS or other techniques. Since 2012, private companies, from OO sector, have subsidised (contributing with an approximate budget of 300,000 Euros) to our research group to develop a GC-IMS method which allow the classification of OO samples. More than 2000 OO samples have already been analysed. The currently proposed methodologies must be fine-tuned to satisfy the demand of the sector before an analytical method can be transferred to routine laboratories.

Table 1 shows the results obtained analysing the fingerprinting information of volatile fraction of OOs using IMS technology. Briefly, modifications to the pre-separation step prior IMS analysis were carried out in these research papers. Firstly, a multi-capillary column (MCC) was used prior to IMS to improve the resolution power obtaining promising results [17]. Later, results provided when using MCC column were compared with the one obtained using a capillary column (GC) showing the enhancement of the latter in a 4 % of

validation success in classification, with a final percentage of validation success in classification of 83 % [18]. A great modification was carried out in [8] where a longer GC column included in a ramp temperature oven was employed which allowed a more exhaustive separation of compound prior to IMS. A 94 % of validation success in classification was obtained in that case for 90 samples analysed. Later, a similar ramped temperature instrument was used to check the possibility of reducing the length of the GC column until 25 m and exploring different chemometric methods [10]. A value of 88 % of success in validation was achieved by using the data of 94 samples. In summary, an average of 88 % (± 5 %) was the percentage of success in validation obtained in the research using an average of more than 80 samples to test each analytical method. Notice that all samples employed in each of these research papers were from a single harvest and all OO samples were tested once in the same panel test. Meanwhile, a total of 701 samples from two harvests were analysed in [9] and when using their fingerprinting, around 79 % of samples were correctly classified in validation. Probably the high number of samples used, and the fact that they belonged to different harvests, influenced these results. It is also important to consider that the 701 samples were not tasted by the same panel and this could have been the reason why the % of validation success decreased compared to previous works. Lastly, in 2020 [19], a 30 m GC-IMS device without a ramp temperature oven similar to the employed ones in previous works [9, 18] was explored to classify 198 commercial OOs. In this case, a semi-targeted approach was employed by focusing on 15 volatile compounds instead of the whole fingerprinting information. The average percentages of correctly classified samples obtained from the two models were satisfactory, namely 77% of validation success.

Anyway, the utility of IMS technology to classify OOs using the fingerprinting of volatile fraction has been demonstrated even though this technology was not initially developed for food analyses. However, an exponential growth of studies which employ IMS in food matrices is currently happening [20]. Since 2017, a project (*Innolivar)* [21] subsidised with public and private funds (more than 800,000 Euros) is using all the experience summarised

in Table 1 to build a new prototype based on IMS technology to classify OOs samples with a high percentage of success.

Table 1. Summary of the results obtained for works related to the fingerprinting information of volatile fraction of OOs using GC-IMS technology.

Number of samples	Pre-separation	% Validation	References
98	MCC column	87	17
55	30 m Capillary column (GC)	83	18
90	60 m GC column and ramped temperature oven	94	8
94	25 m GC column and ramped temperature oven	88	10
701*	30 m GC column	79	9

* Samples from two harvest were employed in this work while the remaining publications used samples from a single harvest.

Separately, the use of the non-volatile or polar fraction information of OOs has been less explored to classify them as EVOO, VOO or LOO. Only two publications were carried out; one using CE-UV to analyse 130 samples [3] and another using an ESI-DMA-MS to measure 30 samples [15]. Both techniques need a previous extraction step based on liquid-liquid extraction to isolate the polar fraction of OOs. These methodologies were very promising according to validation percentages (91 and 89 %, respectively).

In view of all these results, the need to study volatile and non-volatile data of the same samples was detected, in the same period, as an expert panel test does to categorise the OO samples. It was decided to carry out the analysis of a representative group of samples (120 samples) using the most simple and available devices from the studied ones, whose acquisition was

affordable even for small companies. Then, the complementary techniques GC-IMS and CE-UV (instrumental specification included in section 2.3) were explored for the analysis of the same set of samples. Due to CE being a separation technique that is not used in agri-food laboratories, it was decided to test the potential of HPLC to classify OOs according to their polar fraction information.

3.2. Authentication of OOs based on their taste fraction: HPLC vs. CE

The majority fraction of OOs is composed mainly of triglycerides. However, the minor components are the most relevant to differentiate OOs since they influence stability and sensory quality. The most prominent compounds from minor fraction of OOs are polyphenolic compounds, with antioxidant properties, and volatile compounds, which influence the taste and aroma of oils, respectively. For such a purpose, they should be extracted or separated from the matrix of the sample to be detected.

Additionally, OO samples are liquid with a high viscosity and complexity and the direct analysis is not possible using chromatographic techniques. For these reasons, a previous extraction step is necessary.

3.2.1. Exploration of the polar fraction extraction of OO samples

A great number of procedures [16] for the isolation of the polar phenolic fraction of OOs have been developed utilising two basic extraction techniques, LLE or solid phase extraction (SPE). In this study, SPE was discarded as an extraction technique compared to LLE since poorer profiles, which included signals very similar to the background, were recorded for the former through the preliminary exploration of the profiles of both extraction techniques with CE-UV. In this work, SFE was studied as extraction technique of OOs compared to LLE. The untargeted CE-UV profiles found after SFE and LLE were visually acceptable

a priori (see Figure 1) since intense and multiple peaks were observed. The 120 samples selected in this study were extracted through both extraction techniques and were subsequently analysed by CE-UV. PCA-LDA-kNN chemometric models were built and both extraction techniques showed good classification average results of the samples, about 98.9 - 100 % for LLE and 96.6 - 98.9 % for SFE. However, SFE provided low validation average percentages around 59 % while LLE maintained good results (77.3 - 85.5 %). In view of these results, LLE was the extraction techniques selected prior to the analysis of the polar fraction of the OO samples by HPLC or CE.

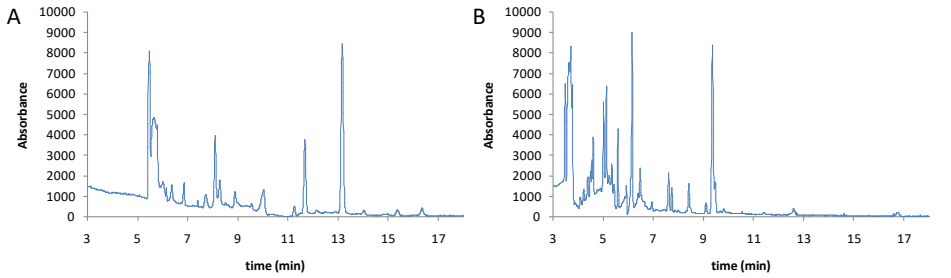

Figure 1. Electropherograms of an olive oil extract obtained through A) SFE and B) LLE.

3.2.2. Selection of the analytical technique for the determination of the polar fraction

Once the extraction technique was selected, two separation techniques, CE and HPLC, were explored to separate the polar extracted compounds from OOs. Good classification results of OOs have already been obtained with the CE-UV method [3]. Since CE is not a popular technique in OOs laboratories, a comparison of the results of this technique with the one provided by HPLC was carried out. UV detector was employed for the detection of the separated compounds for both separation techniques, taking advantage of the fact that any

routine laboratory can use it to classify the samples without requiring highly qualified personnel. FLD data were also acquired after HPLC separation to explore these profiles.

The optimisation procedure of the HPLC method (with UV and FLD detectors) was included in section 1 of supplementary information document. Under optimised conditions, the CE and HPLC fingerprints for both the mixture of polyphenols and some representative OO extracts were studied. Firstly, Figure 2A displays the electropherogram of eleven standards of polyphenols. The identification of individual polyphenols in OO samples (see Figure 2B) was not successfully performed due to the limited powerful of the UV detector to carry out an unequivocal identification of them. However, it is worth noticing that the classification of OOs was carried out using all data found in the electropherogram and not using the information of some specific compounds. In general, the electropherograms of the majority of OO samples presented analogous shape by visual exploration and, for this reason, the use of a chemometric approach is compulsory.

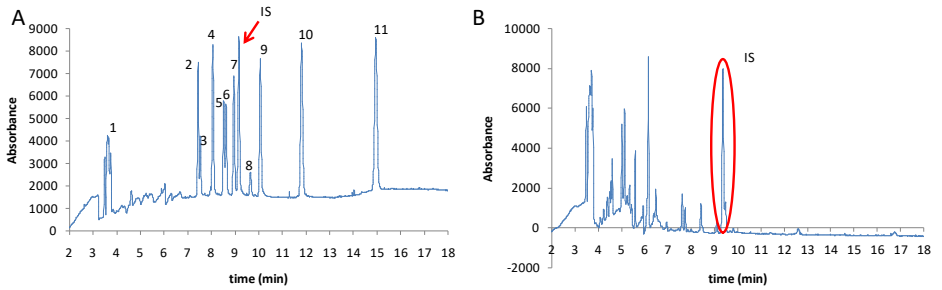

Figure 2. Electropherograms of A) a mixture of 15 mg·L^{-1} of polyphenols and 20 mg·L^{-1} of IS and B) an olive oil extract with IS added. 1. Tyrosol; 2. Trans-cinnamic acid; 3. Sinapic acid; 4. Syringic acid; 5. Gentisic acid; 6. Ferulic acid; 7. o-coumaric acid; 8. p-coumaric acid; 9. Vanillic acid; 10. p-hydroxybenzoic acid and 11. 3,4-dihydroxyphenylacetic acid. IS was bezoic acid.

Secondly, the metabolomic fingerprints for the mixture of polyphenols obtained with HPLC-UV (Figure 3A) and HPLC-FLD (Figure 3B) were also studied. It should be noted that not all polyphenols were fluorescent, as seen in Figure 3B, where only seven polyphenols were detected. The raw chromatograms of an extract of OOs sample were represented in Figure 3C (for UV data) and 3D (for FL data). As in the CE method, the identification of the peaks found in the OO samples was not possible, but that was not necessary for the purpose of this work.

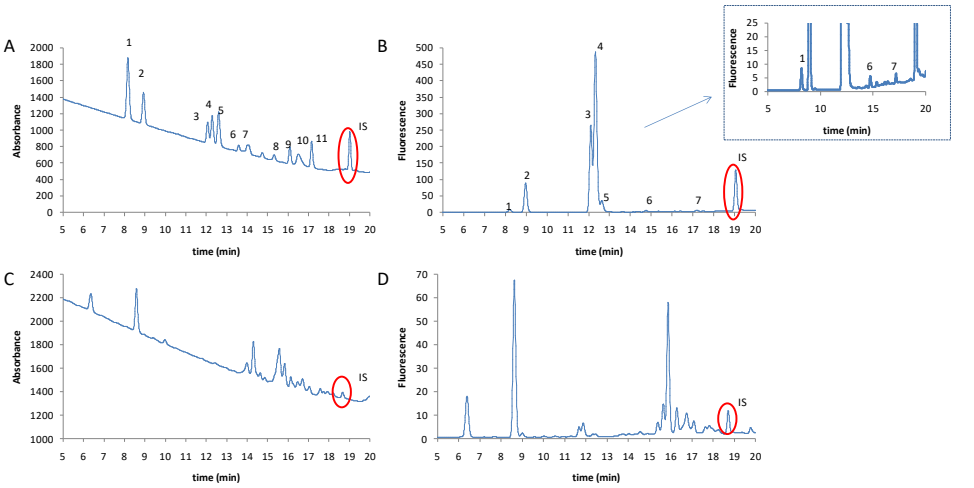

Figure 3. Chromatograms of a mixture of polyphenols at A) 25 mg·L^{-1} with UV and B) 30 mg·L^{-1} with FL detectors, both with 20 mg·L^{-1} of IS. An olive oil extract using C) UV and D) FL detectors with IS added. For UV: 1. 3,4-dihydroxyphenylacetic acid, 2. Tyrosol, 3. Syringic acid, 4. Vanillic acid, 5. p-hydroxybenzoic acid, 6. Sinapic acid, 7. Ferulic acid, 8. p-coumaric acid, 9. o-coumaric acid, 10. Gentisic acid and 11. Trans-cinnamic acid; For FL: 1. 3,4-dihydroxyphenylacetic acid, 2. Tyrosol, 3. Syringic acid, 4. Vanillic acid, 5. p-hydroxybenzoic acid, 6. p-coumaric acid, and 7. Trans-cinnamic acid. IS was 1-naphthol.

Moreover, the validation of CE-UV and HPLC methodologies was carried out using linearity limits of detection (LODs) and limits of quantification (LOQs) of the selected polyphenols (see Table 2), and the precision which was studied using OO extracts. The validation procedure is described in detail in section 2 of the supplementary information document. Consequently, it was found that the LOQs for the 11 polyphenols investigated ranged between 0.7 and 4.5 mg L^{-1} for CE-UV, 2.1 and 27 mg L^{-1} for HPLC-UV and finally 0.4 and 55 mg L^{-1} for HPLC-FLD. When the CE and HPLC results were compared, the LODs and LOQs obtained for the mixture of polyphenols using UV detector with CE and HPLC separation techniques (see Table 2) were lower for CE, except for 3,4-dihydroxyphenylacetic. While for HPLC-FLD, in comparison with HPLC-UV, LODs and LOQs were lower for tyrosol, syringic acid and vanillic acid but higher for 3,4-dihydroxyphenylacetic, p-hydroxybenzoic acid, p-coumaric acid and trans-cinnamic acid. These values, together with the chemometric analyses shown later in section 3.2.3, justify the selection of CE over HPLC to classify OOs. With respect to the precision, in all the cases, acceptable RSD were obtained for intraday precision (< 5.2 % for peak area and < 1.3 % for migration time) and interday precision (< 6.7 % for peak area and < 1.3 % for migration time) with CE-UV. Also, for HPLC, UV and FL measurements, suitable results expressed as RSD were obtained. The values were slightly better for FLD (intraday precision: < 5.3 % for peak area and < 0.9 % for retention time; interday precision: < 11.0 % for peak area and < 1.0 % for retention time) than for UV (intraday precision: < 9.5 % for peak area and < 1.0 % for retention time; interday precision: < 13.0 % for peak area and < 1.0 % for retention time). Comparing the CE and HPLC results, the RSD values assert that both proposed methodologies were precise. In general, the RSD values obtained for time (migration or retention) were slightly higher for CE than for HPLC but acceptable since RSD < 1.3 % was obtained in all cases. Regarding the RSD values for peak areas, the opposite occurs. In any case, the differences related to precision were not significant between CE and HPLC separations. In summary, based on these results, both separation techniques would be suitable to analyse OOs.

Table 2. Statistical and quality parameters obtained in the polyphenol calibration using CE-UV, HPLC-UV and HPLC-FLD.

CE-UV						
Polyphenols	**Intercept**	**Slope**	**R^2**	**Linear range**	**LOD***	**LOQ***
3,4-dihydroxyphenylacetic acid	- 1382.3	779.4	0.984	2.6-75	0.8	2.6
Tyrosol	- 195.6	112.7	0.993	1.2-75	0.4	1.2
Syringic acid	- 970.4	336.4	0.985	4.5-75	1.4	4.5
Vanillic acid	- 1398.1	501.9	0.989	2.8-75	0.8	2.8
p-hydroxybenzoic acid	260.8	752.6	0.985	1.8-75	0.6	1.8
Sinapic acid	- 664.8	191.5	0.983	0.7-75	0.2	0.7
Ferulic acid	- 337.0	249.5	0.978	3.7-75	1.1	3.7
p-coumaric acid	- 683.0	359.0	0.989	3.5-75	1.1	3.5
o-coumaric acid	- 164.0	331.9	0.978	2.4-75	0.7	2.4
Gentisic acid	- 2165.0	302.1	0.996	3.8-75	1.1	3.8
Trans-cinnamic acid	- 569.7	312.8	0.990	4.1-75	1.2	4.1
HPLC-UV						
Polyphenols	**Intercept**	**Slope**	**R^2**	**Linear range**	**LOD***	**LOQ***
3,4-dihydroxyphenylacetic acid	44.78	263.0	0.998	2.1-40	0.6	2.1
Tyrosol	189.1	126.8	0.997	3.9-70	1.2	3.9
Syringic acid	- 45.06	78.52	0.999	7.9-70	2.4	7.9
Vanillic acid	- 61.15	108.7	0.999	6.0-70	1.8	6.0
p-hydroxybenzoic acid	16.46	132.7	0.999	4.3-70	1.3	4.3
Sinapic acid	- 148.5	30.84	0.995	27.2-70	8.2	27.2
Ferulic acid	- 133.9	57.24	0.993	15.0-70	4.5	15.0
p-coumaric acid	1.893	23.41	0.998	23.1-70	6.9	23.1
o-coumaric acid	- 34.74	63.81	0.999	9.1-70	2.7	9.1
Gentisic acid	- 194.7	92.12	0.998	7.2-70	2.2	7.2
Trans-cinnamic acid	- 31.18	96.46	0.999	6.1-70	1.8	6.1
HPLC-FLD						
Polyphenols	**Intercept**	**Slope**	**R^2**	**Linear range**	**LOD***	**LOQ***
3,4-dihydroxyphenylacetic acid	- 2.181	2.711	0.999	28.9-70	8.7	28.9
Tyrosol	- 1.833	28.71	0.999	2.6-70	0.8	2.6
Syringic acid	- 14.08	77.80	0.999	1-35	0.3	1.0
Vanillic acid	8.759	165.0	0.999	1-35	0.1	0.4
p-hydroxybenzoic acid	- 5.378	12.47	0.999	6.2-35	1.9	6.2
p-coumaric acid	0.740	1.369	0.996	48.5-70	14.6	48.5
Trans-cinnamic acid	- 2.999	1.124	0.999	55.3-70	16.6	55.3

* LOD and LOQ were expressed as mg L^{-1}

3.2.3. Olive oils classification using chemometrics: CE vs. HPLC

Once the raw data from liquid-liquid extracts of OO samples were collected using CE-UV, HPLC-UV and HPLC-FLD, raw data pre-processed was needed. The pre-processed electropherograms (alignment and baseline correction) or chromatograms (baseline correction) were used to obtain chemometric models for each data set from each instrumental technique for OOs classification.

The number of samples needed to calibrate the instrumental methodologies is an important issue that is not always considered. Based on the experience of our research group, more than 200 samples should be employed to achieve robust and representative chemometric models for OOs differentiation. These samples should be classified by at least two official sensorial analyses to avoid transferring the error from the panel test to the instrumental analysis. We have also demonstrated that the models are more exhaustive if samples from different harvests are included [9]. However, it is not always possible to get this number of samples equilibrated by categories and properly tasted by official panels. For this reason, in this work, the potential of data fusion was demonstrated with a group of only 120 samples. The results, shown here, do not intend to provide definitive classification and validation percentages. They should only be used as tentative results to demonstrate which technique is more appropriate to be included in the analytical platform.

With respect to chemometric models, two types were built for each data set, specifically, one binary model which differentiated between non-defective (EVOO) and defective (VOO and LOO) samples and another one which allowed differentiation between non-edible (LOO) and edible (EVOO and VOO) samples. Then, in simplified terms, PCA was applied to the spectra of training set of samples as first step to build the chemometric models to reduce dimensionality and extract the most relevant information. Later, LDA was used on the principal components to determine the boundaries of the clustering for the two quality groups of samples. At the end, as a classification method, kNN was applied to obtain the percentages of success in classification and validation.

As result of this procedure, it could first be concluded that when CE-UV and HPLC-UV chemometric models were compared, significantly better validation results were found for CE-UV data (until 85.5 % for EVOO-non EVOO model) with respect to HPLC-UV for which this result was almost a 20 % lower (see Table 3). In view of the results, the separation of chemical compounds from the liquid-liquid polar fraction of OOs carried out with CE was more valuable to differentiate OOs according to their quality compared with the one obtained by HPLC-UV. Additionally, RSD values of classification and validation average percentages were lower for CE-UV since more accurate results were also achieved with this device (see Table 3).

Table 3. Classification (or training) and validation average percentages of the models built for the same sets of OOs samples analysed by LLE-CE-UV, LLE-HPLC-UV, LLE-HPLC-FLD and HS-GC-IMS.

Techniques	**Models**	**% Average percentages of success**			
		Training		Validation	
		average	RSD*	average	RSD*
LLE-CE-UV	EVOO/non EVOO	99.6	0.6	85.5	8.7
	LOO/non LOO	99.8	0.5	77.3	5.9
LLE-HPLC-UV	EVOO/non-EVOO	93.2	1.5	66.4	15.8
	LOO/non-LOO	88.9	4.0	65.5	17.4
LLE-HPLC-FLD	EVOO/non-EVOO	94.1	1.8	66.4	20.9
	LOO/non-LOO	95.0	2.5	65.5	14.4
HS-GC-IMS	EVOO/non-EVOO	100.0	0.0	86.7	5.3
	LOO/non-LOO	98.1	1.1	71.7	13.2

* RSD values were expressed as %.

These results were graphically supported in the PCA-LDA plots of chemometric models, even before comparing success rates. As shown in Figure 4 for EVOO/non EVOO models as an example, grouping of EVOO and non-EVOO

samples was detected for CE-UV data but certainly not in the case of HPLC-UV training dataset.

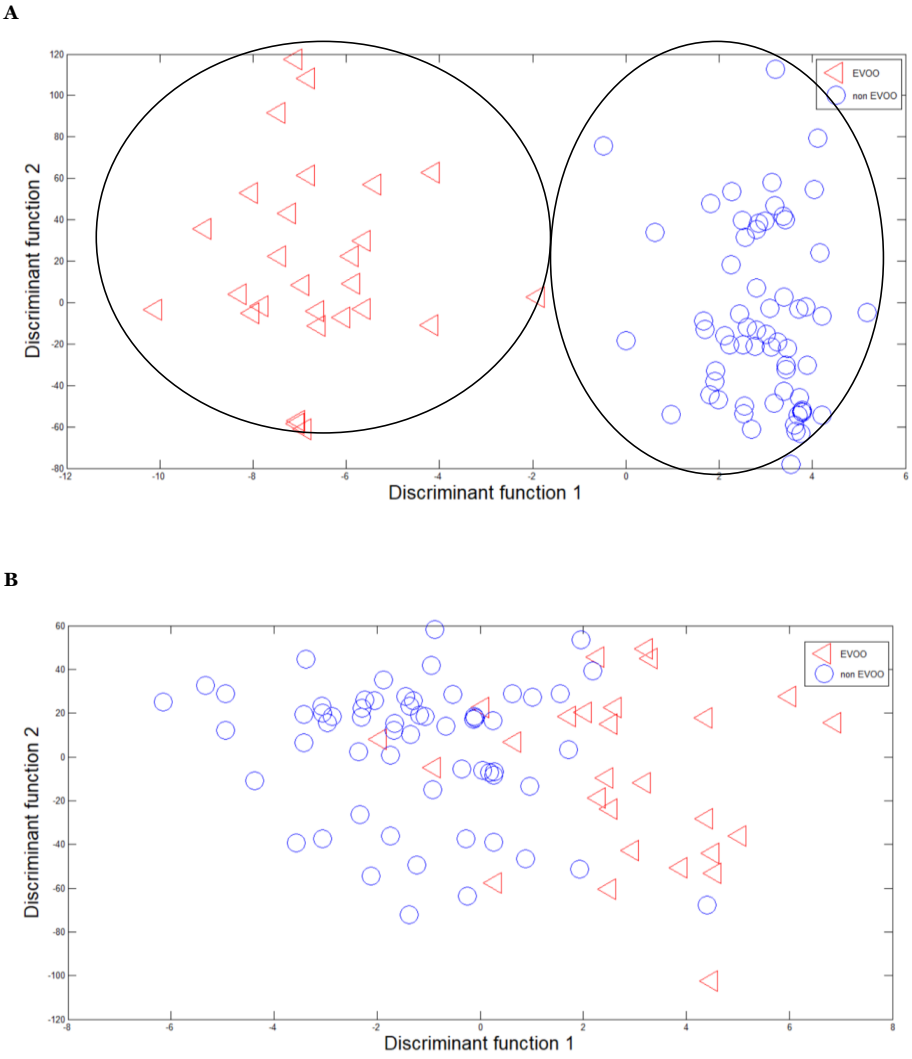

Figure 4. PCA-LDA plots for the same sets of training samples obtained with A) CE-UV and B) HPLC-UV data corresponding to EVOO/non EVOO models.

Furthermore, the possibility of improving the results obtained with HPLC separation by using fluorescence analytical signals instead of UV data was explored. However, the validation average percentages of success obtained were the same as for HPLC-UV although slightly better classification average percentages were reported for FLD. In any case, these results did not exceed those obtained by CE-UV (see Table 3).

Based on these results, CE-UV was chosen as the most suitable instrument to be included in the analytical platform proposed in this work to classify blind OO samples according to their polar fraction composition.

3.3. Authentication of OOs based on aroma fraction

The same set of OOs analysed with CE and HPLC was also analysed to classify them depending on their quality in EVOO, VOO or LOO using their volatile fraction. Based on the wide previous experience of our research group [8, 9, 17, 18], GC-IMS was selected as a suitable instrument to achieve this goal, using HS as sample introduction system.

Binary models were built for the pre-treated GC-IMS data, unknown markers (one-dimension data) selected from the global topographic map as explained in detail in Contreras et al. [9], and the results are summarised in Table 3. Note that validation average percentages between 71.7- 86.7 % were reported for volatile data obtained through GC-IMS (Table 3). As for the rest of the techniques used in this work, the best results were obtained to differentiate EVOO samples from non-EVOO. These results seemed logical since both groups of samples included in these types of models were more different: one group included samples with defects (non-EVOO group) and the other group without defects (EVOO group). However, for LOO-non LOO binary model, one group of samples had defects (LOO group) but the non-LOO group was integrated for samples of the EVOO (free from defects) and VOO categories (defective samples).

For this reason, fixing the barrier between groups should be more complex for this binary group as reflected in the percentages.

3.4. Comparison of OOs classification results of CE-UV and GC-IMS as individual orthogonal techniques

When validation average rates to classify OOs for individual data blocks for the selected instruments (CE-UV and GC-IMS) were compared, an improvement of 5.6 % as maximum was obtained using CE-UV. Conversely, for the least demanding model, EVOO-non EVOO binary model, the results shown by both techniques were practically the same. Based only on success rates, CE-UV may be the preferred option, but it should be considered, for example, that no sample preparation and no solvents were used in the analysis carried out by GC-IMS, which made it a more attractive technique for a routine laboratory in comparison with CE-UV. In addition, it was found that not all blind samples from the validation sets were classified in the same group (EVOO, VOO or LOO) by both techniques. Therefore, we thought that the conclusions drawn by CE-UV and GC-IMS should be considered to obtain the final category of an OO sample since, in the sensory panel, the final category is assigned using the information of the compounds detected in the mouth and nose, as has been done using the analytical platform which combine two orthogonal techniques.

3.5. High-level data fusion of CE-UV and GC-IMS information of OOs

The potential of the synergy between the two technologies selected as the best, CE-UV and GC-IMS, for testing OOs authenticity and quality through analysing their flavour and aroma respectively was researched as part of an analytical platform suitable for classifying OOs.

Different data fusion strategies have been described in the bibliography, called low-level, mid-level and high-level data fusion [22]. In order to explore the most suitable approach for data fusion the characteristic of final data of GC-IMS and CE-UV were studied. Firstly, the intensities of 113 markers were selected (one-dimension data) from the large GC-IMS topographic map (two-dimension data) of each analysed sample to build the chemometric models. This means that a 1×113 vector was obtained for each sample as input data. Moreover, the electropherograms (one-dimension data) registered for CE-UV provided vectors 50 times larger than those obtained by GC-IMS for each sample and so the significantly larger CE-UV data set would have been dominant if the data blocks had been fused directly (low-level data fusion). Therefore, it was decided to carry out a high-level data fusion based on estimating the specific class of the samples according to the models of each individual technique and later these results were combined to provide an updated joint class for each sample.

The classification results of OO samples, belonging to the validation sets, provided for individual techniques and for high-level data fusion were included in Table 4. Note that the assigned class by tasting panels was specified as E1-E8 for EVOO, V1-V8 for VOO and L1-L8 for LOO in the first column. It is of note that after building a chemometric model for each individual technique, the category EVOO, VOO or LOO was not directly assigned to each sample by the binary models. For this reason, a combination of results of both binary models (EVOO-non EVOO and LOO-non LOO) should be carried out for having the final category of each sample.

Delving into the results included in Table 4, it shows how different categories could be assigned to the same sample if only the information of an individual technique is considered. Only if conclusions provided by complementary techniques, such as CE-UV and GC-IMS, are considered at the same time, samples with uncertain grade can be identified (marked with *** in Table 4). Then, the analyst may consider analysing these suspect samples again

by analytical techniques, sending these samples to an official sensorial panel or giving them the lower assigned category.

Notice that when fusing the conclusions of both orthogonal techniques, it was decided to assign the lowest category to the OO samples from the individual provided classes (see Table 4).

Table 4. Quality categories of OOs from validation sets assigned by chemometric models built with CE-UV and GC-IMS data and after data fusion.

Taster category	**CE-UV**			**GC-IMS**			**High-level data fusion**
	E-NE*	**L-NL***	**C****	**E-NE***	**L-NL***	**C****	
E1***	**NE**	**L**	**LOO**	E	**L**	**I***	**LOO**
E2***	E	NL	EVOO	E	**L**	**I**	**VOO**
E3***	E	NL	EVOO	**NE**	NL	**VOO**	**VOO**
E4***	**NE**	NL	**VOO**	E	NL	EVOO	**VOO**
E5	E	E	EVOO	E	E	EVOO	EVOO
E6	E	E	EVOO	E	E	EVOO	EVOO
E7	E	E	EVOO	E	E	EVOO	EVOO
E8	E	E	EVOO	E	E	EVOO	EVOO
V1***	NE	**L**	**LOO**	NE	NL	VOO	**LOO**
V2***	NE	NL	VOO	NE	**L**	**LOO**	**LOO**
V3***	NE	NL	VOO	NE	**L**	**LOO**	**LOO**
V4***	NE	**L**	**LOO**	**E**	NL	**EVOO**	**LOO**
V5***	NE	**L**	**LOO**	NE	NL	VOO	**LOO**
V6	NE	NL	VOO	NE	NL	VOO	VOO
V7	NE	NL	VOO	NE	NL	VOO	VOO
V8	NE	NL	VOO	NE	NL	VOO	VOO
L1***	NE	L	LOO	**E**	**NL**	**EVOO**	LOO
L2***	NE	L	LOO	NE	**NL**	**VOO**	LOO
L3	NE	**NL**	**VOO**	NE	**NL**	**VOO**	**VOO**
L4***	NE	**NL**	**VOO**	NE	L	LOO	LOO
L5***	NE	L	LOO	NE	**NL**	**VOO**	LOO
L6	NE	L	LOO	NE	L	LOO	LOO
L7	NE	L	LOO	NE	L	LOO	LOO
L8	NE	L	LOO	NE	L	LOO	LOO

*The meanings of some abbreviations are:

E-NE: EVOO-non EVOO

L-NL: LOO-non LOO

I: Inconclusive class, since the binary model EVOO-non EVOO says EVOO and the LOO-non LOO says LOO.

**C: Assignation of quality categories of OOs as EVOO, VOO or LOO after building binary classification models by CE-UV or GC-IMS.

*** Samples with uncertain grade when comparing their final category assigned by CE-UV and GC-IMS.

Bold letter indicates that the class assigned to a sample using chemometrics was not coincident with the category assigned by the tasting panel.

This implied that the success in the classification of high-quality samples (EVOO and VOO) after data fusion was usually less (about 20 % lower) than when only one technique is used. In order to verify if the lower category assigned by the analytical platform is correct, this OO sample should be sent to two tasting panels to verify that the results match. Furthermore, it will also be necessary to make a study of the time that an OO sample conserves the category assigned by a tasting panel, considering that OO is a living matrix and deteriorates over time, and therefore its category could decrease. This fact could be used to explain why 20 % of the blind samples shown in Table 4 were classified with a lower category than that provided initially by the panel test.

Summarising, it was found that the high-level data fusion procedure entails the improvement of having greater certainty and security in the final class assigned to the OO samples and detecting suspect samples which are sitting on the border of two groups (e.g. EVOO-VOO or VOO-LOO).

4. Conclusions

After evaluating the average results of classification and validation success obtained for a set of 120 OO samples in EVOO, VOO or LOO through techniques (CE-UV, HPLC-UV and HPLC-FLD) focused on the determination of those flavour components perceived in the mouth, we conclude that CE-UV should be selected as the best analytical technique even though this technique is not implemented in routine laboratories to the same degree as HPLC-UV or HPLC-FLD.

Furthermore, we found that GC-IMS should also be used to classify the same set of OO samples according to their volatile fraction based on the obtained results.

In fact, we recommend using an analytical platform integrating CE-UV, GC-IMS and high-level data fusion from the chemometric models of the complementary techniques to determine compounds detected in the mouth and in the nose in a similar way to what a taster does, which would reduce the work of the highly qualified tasting panels as well as supply the lack of expert panels for the OOs sensory classification.

The high-level data fusion approach allowed us to detect samples for which volatile and non-volatile information was not coincident with respect to the assigned category and only these uncertain samples should be tasted by panel test to confirm their category. Consequently, data fusion gave greater reliability to the classification provided to blind OO samples compared to the use of one individual technique.

Akcnowledgments

Financial support from Innolivar Project (Public Purchase of Innovation in its modality of Pre-Commercial Public Purchase) in accordance with the agreement between the Ministry of Science, Innovation and Universities and the University of Córdoba (Spain) and the Spanish MICINN (PGC2018-098363-B-I00) is acknowledged. This project is co-financed by 80% by FEDER funds, within the Pluriregional Operational Program of Spain 2014-2020. N.J.C. wishes to thank the Spanish Ministry of Education, Culture and Sport for award of a pre-doctoral grant. The authors also acknowledge SOVENA Group for providing the OOs samples and Rocío Rodríguez-Gómez for her collaboration on the optimisation and extraction of samples by SFE.

References

[1] Commission Implementing Regulation (EU) 2019/1604 of 27 September 2019 amending Regulation (EEC) No 2568/91 on the characteristics of olive oil and olive-residue oil and on the relevant methods of analysis, 2019, 14-48.

[2] S. Circi, D. Capitani, A. Randazzo, C. Ingallina, L. Mannina, A. Sobolev, Panel test and chemical analyses of commercial olive oils: a comparative study, Chem. Biol. Technol. Agric., 4 (2017) 18-27. https://doi.org/10.1186/s40538-017-0101-0.

[3] N. Arroyo-Manzanares, F. Gabriel, A. Carpio, L. Arce, Use of whole electrophoretic profile and chemometric tools for the differentiation of three olive oil qualities, Talanta, 197 (2019) 175-180. https://doi.org/10.1016/j.talanta.2019.01.031.

[4] A.C.A Veloso, L.M. Silva, N. Rodrigues, L.P.G. Rebello, L.G. Dias, J.A. Pereira, A.M. Peres, Perception of olive oils sensory defects using a potentiometric taste device, Talanta, 176 (2018) 610-618. https://doi.org/10.1016/j.talanta.2017.08.066.

[5] S. Slim, N. Rodrigues, L.G. Dias, A.C.A Veloso, J.A. Pereira, S. Oueslati, A.M. Peres, Application of an electronic tongue for Tunisian olive oils' classification according to olive cultivar or physicochemical parameters, Eur. Food Res. Technol., 243 (2017) 1459-1470. https://doi.org/10.1007/s00217-017-2856-8.

[6] M. Bobiano, N. Rodrigues, M. Madureira, L.G. Dias, A.C.A Veloso, J.A. Pereira, A.M. Peres, Unmasking sensory defects of olive oils flavored with Basil and Oregano using electronic tongue- chemometric tool, J. Am. Oil Chem. Soc., 96 (2019) 751-760. https://doi.org/10.1002/aocs.12249.

[7] F. Favati, N. Condelli, F. Galgano, M.C. Caruso, Extra virgin olive oil bitterness evaluation by sensory and chemical analyses, Food Chem., 139 (2013) 949-954. https://doi.org/10.1016/j.foodchem.2013.01.098.

[8] M.D.M. Contreras, N. Arroyo-Manzanares, C. Arce, L. Arce, HS-GC-IMS and chemometric data treatment for food authenticity assessment: Olive oil mapping and classification through two different devices as an example, Food Control, 98 (2019) 82-93. https://doi.org/10.1016/j.foodcont.2018.11.001.

[9] M.D.M. Contreras, N. Jurado-Campos, L. Arce, N. Arroyo-Manzanares, A robustness study of calibration models for olive oil classification: Targeted and non-targeted fingerprint approaches based on GC-IMS, Food Chem., 288 (2019) 315-324. https://doi.org/10.1016/j.foodchem.2019.02.104.

[10] N. Gerhardt, S. Schwolow, S. Rohn, P.R. Pérez-Cacho, H. Galán-Soldevilla, L. Arce, P. Weller, Quality assessment of olive oils based on temperature-ramped HS-GC-IMS and sensory evaluation: Comparison of different processing approaches by LDA, kNN, and SVM, Food Chem., 278 (2019) 720-728. https://doi.org/10.1016/j.foodchem.2018.11.095.

[11] L. Cecchi, M. Migliorini, E. Giambanelli, A. Rossetti, A. Cane, F. Melani, N.

Mulinacci, Headspace Solid-Phase Microextraction–Gas Chromatography–Mass Spectrometry Quantification of the Volatile Profile of More than 1200 Virgin Olive Oils for Supporting the Panel Test in Their Classification: Comparison of Different Chemometric Approaches, J. Agric. Food Chem., 67 (2019) 9112-9120. https://doi.org/10.1021/acs.jafc.9b03346.

[12] C. Sales, T. Portolés, L.G. Johnsen, M. Danielsen, J. Beltran, Olive oil quality classification and measurement of its organoleptic attributes by untargeted GC-MS and multivariate statistical-based approach, Food Chem. 271 (2019) 488-496. https://doi.org/10.1016/j.foodchem.2018.07.200.

[13] R. Aparicio-Ruiz, D.L. García-González, M.T. Morales, A. Lobo-Prieto, I. Romero, Comparison of two analytical methods validated for the determination of volatile compounds in virgin olive oil: GC-FID vs GC-MS, Talanta, 187 (2018) 133-141. https://doi.org/10.1016/j.talanta.2018.05.008.

[14] E. Borrás, J. Ferré, R. Boqué, M. Mestres, L. Aceña, A. Calvo, O. Busto, Olive oil sensory defects classification with data fusion of instrumental techniques and multivariate analysis (PLS-DA), Food Chem., 203 (2016) 314-322. https://doi.org/10.1016/j.foodchem.2016.02.038.

[15] M.Y. Piñero, M. Amo-González, R.D. Ballesteros, L.R. Pérez, G.F. De La Mora, L. Arce, Chemical Fingerprinting of Olive Oils by Electrospray Ionization-Differential Mobility Analysis-Mass Spectrometry: A New Alternative to Food Authenticity Testing, J. Am. Soc. Mass Spectrom. 31 (2020) 527-537. https://doi.org/10.1021/jasms.9b00006.

[16] A. Carrasco-Pancorbo, L. Cerretani, A. Bendini, A. Segura-Carretero, T. Gallina-Toschi, A. Fernández-Gutiérrez, Analytical determination of polyphenols in olive oils, J. Sep. Sci., 28 (2005) 837-858. https://doi.org/10.1002/jssc.200500032.

[17] R. Garrido-Delgado, L. Arce, M. Valcárcel, Multi-capillary column-ion mobility spectrometry: a potential screening system to differentiate virgin olive oils, Anal. Bioanal. Chem., 402 (2012) 489-498. https://doi.org/10.1007/s00216-011-5328-1.

[18] R. Garrido-Delgado, M.D.M. Dobao-Prieto, L. Arce, M. Valcárcel, Determination of volatile compounds by GC-IMS to assign the quality of virgin olive oil, Food Chem., 187 (2015) 572-579. https://doi.org/10.1016/j.foodchem.2015.04.082.

[19] E. Valli, F. Panni, E. Casadei, S. Barbieri, C. Cevoli, A. Bendini, D.L. García-González, T. Gallina Toschi, An HS-GC-IMS Method for the Quality Classification of Virgin Olive Oils as Screening Support for the Panel Test, Foods 9 (2020) 657. https://doi.org/10.3390/foods9050657.

[20] M. Hernández-Mesa, D. Ropartz, A.M. García-Campaña, Hélène Rogniaux, G. Dervilly-Pinel, B. Le Bizec, 2019. Ion Mobility Spectrometry in Food Analysis: Principles, Current Applications and Future Trends. Molecules. 24, 2706. https://doi.org/10.3390/molecules24152706.

[21] *Innolivar* project. https://innolivar.es/ (accessed 12 May 2020).

[22] E. Borràs, J. Ferré, R. Boqué, M. Mestres, L. Aceña, O. Busto, Data fusion methodologies for food and beverage authentication and quality assessment - a review, Anal. Chim. Acta, 891 (2015) 1-14. https://doi.org/10.1016/j.aca.2015.04.042.

Supplementary Information

1. Optimisation of the HPLC method

The optimisation of an HPLC separation method to distinguish OOs by analysing their polar extracts was carried out using a mixture of 11 polyphenols as a test mixture. These chemicals were selected as model compounds because they belong to the unsaponifiable fraction (water soluble part) of OOs. Also, the detected peaks from OO extracts were considered in order to tackle this issue.

The method was developed on the basis of the Farrés et al. work [1] in which HPLC-UV polyphenolic profiles were obtained to classify olive and other vegetable oils. However, the parameters related to mobile phase (composition and gradient) and detection wavelength were re-optimised for UV and FLD detectors in this work.

Firstly, the composition of the mobile phase was explored. As a result, the best separation of the selected polyphenolic mixture and for the separation of the compounds detected in the OO samples was obtained using methanol as organic solvent in mobile phase. Acetonitrile and methanol:acetonitrile (1:1) were also tested but poorer resolutions were obtained. Later, different percentages of formic acid were explored to be part of the composition of the aqueous solution of the mobile phase. When no acid was used, the intensity of the peaks for polyphenols and compounds detected in OO samples were lower than when the acid was used. At values over 0.25 % of formic acid, no improvement in intensity or resolution of peaks was observed. Therefore, 0.25 % of formic acid dissolved in water was selected as the optimum.

Moreover, the effect of the mobile phase gradient was studied. In our case, we avoided the gradual increase of methanol content, unlike the Farrés et al. work [1], at the beginning of the separation. A suitable chromatographic separation of the studied compounds was achieved with an increase in methanol

content from 10 to 90 %, in one step, over 20 min (after an isocratic step of 2 min at initial conditions), followed by an isocratic step of 2 min at 90 %.

Regarding detection parameters, three wavelengths were tested for UV measurements: 200, 250 and 280 nm. It was found that the results corresponding to the lowest scanned wavelength were more appropriate, since richer profiles were obtained for OOs extracts and more intense peaks were collected for the mixture of polyphenols. For the FLD detection, the excitation and emission wavelengths were also studied and values of 200, 250 and 280 nm were selected for the former, while 350 and 400 nm were the chosen for the latter. The optimal values, in terms of resolution and peak intensities, were obtained at 280 (excitation wavelength) and 350 nm (emission wavelength).

2. Validation of CE-UV and HPLC methodology

In order to compare the proposed CE method [2] with the new optimised HPLC method for the authentication of quality of OO samples, linearity, limits of detection (LODs) and limits of quantification (LOQs) were evaluated using 11 polyphenols as test compounds. The precision was also studied using OO extracts.

The calibration regressions considering the peak areas were built from standard solutions of the 11 polyphenols at different concentration levels from 0.5 to 75 mg L^{-1} for CE and 0.4 to 70 mg L^{-1} for HPLC. Each concentration level was prepared in triplicate and also injected in triplicate. The statistical and quality parameters calculated by means of the least square regression are included in Table 2 of the main text. The coefficients of determination (R^2) obtained confirmed that the responses for the polyphenols conformed to a linear model in the range studied. The LOD and LOQ values were calculated as 3×S/N and 10×S/N ratio, respectively.

For the evaluation of precision, the selection of three unknown peaks from one OOs extract analysed by CE-UV was carried out (peak 1: 7.18 min, peak 2: 7.80 min and peak 3: 10.25 min). The same was carried out for HPLC-UV and FLD (peak 1: 6.19 min, peak 2: 12.28 min and peak 3: 15.74 min). Relative areas (peak area/IS area) and relative migration times (peak migration time/IS migration time) were calculated to correct their variations in CE profiles of OO samples. The selected IS was benzoic acid because its structure is similar to polyphenols and its migration time is well-separated from the rest of the polyphenols considered in this study by CE (see Figure 2A). The IS selected for HPLC separations was the 1-naphthol instead of benzoic acid, since the latter eluted from the column at a retention time (15.4 min) which prevent its differentiation from the rest of the polyphenols and was not fluorescent. However, 1-naphthol was fluorescent and eluted about 19.0 min. Precision was evaluated as repeatability (intraday precision) and as intermediate precision (interday precision), expressed as relative standard deviation percent (% RSD) of relative areas and relative migration times. Repeatability was evaluated by application of the whole procedure on the same day to nine OO samples. Intermediate precision was assessed in the same way but with nine samples analysed on three different days.

References

[1] M. Farrés-Cebrián, R. Seró, J. Saurina, O. Núñez, HPLC-UV Polyphenolic Profiles in the Classification of Olive Oils and Other Vegetable Oils via Principal Component Analysis, Separations, 3 (2016) 33. https://doi.org/10.3390/separations3040033.

[2] N. Arroyo-Manzanares, F. Gabriel, A. Carpio, L. Arce, Use of whole electrophoretic profile and chemometric tools for the differentiation of three olive oil qualities, Talanta, 197 (2019) 175-180. https://doi.org/10.1016/j.talanta.2019.01.031.

Exploration of the potential of different analytical techniques to authenticate organic *vs.* conventional olives and olive oils from two varieties using untargeted fingerprinting approaches

CHAPTER IX

To send

Exploration of the potential of different analytical techniques to authenticate organic *vs.* conventional olives and olive oils from two varieties using untargeted fingerprinting approaches

Natividad Jurado-Campos[a], María García-Nicolás[b], Marta Pastor-Belda[b], Tom Bußmann[c], Natalia Arroyo-Manzanares[b], Brígida Jiménez[d], Pilar Viñas[b] and Lourdes Arce[a]

[a]*Department of Analytical Chemistry, University of Córdoba. Institute of Fine Chemistry and Nanochemistry. International Agrifood Campus of Excellence (ceiA3), Marie Curie Annex Building. Campus de Rabanales. 14071 Córdoba (Spain).*

[b]*Department of Analytical Chemistry, Faculty of Chemistry, Regional Campus of International Excellence "Campus Mare-Nostrum", University of Murcia, E-30100, Murcia, Spain*

[c]*Hamm-Lippstadt University of Applied Sciences, Hamm, Germany.*

[d]*Department of Technology, Postharvest, and Food Industries, IFAPA 'Cabra' Centre, Institute for Research and Training in Agriculture and Fisheries, Ctra. Cabra-Doña Mencía, Km. 2.5, 14940, Cabra, Córdoba, Spain.*

Exploration of the potential of different analytical techniques to authenticate organic vs. conventional olives and olive oils from two varieties using untargeted fingerprinting approaches

Natividad Jurado-Campos, María García-Nicolás, Marta Pastor-Belda, Tom Bußmann, Natalia Arroyo-Manzanares, Brígida Jiménez, Pilar Viñas and Lourdes Arce

ABSTRACT

Authentication of organic olives and olive oils is of growing interest due to the marked development of organic olive agriculture worldwide. In this work, for first time, the potentiality of using the untargeted volatile fingerprinting of organic and conventional olives obtained with a low-cost and fast methodology based on ultraviolet - ion mobility spectrometry (UV-IMS) was investigated. The results showed the suitability of the optimised method since a 94.39 % of classification success was achieved. However, this UV-IMS device did not provided good results for olive oils samples. Thus, two different and more powerful analytical techniques (gas chromatography coupled to IMS with tritium source (GC-IMS) and capillary electrophoresis coupled to UV detector (CE-UV)) were employed respectively to analyse the volatile fingerprinting and the polar compounds extracted from organic and conventional olive oils from two varieties and harvests. It was found that both devices could provide good classification results, above 93.20 %, if an adequate number of samples (n > 50) from a single harvest was used. However, it was demonstrated that CE-UV is the best option since it provided more robust classification results over the years (95.76 %) in comparison with GC-IMS (75.16 %). An improvement of classification percentages of GC-IMS data was observed when samples from two harvest were separated into *Picual* (98.73 %) and *Hojiblanca* (98.78 %) variety sets. GC-mass spectrometry (GC-MS) with a single quadruple was employed to contrast the results obtained for the volatile fraction of olive and olive oils with UV-IMS and

GC-IMS devices. Also, up to 12 compounds were identified in olive and olive oil samples using GC-MS but only the 3-hexenyl acetate was able to differentiate organic and conventional olive oils.

Keywords: Organic, Olive, Olive Oil, Classification, Ion Mobility Spectrometry, Capillary Electrophoresis, Gas Chromatography, Mass Spectrometry

1. Introduction

Olives are the fruit of the olive tree (*Olea europaea*) and they are globally consumed as table olives or indirectly as olive oil (OO). In any case, olives can be cultivated through an organic production system, avoiding the use of agrochemicals and contributing to the protection of the environment, animal welfare and rural development, or in a conventional way. Organic olives are susceptible to fraud since the price of them and their by-products is higher.

Olive growers lose yield annually through the attack of some pests and thus large quantities of pesticides are applied to olive groves. However, persistent pesticides can adversely affect human health as well as other agrochemicals such as mineral fertilizers or hormones used in conventional production. This is one of the main reasons of the increasing of organic farming in general [Bertrand et al., 2018], and in the case of olives and OOs in particular [Pleguezuelo et al., 2018]. A critical aspect is also the environmentally friendly contribution of organic orchards to reduce the pollution, water consumption or over the quality of soils which influence on the quality of the cultivated fruit as have been demonstrated for olives [Aranda et al., 2011; Sofo et al., 2019].

When a food product is labelled as "Organic" means that its production and elaboration agree with the community regulations, as European regulation [Council, 2007]. Typically, certified organic products are more expensive so,

DISCUSSION OF THE RESULTS

The present Thesis Book is based on the format of articles compilation (published or next to publication) regulated by University of Córdoba. Therefore, articles were included as such. A joint discussion of the results obtained according to the objectives initially planned is necessary to provide a global vision of the main results derived from the Doctoral Thesis.

The highest present challenge in IMS is to maximize the selectivity of the analytical methods to achieve unequivocal identification of analytes, thus making possible to generate representative results of complex samples. Associated to this challenge, one general objective of this Doctoral Thesis was to propose innovations and/or approaches in the different stages of the analytical process involving sampling, sample preparation, detection and data analysis to improve the selectivity and/or identification capacity of analytical methods as well as other analytical properties such as sensitivity or speed of analysis. Also, extending the boundaries of IMS's applications well beyond the conventional ones such as detection of warfare agents, explosives and illicit drugs, is a current goal of the scientific community related to this technique. For this reason, other main objective of this Doctoral Thesis was to develop more innovative IMS applications through making the mentioned improvements in conventional areas of application and exploiting other unconventional samples in IMS such as soil, olive and mainly olive oils. The research developed in this Thesis Book is divided into three Blocks. One common link among blocks is the main detection technique: IMS with several variations.

Block I. Theoretical study of Ion Mobility Spectrometry

The use of a GC column prior the IMS system provides an additional separation dimension giving both retention time and drift time of the product ions which increases the accuracy of the qualitative analysis by improving

selectivity of the technology. This coupling can also mean an enhancement in the sensitivity of the IMS measurements since it can avoid the competition of volatile compounds to be ionized in the ionization chamber.

Concretely, in Chapter I, an exceptional finding was detected when proton-bound trimers, which are seldom observed in mobility spectra due to their low stability in the drift tube, were only observed for n-alcohols, at concentrations above 0.5 mg L^{-1} and for carbon numbers of 5 and above at low drift tube temperature (35-40 °C) as shown Figure 3 included in Chapter I of this Doctoral Thesis book. This experimental observation was explained by using structural calculations through quantum computations. It was found that this finding was due to the V-shape conformational structure of the two O-H bonds of protonated monomers of these alcohols (see Figure 6a included in Chapter I) and, the presence of two free O–H bonds for proton-bound dimers of alcohols that have the potential to participate in the formation of stable proton-bound trimers (see Figure 6b included in Chapter I). These results suppose an important contribution to IMS users to help to interpret the signals obtained when analysing these alcohols and even as a beginning to explain abnormal behaviours of other chemical compounds measured by IMS.

In Chapter II, an innovative tandem IMS device with a reactive stage which could produce field induced fragmentation (FIF) spectra of isolated product ions was used to prove its usefulness in improving the interpretation and identification capacity over the results obtained by IMS. For that, the rates of categorization of FIF spectra (expressed as adjusted average value (AAV)) by chemical class of compounds using neural networks were determined. It was demonstrated that when FIF was applied, the performance in categorization of compound was better in comparison only to mobility-selected spectra without fragmentation (see Table 3 included in Chapter II) for familiar strategy (spectra of all the compounds were included in training and testing sets at different concentration) since the additional energy promoted the formation of structural information in FIF spectra by increasing ion energies beyond thresholds for fragmentation. For unfamiliar strategy (one compounds from each chemical

family is included in testing set and the remaining compounds are maintained in the training set), the results were dependent on chemical family where classification was improved significantly for alcohols and ketones, improved moderately for acetates, and improved slightly for aldehydes. There was no improvement in classification observed with ethers.

Thus, it was demonstrated that using FIF data facilitates the categorization of some compounds within a chemical family since it provides important structural information for their identification. These findings fit with what happens with tandem MS technology whose identification power is higher than for stand-alone MS devices. However, tandem IMS is still too recent and needs further study and effort by researchers to achieve the usefulness of its counterpart in MS technology in qualitative analysis.

Block II. Applied study of Ion Mobility Spectrometry

The main aims of Block II were to develop new strategies or use existing alternatives applied throughout different steps of the analytical process to improve the detection and identification capacity in IMS analysis. The main results provided in this Block and the step of the analytical procedure that they affect are summarized below.

In Chapter III, the TD unit demonstrated to be a suitable alternative to detect cannabinoids in Cannabis herbal samples despite they have a relatively high boiling point. In preliminary tests, a HS system was checked as SIS and it was not suitable to detect these analytes by IMS since they were highly condensed before entering the instrument. Note that, an UV-IMS was employed during this preliminary tests instead of an IMS with ^{63}Ni ionization source as the case of the selected TD-IMS. Then, TD unit influenced the sensitivity of the method allowing the detection of the mentioned analytes. The spectral fingerprints of Cannabis herbal samples, which included these cannabinoids, were collected with the portable TD-IMS instrument, with and without pretreatment of the samples, in

solid-liquid extracts with n-hexane or in residues of Cannabis plants on fingers, respectively. PCA and LDA were used as chemometric strategies to perform the chemotyping of different Cannabis varieties to demonstrate the potential of TD-IMS for the screening of cannabinoids. Class grouping was successful in most cases so it was demonstrated that this method can be used for the discrimination of Cannabis chemotypes, without the requirement of a pre-extraction method, and faster than other methodologies employed for companies of this sector such as GC-MS. Then, the portability and quickness of IMS were exploited in this Chapter III thanks to find a suitable SIS for the detection of the cannabinoids with enough sensitivity.

Meanwhile, Chapter V was focused on the pioneer online coupling of SFE as SIS prior IMS using a column filled with Tenax TA material as sorbent trap to couple both devices. The robust, proper and reliable functioning of this new instrumental development and its utility was demonstrated by analyzing toluene and benzene as contaminants in soil samples and through the extraction and detection of eucalyptol in rosemary plants. This coupling could improve analytical properties of future IMS methods such as sensitivity and selectivity thanks to both the extraction of analytes or inferences using SFE and the separation and preconcentration of analytes using the Tenax TA column.

Finally, in Chapter IV, a tandem IMS with reactive stage was proposed to improve the selectivity of analytical methods which employ IMS technology in the detection step of the analytical process. Again, a TD inlet was employed as SIS, without relying on chromatograph pre-separation or drift tubes with high resolving powers (greater than 130). The selective determination of TNT in mobility dimension was carried out in presence of an interference (called as Interferent B) through reactive removal of interfering ions of Interferent B, through its fragmentation, following mobility isolation using the mentioned device as detection system. However, the sensitivity of this method could not be improved since suppression of ionization in the source from excessive amounts of

Interferent B could not be avoided due to a pre-separation stage was not used with the proposed instrument to maintain speed of measurements.

As summary, the improvement in selectivity using a tandem IMS with reactive stage observed in this Chapter can be extrapolated to other applications avoiding the use a pre-separation stage such as GC or HPLC that restricts one of the most attractive properties of the IMS, the speed of the measurements.

Block III. Applied study of Gas Chromatography coupled to Ion Mobility Spectrometry

Following with challenges of IMS technology, this Block III was mainly focused on using a pre-separation step, concretely a GC column prior IMS. The use of this step can improve both sensitivity by avoiding or reducing competitive ionization effects, and selectivity by providing a dual separation of IMS methods at the expense of quickness. In this Block, the mentioned opportunities of GC-IMS devices were applied for food analysis which is an expanding application area in IMS [1]. Specifically, the main objective of Chapters VI, VII and VIII was to authenticate olive oils depending on their quality in three categories using instrumental technique to support the current panel test method [2]. Meanwhile, Chapter IX was focused on the authentication of olive oil and olive samples according to their production system which provide to these matrices the organic or conventional category using GC-IMS and IMS equipments. Untargeted analysis methods, which do not aim the determination of individual analytes but on analyte profiles that are as comprehensive as possible, were used in this Block as it has been the trend in food authentication in the past 5 years [3]. This kind of methods allow that they can be easily established in routine laboratories avoiding the need of authentic reference material, high resolution laboratory infrastructure, extensive expertise in processing and storing very large amounts of data and so on which is required when using targeted approaches. In Chapters

VIII and IX, complementary techniques to IMS such as CE and/or HPLC were also explored to achieve the goal of each Chapter.

In Chapter VI it was found that the most consolidated techniques to determine VOCs from olive oils to classify them as EVOO, VOO or LOO were the GC-MS as well as the GC-IMS. Furthermore, CE-UV appears as an appropriate alternative or complement to complete the panel test by analysing extracts of the polar fraction of olive oil samples. For this reason, CE-UV was employed together with IMS devices in Chapters VIII and IX of this Doctoral Thesis.

The remaining Chapters of this Block were experimental and three specific studies were carried out in each of them related to the authentication of olive oils (in Chapters VII, VIII and IX) and olives (in Chapter IX). As a brief outline, in Chapter VII a huge amount of olive oil samples (701) of the categories EVOO, VOO and LOO, from two different olive oil harvests were measured. Two different chemometric approaches for olive oil classification using GC-IMS in an attempt to get the most robust model over time were compared. The results demonstrated that using either spectral fingerprint or markers data processing strategies for olive oil grading, the prediction abilities were enhanced recalibrating the models with samples from a new harvest. However, markers strategy was found the easiest and fastest alternative to be implemented in companies of this sector. In addition, after using 15 markers which correspond with identified compound by injecting real standards to perform an ANOVA test over their normalized intensity it was demonstrated that using targeted analysis of some compound, similar to what has been done previously in the bibliography with other instruments, was not enough to address this issue.

Whereas, in Chapter VIII, the combination of the results of GC-IMS with an orthogonal instrumental technique to differentiate olive oil samples according to their quality to imitate the expert panels was explored. CE-UV (in comparison with HPLC-UV and HPLC-FLD) was chosen as the most suitable instrument to complement GC-IMS. Also, it was found that the high-level data fusion procedure entails the improvement of having greater certainty and security in the final class

assigned to the olive oil samples and detecting suspect samples which are sitting on the border of two groups (e.g. EVOO-VOO or VOO-LOO). In my opinion, CE-UV and GC-IMS data fusion should be explored in future research work using samples tested by two panel tests and evaluating the time that olive oil samples conserves the category assigned by these panels to decide about the implementation of this platform in industries instead of a single GC-IMS.

Finally, in Chapter IX, the authentication of olive and olive oil samples according with their production system to categorize them as organic or conventional was the objective. Note that this problem has not been largely treated in bibliography yet. Firstly, it was demonstrated that UV-IMS device was enough for the authentication of olives taking advantages of its faster functioning by avoiding a pre-separation step. However, this technique was not enough to authenticate olive oil samples. For this reason, GC-IMS and CE-UV were studied based on the previous experience for the authentication of olive oils according to quality (in Chapters VII and VIII). In this case, both techniques were appropriate to classify samples of olive oil from the same harvest, but only the CE-UV remained as effective with samples from two harvests. This could be due to the non-volatile fraction of olive oils remains more constant over time than the volatile one which could be modified during the storage time of the samples easily. The GC-IMS proved to be valid for authentication of samples from two harvests only if the samples belonged to the same variety of olive (*Hojiblanca* or *Picual*) and there was no mixture of two varieties as until now. The results obtained for the techniques related to the volatile fraction of olives (UV-IMS) and olive oils (GC-IMS) were successfully contrasted with GC-MS data. Again, similarly that happened in Chapter VII but that time in a different context, using some identified compounds (up to 12 volatile compounds in olive and olive oil samples) was not enough to meet the objective described in Chapter IX.

Therefore, this block demonstrates the great potential of GC-IMS mainly for the authentication of olive oils as a technique that does not require sample treatment, does not use solvents and does not require a high cost, providing

promising results for the olive oil industry as described above. In fact, results derived from Chapters VII and VIII are being considered in a project (*Innolivar)* [4] subsidized with public and private funds (more than 800,000 Euros) to build a new prototype based on IMS technology to classify olive oil samples according to their quality with a high percentage of success to transfer this technology to companies in the sector. In addition, the usefulness of a complementary or orthogonal technique to GC-IMS, such as CE-UV, which is not implemented in routine laboratories is proved. In spite of CE-UV is more effective, efficient and simple than HPLC-UV and required low volume of sample and solvent, it is not widely implemented yet due to this technique provides lower reproducibility and higher detection limit compared to HPLC. The demonstrated success for CE-UV in the analysis of olive oil samples may arouse the interest of other authors in this technique for other sectors.

To finish this section, the improvements over the IMS properties described along all the Chapters included in this Doctoral Thesis book and discussed here were summarized in Table 1.

Table 1. Improvements achieved over IMS properties throughout this Doctoral Thesis.

Blocks	Chapters	Analytes	Matrices	Tools	Improvements on IMS properties
Block I	Chapter I	Alcohols Aldehydes ketones	*	GC-IMS Quantum computation	Interpretation of IMS data (identification) Selectivity
	Chapter II	Alcohols Acetates Aldehydes Ketones Ethers	*	GC-Tandem IMS with reactive stage Chemometrics	Interpretation of IMS data (identification) Selectivity

Block II	Chapter III	Cannabinoids	*Cannabis sativa* L. plant	TD-IMS Chemometrics	Portability Quickness Sensitivity
	Chapter IV	TNT	Explosive	Tandem IMS with reactive stage	Sensitivity Selectivity Quickness
	Chapter V	Benzene and toluene Eucalyptol	Soil Rosemary plant	SFE-IMS	Sensitivity Selectivity
Block III	Chapter VI	**	**	**	**
	Chapter VII	Unknown VOCs	Olive oils: EVOO, VOO and LOO	GC-IMS Chemometrics	Selectivity
	Chapter VIII	Unknown VOCs	Olive oils: EVOO, VOO and LOO	GC-IMS Chemometrics	Selectivity
	Chapter IX	Unknown VOCs	Organic and conventional olives Organic and conventional olive oils	UV-IMS Chemometrics GC-IMS Chemometrics	Quickness (UV-IMS) Selectivity (GC-IMS)

* These studies were carried out with standards.

** This Chapter is a bibliographical study.

References

[1] M. Hernández-Mesa, D. Ropartz, A.M. García-Campaña, H. Rogniaux, G. Dervilly-Pinel, B. Le Bizec, 2019. Ion Mobility Spectrometry in Food Analysis: Principles, Current Applications and Future Trends. Molecules. 24, 2706.

[2] International Olive Oil Council – IOOC. (2013). Sensory analysis of olive oil method for the organoleptic assessment of virgin olive oil (COI/T.20/Doc. No 15/Rev. 6). Madrid: IOOC.

[3] M. Creydt, M. Fischer, Food authentication in real-life: How to link non-targeted approaches with routine analytics? Electrophoresis (2020).

[4] *Innolivar* project. https://innolivar.es/ (accessed 12 May 2020).

CONCLUSIONS

CONCLUSIONES

The research conducted in this Doctoral Thesis was aimed at exploring the potential of IMS by using theoretical and applied strategies to improve the detection and identification coverage in analysis carried out with this technology.

The most salient conclusions drawn from this work can be summarized as follows according to the objectives:

1. Benefits derived from the study of theoretical aspects of IMS for improving the interpretation of IMS spectra and from the use of additional features such as structural information to enhance qualitative analysis.

    i) Only n-alcohols from 1-pentanol to 1-octanol produced proton-bound trimers which are sufficiently stable to be observed at 35 ºC since only alcohols formed a V-shaped arrangement for proton-bound trimers that strengthened their stability along the drift tube according to the computational modeling. Collision cross sections derived from reduced mobility coefficients in nitrogen gas atmosphere support the predicted ion structures and approximate degrees of hydration.

    ii) FIF spectra obtained using a tandem IMS spectrometer with a reactive stage presented a high efficiency of fragmentation for single bond cleavage of alcohols and in six-member ring rearrangements of acetates. Fragmentation was not observed, or seen weakly, with aldehydes, ethers, and ketones due to their strained four-member ring transition states. Neural networks were trained to categorize spectra by chemical class. Rates of categorization were class dependent with best performance for alcohols and acetates, moderate performance for ketones, and worst performance for ethers and aldehydes.

2. Improvement of the analytical process through new methodological developments to enhance the detection and identification capacity using IMS.

   (iii) The rapid detection of cannabinoids of Cannabis sativa L. plants using a portable TD-IMS was used to chemotyping these plants by analysing their solid-liquid extracts and the residues of plants on hands after their manipulation. PCA and LDA were applied over the pre-treated data and suitable results for on-site chemotaxonomic discrimination of Cannabis varieties and detection of illegal marijuana were obtained in less than 2 min.

   (iv) The use of a tandem IMS with reactive stage allowed the selective detection of TNT in presence of Interferent B. The peaks of the product ions of both, $(M-1)^-$ and M_2Cl^-, were more than 90% convolved even with mobility isolation of peaks in a tandem IMS drift tube. When using the reactive stage through applying an electric field of 123 Td more than 95 % of peak area for M_2Cl^- was decomposed to $M\cdot(M-1)^-$ which is almost completely separated from TNT. Only a 5% convolution was observed which was easily removed through peak deconvolution. However, suppression of ionization in the source from excessive amounts of Interferent B was observed which caused 30% loss in response to TNT with amounts of Interferent B of 200 ng or more on a sample swipe.

   (v) A pioneer on-line and environmentally-friendly hyphenation between a SFE and an IMS detector through a Tenax TA sorbent trap as retention interface was carried out for first time. This new coupling allows to extract and preconcentrate analytes and in a second step to determine them eliminating the manual transfer of samples from one device to another, which increase the accuracy and speed of the analytical process. The coupling was

successfully evaluated determining benzene and toluene present in samples of soil and eucalyptol in rosemary aromatic plants. It was concluded that the proposed new hyphenation can have a strong impact on extracting and detecting different volatile analytes present in complex matrices. The SFE-UV-IMS coupling improves the sensitivity and / or selectivity of the methods optimized with this technique, expanding its scope to other research areas or even in different industrial applications.

3. Exploitation of the opportunities of GC-IMS and IMS devices for food analysis as an expanding application area in IMS based on untargeted analysis methods.

   (vi) A bibliographical study of the publications dealing with the classification of olive oils according to their quality in the EVOO, VOO or LOO categories was carried out using non-separation and separation analytical techniques to complement the official methods, demonstrating that GC-IMS, GC-MS and CE-UV were the most promising and successful techniques for classifying olive oils.

   (vii) It has been shown that both the use of fingerprinting and the use of peak areas of the markers found in the topographic maps obtained in the GC-IMS equipment can be used for classification of the EVOO, VOO or LOO to build classification models of samples from the same harvest. However, when these models were applied for classifying olive oil samples from the next harvest, better classification values were obtained using markers from the topographic plots. The combination of data from the two harvests to build the chemometric models improved the percentages of prediction success for samples of the second harvest (> 90%). These results confirm the suitability of the

recalibration of the models with samples from at least two different harvests.

(viii) LLE-CE-UV was selected to determine the compounds appreciated in the mouth as the orthogonal technique of the HS-GC-IMS that is used to determine the compounds that the taster appreciates in the nose. The data obtained in the analytical platform (LLE-CE-UV and HS-GC-IMS) were merged to classify the olive oils that are sitting on the border of two groups (e.g. EVOO-VOO or VOO-LOO).

(ix) Organic or conventional olives of two varieties and a single harvest can be classified quickly and at low cost by chemometric treatment of the spectral fingerprint data obtained with UV-IMS. However, this technique did not provide good results for classifying organic or conventional olive oil samples.

Organic or conventional olive oils of two varieties and harvests could be classified using both HS-GC-IMS and LLE-CE-UV. However, when samples from two harvests are used together, the use of the LLE-CE-UV to obtain a good classification of the samples is recommended.

Results related to volatile fraction of olives and olive oils obtained with UV-IMS and GC-IMS, respectively, were contrasted with those obtained using HS-GC-MS (considered as a more implemented technique in analysis laboratories) and a good correlation of percentages of success obtained with both IMS and MS was achieved. GC-MS device was also employed to identify a total of 12 compounds in both matrices (olive oils and olives). However, the categorization of olives was not possible with this information and only the 3-hexenyl acetate allowed differentiation between organic and conventional olive oils.

La investigación realizada en esta Tesis Doctoral tenía como objetivo explorar el potencial de la IMS mediante el uso de estrategias teóricas y aplicadas para mejorar la capacidad de detección e identificación en los análisis realizados con esta tecnología.

Las conclusiones más destacadas de este trabajo de acuerdo con los objetivos inicialmente propuestos, se resumen a continuación:

1. Beneficios derivados del estudio de los aspectos teóricos de la IMS para mejorar la interpretación de los espectros de IMS y del uso de características adicionales como información estructural para mejorar el análisis cualitativo.

    i) Solo los n-alcoholes desde el 1-pentanol al 1-octanol produjeron trímeros protonados que son suficientemente estables para ser observados a 35 ºC ya que solo los alcoholes presentaban una disposición en forma de V para los trímeros protonados que fortalecía su estabilidad a lo largo del tubo de deriva de acuerdo con el modelo computacional. Las secciones transversales de colisión obtenidas a partir de los coeficientes de movilidad reducida en atmósfera de nitrógeno gaseoso apoyan las estructuras iónicas predichas y los grados aproximados de hidratación.

    ii) Los espectros FIF obtenidos usando un espectrómetro de IMS en tándem con una etapa reactiva, presentaron una alta eficiencia de fragmentación mediante la escisión de un solo enlace en alcoholes y el reordenamiento de anillos de seis miembros en acetatos. La fragmentación no se observó, o se vio débilmente, con aldehídos, éteres y cetonas debido a sus estados de transición tensos de anillos de cuatro miembros. Las redes neuronales se

entrenaron para clasificar los espectros por clase química. Las tasas de categorización fueron dependientes de la clase obteniéndose las mejores para alcoholes y acetatos, moderadas para cetonas y las peores para éteres y aldehídos.

2. Mejora del proceso analítico a través de nuevos desarrollos metodológicos para mejorar la capacidad de detección e identificación usando IMS.

   (iii) La detección rápida de los cannabinoides de las plantas de Cannabis sativa L. usando un TD-IMS portátil se usó para agrupar en función de su quimiotipo estas plantas mediante el análisis de sus extractos sólido-líquido y los residuos de las plantas en las manos después de su manipulación. Se aplicaron PCA y LDA sobre los datos pretratados y se obtuvieron resultados adecuados para la discriminación quimiotaxonómica in situ de las variedades de cannabis y la detección de marihuana ilegal en menos de 2 minutos.

   (iv) El uso de un IMS en tándem con etapa reactiva permitió la detección selectiva de TNT en presencia de Interferente B. Los picos de los iones producto de ambos, $(M-1)^-$ y M_2Cl^-, estaban solapados en más del 90% incluso con el aislamiento de iones en un tubo de deriva en tándem. Al usar la etapa reactiva mediante la aplicación de un campo eléctrico de 123 Td, más del 95% del área de pico para M_2Cl^- se descompuso en $M\cdot(M-1)^-$, que está casi completamente separado del TNT. Solo se observó un solapamiento del 5% que se eliminó fácilmente a través de la deconvolución de picos. Sin embargo, se observó la supresión de la ionización en la fuente debido a cantidades excesivas de Interferente B que causó una pérdida del 30% en la respuesta del TNT con cantidades de Interferente B de 200 ng o más.

(v) Un acoplamiento pionero on-line y respetuoso con el medio ambiente entre un SFE y un detector IMS a través de una trampa sorbente de Tenax TA como interfaz de retención se llevó a cabo por primera vez. Este nuevo acoplamiento permite extraer y preconcentrar analitos y, en un segundo paso, determinarlos eliminando la transferencia manual de muestras de un dispositivo a otro, lo que aumenta la precisión y la velocidad del proceso analítico. El acoplamiento se evaluó con éxito determinando el benceno y el tolueno presentes en muestras de suelo y el eucaliptol en plantas de romero. Se demostró que el nuevo acoplamiento propuesto puede tener un fuerte impacto en la extracción y detección de diferentes analitos volátiles presentes en matrices complejas. Con el acoplamiento SFE-UV-IMS se mejora la sensibilidad y/o selectividad de los métodos optimizados con esta técnica, ampliando su alcance a otras áreas de investigación o incluso en diferentes aplicaciones industriales.

3. Aprovechar las oportunidades de la GC-IMS y dispositivos IMS para el análisis de alimentos como un área de aplicación en expansión en IMS basada en métodos de análisis no dirigidos.

(vi) Se realizó un estudio bibliográfico de las publicaciones que tratan sobre la clasificación de los aceites de oliva según su calidad en las categorías AOVE, AOV o AOL utilizando técnicas analíticas no-separativas y separativas para complementar los métodos oficiales, demostrándose que la GC-IMS, GC-MS y CE-UV fueron las técnicas más prometedoras y exitosas para clasificar aceites de oliva.

(vii) Se ha demostrado que tanto el uso de huellas espectrales como el uso de áreas de pico de los marcadores encontrados en los mapas topográficos obtenidos en el equipo GC-IMS se pueden usar para la clasificación del AOVE, AOV y AOL para construir modelos de

clasificación de muestras de una misma campaña. Sin embargo, cuando estos modelos se aplicaron para clasificar muestras de aceite de la campaña siguiente, se obtuvieron mejores valores de clasificación usando los marcadores de los mapas topográficos. La combinación de datos de las dos campañas para construir los modelos quimiométricos mejoró los porcentajes de éxito de predicción para muestras de la segunda campaña (> 90%). Estos resultados confirman la idoneidad de la recalibración de los modelos con muestras de al menos dos campañas diferentes.

(viii) La LLE-CE-UV se seleccionó para determinar los compuestos apreciados en boca como técnica ortogonal de la HS-GC-IMS que se usa para determinar los compuestos que el catador aprecia en nariz. Los datos obtenidos en la plataforma analítica (LLE-CE-UV y HS-GC-IMS) se fusionaron para clasificar los aceites de oliva que se encuentran en el borde de dos grupos (por ejemplo, AOVE-AOV o AOV-AOL).

(ix) Se pueden clasificar de forma rápida y a bajo coste aceitunas ecológicas o convencionales de dos variedades y una sola campaña tratando quimiométricamente los datos de las huellas espectrales obtenidos con UV-IMS. Sin embargo, esta técnica no proporcionó buenos resultados para clasificar muestras de aceites de oliva ecológicas o convencionales.

Los aceites de oliva ecológicos o convencionales de dos variedades y campañas sí se pudieron clasificar usando tanto la HS-GC-IMS como la LLE-CE-UV. Sin embargo, cuando se usan muestras de dos campañas de forma conjunta, se recomienda usar la LLE-CE-UV para obtener una buena clasificación de las muestras.

Los resultados relativos a la fracción volátil de aceitunas y aceites de oliva obtenidos con UV-IMS y GC-IMS, respectivamente, se

compararon con los obtenidos usando HS-GC-MS (considerada como una técnica más implementada en los laboratorios de análisis) y se logró una buena correlación de los porcentajes de éxito obtenidos tanto con IMS como con MS. El dispositivo GC-MS también se empleó para identificar un total de 12 compuestos en ambas matrices (aceite y aceitunas). Sin embargo, la categorización de las aceitunas no fue posible con esta información y solo el acetato de 3-hexenilo permitió la diferenciación entre los aceites de oliva ecológicos y convencionales.

ANNEXES

ANNEX I

Other publications co-authored by PhD student

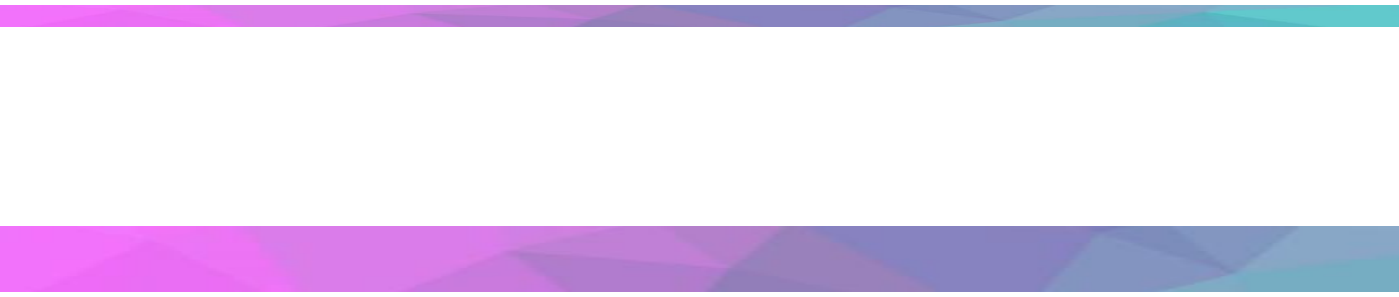

Other publications co-authored by the PhD student

Collaborations with other members of the group and with other group, which have provided 3 articles published.

1. Evaluation of different strategies to extract and preconcentrate penicillins present in milk prior determination by capillary electrophoresis.
   M.Y. Piñero, ***N. Jurado-Campos****, R. Bauza, L. Arce*
   Revista Científica de Veterinaria 24 (2014) 55-63

---

2. Target vs spectral fingerprint data analysis of iberian ham samples for avoiding labelling fraud using headspace - gas chromatography - ion mobility spectrometry.
   N. Arroyo-Manzanares, A. Martín-Gómez, ***N. Jurado-Campos****, R. Garrido-Delgado, C. Arce, L. Arce*
   Food Chemistry 246 (2018) 65-73

---

3. Deep learning techniques to improve the performance of olive oil classification
   B. Vega-Márquez, I.A. Nepomuceno-Chamorro, ***N. Jurado-Campos****, C. Rubio-Escudero*
   Frontiers in Chemistry 7 (2020) 929

Revista Científica, FCV-LUZ / Vol. XXIV, Nº 1, 55 - 63, 2014

EVALUATION OF DIFFERENT STRATEGIES TO EXTRACT AND PRECONCENTRATE PENICILLINS PRESENT IN MILK PRIOR DETERMINATION BY CAPILLARY ELECTROPHORESIS

Evaluación de diferentes estrategias para extraer y preconcentrar penicilinas presentes en leche previa determinación por Electroforesis Capilar

María Ysabel Piñero [1], ***Natividad Jurado*** [2], ***Roberto Bauza*** [3], ***Lourdes Arce*** [2] ***and Miguel Valcárcel*** [2]*

[1]*Faculty of Veterinary, University of Zulia, PO Box 126, Maracaibo, Venezuela.* [2]*Department of Analytical Chemistry, Institute of Fine Chemistry and Nanochemistry (IQFN), University of Córdoba, Annex C3 Building, Campus of Rabanales, E-14071 Córdoba, Spain.* [3]*Department of Chemistry, Faculty of Science, University of Zulia, PO Box 126. Maracaibo, Venezuela.*
**qa1meobj@uco.es - Fax: +34 957 218616*

ABSTRACT

One of the main problems concerning the determination of residues of penicillins (PENs) in complex matrix, as milk samples of animal origin, is the sample treatment. The aim of this work was to evaluate the influence of different background electrolyte (BGE) composition and pH, found in the literature, in the determination of PENs by capillary electrophoresis (CE) and, different sample treatments for the determination of PENs in bovine milk samples by CE. Off-line preconcentration, as classical solid-phase extraction (SPE) and QuEChERS (namely quick, easy, cheap, effective, rugged and safe) methodology and in-line preconcentration strategies, as large volume sample stacking (LVSS) were applied. In general, the milk sample treatment included protein precipitation prior to preconcentration. For this purpose, hydrochloric acid (HCl) and trichloroacetic acid (TCA) were mainly used. To evaluate the SPE steps, several commercial sorbents (Oasis HLB, Bond Elut C18 and Strata-X) were studied. In order to provide useful information enabling the determination of these analytes in routine laboratories, the strengths and weaknesses of each of the sample treatments tested are presented. Protein precipitation with HCl followed by SPE or QuEChERS procedure proved to be efficient for removing matrix interferences, showing higher selectivity than other procedures evaluated.

Key words: Capillary electrophoresis, penicillins, milk, QuEChERS, SPE.

Recibido: 22 / 07 / 2013 . Aceptado: 26 / 11 / 2013.

RESUMEN

El tratamiento de muestra es uno de los principales problemas relacionado con la determinación de residuos de penicilinas (PENs) en una matriz compleja, como leche de origen animal. El objetivo de este trabajo fue evaluar la influencia de la composición y pH de diferentes electrolitos de fondo o BGE (por sus siglas en inglés: background electrolyte) encontrados en la literatura para la determinación de PENs por electroforesis capilar (CE) y diferentes tratamientos de muestras para la determinación de PENs en muestras de leche bovina por CE. Para ello se aplicó una estrategia de preconcentración en línea, llamada *large volume sample stacking (LVSS)*, y preconcentración fuera de línea, como extracción en fase sólida (SPE) y la metodología QuEChERS (llamada así por sus siglas en inglés: Quick, Easy, Cheap, Effective, Rugged y Safe). En general, el tratamiento de la muestra de leche incluyó la precipitación de proteínas previo a la preconcentración. Para este propósito fueron empleados principalmente, ácido clorhídrico (HCl) y ácido tricloroacético (TCA). Para evaluar la SPE, se estudiaron varios sorbentes comerciales (Oasis HLB, Bond Elut C18 y Strata-X). En este trabajo se presentan las debilidades y fortalezas de cada uno de los tratamientos de muestras estudiados, con el fin de suministrar información útil para la determinación de estos analitos en laboratorios de rutina. La precipitación de proteínas con HCl seguido de SPE o QuEChERS resultaron ser los procedimientos más eficientes para la eliminación de interferentes de matriz demostrando mayor selectividad en comparación con otros procedimientos evaluados.

Palabras clave: Electroforesis capilar, penicilinas, leche, QuEChERS, SPE.

Food Chemistry 246 (2018) 65–73

Contents lists available at ScienceDirect

Food Chemistry

journal homepage: www.elsevier.com/locate/foodchem

Target vs spectral fingerprint data analysis of Iberian ham samples for avoiding labelling fraud using headspace – gas chromatography–ion mobility spectrometry

Natalia Arroyo-Manzanares[a], Andrés Martín-Gómez[a], Natividad Jurado-Campos[a], Rocío Garrido-Delgado[a], Cristina Arce[b], Lourdes Arce[a,*]

[a] Department of Analytical Chemistry, Institute of Fine Chemistry and Nanochemistry, Marie Curie Annex Building, Campus de Rabanales, 14071 Córdoba, Spain
[b] Department of Animal Production, University of Córdoba, Campus de Rabanales, E-14071 Córdoba, Spain

ARTICLE INFO

Keywords:
Iberian ham classification
Commercial fraud
Ion mobility spectrometry
Gas chromatography and Chemometrics

ABSTRACT

The data obtained with a polar or non-polar gas chromatography (GC) column coupled to ion mobility spectrometry (IMS) has been explored to classify Iberian ham, to detect possible frauds in their labelling. GC–IMS was used to detect the volatile compound profile of dry-cured Iberian ham from pigs fattened on acorn and pasture or on feed.

Due to the two-dimensional nature of GC–IMS mensurements, great quantities of data are obtained and an exhaustive chemometric processing is required. A first approach was based on the processing of the complete spectral fingerprint, while the second consisted of the selection of individual markers that appeared throughout the spectra. A classification rate of 90% was obtained with the first strategy, and the second approach correctly classified all Iberian ham samples according to the pigs' diet (classification rate of 100%). No significant differences were found between the GC columns tested in terms of classification rate.

1. Introduction

The Iberian pig constitutes a breed of great economic importance in Spain. Iberian pigs are raised under different rearing systems and one of their dry-cured products, ham, is classified in different categories, such as acorn or feed, depending on the feeding regime provided. Acorn-fed ham comes from Iberian pigs raised on free-range farms with a diet of acorns and grass, while feed-fed ham comes from pigs raised on confined farms and fed with concentrated feed. It is regulated by the Spanish government (Royal Decree 4/, 2014) and causes great differences in quality and final prices implying that Iberian ham is susceptible to fraud. In fact, labelling fraud is a serious problem that causes major economic loss in the sector, since in many cases Iberian hams from pigs fed with concentrated feed are labelled as Iberian acorn-fed hams.

Despite this problem, there are no analytical methods included in current legislation to control and ensure the authenticity of final dry-cured products or detect possible fraud in their labelling. Consequently, in recent years, researchers have switched their attention to the development of different analytical methodologies to predict the feeding diets given to Iberian pigs. Most of the developed analytical methods are based on gas chromatography (GC) coupled to flame ionization detection (Flores, Biron, Izquierdo, & Nieto, 1988; Ordóñez, López, Hierro, Cambero, & De la Hoz, 1996; Osorio, Montero de Espinosa, Sánchez, & Lozano, 1991; Viera-Alcaide, Vicario, Escudero-Gilete, Graciani-Constante, & León-Camacho, 2008) or mass spectrometry (Gamero-Pasadas et al., 2006; Hernández-Matamoros, González, García-Casco, & Tejeda, 2013; López-Vidal, Rodríguez-Estévez, Lago, Arce, & Valcárcel, 2008), determining different analytes as markers of feeding diets: fatty acids (Flores et al., 1988; López-Vidal et al., 2008; Ordóñez et al., 1996; Osorio et al., 1991) or their stable isotopes (^{13}C) (González-Martín, González-Pérez, Hernández Méndez, & Sánchez-González, 2001), triglyceride fraction (Viera-Alcaide et al., 2008) and hydrocarbons (Gamero-Pasadas et al., 2006; Hernández-Matamoros et al., 2013). In addition, the quantification of alpha and gamma tocopherol by high-performance liquid chromatography-ultraviolet detector (Rey, Daza, López-Carrasco, & López-Bote, 2006; Rey, Isabel, Cava, & López-Bote, 1998) and the near-infrared signal (Arce et al., 2009; de Pedro, Garrido, Lobo, Dardenne, & Murray, 1995; García-Olmo, Garrido-Varo, & de Pedro, 2009) and the determination of volatile compounds by proton transfer reaction time of flight mass spectrometry (Sánchez del Pulgar et al., 2013) or flow tube-mass

* Corresponding author.
E-mail address: lourdes.arce@uco.es (L. Arce).

https://doi.org/10.1016/j.foodchem.2017.11.008
Received 11 April 2017; Received in revised form 16 October 2017; Accepted 2 November 2017
Available online 04 November 2017

frontiers in Chemistry

ORIGINAL RESEARCH
published: 17 January 2020
doi: 10.3389/fchem.2019.00929

Deep Learning Techniques to Improve the Performance of Olive Oil Classification

Belén Vega-Márquez[1], Isabel Nepomuceno-Chamorro[1], Natividad Jurado-Campos[2] and Cristina Rubio-Escudero[1]*

[1] Department of Computer Languages and Systems, University of Sevilla, Sevilla, Spain, [2] Department of Analytical Chemistry, Institute of Fine Chemistry and Nanochemistry, International Agrifood Campus of Excellence (ceiA3), University of Córdoba, Córdoba, Spain

The olive oil assessment involves the use of a standardized sensory analysis according to the "panel test" method. However, there is an important interest to design novel strategies based on the use of Gas Chromatography (GC) coupled to mass spectrometry (MS), or ion mobility spectrometry (IMS) together with a chemometric data treatment for olive oil classification. It is an essential task in an attempt to get the most robust model over time and, both to avoid fraud in the price and to know whether it is suitable for consumption or not. The aim of this paper is to combine chemical techniques and Deep Learning approaches to automatically classify olive oil samples from two different harvests in their three corresponding classes: extra virgin olive oil (EVOO), virgin olive oil (VOO), and lampante olive oil (LOO). Our Deep Learning model is built with 701 samples, which were obtained from two olive oil campaigns (2014–2015 and 2015–2016). The data from the two harvests are built from the selection of specific olive oil markers from the whole spectral fingerprint obtained with GC-IMS method. In order to obtain the best results we have configured the parameters of our model according to the nature of the data. The results obtained show that a deep learning approach applied to data obtained from chemical instrumental techniques is a good method when classifying oil samples in their corresponding categories, with higher success rates than those obtained in previous works.

Keywords: olive oil classification, chemometric approaches, GC-IMS method, machine learning, deep learning, feed-forward neural network

OPEN ACCESS

Edited by:
John C. Cancilla,
Scintillon Institute, United States

Reviewed by:
Ricard Boqué,
University of Rovira i Virgili, Spain
Ramesh L. Gardas,
Indian Institute of Technology Madras, India

****Correspondence:***
Belén Vega-Márquez
bvegas@us.es

Specialty section:
This article was submitted to Theoretical and Computational Chemistry, a section of the journal Frontiers in Chemistry

Received: *15 February 2019*
Accepted: *20 December 2019*
Published: *17 January 2020*

Citation:
Vega-Márquez B, Nepomuceno-Chamorro I, Jurado-Campos N and Rubio-Escudero C (2020) Deep Learning Techniques to Improve the Performance of Olive Oil Classification. Front. Chem. 7:929. doi: 10.3389/fchem.2019.00929

1. INTRODUCTION

Olive oil is a fatty substance which is obtained from the fruit of the olive tree *Olea europea L.*. There are three different olive oil categories that in descending order of quality are named as extra virgin olive oil (EVOO), virgin olive oil (VOO), and *lampante* olive oil (LOO). The first two are edible while the last one should be refined prior to be consumed. The EVOO flavor is characterized by a pleasant balanced flavor of green and fruity sensory characteristics. In the VOO and LOO, some negative attributes (chemical compounds associated to defects) can be detected in different proportions. The EVOO is the only non-defective olive oil and therefore it is the most appreciated and expensive. Moreover, selling lower quality olive oils as EVOO is one of the most common olive oil commercial frauds. The classification of olive oil depends on (i) chemical parameters such as free

ANNEX II

Book chapters non-included in the Thesis

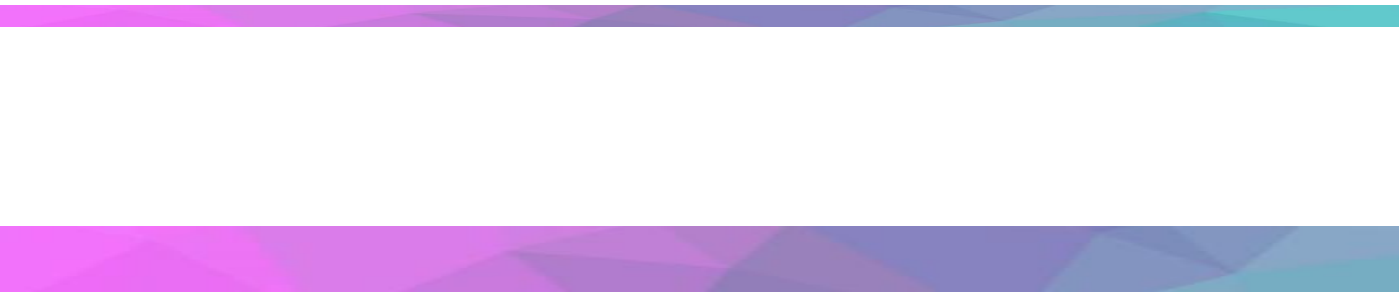

Book chapters non-included in the Thesis

1. B. Vega-Márquez, A. Carminati, **N. Jurado-Campos**, A. Martín-Gómez, L. Arce-Jiménez, C. Rubio-Escudero, I.A. Nepomuceno-Chamorro, Convolutional neural network for olive oil classification. From Bioinspired systems and biomedical applications to machine learning. Suiza. Springer. 2019. ISBN: 978-3-030-19650-9.

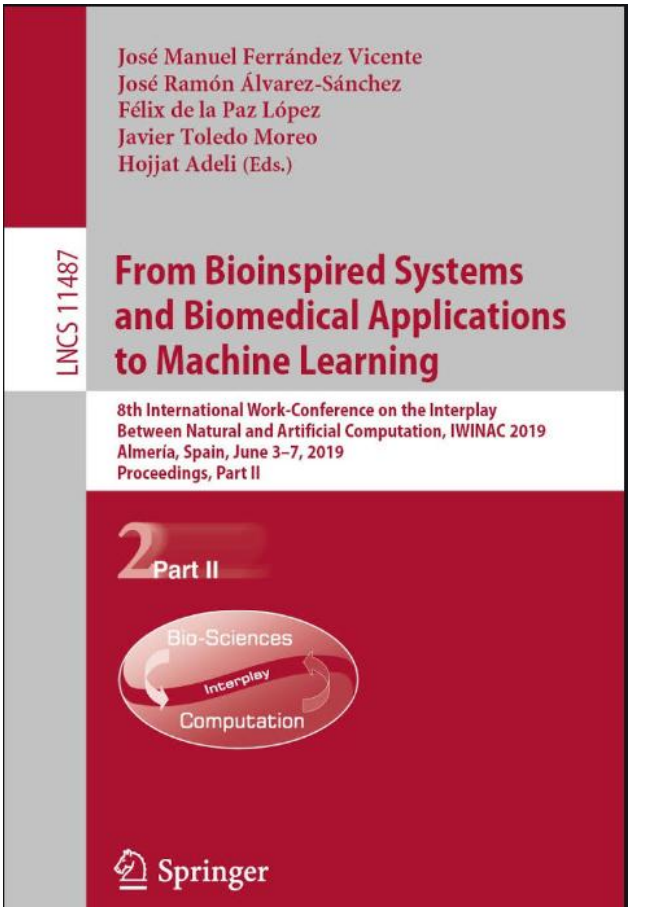

Applications

Bioinspired Systems

2. M. Esteki, M.J. Cardador, **N. Jurado-Campos**, A. Martín-Gómez, L. Arce and J. Simal-Gandara, Chapter X- Innovation in analytical methods for food authenticity. From Innovative Food Analysis. Elsevier. Published Date: 1st January 2021.

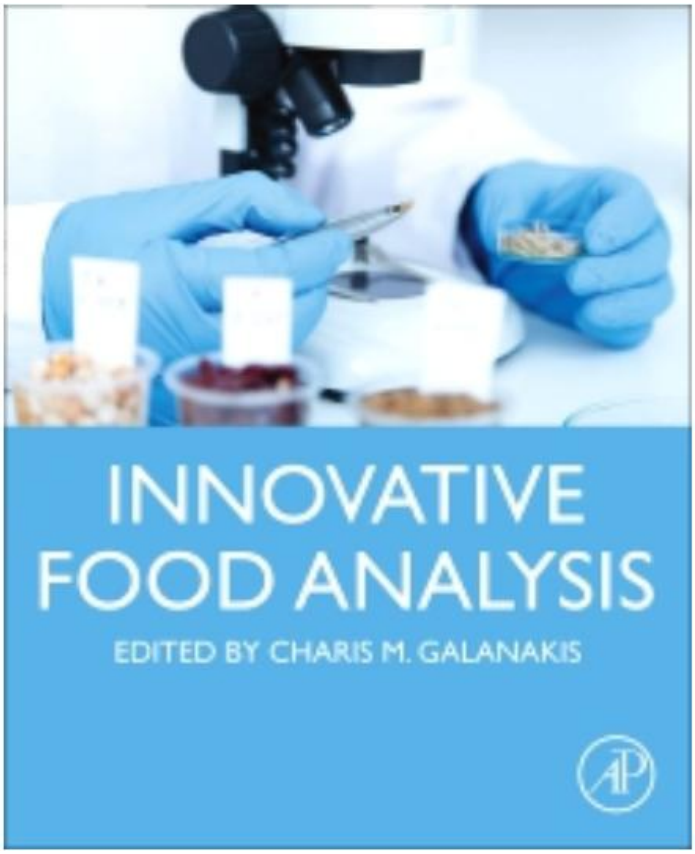

3. M.J. Cardador, **N. Jurado-Campos** and L. Arce, Chapter 15- Ion Mobility Detectors for Gas Chromatography. From Gas Chromatography 2nd edition. Elsevier. In press 2020.

ANNEX III

Oral and poster communications in national or international meetings

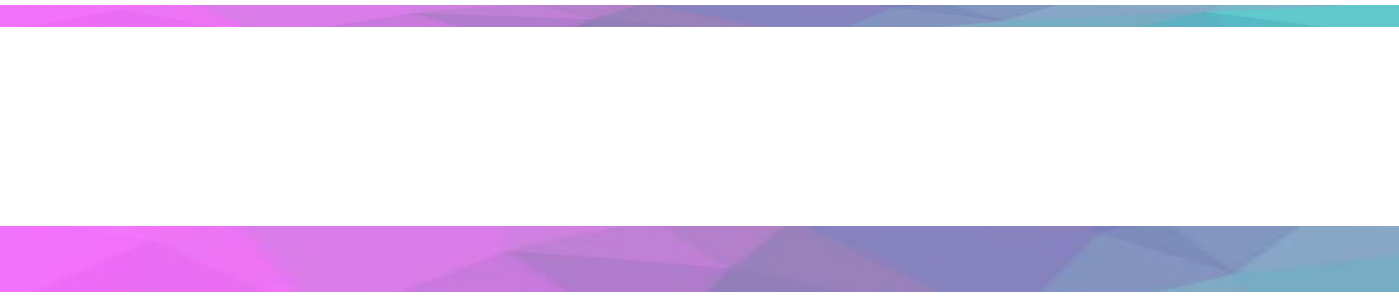

1. Evaluation of different strategies to extract and preconcentrate penicillins present in milk prior determination by capillary electrophoresis

M.Y. Piñero, N. Jurado-Campos, R. Bauza, L. Arce, M. Valcárcel

20TH INTERNATIONAL SYMPOSIUM ON ELECTRO- AND LIQUID PHASE-SEPARATION TECHNIQUES (ITP2013)

Tenerife, Spain, 2013

Type of communication: Poster **Level:** International

2. Study of the experimental conditions needed to detect trimers in linear ion mobility spectrometry

N. Jurado-Campos, R. Garrido-Delgado, B. Martínez-Haya, L. Arce.

25TH INTERNATIONAL CONFERENCE ON ION MOBILITY SPECTROMETRY

Boston, USA, 2016

Type of communication: Oral communication **Level:** International

3. Authentication of Iberian ham using volatile compounds by headspace-gas chromatography-ion mobility spectrometry

N. Jurado-Campos, A. Martín-Gómez, N. Arroyo-Manzanares, R. Garrido-Delgado, C. Arce, L. Arce

XVI SCIENTIFIC MEETING OF THE SPANISH SOCIETY OF CHROMATOGRAPHY AND RELATED TECHNIQUES - SECyTA 2016

Sevilla, Spain, 2016

Type of communication: Poster **Level:** International

4. Target vs. spectral fingerprint data analysis of ham samples using headspace-gas chromatography-ion mobility spectrometry

N. Jurado-Campos, A. Martín-Gómez, N. Arroyo-Manzanares, R. Garrido-Delgado, C. Arce, L. Arce

V CONGRESO CIENTÍFICO DE INVESTIGADORES EN FORMACIÓN DE LA UNIVERSIDAD DE CÓRDOBA

Córdoba, Spain, 2016

Type of communication: Oral communication **Level:** Regional

5. Design, adaptation and evaluation of an interface for supercritical fluid extraction-ion mobility spectrometry coupling

N. Jurado-Campos, A. Carpio, N. Arroyo-Manzanares, M. Zougagh, L. Arce

26TH ANNUAL CONFERENCE ON ION MOBILITY SPECTROMETRY

Varsaw, Poland, 2017

Type of communication: Oral communication **Level:** International

6. Uso de técnicas ortogonales (GC-IMS/CE-UV) para clasificar aceites de oliva virgen extra

N. Arroyo-Manzanares, M.M. Contreras, N. Jurado-Campos, L. Arce

XXI REUNIÓN DE LA SOCIEDAD ESPAÑOLA DE QUÍMICA ANALÍTICA

Valencia, Spain, 2017

Type of communication: Poster **Level:** National

7. Ion mobility spectrometer: a suitable detector to optimize the extraction process when a supercritical fluid extractor is used in an analytical lab

N. Jurado-Campos, N. Arroyo-Manzanares, L. Arce

VI CONGRESO CIENTÍFICO DE INVESTIGADORES EN FORMACIÓN DE LA UNIVERSIDAD DE CÓRDOBA

Córdoba, Spain, 2018

Type of communication: Poster **Level:** Regional

8. Gas Chromatography-ion mobility spectrometry: a powerful combination to support sensorial analysis of foodstuff. Classification of olive oil samples as a case of study

L. Arce, C. Arce, N. Arroyo-Manzanares, M.M. Contreras-Gámez, N. Jurado-Campos, A. Martin-Gómez

27TH ANNUAL CONFERENCE ON ION MOBILITY SPECTROMETRY

Calgary, Canada, 2018

Type of communication: Oral communication **Level:** International

9. A new sensor for the detection of cannabinoids and discrimination of cannabis sativa L. chemotypes

M.M. Contreras, N. Jurado-Campos, C. Sanchez-Carnerero Callado, N. Arroyo-Manzanares, L. Fernandez, S. Casano, S. Marco, L. Arce, C. Ferreiro-Vera

27TH ANNUAL CONFERENCE ON ION MOBILITY SPECTROMETRY

Calgary, Canada, 2018

Type of communication: Poster **Level:** International

10. HS-GC-IMS as a powerful analytical tool to classify olive oil: exploring data treatment and characteristics of two devices

N. Jurado-Campos, M.M. Contreras, N. Arroyo-Manzanares, L. Arce

XVIII MEETING OF THE SPANISH SOCIETY OF CHROMATOGRAPHY AND RELATED TECHNIQUES - SECyTA 2018

Granada, Spain, 2018

Type of communication: Poster **Level:** International

11. Is GC-IMS a suitable instrument for routine analysis?

A. Martín-Gómez, N. Jurado-Campos, M.C. Alcudia-León, N. Arroyo-Manzanares, L. Arce

XVIII MEETING OF THE SPANISH SOCIETY OF CHROMATOGRAPHY AND RELATED TECHNIQUES - SECyTA 2018

Granada, Spain, 2018

Type of communication: Poster **Level:** International

12. Determinación de drogas de abuso usando la espectrometría de movilidad iónica

N. Jurado-Campos

VII CONGRESO CIENTÍFICO DE INVESTIGADORES EN FORMACIÓN DE LA UNIVERSIDAD DE CÓRDOBA

Córdoba, Spain, 2019

Type of communication: Oral communication **Level:** Regional

13. Molecular classification and identification using tandem ion mobility spectrometry with neural networks analysis of mobility selected ions and full spectra

H. Shokri, N. Jurado-Campos, B. Gardner, H-C Niu, E. Nazarov, G.A. Eiceman

67TH CONFERENCE ON MASS SPECTROMETRY AND ALLIED TOPICS

Atlanta, USA, 2019

Type of communication: Poster **Level:** International

14. Convolutional neural networks for olive oil classification

B. Vega-Márquez, A. Carminati, N. Jurado-Campos, A. Martín-Gómez, L. Arce-Jiménez, C. Rubio-Escudero, I.A. Nepomuceno-Chamorro

8TH INTERNATIONAL WORK-CONFERENCE ON THE INTERPLAY BETWEEN NATURAL AND ARTIFICIAL COMPUTATION - IWINAC 2019

Almería, Spain, 2019

Type of communication: Poster **Level:** International

15. Selective and quantitative determination of TNT by tandem ion mobility spectrometry through decomposition of interfering ions in a reactive stage

U. Chiluwal, N. Jurado-Campos, G.A. Eiceman

28TH ANNUAL CONFERENCE ON ION MOBILITY SPECTROMETRY

Hannover, Germany, 2019

Type of communication: Oral communication **Level:** International

16. Is identification and quantification a challenge for IMS applications?

L. Arce, N. Jurado-Campos, A. Martín-Gómez, N. Reichelt, D. Saavedra, M.M. Contreras

28TH ANNUAL CONFERENCE ON ION MOBILITY SPECTROMETRY

Hannover, Germany, 2019

Type of communication: Oral communication **Level:** International

17. Portable ion mobility spectrometry to classify cannabis plant depending on their cannabinoids content

N. Jurado-Campos, M.M. Contreras, C. Sánchez-Carnerero Callado, N. Arroyo-Manzanares, L. Fernández, S. Casano, S. Marco, L. Arce, C. Ferreiro-Vera

4TH INTERNATIONAL MASS SPECTROMETRY SCHOOL

Sitges, Spain, 2019

Type of communication: Oral communication **Level:** International

18. Use of whole electrophoretic profile and chemometric tools for the differentiation of three olive oil qualities using the compounds extracted by liquid-liquid extraction and supercritical fluid extraction

N. Jurado-Campos, L. Valbuena, R. Rodríguez-Gómez, N. Arroyo-Manzanares, L. Arce

25TH LATIN-AMERICAN SYMPOSIUM ON BIOTECHNOLOGY, BIOMEDICAL, BIOPHARMACEUTICAL, AND INDUSTRIAL APPLICATIONS ON CAPILLARY ELECTROPHORESIS AND MICROCHIP TECHNOLOGY (LACE 2019)

Alcalá de Henares, Spain, 2019

Type of communication: Oral communication **Level:** International

ANNEX IV

Co-direction of two Final Degree Projects (TFGs) of Degree in Chemistry students (University of Córdoba, Spain)

1. **Co-direction of Final Degree Project (TFG) of Degree in Chemistry**

Student: Andrés Martín Gómez

Title: Uso de la Cromatografía de Gases-Espectrometría de Movilidad Iónica para autentificar un jamón ibérico de bellota.

Academic year: 2015/2016.

2. **Co-direction of Final Degree Project (TFG) of Degree in Chemistry**

Student: María Palma Chaves Aracena

Title: Clasificación de aceites de olivas vírgenes extras usando la Electroforesis Capilar y la Cromatografía Líquida con detector UV-visible previa extracción líquido-líquido.

Academic year: 2018/2019.

DEPARTAMENTO DE QUÍMICA ANALÍTICA
Edificio Marie Curie (Anexo)
Campus Universitario de Rabanales
Facultad de Ciencias. Universidad de Córdoba
14071 Córdoba (Spain)
Tfno: 34 957 218614 Fax: 34 957 218614

Doña Natividad Jurado Campos, adscrita al Departamento de Química Analítica como Investigadora del Grupo de Investigación FQM-215, ha colaborado con la Profesora Doña Lourdes Arce Jiménez en la tutorización del Trabajo Fin de Grado cuyos datos se refieren más abajo.

Alumno:	Andrés Martín Gómez		
Título del TFG:	Uso de la Cromatografía de Gases-Espectrometría de Movilidad Iónica para autentificar un jamón ibérico de bellota (QM15-21-QAN)		
Grado:	Química		
Tutor/es	Lourdes Arce Jiménez		
Fecha de defensa:	15 septiembre 2016	Créditos de la asignatura TFG:	15

Y para que conste y surta los efectos oportunos, firman el presente en Córdoba, a veintiuno de noviembre de 2016

Tutor del TFG	Tutor del TFG	El Director del Departamento
Fdo.: Lourdes Arce Jiménez	Fdo.: _____	Fdo.: Manuel Silva Rodríguez

Vº Bº

El Decano

FACULTAD DE CIENCIAS · UNIVERSIDAD DE CÓRDOBA · DECANATO

UNIVERSIDAD DE CÓRDOBA

Facultad de Ciencias

MARTA ROSEL PÉREZ MORALES, SECRETARIA DE LA FACULTAD DE CIENCIAS DE LA UNIVERSIDAD DE CÓRDOBA,

CERTIFICA:

Que **Dª. NATIVIDAD JURADO CAMPOS,** con D.N.I.: 50615863Q, ha sido tutora del siguiente Trabajo de Fin de Grado:

- QM17-19-QAN "CLASIFICACIÓN DE ACEITES DE OLIVAS VÍRGENES EXTRAS USANDO LA ELECTROFORESIS CAPILAR Y LA CROMATOGRAFÍA LÍQUIDA CON DETECTOR UV-VISIBLE PREVIA EXTRACCIÓN LÍQUIDO-LÍQUIDO" Dicho trabajo fue defendido en la convocatoria de septiembre del curso 2018/2019 y obtuvo la calificación de 8,6 Notable.

Y para que conste y surta los efectos oportunos, firmo el presente en Córdoba, a 19 de noviembre de 2019.

Código Seguro de Verificación	VYQAC5ATAI3X4U5ABVUGIIGTVA	Fecha y Hora	19/11/2019 11:20:02
Normativa	Este documento incorpora firma electrónica reconocida de acuerdo a la ley 59/2003, 19 de diciembre, de firma electrónica		
Firmado por	MARTA ROSEL PEREZ MORALES		
Url de verificación	https://sede.uco.es/verifirma/	Página	1/1

ANNEX V

Co-direction of three Practical semester project of German Erasmus students from Hamm-Lippstadt University of Applied Sciences, Germany

1. Co-direction of Practical Semester Project of German Erasmus students

Student: Hannah Schanzmann

Title: Identification of different markers which allow the differentiation of three olive oil categories using gas chromatography - ion mobility spectrometry.

Academic year: 2018/2019.

2. Co-direction of Practical Semester Project of German Erasmus students

Student: Tom Bußmann

Title: Fingerprinting to classify extra virgin olive oil samples using Capillary Electrophoresis.

Academic year: 2019/2020.

3. Co-direction of Practical Semester Project of German Erasmus students

Student: Kai Ordon

Title: Differentiation of olives according to their volatile profile using UV-IMS.

Academic year: 2019/2020.

Identification of different markers which allow the differentiation of three olive oil categories using gas chromatography - ion mobility spectrometry

Practical semester report

in study course Environmental Monitoring and Forensic Chemistry - exchange semester - food and environmental analytics (UFC-B-1-6.01)
Hamm-Lippstadt University of Applied Science

presented by Hannah Schanzmann
Am Mühlenteich 4, 46499 Hamminkeln
Hannah.schanzmann@stud.hshl.de
Matriculation number: 1150755

accomplished at University of Córdoba, Annex C3 "Marie Curie" Building, Campus of Rabanales, Córdoba, Spain
Department of Analytical Chemistry

supervised by Prof. Dr. Lourdes Arce Jiménez (lourdes.arce@uco.es, +34 957 218562) and Natividad Jurado Campos (nati_jurado@hotmail.com)

Hochschule Hamm-Lippstadt

Fingerprinting to classify extra virgin olive oil samples using Capillary Electrophoresis

Practical Semester Report

Study course: Environmental Monitoring and Forensic Chemistry - Specialization Chemical Forensics

Modul Number UFC-B-1-5.01 WS 19/20

Written by

Tom Bußmann

Neue Ostenheide 4, 59071 Hamm

tom.bussmann2@stud.hshl.de

Matriculation Number 1170726

Supervised by

Prof. Lourdes Arce Jiménez

lourdes.arce@uco.es, (+34) 957 21 85 62

Natividad Jurado Campos

nati_jurado@hotmail.com

Accomplished at

FQM-215 Research Group

University of Córdoba

Department of Analytical Chemistry

Marie Curie Building, C. U. Rabanales

14071 Córdoba, Spain

Differentiation of olives according to their volatile profile using UV-IMS

Practical semester report

Study course: Environmental Monitoring and Forensic Chemistry – Semester abroad - Specialization Chemical Forensics
Modul Number UFC-B-1-5.01

Presented by
Kai Ordon
Hesslerstraße 29, 59065 Hamm
Kai-Tino.Ordon@stud.hshl.de
Matriculation Number 2170013

Supervised by
Prof. Lourdes Arce Jiménez
lourdes.arce@uco.es (+34) 957 21 85 62
and
Natividad Jurado Campos (nati_jurado@hotmail.com)

Accomplished at
FQM-215 Research Group
University of Córdoba
Department of Analytical Chemistry
Marie Curie Building, C. U. Rabanales
14071 Córdoba, Spain

ANNEX VI

Simultaneous research in education

Simultaneous research in education, which has provided 1 article published and participation in a teaching innovation project

1. Promotion of self-employed work in the laboratory practices of students of the Degree in Chemistry: case study.
   M. A. López-Bascón, ***N. Jurado-Campos****, E. Romera-García, F. Priego-Capote, L. Arce*
   Accepted in Revista de Innovación y Buenas Prácticas Docentes 193 (2019)

2. Participation in a teaching project of University of Córdoba
   Title: Fomento del trabajo autónomo en las prácticas de laboratorio de alumnos del grado de Química
   Code: 2018-2-2002

REVISTA DE INNOVACIÓN Y BUENAS PRÁCTICAS DOCENTES

PROMOTION OF SELF-EMPLOYED WORK IN THE LABORATORY PRACTICES OF STUDENTS OF THE DEGREE IN CHEMISTRY: CASE STUDY

FOMENTO DEL TRABAJO AUTÓNOMO EN LAS PRÁCTICAS DE LABORATORIO DE ALUMNOS DEL GRADO DE QUÍMICA: CASO DE ESTUDIO

María Asunción López-Bascón, Natividad Jurado-Campos, Encarnación Romera-García, Feliciano Priego-Capote, Lourdes Arce

Abstract:

In this study we have sought to increase the participation of students in laboratory practices. The main reason has been to prevent the student from memorizing the theoretical concepts without being able to apply them to the resolution of real problems, and thus acquire useful competences for when entering into the working world. The new methodology was developed in the optional subject of the Degree in Chemistry, Applied Analytical Chemistry. In laboratory sessions, the common is to carry out a practical exercise following a script established by the teaching staff. Therefore, it was proposed that they themselves elaborate the protocols of three practices, on three subjects proposed by the teaching staff, and that they carried them out independently in the laboratory.

The evaluation of the students' work was carried out through three activities: preparation of the practical protocols, carrying out of the laboratory practices (using a rubric) and interactive questionnaire on theoretical concepts (using the Kahoot tool). Finally, the degree of acceptance of the new teaching methodology by the students was evaluated. This allowed to detect the aspects to be improved for the implementation of this methodology in the next academic year.

Key words: laboratory work, competences, chemistry, criterion-referenced evaluation, self-employed work

ANEXO V. MEMORIA FINAL DE PROYECTOS. MODALIDADES 1, 2, 3 Y 4

CURSO ACADÉMICO 2018/2019

DATOS IDENTIFICATIVOS:

1. Título del Proyecto

Fomento del trabajo autónomo en las prácticas de laboratorio de alumnos del grado de Química

2. Código del Proyecto

2018-2-2002

3. Resumen del Proyecto

En este proyecto se ha perseguido incrementar la participación de los alumnos en las prácticas de laboratorio. El motivo principal para plantear este proyecto ha sido evitar que el alumno simplemente memorice los conceptos teóricos, y que por tanto los comprenda y sea capaz de aplicarlos a la resolución de problemas reales, adquiriendo compentencias útiles para cuando se introduzca en el mundo laboral.

El proyecto se desarrolló en las clases prácticas de aula y laboratorio de una asignatura optativa del Grado de Química, Química Analítica Aplicada. En este tipo de clases, lo más común es realizar un ejercicio práctico siguiendo un guión. Sin embargo, el alumno no es consciente del trabajo que supone elaborar dicho guión para que la práctica se desarrolle con éxito, seleccionando los procedimientos más correctos desde un punto de vista analítico, medioambiental y económico. Por consiguiente, se les propuso que ellos mismos elaboraran los protocolos de tres prácticas, sobre tres temas concretos propuestos por el profesorado, y que las llevaran a cabo de forma autónoma en el laboratorio.

La evaluación del trabajo de los alumnos se realizó mediante tres actividades: elaboración de los protocolos de prácticas, realización de las prácticas de laboratorio (evaluada mediante rúbrica) y cuestionario interactivo sobre conceptos teóricos (mediante el uso de la herramienta Kahoot!). Como resultado, el 93.75% del alumnado obtuvo una calificación superior a 8.5 (sobre 10). La actividad en la que más discreparon sus resultados fue en la actividad programada con Kahoot!. Por otra parte, se evaluó el grado de aceptación de la metodología docente propuesta en este proyecto por parte del alumnado y el resultado general fue positivo. Se pudieron detectar los aspectos a mejorar para la implementación de esta metodología en el año académico próximo, siendo estos: el horario, el tiempo para desarrollar la actividad y la dificultad para encontrar información.

LIST OF ABBREVIATIONS

2,6-DtBP: 2,6-di-tbutylpyridine
AAVs: Adjusted Average Values
ALS: Alternating Least Squares
ANN: Artificial Neural Networks
ANOVA: Analysis of Variance
APCI: Atmospheric Pressure Chemical Ionization
AsLS: Assymetric Least Squares
AUROC: Area under ROC curve
BPR: Back Pressure Regulator
BSTFA: N,O-Bis(Trimethylsilyl)Trifluoro-Acetamide
BTEX: Benzene, Toluene, Ethylbenzene and Xilenes
CBC: Cannabichromene
CBD: Cannabidiol
CBDA: Cannabidiolic acid
CBDV: Cannabidivarin
CBG: Cannabigerol
CBGA: Cannabigerolic acid
CBN: Cannabinol
CC: Capillary column
CCl_4: Carbon Tetrachloride
CCS: Collision Cross Section
CD: Corona Discharge
CE: Capillary Electrophoresis
CID: Collision Induced Dissociation
d3-CBD: Deuterated Cannabidiol
DA: Discriminant analysis
DART: Direct Analysis in Real Time
DESI: Desorption Electrospray Ionization
DFT: Density Functional Theory
DLLME: Dispersive Liquid-Liquid Microextraction
DMA: Differential Mobility Analyzers

DMS: Differential Mobility Spectrometry
DTIMS: Drift Time Ion Mobility Spectrometry
EA-IRMS: Elemental Analysis-Isotope Ratio Mass Spectrometry
EGDN: Ethylene Glycol Dinitrate
EI: Electronic Impact
E-nose: Electronic Nose
ESI: Electrospray ionization
ETDs: Explosive Trace Detectors
E-tongue: Electronic Tongue
EVOO: Extra Virgin Olive Oil
FA: Fatty Acid
FAIMS: High Field Asymmetric Waveform Ion Mobility Spectrometry
FC: Folin Ciocalteu
FID: Flame Ionization Detector
FIF: Field Induced Fragmentation
FLD: Fluorescence Detector
FT: Fourier Transform
FWHM: Peak width or full width-half-maximum
GA: Genetic Algorithms
GC: Gas Chromatography
GNPs: Gold Nanoparticles
HCA: Hierarchical Cluster Analysis
HCl: Hydrochloride Acid
HDMS: High-definition Mass Spectrometry
HFLPME: Hollow Fibre Liquid Phase Microextraction
HMX: Octogen
HPLC: High Performance Liquid Chromatography
HS: Headspace
ILs: Ionic Liquids
IM-MS: Hybrid Ion Mobility-Mass Spectrometry
IMS: Ion Mobility Spectrometry

IR: Infrared
IS: Internal Standard
KNN: k-Nearest Neighbor
LC: Liquid Chromatography
LDA: Linear Discriminant Analysis
LLE: Liquid-Liquid Extraction
LLME: Liquid-Liquid Microextraction
LOD: Limit of Detection
LOO: Lampante Olive Oil
LOQ: Limit of Quantification
LOWESS: Locally Weighted Scatterplot Smoothing
LPME: Liquid Phase Microextraction
MALDI: Matrix-Assisted Laser Desorption Ionization
MCC: Multi-capillary column
MCR: Multivariate Curve Resolution
MDMA: 3,4-Methylenedioxy-Methamphetamine
MDS: Multidimensional Scaling
ME: Matrix Effect
MEPS: Microextraction in Packed Syringe
MIPS: Modular Intelligent Power Sources
MIPs: Molecularly Imprinted Polymers
MIR: Mid-Infrared Spectroscopy
MOS: Metal Oxide Sensors
MPCL: Merged Peak Cluster Localization
MPS: Multipurpose Sampler
MS: Mass Spectrometry
MTBE: Methyl Tert-Butyl Ether
NaOH: Sodium hydroxide
nESI: Nanoelectrospray Ionization
NG: Nitroglycerine
NIR: Near Infrared Spectroscopy

NN: Neural Networks
O: Olfactometry
OLIMS: open loop Ion Mobility Spectrometry
OMS: Overtone Mobility Spectrometers
OO: Olive Oil
OPLS-DA: Orthogonal Partial Least Squares-Discriminant Analysis
OPO: Olive Pomace Oil
PCA: Principal Component Analysis
PCR: Principal Component Regression
PEs: Potential Energies
PETN: Pentaerythritol Tetranitrate
PLSR: Partial Least Squares Regression
PME: Peak Model Estimation
PTFE: Polytetrafluoroethylene, Teflon
PTR-MS: Proton Transfer Reaction-Mass Spectrometry
QCM: Quartz Crystal Microbalance
Q-TOF: Hybrid Quadrupole Time-of-Flight
RDX: Cyclonite
RF: Random Forests
RIP: Reactant Ion Peak
RMSEP: Root Mean Square Error of Prediction
RSD: Relative Standard Deviation
RSIMPLISMA: Recursive Simple-to-use Interactive Self-Modeling Mixture Analysis
r-SVM: Recursive Supporting Vector Machine
SA: Simulated Annealing
SAW: Surface Acoustic Wave
SBSE: Stir-Bar Sorptive Extractors
SESI: Secondary Electrospray Ionization
SFC: Supercritical Fluid Chromatography
SFE: Supercritical Fluid Extraction

SIMCA: Soft Independent Modelling of Class Analogy

SIMPLISMA: Simple-to-use Interactive Self-Modeling Mixture Analysis

SIS: Sample Introduction System

SLDA: Stepwise Linear Discriminant Analysis

SOMs: Self-Organizing Maps

SPE: Solid Phase Extraction

SPME: Solid Phase Microextraction

SVM: Support Vector Machines

TD: Thermal Desorption

TIC: Total Ion Chromatogram

TIMS: trapped Ion Mobility Spectrometry

TLC: Thin Layer Chromatography

TMCS: Trimethylchlorosilane

TMIMS: Transversal Modulation Ion Mobility Spectrometry

TNT: trinitrotoluene

TOF: Time of Flight

TWIMS: Travelling-Wave Ion Mobility Spectrometry

UV: Ultraviolet

VOCs: Volatile Organic Compounds

VOO: Virgin Olive Oil

WST: Watershed Transformation

Δ^8-THC: Δ^8-Tetrahydrocannabinol

Δ^9-THC: Δ^9-Tetrahydrocannabinol

Δ^9-THCA: Δ^9-tetrahydrocannabinolic acid

Δ^9-THCV: Δ^9-Tetrahydrocannabivarin